

**STOICHIOMETRY AND TRANSPORT PROPERTIES OF THE GLUTAMATE
UPTAKE CARRIER IN SALAMANDER MÜLLER CELLS**

Muriel Bouvier

A thesis submitted for the degree of
Doctor of Philosophy
in the
University of London

Department of Physiology
University College London

September 1993

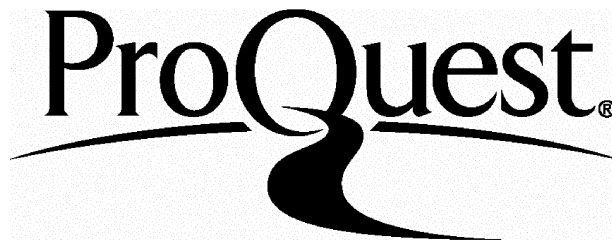
ProQuest Number: 10106743

All rights reserved

INFORMATION TO ALL USERS

The quality of this reproduction is dependent upon the quality of the copy submitted.

In the unlikely event that the author did not send a complete manuscript and there are missing pages, these will be noted. Also, if material had to be removed, a note will indicate the deletion.



ProQuest 10106743

Published by ProQuest LLC(2016). Copyright of the Dissertation is held by the Author.

All rights reserved.

This work is protected against unauthorized copying under Title 17, United States Code.
Microform Edition © ProQuest LLC.

ProQuest LLC
789 East Eisenhower Parkway
P.O. Box 1346
Ann Arbor, MI 48106-1346

Abstract

Glutamate is a major neurotransmitter in the central nervous system (CNS). The synaptic action of neurotransmitter glutamate is ultimately terminated by its uptake into glial cells and neurones. Uptake of glutamate is also important because it maintains the extracellular glutamate concentration below neurotoxic levels. Some of the sulphur-containing analogues of glutamate are also thought to have a possible role as neurotransmitters in the CNS and some of them may accumulate extracellularly and cause neuronal death.

The uptake of glutamate, aspartate and of their sulphur-containing analogues was studied in salamander retinal glial cells, using the whole-cell configuration of the patch-clamp technique.

Sulphur-containing analogues of glutamate and aspartate were shown to be transported on the glutamate uptake carrier with different affinities. The low affinity for transport of some of the analogues might explain their neurotoxic effect.

The possible transport of a pH-changing ion on the glutamate uptake carrier was investigated. Glutamate uptake was shown to be accompanied by an intracellular acidification and an intracellular alkalinization. These pH changes have the sodium-and potassium-dependence and the pharmacology of glutamate uptake. They were shown not to be due to metabolism nor to secondary activation of pH-regulating mechanisms.

The effect of certain anions inside the cell on the amplitude of the current evoked by glutamate uptake was investigated. This approach was used to show that the pH changes described above were due to an anion such as hydroxyl or bicarbonate being transported out on the glutamate uptake carrier, rather than due to a proton being transported into the cell. Anion-sensitive electrodes provided direct evidence for the transport of anions out of the cell on the glutamate uptake carrier.

The possible modulatory effects of various agents such as ATP, adenosine, ascorbate and annexin I were tested on the magnitude of the current evoked by the transport of glutamate. The effect of activating or inhibiting protein kinases was also studied.

Contents

Abstract	2
Contents	3
List of figures	9
List of tables	12
List of abbreviations	13

Chapter 1

Introduction

1.1	Glutamate receptors	18
1.1.1	NMDA receptors	19
1.1.2	Non-NMDA receptors	20
1.1.3	Metabotropic receptors	20
1.1.4	Glutamate-gated chloride channels	21
1.2	Sulphur-containing analogues of glutamate and aspartate	21
1.3	Long Term Potentiation	24
1.3.1	Properties of LTP	24
1.3.2	Induction of LTP	25
1.4	Glutamate and neurotoxicity	26
1.5	Glutamate and pathology	27
1.5.1	Epilepsy	27
1.5.2	Huntington's chorea	27
1.5.3	Parkinson's disease	28
1.5.4	Amyotrophic lateral sclerosis (ALS)	28
1.6	Glutamate transport	28
1.6.1	Stoichiometry of the glutamate uptake carrier	29
1.6.2	Affinity and pharmacology of glutamate uptake carriers	33
1.6.3	Modulation of uptake	35
1.6.4	Neuroprotective role of glutamate uptake	37
1.6.5	Cloning of the glutamate uptake carrier	37
1.6.6	Vesicular glutamate transporter	41
1.7	Other neurotransmitter and amino-acid transporters	48
1.8	Release of neurotransmitters	52

1.8.1	Ca ²⁺ -dependent release	52
1.8.2	Ca ²⁺ -independent release	52
1.9	Changes of pH during brain stimulation	54
1.9.1	Intracellular pH changes	54
1.9.2	Extracellular pH changes	54
1.10	pH-regulating mechanisms	55
1.11	Role of glial cells	56
1.11.1	K ⁺ buffering	56
1.11.2	pH regulation	57
1.11.3	Re-uptake of neurotransmitters	57
1.11.4	Glutamine synthesis and transport	58
1.12	Experiments performed for this thesis	59

CHAPTER 2

Methods

2.1	Cell preparation	61
2.2	Solutions and superfusion	64
2.2.1	External solutions	64
2.2.2	Internal solutions	65
2.2.3	Concentration of free glutamate in the superfusion solution	66
2.3	Recording from cells	66
2.3.1	Whole-cell patch-clamp recording	66
2.3.1	Correction for liquid junction potentials	67
2.3.2	Voltage-clamp quality	68
2.3.3	Series resistance error	70
2.3.4	Data acquisition	71
2.3.5	Data analysis	71
2.4	Internal pH measurements	74
2.4.1	Experimental apparatus	74
2.4.2	Calibration of BCECF fluorescence with weak acids and bases	75
2.4.3	Calculation of the absolute pH, the buffering power of the cell and the pH changes	76
2.4.4	Calibration of the fluorescence using nigericin	84
2.4.5	Calculation of the contribution of BCECF to the buffering power of the intracellular medium	87

2.5	External pH measurements	88
2.5.1	pH-sensitive electrodes	88
2.5.2	Electrical apparatus	89
2.5.3	Calibration of the pH microelectrode	89
2.5.4	Calculation of the pH at various times during the experiment, and of the corresponding $[H^+]$ change	89
2.6	Measurements of external ClO_4^- concentrations	91
2.6.1	Experimental apparatus	91
2.6.2	Anion-sensitive electrode	91
2.6.3	Calibration of the electrode and calculation of the change in $[ClO_4^-]$	91
2.7	Diffusion of a substance from the patch pipette into the cell	93

CHAPTER 3

Electrogenic Uptake of Sulphur-containing Analogues of Glutamate and Aspartate

3.1	Introduction	102
3.2	Dose-dependence of currents evoked by sulphur-containing amino-acids	102
3.3	Voltage-dependence of the current evoked by sulphur-containing amino-acids	108
3.4	Sodium-dependence of the sulphur-containing amino-acid uptake current	108
3.5	Dependence of the current on intracellular potassium	111
3.6	Lack of summation of currents produced by glutamate and the sulphur-containing analogues	116
3.7	Conclusion	119

CHAPTER 4

Changes of pH induced during glutamate uptake into glial cells

4.1	Introduction	120
4.2	External pH changes induced during L-glutamate and D-aspartate uptake	120
4.3	Voltage-dependence of the pH_o change	122
4.4	Sodium-dependence of the pH_o change	125
4.5	Changes of pH evoked during glutamate uptake when using patch pipettes of different series resistance	125
4.6	Effect of amiloride on the pH_o change evoked by glutamate uptake	131
4.7	Measurements of the extracellular pH changes at different parts	

	of the cell	133
4.8	Internal pH changes induced during L-glutamate and D-aspartate uptake	136
4.9	Is the intracellular pH change evoked by L-glutamate due to metabolism?	139
4.10	Sodium dependence of the pH_i change	143
4.11	Amiloride sensitivity of the internal pH acidification	145
4.12	Effect of DIDS on the internal pH change induced during glutamate uptake	147
4.13	Intracellular pH changes in unclamped cells	147
4.14	Pharmacology of the pH change in unclamped cells	150
4.15	Conclusion	150

CHAPTER 5

Effect of internal anions on the glutamate uptake carrier

5.1	Introduction	153
5.2	Substitutions of anions in the intracellular solution: effect on the amplitude of the glutamate uptake current	153
5.3	External pH changes accompanying glutamate uptake when internal Cl^- is replaced with NO_3^- or ClO_4^-	156
5.4	Efflux of ClO_4^- during glutamate uptake	158
5.5	Voltage-dependence of the ClO_4^- efflux	161
5.6	Dependence of the ClO_4^- efflux on external sodium	161
5.7	Dependence of the uptake current on internal potassium when ClO_4^- or NO_3^- is present inside the cell	165
5.8	Pharmacology of the efflux of ClO_4^-	167
5.9	Measurement of the efflux of ClO_4^- when the cells were whole-cell clamped with a solution containing a high concentration of sodium	167
5.10	Harmaline sensitivity of the ClO_4^- efflux	170
5.11	Measurements of the continuous efflux of ClO_4^- in the presence of 9AC	170
5.12	Summary of the chapter so far	172
5.13	Effect of intracellular bicarbonate on the amplitude of the uptake current	172
5.14	Internal pH changes with and without 10mM internal HCO_3^-	174
5.15	Effect of depleting the intracellular bicarbonate concentration on the amplitude of the uptake current	176
5.16	Effect of external acetazolamide on the extracellular pH change evoked during glutamate uptake	176
5.17	Effect of acetazolamide outside on the internal pH change induced by glutamate uptake	178
5.18	Conclusion	180

Chapter 6

Modulation of the rate of glutamate uptake

6.1	Introduction	182
6.2	Effect of ascorbate on the amplitude of the glutamate-evoked current	182
6.3	Effect of external ATP on the inward current evoked by glutamate uptake	183
6.4	Effect of external adenosine on the glutamate-evoked current . . .	183
6.5	Effect of external annexin I on the the glutamate uptake carrier .	184
6.5.1	Effect of external annexin I on the amplitude of the glutamate-evoked current	184
6.5.2	Effect of external annexin I on the inhibition of the glutamate uptake carrier by arachidonic acid	185
6.6	Effect of PKA catalytic subunit and of a peptide inhibitor of PKA present inside the cell on the amplitude of the glutamate evoked current	185
6.6.1	Protein kinase A catalytic subunit	186
6.6.2	Peptide inhibitor of protein kinase A	186
6.7	Effect of TPA, an activator of protein kinase C, on the amplitude of the inward current evoked by glutamate uptake	187

Chapter 7

Discussion

7.1	Electrogenic uptake of sulphur-containing analogues of glutamate and aspartate	190
7.1.1	Sulphur-containing amino-acids activate the electrogenic glutamate uptake carrier	190
7.1.2	Inhibition of HCA transport with β -p-chlorophenylglutamate	191
7.1.3	Termination of postulated neurotransmitter action	192
7.1.4	Excitotoxic actions of the sulphur-containing amino-acids . .	193
7.1.5	Mechanism of release of sulphur-containing amino-acids . . .	197
7.2	Stoichiometry of the glutamate uptake carrier	197
7.2.1	Glutamate	197
7.2.2	Sodium	198
7.2.3	Potassium	198
7.2.4	pH-changing ions	199
7.2.5	Most likely stoichiometry	203
7.3	Accumulative power of the carrier	203

7.4	Function of hydroxyl counter-transport	204
7.5	How similar are amphibian and mammalian glutamate uptake transporters?	204
7.6	Neuronal vs glial glutamate uptake	206
7.7	Glutamate uptake is associated with intra- and extracellular pH changes	206
7.7.1	Likely pH changes observed <i>in vivo</i> due to glutamate uptake	206
7.7.2	How do uptake-evoked pH changes affect cells?	207
7.8	Modulation of glutamate uptake	209
7.8.1	Effect of ascorbate on glutamate uptake	209
7.8.2	Effect of activating or inhibiting cAMP-dependent protein kinase	211
7.8.3	Effect of activating protein kinase C	211
7.8.4	Effect of annexin I on the inhibition of glutamate uptake by arachidonic acid	212
7.9	Role of glutamate uptake in neurotoxicity and pathology	212
7.10	Suggestions for future work	213
	References	218

List of Figures

Fig 1.1	Sulphur-containing analogues formulas	23
Fig 1.2	Stoichiometry of the glutamate uptake carrier	32
Fig 1.3	Aligned sequences of the glutamate uptake carriers	43
Fig 1.4	Hydrophobicity plots of the glutamate uptake carriers cloned to date	45
Fig 1.5	Alignment of the sequences of the glutamate uptake carrier GLT1 with glutamate proton transporter (<i>gltP</i>) from <i>E. coli</i> ..	47
Fig 1.6	Stoichiometries of various neurotransmitter transporters and proposed secondary structure	51
Fig 2.1	Müller cell from the salamander retina	63
Fig 2.2	Capacity transient analysis	73
Fig 2.3	Apparatus for fluorescence recordings	79
Fig 2.4	Calibration of the fluorescence of BCECF with weak acids and bases	80
Fig 2.5	Characteristics of the fluorescent dye BCECF	82
Fig 2.6	Calibration of the fluorescence of BCECF with nigericin	86
Fig 2.7	Calibration of a pH electrode	90
Fig 2.8	Calibration of an anion-sensitive electrode	92
Fig 3.1	Inward membrane current evoked by the different sulphur-containing analogues of glutamate and aspartate	104
Fig 3.2	Dose response curves for the action of CA, CSA, HCA and HCSA on the membrane current of Müller cells	107
Fig 3.3	Voltage-dependence of the current evoked by CA, CSA, HCA, HCSA and SC	110
Fig 3.4	Sodium-dependence of the current evoked by CA, CSA, HCA, HCSA and SC	113
Fig 3.5	Dependence of the CA, CSA, HCA, HCSA and SC induced	

	current on intracellular potassium	115
Fig 3.6	Competition of glutamate and sulphur-containing analogues for activation of electrogenic glutamate uptake carrier.	118
Fig 4.1	Extracellular alkalinization induced when glutamate uptake is activated	121
Fig 4.2	Voltage-dependence of the extracellular alkalinization	124
Fig 4.3	Dependence of the external pH change on external sodium	126
Fig 4.4	Calculation of the rise of $[Na^+]_i$ during glutamate uptake	128
Fig 4.5	Plot of the extracellular alkalinization induced during glutamate uptake for cells whole-cell clamped with pipettes of different series resistances.	130
Fig 4.6	Lack of amiloride-sensitivity to the extracellular alkalinization	132
Fig 4.7	Mapping of the external pH change	135
Fig 4.8	Intracellular acidification induced during glutamate uptake	138
Fig 4.9	Metabolic pathways by which glutamate can be metabolised	141
Fig 4.10	Intracellular acidification induced during L-glutamate and D-aspartate uptake	142
Fig 4.11	Dependence of the intracellular acidification on external sodium	144
Fig 4.12	Amiloride-sensitivity of the internal pH acidification	146
Fig 4.13	Effect of DIDS on the glutamate uptake current	148
Fig 4.14	Effect of DIDS on the internal pH change induced during glutamate uptake	149
Fig 4.15	Pharmacology of the intracellular pH changes in unclamped cells	151
Fig 5.1	Substitutions of anions in the intracellular solution: effect on the amplitude of the glutamate uptake current	155
Fig 5.2	Two possible explanations for the effect of NO_3^- , ClO_4^- or	

	SCN ⁻ present inside the cell on the amplitude of the current induced by glutamate uptake	157
Fig 5.3	Effect of the presence of NO ₃ ⁻ inside the cell on the amplitude of extracellular pH change induced by glutamate ..	159
Fig 5.4	Efflux of ClO ₄ ⁻ during glutamate uptake	160
Fig 5.5	Voltage-dependence of the efflux of ClO ₄ ⁻	163
Fig 5.6	Dependence of the efflux of ClO ₄ ⁻ on external sodium	164
Fig 5.7	Dependence of the current evoked by glutamate on internal potassium when ClO ₄ ⁻ is present inside the cell	166
Fig 5.8	Pharmacology of the efflux of ClO ₄ ⁻	168
Fig 5.9	Dependence of the efflux of ClO ₄ ⁻ on the concentration of internal sodium	169
Fig 5.10	Sensitivity of the glutamate-evoked ClO ₄ ⁻ efflux to the presence of harmaline	171
Fig 5.11	Effect of internal HCO ₃ ⁻ on the amplitude of the current evoked by glutamate uptake	173
Fig 5.12	Changes of intracellular pH evoked by glutamate when the cell is whole-cell clamped with an internal solution containing added HCO ₃ ⁻	175
Fig 5.13	Acetazolamide sensitivity of the extracellular pH change induced during glutamate uptake	177
Fig 5.14	Sensitivity of the intracellular acidification on the presence of external acetazolamide	179
Fig 5.15	Proposed stoichiometry for the glutamate uptake carrier	181
Fig 6.1	Effect of prolonged applications of TPA on the magnitude of the glutamate uptake current	189
Fig 7.1	Minimum [Glu] _o maintainable by the glutamate uptake carrier in pathological conditions	215

List of Tables

Table 1.1	Characteristics of glutamate uptake carriers cloned to date	39
Table 2.1	Extracellular solutions A-E	96
Table 2.2	Extracellular solutions F-I	97
Table 2.3	Internal solutions J-M	98
Table 2.4	Internal solutions N-Q	99
Table 2.5	Internal solutions R-V	100
Table 2.6	Internal solutions W- Ω	101
Table 7.1	Excitotoxic index values of glutamate, aspartate and their sulphur-containing analogues	195

List of Abbreviations

Ac	acetate
9AC	anthracene-9-carboxylic acid
Acetazol	acetazolamide
ALS	amiotrophic lateral sclerosis
AMPA	α -amino-3-hydroxy-5-methyl-4-isoxazole propionate
L-AP3	L-2-amino-3-phosphonopropionate
L-AP4	L-2-amino-4-phosphonobutyrate
D-AP5	D-2-amino-5-phosphonopentanoate (also known as APV)
D-APV	D-2-amino-5-phosphonovalerate (also known as AP5)
Asp	aspartate
ATP	adenosine triphosphate
BCECF	2',7'-bis-(carboxyethyl)-5 (6')-carboxyfluorescein
BCECF-AM	BCECF (acetoxymethyl ester form)
β	buffering power
CA	cysteic acid
cAMP	cyclic adenosine monophosphate
cDNA	complementary deoxyribose nucleic acid
cGMP	cyclic guanosine monophosphate
CNQX	6-cyano-7-nitroquinoxaline-2,3-dione
CO	carbon monoxide
CPP	3-((\pm)-2-carboxypiperazin-4-yl) propyl-1-phosphonic acid
CSA	cysteine sulphinic acid
CSF	cerebrospinal fluid
DA	dopamine
DIDS	4,4'-diisothiocyanatostilbene-2,2'-disulfonic acid
DMSO	dimethyl sulphoxide
DNDS	4,4'-dinitrostilbene-2,2'-disulfonate
L-Dopa	L-3,4-dihydroxyphenylalanine
EGTA	ethyleneglycol-bis-(β -aminoethylether) <i>N,N'</i> -tetraacetic acid
GABA	γ -amino-butyric acid

Glu	glutamate
Gly	glycine
G-protein	guanine nucleotide binding protein
HCA	homocysteic acid
HCSA	homocysteine sulphinic acid
Hepes	<i>N</i> -2-hydroxyethylpiperazine- <i>N'</i> -ethanesulphonic acid
5HT	serotonin
IP ₃	inositol trisphosphate
KA	kainate
LTP	long term potentiation
MCPG	(<i>RS</i>)- α -methyl-4-carboxyphenylglycine
MK801	dizocilpine/(+)-5-methyl-10,11-dihydroxy-5H-dibenzo (a,d) cyclohepten-5,10-imine
MPTP	1-methyl-4-phenyl-1,2,3,6 tetrahydropyridine
NA	noradrenaline
NAD ⁺	nicotinamide adenine dinucleotide
NADH	nicotinamide adenine dinucleotide (reduced form)
NADP ⁺	nicotinamide adenine dinucleotide phosphate
NADPH	nicotinamide adenine dinucleotide phosphate (reduced form)
NMDA	<i>N</i> -methyl-D-aspartate
NMDG	<i>N</i> -methyl-D-glucamine
NO	nitric oxide
PCP	phencyclidine or phenyl-cyclohexyl-piperidine
PDC	<i>L-trans</i> -pyrrolidine-2,4-dicarboxylate
pH _i	intracellular pH
pH _o	extracellular pH
Pipes	piperazine- <i>N,N'</i> -bis-2-ethanesulfonic acid
PKA	cAMP-dependent protein kinase
PKC	protein kinase C
PLC	phospholipase C
SC	S-sulpho-L-cysteine
SITS	4-acetamido-4'-isothiocyano-2,2'-disulphonic acid

THDA	threo-3-hydroxy-DL-aspartate
TMA	trimethylamine
TPA	12-O-tetradecanoylphorbol-13-acetate
<i>trans</i> -ACPD	<i>trans</i> -1-amino-cyclopentyl-1,3-dicarboxylate
ZnPP	zinc protoporphyrin

Acknowledgements

I would like to thank my supervisor, David Attwell, for his support and encouragement throughout the three years of my PhD.

I would also like to thank people associated with David Attwell's lab, in particular Marek Szatkowski with whom I had the pleasure of working for much of my first year in the lab. I am grateful to Beverley Clark, Barbara Miller, Peter Mobbs and Monique Sarantis for many helpful and stimulating discussions and moral support.

I would like to thank Sara "change her mind" Jacob for fun discussions and valuable friendship and Wen-Jun Shen for guiding my first steps into the computer program UWGCG.

Plusieurs de mes amis en France ont dû entendre mes sempiternelles discussions sur la possibilité de faire ma thèse en Angleterre. Ils n'ont pourtant jamais montré d'impatience. J'aimerais donc tout spécialement remercier Brigitte Chamak, Jean-Marie Desce, Thérèse Jay et Philippe Marin.

Last but not least, I wish to thank Steve Moss for his inexhaustible patience and encouragement all through the three years of my PhD and for reassembling me so often as I was falling into pieces.

This work was supported by the Wellcome Trust.

CHAPTER 1

Introduction

Glutamate was shown to have an important metabolic role and to be involved in protein synthesis, long before its possible role as a neurotransmitter was proposed. Indeed, a substance that is not specifically found in neurones, is involved in the metabolism of all cells and is a component of proteins was, at first, not readily accepted as a neurotransmitter. Furthermore, it was impossible to demonstrate the presence of an enzyme capable of degrading glutamate in the synaptic cleft (an enzyme was originally believed to be required for inactivation of the synaptic action of neurotransmitters, by analogy with acetylcholine). Glutamate was known to produce excitation when applied iontophoretically to the brain (Curtis & Watkins, 1963) but high doses of glutamate were needed and the effect of the amino acid did not seem very specific since it was observed in most of the brain. The effect of glutamate was therefore believed to be a non-specific effect on the membranes of all cells. However, glutamate was later shown to have all the characteristics required for a substance to be recognised as a neurotransmitter (the history of these discoveries was reviewed by Watkins (1986)), as follows:

- (1) glutamate is localised in the presynaptic terminals in synaptic vesicles;
- (2) stimulation of nerve terminals provokes its release;
- (3) this release is Ca^{2+} -dependent;
- (4) glutamate applied exogenously mimics the effects of the endogenous transmitter;
- (5) the effects of endogenous or exogenously applied glutamate are affected by the presence of antagonists;
- (6) a system exists for inactivation of the action of the neurotransmitter at the synapse.

It is now apparent that the vast majority of fast excitatory synapses in the central nervous system (CNS) are glutamatergic synapses (for review see Monaghan *et al*, 1989). Glutamate acts on two different kinds of receptors:

ionotropic receptors (linked to cation channels) and metabotropic receptors (coupled to G-proteins). The system which inactivates glutamate's synaptic action was eventually found to be, not an enzyme, but removal into cells by uptake.

This introduction covers the background to the experiments from this thesis, characterising the properties of the glutamate uptake carrier in salamander Müller (glial) cells. I will first of all review the properties of glutamate receptors and their involvement in long term potentiation, neurotoxicity and neuropathology. This part of the introduction also deals with actions of sulphur-containing analogues of glutamate and aspartate, which also activate glutamate-gated channels and are transported on the glutamate uptake carrier (see chapter 3 of this thesis). I then review the characteristics of glutamate transport across the plasma membrane, and compare it to the transport of other neurotransmitters and amino acids. A further part of this introduction deals with the mechanisms of glutamate release, which can occur via calcium-dependent vesicular release, but also in a calcium-independent manner by the reversed operation of glutamate transporters. I then discuss pH changes occurring during brain stimulation. This is highly relevant to the work described in this thesis, since I show in chapter 4 that glutamate transport is accompanied by an intracellular acidification and an extracellular alkalinization. The pH-regulating mechanisms available to cells, especially glial cells from the salamander retina (the preparation used throughout this thesis) are also described. Lastly, I examine briefly the possible roles of glial cells which are relevant to the work described in this thesis.

1.1 Glutamate receptors

Glutamate receptors can be sub-divided into two categories: ionotropic receptors (for which glutamate binding induces channels to open) and metabotropic receptors (where glutamate binding stimulates or inhibits the production of an intracellular messenger). Ionotropic receptors can be further divided into NMDA (N-methyl-D-aspartate) receptors and non-NMDA receptors (or α -amino-3-hydroxy-5-methyl-4-isoxazole propionate (AMPA)/kainate receptors).

For the pharmacological experiments described in this thesis, it is important to know how the properties of these receptors differ from those of the glutamate uptake carrier.

1.1.1 NMDA receptors

NMDA receptors are permeable to sodium, potassium and calcium ions (Ascher *et al*, 1988; Vyklícký *et al*, 1988; Mayer *et al*, 1987). In fact, the increase of intracellular calcium concentration resulting from the activation of NMDA receptors is thought to play a major role in neuroplasticity and neurotoxicity (see below). NMDA receptors have a key characteristic: they are blocked by Mg^{2+} at negative membrane potentials (Nowak *et al*, 1984; Mayer *et al*, 1984). Glutamate on its own is therefore unable to open these channels in a hyperpolarised cell: the cell must also be depolarised (for example when AMPA receptors are co-activated, see below) to release Mg^{2+} from the channel. However, several studies have now described NMDA receptors with a different voltage-dependence of Mg^{2+} block (Novelli *et al*, 1987; Schmidt *et al*, 1987; Ben-Ari *et al*, 1988; Bowe & Nadler, 1990; Marin *et al*, 1992; Gonzales, 1992) suggesting heterogeneity of NMDA receptors. Several other modulatory sites on these receptors have been described, including a site for glycine. Glycine on its own is not sufficient to open NMDA channels but its presence is obligatory for the opening of the channel. Glycine (at nanomolar levels) potentiates NMDA responses via a strychnine-insensitive site (Johnson & Ascher, 1987). Zn^{2+} ions are also able to block NMDA channels by binding to a site located on the extracellular domain of the receptor (Westbrook & Mayer, 1987). Interestingly, Zn^{2+} ions have been found to be co-released with glutamate at certain synapses (Mayer *et al*, 1989). Other modulatory agents acting on NMDA receptors include polyamines (Ransom & Stec, 1988; Williams *et al*, 1990), arachidonic acid (Miller *et al*, 1992), H^+ ions (Tang *et al*, 1990; Traynelis & Cull-Candy, 1990, 1991) and reducing or oxidizing agents (Aizenman *et al*, 1989, 1990).

NMDA receptors are selectively antagonised by D-2-amino-5-phosphonovaleric acid (D-APV) and 3-((±)-2-carboxypiperazin-4-yl)propyl-1-phosphonic acid (CPP) (competitive antagonists). Non-competitive antagonists

include dissociative anesthetics such as MK 801, phencyclidine (PCP) and ketamine which block the channel in a voltage-dependent manner (MacDonald & Nowak, 1990).

Several sub-units of the NMDA receptor have now been cloned (Moriyoshi *et al*, 1991; Meguro *et al*, 1992; Monyer *et al*, 1992). The subunit NMDAR1 is able to form homomeric channels but subunits NMDAR2A-D potentiate NMDAR1 currents when incorporated into heteromeric channels.

1.1.2 Non-NMDA receptors

Non-NMDA receptors are sometimes sub-divided into AMPA (α -amino-3-hydroxy-5-methyl-4-isoxazole propionate) and kainate receptors. They were the first glutamate receptors to be cloned and, according to their sequence similarities, they can be sub-divided into AMPA receptors (subunits GluR1, GluR2, GluR3 and GluR4), kainate receptors (subunits GluR5, GluR6 and GluR7) and high affinity kainate receptors (subunits KA1 and KA2). Several subunits are required to form a functional channel (probably five subunits for the AMPA receptor, not necessarily in heteromeric assembly; Wenthold *et al*, 1992). These channels are permeable to sodium and potassium, and also to calcium if GluR2 is not one of the subunits of the channel (Hollmann *et al*, 1991; Verdoorn *et al*, 1991). The non Ca^{2+} permeability conferred by GluR2 subunits is due to the presence of an arginine residue within the second transmembrane segment. Subunits GluR1, GluR3 and GluR4 have glutamine residues instead of this arginine. The arginine residue appears at the mRNA level (genomic DNA encodes for glutamine) after RNA editing (Sommer *et al*, 1991). This RNA editing process may be also active on GluR5 and GluR6 but to a lesser extent (they exist both in edited and unedited forms) (Sommer *et al*, 1991).

1.1.3 Metabotropic receptors

Metabotropic glutamate receptors were first described by Sladeczek *et al* (1985) for cultured striatal neurones. These receptors are coupled to G-proteins (Sugiyama *et al*, 1987; Nicoletti *et al*, 1988). Seven metabotropic receptors have been cloned to date: mGluR1 (Masu *et al*, 1991; Houamed *et al*, 1991; Tanabe

et al, 1992) and mGluR5 (Abe *et al*, 1992) are coupled to phospholipase C (PLC) and induce an increase in inositol trisphosphate (IP₃) concentration, while mGluR2 (Tanabe *et al*, 1992), mGluR3 (Tanabe *et al*, 1992), mGluR4 (Hayashi *et al*, 1992) and mGluR6 (Nakanishi, 1992) inhibit adenylate cyclase. The intracellular mechanism to which mGluR7 is coupled has not yet been determined (Saugstad *et al*, 1992). These receptors can be activated by glutamate, *trans*-1-amino-cyclopentyl-1,3-dicarboxylate (*trans*-ACPD), quisqualate or ibotenate. The most effective blockers of these receptors are L-2-amino-3-phosphonopropionate (AP3), 2-amino-4-phosphonobutyrate (L-AP4; which is in fact an agonist at some metabotropic receptors (see below)) and (RS)- α -methyl-4-carboxyphenylglycine (MCPG; Eaton *et al*, 1993; Bashir *et al*, 1993) (competitive blocker).

In the brain and spinal cord, L-AP4 inhibits release of glutamate (by acting on a presynaptic metabotropic receptor) and therefore reduces synaptic transmission (Cotman *et al*, 1986). In the retina, this glutamate analogue hyperpolarises ON-bipolar cells by activating a metabotropic receptor linked to a cGMP phosphodiesterase and thus closing cGMP-gated cation channels (Nawy & Jahr, 1990; Shiells & Falk, 1990).

1.1.4 Glutamate-gated chloride channels

Glutamate opens chloride-selective channels in locust muscle (Cull-Candy, 1976), *Helix* neurones (Szczepaniak & Cottrell, 1973) and in cone photoreceptors (Sarantis *et al*, 1988). The cone receptor is localised in the synaptic terminal of the cone and its effect is abolished when sodium is removed from the extracellular space. It is thought to act as a positive feed-back autoreceptor, responding to glutamate released from the cone synapse and increasing the gain of phototransduction.

1.2 Sulphur-containing analogues of glutamate and aspartate

Sulphur-containing analogues of glutamate (L-homocysteic acid (HCA) and L-homocysteinesulphinic acid (HCSA)) and aspartate (L-cysteic acid (CA) and L-cysteinesulphinic acid (CSA)), as well as S-sulpho-L-cysteine (SC, an analogue of HCA), have been suggested to act as neurotransmitters in the

central nervous system (Mewett *et al*, 1983) (Fig 1.1). Some of the experiments described in this thesis are on the transport of these substances by the glutamate uptake carrier. This is of interest because they are released in a calcium-dependent manner following depolarization by potassium (Do *et al*, 1986), and they depolarise neurones (Curtis & Watkins, 1963; Cox *et al*, 1977; Turski *et al*, 1987) by activating glutamate receptors, predominantly NMDA receptors but also AMPA receptors (Patneau & Mayer, 1990).

One of the criteria that defines a neurotransmitter is the presence of a potent mechanism to remove it from the extracellular space (or degrade it). The existence of such an uptake mechanism for the sulphur-containing amino acids has been shown in most cases. However, it is still unclear whether the uptake mechanisms described by different laboratories are powerful enough to lower the extracellular concentrations of the sulphur-containing analogues below levels that would activate glutamate receptors. There is some controversy over the mechanism by which sulphur-containing analogues are removed from the extracellular space after being released. Wilson & Pastuszko (1986) found that CA and CSA were transported by an uptake mechanism similar to that for glutamate and aspartate (see below). However, certain authors claim that sulphur-containing analogues are transported on a carrier other than the high-affinity glutamate uptake carrier (Cox *et al*, 1977; Parsons & Rainbow, 1984). Davies *et al* (1985) argued in favour of two different re-uptake systems based on the finding that β -p-chlorophenylglutamate selectively blocked the transport of radioactive HCA but not that of glutamate, but I will argue against this interpretation of their data in the discussion chapter (section 7.1.2).

In addition to being transmitter candidates, sulphur-containing analogues of glutamate and aspartate are also interesting because they are thought to be involved in certain neurodegenerative diseases. In cystathionine synthetase deficiency (a disease which leads to mental retardation), Ohmori *et al* (1972) and Mudd & Levy (1989) found that high concentrations of homocysteine and its metabolites (including HCA) were produced in the brain, blood and urine. It has been suggested that the cause of the neurological symptoms was an excitotoxic action of HCA on glutamate receptors, since HCA is able to induce glutamate-

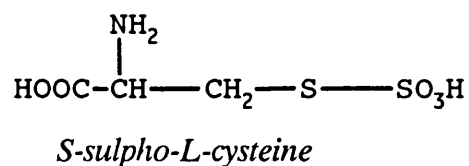
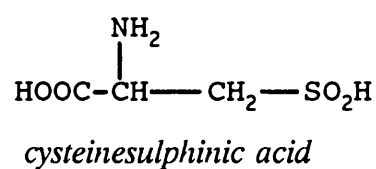
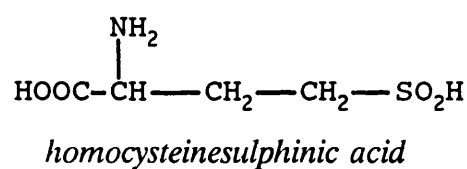
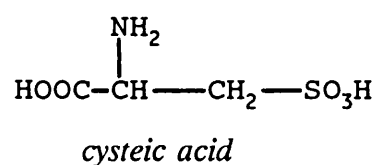
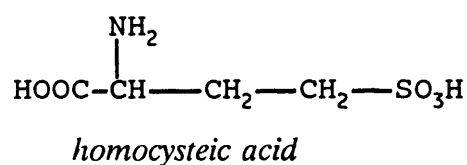
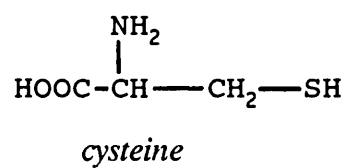
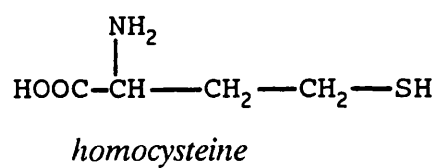
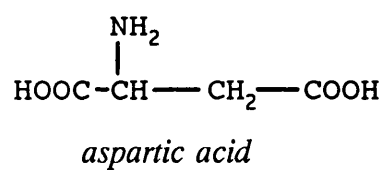
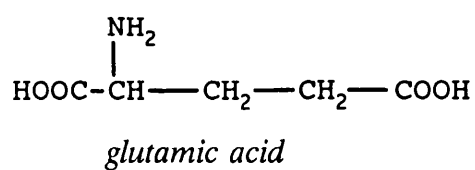


Fig 1.1: Structures of the sulphur-containing analogues of glutamate (left column) and aspartate (right column).

type neurotoxicity (Olney *et al*, 1971; Kim *et al*, 1987). In sulphite oxidase deficiency (a rare disease leading to mental retardation), it is the analogue of HCA, S-sulpho-L-cysteine (SC) which is found to accumulate in brain, blood and urine. Patients suffering from this disease have the same type and pattern of brain damage as that produced by glutamate (Olney *et al*, 1975) which is in accordance with the finding by Patneau & Mayer (1990) that SC is able to activate NMDA and AMPA receptors.

1.3 Long Term Potentiation

Long term potentiation (LTP), an activity-dependent increase in the strength of synaptic transmission, was first described in detail by Bliss & Lømo (1973) and Bliss & Gardner-Medwin (1973), and was recently reviewed by Bliss & Collingridge (1993). It was first shown to take place in the hippocampus but was later described in other parts of the brain.

1.3.1 Properties of LTP

LTP exhibits several important properties: first of all, both pre- and postsynaptic cells have to be active for LTP to occur. In other words, the presynaptic cell has to release glutamate and the postsynaptic cell has to be depolarised (see below). This is known as the associativity of LTP, and can be achieved by the application of a strong tetanus leading to the generation of action potentials in the postsynaptic cell (McNaughton *et al*, 1978). Alternatively, weak stimulation (which does not induce the postsynaptic cell to fire action potentials) of the studied input induces LTP if the postsynaptic cell is depolarised by the application of a strong tetanus on a convergent input (McNaughton *et al*, 1978; Levy & Steward, 1979), or by passing current into the cell with a voltage-clamp electrode while activating the input being studied ("pairing"). The second important characteristic of LTP is its specificity: only the stimulated input undergoes LTP (Andersen *et al*, 1977; Lynch *et al*, 1977).

1.3.2 Induction of LTP

The role of NMDA receptors in LTP induction explains both the associativity and specificity of LTP. Associativity results from the need for postsynaptic depolarisation (to remove Mg^{2+} block; see section 1.1.1) at the same time as the presynaptic cell is active (i.e. releasing glutamate to activate NMDA receptors). Specificity results from the need for glutamate release at the potentiated synapse to activate NMDA receptors and thus raise $[Ca^{2+}]_i$ locally (probably in the postsynaptic spines on which the synapses are made). Several lines of evidence indicate that calcium entry is a trigger for LTP. The induction of LTP can be blocked by the injection of EGTA (a calcium chelator) into the cells (Lynch *et al*, 1983). Moreover, light-evoked release of caged calcium is enough to induce a form of potentiation (Malenka *et al*, 1988). Calcium ions involved in the induction of LTP probably come from external sources via NMDA channels, as well as being released from intracellular stores (Obenaus *et al*, 1989; Harvey & Collingridge, 1992; Bortolotto & Collingridge, 1993). Several intracellular signalling molecules have been suggested to play a role in LTP. Blocking protein kinase C (PKC) or calcium/calmodulin-dependent kinase (CaM kinase) prevents the induction of LTP (Malinow *et al*, 1988; Klann *et al*, 1991, Ito *et al*, 1991). Protein tyrosine kinases have also been suggested to be needed for the induction of LTP but not to maintain it (O'Dell *et al*, 1991). Blocking the calcium-dependent enzymes phospholipase A_2 or nitric oxide synthase also blocks LTP (Linden *et al*, 1987; Okada *et al*, 1989; O'Dell *et al*, 1991). However, the evidence for nitric oxide (NO) as a candidate for the retrograde messenger acting during LTP is not conclusive. A more likely intercellular messenger suggested to play an important role in the induction of LTP is carbon monoxide (CO). This gas is synthesised in the brain by the enzyme haem-oxygenase (present in hippocampal pyramidal cells). Blocking this enzyme (with zinc protoporphyrin IX; ZnPP) inhibits the induction of LTP (Stevens & Wang, 1993; Zhuo *et al*, 1993). However, it is not clear how the enzyme haem-oxygenase would be up-regulated by the activation of NMDA receptors or by an increase in intracellular Ca^{2+} concentration. The hypothesis that CO is the retrograde messenger involved in LTP remains, therefore, to be proven.

It is still not clear the extent to which LTP is due to an increase of the amount of glutamate released by the presynaptic cell, a modification of the number or properties of post-synaptic receptors, or a change in the morphological characteristics of the synapse.

1.4 Glutamate and neurotoxicity

The brain is very sensitive to hypoxic-ischemic damage. Van Harreveld (1959) analysed the composition of extracts prepared from cortex exposed to 5 minutes of circulatory arrest. These experiments led him to suspect that this damage was related to the release of a compound present in the extracts (which was identified as being the amino acid glutamate). The neurotoxic action of glutamate was later established by Olney & Sharpe (1969) who observed acute neuronal death (observed by light or electron microscopy) after the subcutaneous injection of monosodium glutamate. Under physiological conditions, the glutamate concentration in the extracellular space is kept low by glutamate uptake carriers present in the membrane of glial cells and neurones (see below). However, under pathological conditions such as during anoxia or ischemia, because the amount of oxygen available to the cells decreases, ATP levels fall and the Na^+/K^+ ATPase is unable to maintain the ionic gradients across the cell membrane. Consequently, $[\text{K}^+]_o$ and $[\text{Na}^+]_i$ slowly rise and as a result, the membrane potential becomes depolarised. These pathological changes have several effects, including an increase of glutamate release (initially because neurones are depolarised and fire action potentials) and an inhibition of the glutamate uptake carrier (both because of the depolarisation of the cell membrane and the rise of $[\text{K}^+]_o$, see introduction, section 1.6 and discussion, section 7.9). These effects lead to a rise of extracellular glutamate concentration.

Glutamate neurotoxicity is thought to be due to a raised extracellular glutamate concentration, activating glutamate receptors excessively and thereby promoting the excessive entry of Na^+ and Ca^{2+} . This massive entry of ions has several effects including the induction of cell swelling and the activation of proteases, lipases and endonucleases (by high $[\text{Ca}^{2+}]_i$). Swelling can be prevented by removal of Na^+ and Cl^- from the extracellular medium (Rothman, 1985;

Olney *et al*, 1986). However, this operation is insufficient to prevent neuronal death: Ca^{2+} entry on its own is able to provoke a delayed degeneration. Removal of extracellular calcium was found to attenuate this degeneration in several preparations (cortical and hippocampal neurones in culture and cerebellar slices; Choi, 1985; Rothman *et al*, 1987; Garthwaite & Garthwaite, 1986). Glutamate neurotoxicity was also found to be blocked by antagonists to glutamate-gated channels, especially blockers of the NMDA-type channel (Rothman, 1984). These results are consistent with the findings of MacDermott *et al* (1986) i.e. that NMDA channels are permeable to calcium. However, excessive activation of glutamate-gated channels is probably only a partial explanation of processes leading to neuronal death during anoxia and ischemia and several other factors may be involved (e.g. release of calcium from internal stores following activation of metabotropic glutamate receptors, cell membrane breakdown releasing unsaturated fatty acids which generate toxic free radicals).

1.5 Glutamate and pathology

In this section, I will review briefly the clinical disorders in which glutamate may play a role.

1.5.1 Epilepsy

A convulsive effect of glutamate when applied to the brain was the first action of this neurotransmitter to be demonstrated (reviewed by Watkins, 1986). Moreover, MK-801, which is now known to be an NMDA antagonist, was first isolated for its anti-convulsive action (Wong *et al*, 1986). Glutamate depolarising cells presumably underlies its role in epilepsy.

1.5.2 Huntington's chorea

The major clinical signs of this disease are abnormal involuntary movements of the body. The pathology shows lesions of the brain limited to the striatum. An experimental model of Huntington's disease consists of the injection of quinolinic acid (an NMDA agonist) in the striatum (Beal *et al*, 1986), leading to striatal lesions resembling those observed in Huntington's chorea. Patients

suffering from Huntington's chorea show a diminution of the number of NMDA receptors in the striatum (Greenamyre *et al*, 1985). Since the striatum (caudate and putamen) receives numerous afferent fibres from the cortex (Alexander & Crutcher, 1990), it has been suggested that abnormalities in glutamatergic functions may play a role in this disease.

1.5.3 Parkinson's disease

In this disease, patients suffer from tremor and rigidity. Several lines of evidence suggest a role for excitatory amino acids in this disease. The locomotor enhancing effect of L-Dopa is greatly potentiated by low doses of MK-801 or CPP (NMDA antagonists) (Olney *et al*, 1987; Bormann, 1989). Moreover, NMDA antagonists protect against 1-methyl-4-phenyl-1,2,3,6-tetrahydropyridine (MPTP)-induced degeneration of dopamine neurones from the substantia nigra (Turski *et al*, 1991) and Parkinsonian patients have an increased concentration of glutamate and aspartate in the plasma (Iwasaki *et al*, 1992). These data suggest that excitotoxic mechanisms may play a role in Parkinson's disease.

1.5.4 Amyotrophic lateral sclerosis (ALS)

In this disease, motorneurones from the brainstem, spinal cord and cerebral cortex are found to progressively degenerate. In the cerebrospinal fluid (CSF) of patients suffering from ALS, concentrations of glutamate and aspartate were found to be increased (Rothstein *et al*, 1990). This has been suggested to result from a deficiency in glutamate uptake (Rothstein *et al*, 1992). However, a more recent study (Battaglioli *et al*, 1993) performed on a mutant mouse with a motor neurone disease mimicking ALS suggested that the decline in glutamate uptake is a consequence of the loss of the motorneurones, rather than the cause.

1.6 **Glutamate transport**

Uptake into neurones and glial cells ultimately terminates the synaptic action of neurotransmitter glutamate, possibly after diffusion out of the synaptic cleft to surrounding regions where the glutamate concentration is maintained low by uptake. A considerable amount of work has been done on glutamate uptake

transport, most of it using radiotracing methods, to study the movement of glutamate into either cells or synaptosomes (for review, see Hertz, 1979). More recently, glutamate uptake has been studied by whole-cell patch clamping, measuring the inward current that reflects the uptake of glutamate (Brew & Attwell, 1987).

1.6.1 Stoichiometry of the glutamate uptake carrier

The accumulative power of an uptake carrier (defined as the maximum ratio of intracellular to extracellular concentration of transported substance it can produce) is determined exclusively by its stoichiometry. It is well established now that the glutamate uptake carrier transports sodium into the cell with glutamate on each of its cycles (Balcar & Johnston, 1972; Kanner & Sharon, 1978a). The sigmoidal shape of the dependence of uptake on the extracellular concentration of sodium suggests that at least two sodium ions are transported. Most of the studies do not enable a distinction to be made between two and three sodium ions being transported due to poor resolution at low $[Na^+]_o$ (e.g. Barbour *et al*, 1991). However, studies of how the equilibrium gradient of labelled D-aspartate depends on the sodium gradient have shown that aspartate is transported on the glutamate uptake carrier together with two sodium ions (Erecińska *et al*, 1983).

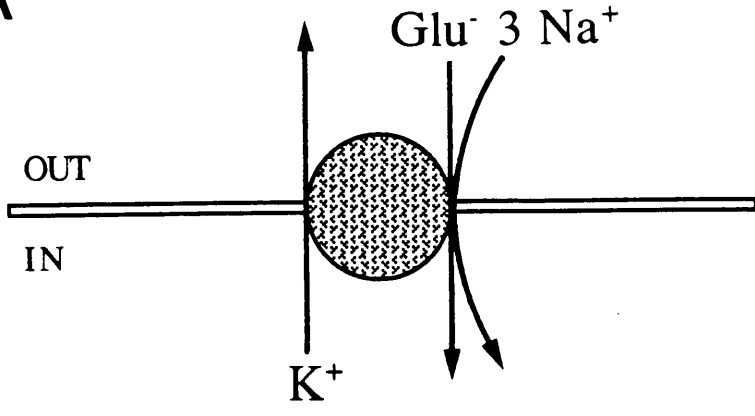
Several groups have also suggested that potassium ions are transported out on the glutamate uptake carrier. The first indication of this transport was from radiotracing experiments (Kanner & Sharon, 1978a; Kanner & Marva, 1982) in which glutamate uptake was abolished by removing K^+ from inside synaptosomes. However, since the glutamate uptake process is electrogenic (Kanner & Sharon, 1978a; Brew & Attwell, 1987) the effect of potassium could have been an indirect effect, due to the change in potassium concentration altering the potential across the membrane. Barbour *et al* (1988) took advantage of the electrogenicity of the carrier to monitor glutamate uptake as a membrane current while whole-cell clamping the cell membrane at constant voltage (see below), and thus showed that internal (i.e. whole-cell pipette) potassium was required for the transport of glutamate into the cell. However, these results were later contradicted by the findings of Schwartz & Tachibana (1990): in salamander

Müller cells, the same preparation as used by Barbour *et al* (1988), the uptake of aspartate on the carrier was independent of the concentration of potassium ions in the whole-cell pipette. Szatkowski *et al* (1991) resolved this controversy by showing that the pipettes used by Schwartz & Tachibana (1990) had too small a tip size to allow adequate control of the intracellular potassium concentration, so the intracellular $[K^+]$ was non-zero, even when the pipette $[K^+]$ was zero. After the work of Barbour *et al* (1988), the stoichiometry of the uptake carrier was postulated to be as shown in Fig 1.2A, where one glutamate is transported into the cell with three sodium ions and one potassium ion is transported out. Although, as discussed above, some evidence suggested that only two sodium ions are transported on the carrier (Wheeler, 1979; Erecińska *et al*, 1983), the transport of three sodium ions was postulated in order to explain the electrogenicity of the carrier.

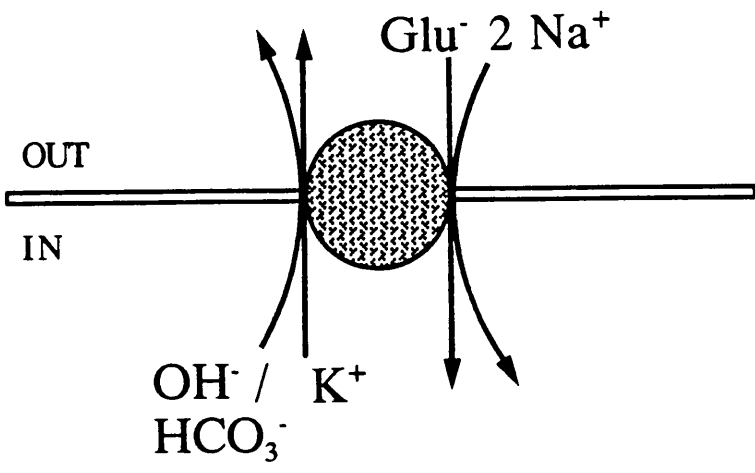
There has been controversy over the transport of protons into the cell on the glutamate uptake carrier for a long time. Erecińska *et al* (1983) found that aspartate transport into synaptosomes from rat brain evoked an extracellular alkalization, suggesting that protons are transported in on the carrier (or that OH^- are transported out). Nelson *et al* (1983) made a similar finding when working on the transport of glutamate in the kidney. However, Schwartz & Tachibana (1990) could not detect any intracellular pH change (measured with the pH-sensitive fluorescent dye, BCECF) in the salamander Müller cell when uptake of aspartate was elicited. Work from this thesis shows that hydroxyl ions (or possibly bicarbonate ions) are counter-transported on the glutamate uptake carrier. As a result, uptake of glutamate (and aspartate) is accompanied by an extracellular alkalization and an intracellular acidification (see results chapters 4 and 5). The likely stoichiometry of the glutamate uptake carrier derived from this work is as shown in Fig 1.2B where one glutamate anion is transported into the cell on the glutamate uptake carrier with two sodium ions and one potassium ion is counter-transported together with one hydroxyl ion (or possibly one bicarbonate). As a result of the stoichiometry discussed above, the glutamate uptake carrier is electrogenic (Brew & Attwell, 1987). Bath applied glutamate evokes an inward membrane current when these cells are whole-cell clamped.

Fig 1.2: Stoichiometry of the glutamate uptake carrier in salamander Müller cells. A- Proposed stoichiometry from the work of Brew & Attwell (1987) and Barbour *et al* (1988) suggesting that one glutamate anion is transported into the cell with three sodium ions and one potassium ion is counter-transported. This stoichiometry implies that glutamate transport on the carrier is electrogenic (glutamate uptake generates an inward membrane current). B- Proposed stoichiometry showing that one glutamate anion is transported into the cell on each cycle of the carrier with two sodium ions and that one potassium ion and one hydroxyl (or bicarbonate) ion are counter-transported (work from this thesis). This stoichiometry also results in an inward membrane current being generated by the uptake of glutamate, as is observed experimentally.

A



B



The inward current accompanying glutamate uptake is generated by a net positive charge transported into the cell on each cycle of the carrier (Fig 1.2B). Each glutamate anion is taken up with two sodium ions while one potassium ion is transported out together with a hydroxyl ion or a bicarbonate ion (Brew & Attwell, 1987; Barbour *et al*, 1988; and work from this thesis). Studying glutamate uptake by whole-cell patch clamping presents several advantages over radiotracing studies. The most important advantage it provides is control of the membrane potential. Because it transports one net positive charge into the cell on each cycle of the carrier, the glutamate transporter is inhibited at positive potentials and activated at negative potentials (Brew & Attwell, 1987). This property was used in the experiments described in chapter 4 to study extracellular pH changes. Being able to clamp the voltage of the cell via the whole-cell pipette also means that it is possible to change the composition of the intracellular and extracellular media at will without affecting the membrane potential. Moreover, being able to change the intracellular medium via the whole-cell patch pipette allows study of the effect of various ions when present inside the cell. Müller cells are a particularly convenient preparation to study glutamate uptake with whole-cell-clamping because these cells do not express glutamate-gated channels, and because they express enough uptake carriers to produce an easily detectable current. Furthermore, monitoring the uptake of glutamate by a fluorescence technique has shown that the uptake current is proportional to the amount of glutamate entering the cell (Barbour *et al*, 1993), so the membrane current generated by the carrier can be used to monitor glutamate uptake electrically. An example of the current evoked by the application of glutamate to a whole-cell clamped Müller cell from the salamander retina is shown in Fig 4.10.

1.6.2 Affinity and pharmacology of glutamate uptake carriers

Glutamate uptake transporters from several preparations have now been described. Their affinity for glutamate is usually around 10-20 μ M (considered as high affinity glutamate transporters) (Logan & Snyder, 1971; Balcar & Johnston, 1972; Brew & Attwell, 1987; Sarantis & Attwell, 1990; Wyllie *et al*, 1991). The

glutamate uptake carrier does not transport glutamate-gated channel and metabotropic receptor agonists such as kainate, NMDA, quisqualate, AMPA or *trans*-ACPD (Barbour *et al*, 1991). Similarly, it is not affected by glutamate-gated channel blockers like APV, CNQX or kynurenate (Barbour *et al*, 1991).

Several pharmacological studies have tentatively divided high affinity glutamate transporters into different categories. In 1983, Waniewski & Martin suggested that glial glutamate uptake was selectively inhibited by a stilbene: 4-acetamido-4'-isothiocyano-2,2'-disulfonic acid (SITS). Several laboratories have found two pharmacologically distinct high affinity glutamate transporters (Ferkany & Coyle, 1986; Robinson *et al*, 1991, 1993). L-amino adipate was 15 to 20 fold more potent at inhibiting uptake into synaptosomes isolated from the cerebellum than from the forebrain. Conversely, dihydrokainate was a potent inhibitor of glutamate uptake in the forebrain but not in the cerebellum (Johnston *et al*, 1979; Ferkany & Coyle, 1986; Robinson *et al*, 1991). This inhibitor only has a small effect on the glutamate uptake carrier from salamander Müller cells (Barbour *et al*, 1991). Robinson *et al* (1991) also found kainate-sensitive and insensitive transport both in the cerebellum and in the cortex, suggesting the possible existence of a further sub-division of glutamate transporters in the brain. However, the inhibition of glutamate uptake by kainate could be the consequence of a depolarisation of cells expressing both kainate receptors and glutamate carriers rather than a direct inhibition of the transporter. Cells lacking kainate receptors would in that case show a "kainate-insensitive" glutamate transport. Threo-3-hydroxy-DL-aspartate (THDA) was also found to reduce glutamate uptake (Balcar & Johnston, 1972) by competing with glutamate for transport (Barbour *et al*, 1991). A more selective and more potent uptake blocker has recently been discovered: L-trans-pyrrolidine-2,4-dicarboxylate (PDC, Bridges *et al*, 1991). It was found to block glutamate uptake competitively in salamander glial cells and to be transported on the transporter at a low rate and produce a current in this preparation (Sarantis *et al*, 1993).

A number of studies have also reported a low affinity (K_m values of 100 μ M-5mM) component to glutamate uptake. However, it seems likely that this reflects either (in slice preparations) a reduction of glutamate concentration at

the site of uptake by virtue of uptake in more superficial cell layers (so a higher superfused glutamate concentration is needed to saturate total uptake) or else, movement of uncharged glutamate directly through the cell membrane (i.e. not on a carrier). In most studies, this low affinity uptake represents less than 15% of the total uptake of glutamate (applied at a concentration of 1mM) into the cell (Hertz *et al*, 1978; Stallcup *et al*, 1979). Low-affinity glutamate uptake was reported to be sodium-independent in synaptosomes from rat brain and in a cerebellar nerve cell line (Benett *et al*, 1973; Stallcup *et al*, 1979). However, White & Neal (1976) described Na⁺-dependent low-affinity glutamate uptake ($K_m = 630\mu\text{M}$) in the rat retina. This transport process was found to have a V_{max} 25 times higher than the high affinity uptake from the same preparation. The other characteristics of the two transport systems reported in their study appear to be otherwise very similar: both are sodium-dependent and have similar pharmacological profile and sensitivity to metabolic blockers). These results could be explained simply by the presence of only one high-affinity glutamate uptake process, with part of the carriers being present at the surface of the retina (and therefore in contact with the superfused glutamate) and the rest of the carriers being deeply buried in the retina at location to which glutamate has to diffuse before being taken up by the carriers.

1.6.3 Modulation of uptake

Several agents can modulate the rate of glutamate uptake. It is inhibited by arachidonic acid in salamander Müller cells as well as in synaptosomes and astrocyte cultures from rat cerebral cortex (Chan *et al*, 1983; Barbour *et al*, 1989; Volterra *et al*, 1992). This effect occurs even in the presence of cyclo-oxygenase and lipoxygenase inhibitors (blockers of enzymes for arachidonic acid metabolism) (Barbour *et al*, 1989), and could be mimicked by melittin which activates phospholipase A₂ or by thimerosal which inhibits fatty acid reacylation in phospholipids (Volterra *et al*, 1992). This suggests that arachidonic acid may have a direct effect on the uptake carrier. However, the glutamate uptake carriers recently cloned (see below) do not have the putative fatty acid binding site described as being present in NMDA receptors and postulated to explain the

modulatory action of arachidonic acid on these receptors (Petrou *et al*, 1993). Glutamate uptake is also activated by protein kinase C (PKC) activators such as phorbol esters (Casado *et al*, 1991), and inhibited by glucocorticoids (Virgin *et al*, 1991). Activation of dopaminergic receptors inhibits glutamate uptake in homogenates from rat striatum (Nieoullon *et al*, 1983; Kerkerian *et al*, 1987), whereas the activation of α_1 -adrenergic receptors stimulates uptake of glutamate by a mechanism involving a pertussis toxin-sensitive G-protein and protein kinase C (Fahrig, 1993). Noradrenaline was shown to act through an increase of the V_{\max} of the transporter while the K_m remained unchanged. Voisin *et al* (1993) found that glutamate uptake in cerebellar astrocytes from newborn mice could be upregulated by an unknown factor present in horse serum as well as by the presence of neurones in the culture. This plasticity was lost in cultures from eight day old mice.

Unlike GABA uptake, which has been found to control the duration of the inhibitory synaptic current (Thompson & Gähwiler, 1992), the rate of uptake of glutamate out of the synaptic cleft apparently does not determine the decay rate of the non-NMDA component of the synaptic current (Sarantis *et al*, 1993). Thus, modulation by the agents described above, at least within certain limits, may not greatly alter the synaptic current waveform, although a rise in background $[\text{Glu}]_o$ produced by inhibiting uptake may desensitise postsynaptic receptors and reduce the amplitude of the postsynaptic current (Sarantis *et al*, 1993)

Finally, in ischemic or hypoxic conditions, when the ATP level falls and the ion gradients across the plasma membrane are disrupted, glutamate uptake is expected to be inhibited by several factors including the rise of $[\text{K}^+]_o$ and $[\text{Na}^+]_i$ and the depolarisation of the cells occurring. Swanson (1992) showed that glutamate uptake into astrocytes in culture was inhibited to about 50% of the control values in hypoxic conditions (modelled by blocking aerobic metabolism) and to 95% if both aerobic and anaerobic metabolism were blocked. However, since neither the extracellular potassium concentration nor the membrane voltage of the astrocytes were monitored during these experiments, it is difficult to interpret these results in terms of what is likely to happen *in vivo*.

1.6.4 Neuroprotective role of glutamate uptake

Astrocytic glutamate uptake plays an important role in the protection of neurones from the neurotoxic effects of added glutamate in culture (Rosenberg *et al*, 1992), and blocking it was shown to greatly elevate the neurotransmitter's neurotoxic potential: glutamate was shown to be a potent neurotoxic agent in cultures of rat cerebral cortex poor in astrocytes or in cultures superfused with a sodium-free medium (inhibiting uptake) while it was a lot less potent if the culture was rich in astrocytes. In parallel experiments, the authors showed that the uptake of glutamate was reduced by about 25 fold in astrocyte poor cultures. These results, although not surprising, give a more direct piece of evidence for the neuroprotective role of glutamate uptake.

1.6.5 Cloning of the glutamate uptake carrier

Recently, three different glutamate uptake carriers have been cloned and sequenced (see table 1.1). These three clones show very different patterns of expression. GLT1 (isolated from rat brain; Pines *et al*, 1992; Kanner, 1993) is only expressed in the brain (absent from the spleen, liver, heart, lung or kidney) and has been shown to be of glial origin (Danbolt *et al*, 1992). EAAC1 (Kanai & Hediger 1992) was initially cloned from rabbit small intestine, where it is expressed at high levels, but was later found to be also expressed in neurones of specific areas of the brain (hippocampus, cerebellum and cortex). GLAST (isolated from rat brain; Storck *et al*, 1992) is expressed in the brain, mainly in the Purkinje cell layer of the cerebellum (presumably in the Bergmann glial cells, since unlike Purkinje cells, these have been shown by radiotracing studies to express glutamate uptake (Garthwaite & Garthwaite, 1985)), but also at low levels in the rest of the brain, testis and kidney (the last two sites of expression were found by Tanaka (1993) who cloned a carrier that only differs from GLAST by one amino acid (valine 302 is leucine 302 in GLAST)). All three clones are of similar size: GLT1 codes for a protein comprising 573 amino acids and has a molecular weight of approximately 64kDa; EAAC1 encodes a 524 amino acid protein which predicts a molecular weight of 57kDa, and GLAST codes for a 543 amino acid protein with a predicted molecular weight of 60kDa. Alignment of

Table 1.1: Characteristics of the glutamate uptake carriers cloned to date. The table shows the molecular characteristics, functional properties and tissue distribution of the cloned glutamate uptake carriers. n/d = non determined; THDA = threo-3-hydroxy-DL-aspartate; PDC = L-*trans*-pyrrolidine-2,4-dicarboxylate; PKC = protein kinase C; PKA = cAMP-dependent protein kinase; SITS = 4-acetamido-4'-isothiocyano-2,2'-disulphonic acid; *: personal communication

	GLAST	GLT-1	EAAC1	Glu-1
Reference	Storck <u>et al, 1992</u>	Pines <u>et al, 1992</u>	Kanai & Hediger, 1992	Tanaka, 1993
No. of amino acids	543	573	524	543
Number of predicted transmembrane domains	6	8	10	6-8
Molecular weight	60kD (predicted) 66kD (purified prot.)	64kD (predicted) 73kD (isolated prot.)	57kD (predicted)	
Putative glycosylation sites	2	2	n/d	2
Putative phosphorylation sites	PKC: 3 PKA: 2	PKC: 3 PKA: 1	n/d	n/d
K _m for Glutamate	77μM	2-10μM	12μM	62μM
Na ⁺	Yes	Yes	Yes	Yes
K ⁺	n/d	Yes	Yes	n/d
OH ⁻ /H ⁺	n/d	n/d	Yes*	n/d
Cl ⁻	n/d	No	No	Yes
Electrogenicity	n/d	n/d	Yes	n/d
Inhibitors	THDA	THDA PDC dihydrokainate (weak) L-amino-adipate (weak)	THDA (IC ₅₀ =7μM) L-amino-adipate (IC ₅₀ =165μM) dihydrokainate (weak)	L-cystein- sulfinat & β-glutamate (at high concentrations) SITS
Present in	brain (mainly cerebellum)	brain	brain small intestine kidney (liver, heart)	forebrain cerebellum testis kidney
Type of brain cell	Glial cells	Glial cells	Neurones	Glial cells
Absent from	peripheral tissues	spleen, liver heart, lungs kidney		liver

the sequences of these carriers (shown in Fig 1.3), done using the computer program UWGCG, reveals a striking sequence similarity. However, the three groups who cloned them predicted different numbers of transmembrane regions for the carriers: 6 for GLAST, 8 for GLT1 and 10 for EAAC1. The three groups agreed only on the position of the six first putative transmembrane regions. As seen on the hydrophobicity plots of Fig 1.4, the last 2-4 putative membrane spanning segments are either less hydrophobic or shorter, so their identification as transmembrane regions is less definite. According to the position of predicted cytoplasmic and external domains, GLT1 presents two putative extracellular glycosylation sites, three putative intracellular sites for phosphorylation by protein kinase C (PKC) and one for phosphorylation by the cAMP-dependent protein kinase (PKA), while GLAST has two putative glycosylation sites, three putative phosphorylation sites for PKC and two for PKA. The arrangement of the transmembrane domains predicted by Kanai and Hediger for the EAAC1 transporter eliminates a putative PKA phosphorylation site located in the most highly conserved stretch of the protein (Thr-355), by placing it on the extracellular side of the membrane. As no cleavable signal sequence was found, the N-terminus of the protein was assumed to be located in the cytoplasm.

The characteristics of these three clones were very similar when expressed in different expression systems (*Xenopus* oocytes or HeLa cells). Their uptake of glutamate was found to be strictly dependent on the presence of sodium ions in the extracellular medium, and was activated by intracellular potassium for GLT1 and inhibited by extracellular K^+ for EAAC1. EAAC1 was also shown to take up glutamate in an electrogenic fashion. Other amino acids or monoamines (alanine, leucine, glutamine, arginine, methionine, lysine, taurine, proline, cystine, β -alanine, GABA, dopamine, noradrenaline and serotonin) as well as L-malate were tested for their putative transport on the cloned glutamate uptake carriers. The results of these experiments were always negative. The three cloned glutamate transporters were inhibited by the presence of DL-threo-3-hydroxyaspartate (THDA), a commonly used glutamate transport blocker. Kanai and Hediger showed that this inhibition was due to competition with glutamate and that THDA was transported on the carrier in place of glutamate. Two of the

transporters (GLT1 and EAAC1) were also shown to be partially inhibited by dihydrokainate but with much less efficacy. The affinity of the three proteins for glutamate varied slightly but GLT1 ($K_m=2-10\mu\text{M}$), EAAC1 ($K_m=12\mu\text{M}$) and GLAST ($K_m=77\mu\text{M}$) could all be classified as high affinity glutamate uptake carriers. None of the three clones showed any significant sequence similarity with any other known eukaryotic proteins (including the Na^+ /glucose transporter (Hediger *et al*, 1987) or with the superfamily of neurotransmitter transporters which carry GABA, noradrenaline, dopamine, serotonin, glycine, proline, choline and betaine). However, sequence similarities of about 30% were found with *gltP*, the proton-coupled glutamate transporter from *Escherichia coli* (Tolner *et al*, 1992), the sodium-proton-glutamate transporter *gltT* of *Bacillus stearothermophilus* (de Vrij *et al*, 1989) and with the dicarboxylate transporters *DctA* of *Rhizobium meliloti* (Engelke *et al*, 1989) (especially a stretch AAIFIAQ (residues 408-413) proposed as being the glutamate binding site for GLT1 (Pines *et al*, 1992); this peptide is located within the seventh putative transmembrane region of GLT1, on the cytoplasmic side of the membrane). Fig 1.5 shows the alignment (sequences aligned by using the computer program UWGCG) of the consensus sequence of the three cloned glutamate transporters and of the sequence of GLT1 with the sequence of *gltP*, the proton-coupled glutamate transporter from *Escherichia coli*. The putative sodium binding site proposed by Deguchi *et al* (1990) based on the alignment of four Na^+ -coupled transporters (E.coli glutamate and proline transporters, rabbit Na^+ /glucose co-transporter and human Na^+ /glucose co-transporter) does not occur in any of the cloned glutamate transporters.

1.6.6 Vesicular glutamate transporter

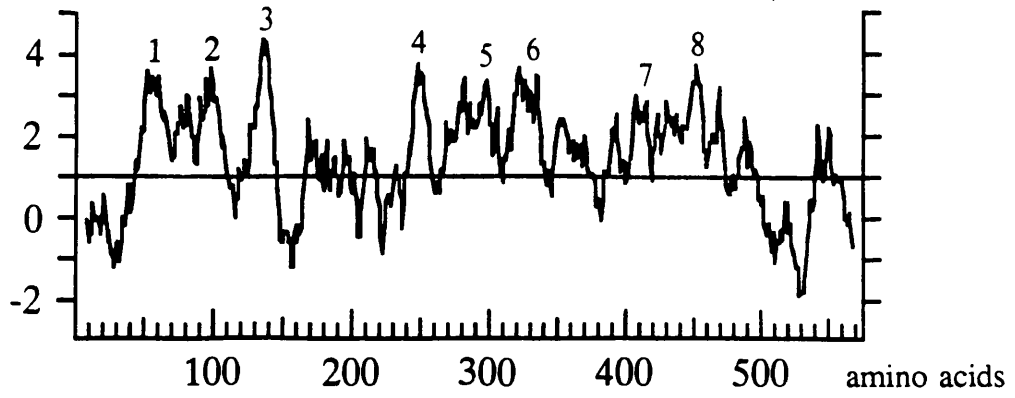
It is now widely accepted that neurotransmitters are released, following entry of calcium into the cell, by fusion of synaptic vesicles with the presynaptic membrane (reviewed by Jessel & Kandel, 1993). These vesicles are capable of accumulating neurotransmitters in a specific manner against their concentration gradient. Using cerebellar mutant mice, Fischer-Bovenkerk *et al* (1988) have shown that the ATP-dependent vesicular glutamate uptake system is located in

Fig 1.3: Comparison of the sequences of the three glutamate uptake carriers cloned to date. Alignment was done using the computer program UWGCG. Sequences in blue indicate intracellular domains, whereas green are transmembrane segments and red are the extracellular domains: this secondary structure is as predicted by the various authors (see introduction, section 1.6.5). The sequence in black is the consensus sequence for the three carriers indicating the strict conservation of the amino acids and conservative substitutions (indicated by x). Putative glycosylated sites for GLT-1 are indicated above the sequences by ψ , putative sites for phosphorylation by PKC are indicated (for GLT-1) by \circ and for phosphorylation by PKA by ∇ . Charges conserved across all the sequences are shown above the sequences.

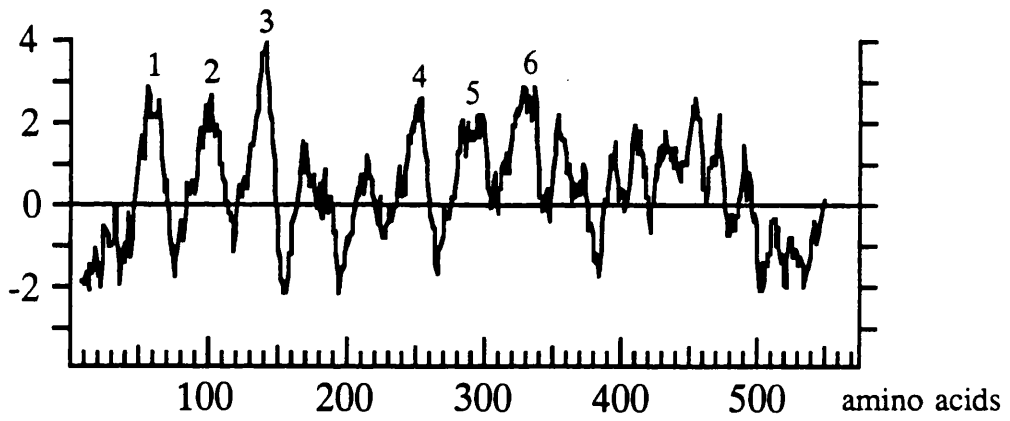
MASTEGANNMPKQVEVRMHDSHLSSEEPKHRNLGMRMCDKLGKNLLLSL	GLT1
MGKPARKGCDKRFLKNNWLLLS	EAAC1
MTKSNGEPRMGSRMERFQQGVRKRTLLAKKKVQNITKEDVKSYLFRNAFVLL	GLAST
L N xx	consensus
+ - +	
TVFGVILGAVCGLLRLAAPIHDPDVVMLIAFPGDILMRMLKMLILPLIISSLI	GLT1
TVVAVVLGIVIGVLVREYSNLSTLDKIFYFAFPGEILMRMLKLVILPLIVSSMI	EAAC1
TVSAVIVGTILGFALRPY.KMSYREVKYFSFPGELLMRMLQMLVLPPLIISSLV	GLAST
TV VxxG x G xxR x FPGxxLMRML xxLPLIxSS x	consensus
- ⊕ + +	
TGLSGLDAKASGRLGTRAMVYYMSTTIIAAVLGVILVLAIHGPNPKLKKQLGP	GLT1
TGVAALDSNVSGKIGLRAVLYYFCTTIIAVILGIVLVVSIKPGVTQKVDEIDR	EAAC1
TGMAALDSKASGKMGMRVYYMSTTIIAVVIGIIIVIIIHPGKGTK.ENMYR	GLAST
TG LD xSGx G RA xYY TTIIAxxxGxxxVx I PG	consensus
- - +	
GKKNDEVSSLD AFLDLIRNLFPENLVQACFQQIQTVTKKVLVAPPSEEANTTK	GLT1
TGSTPEVSTVDAMLDLIRNMFPENLVQACFQQYKTTREEVTASDDTGKNGTEE	EAAC1
EKGIVQVTAADAFDLIRNMFPPNLVEACFKQFKTSYEKRSFKVPIQANETLL	GLAST
Vx xDA LDLIRN FP NLV ACF Q T x T	consensus
ψ - -	
AVISLLNETMNEAPEETKIVIKKGLEFKDGMNVLGLIGFFIAFGIAMGKMGEQ	GLT1
SVTAVMTTAVSENRTKEY...RVVGLYSDGINVLGLIVFCLVFGLVIGKMGEK	EAAC1
GAVINNVSEAMETLTRIREEMVPPVPGSVNGVNALGLVVFMSCFGVIGNMKEQ	GLAST
x E G NxLGLx F FGxx G M E	consensus
- - + + -	
AKLMVEFFNILNEIVMKLVIMIMWYSPLGIACLICGKIIAIKDLEVVARQLGM	GLT1
GQILVDFFNALS DATMKIVQIIMCYMPLGILFLIAGKII EVEDWEIF.RKLGL	EAAC1
GQALREFFDSLNEAIMRLVAVIMWYAPLGILFLIAGKILEMEDMGVIGGQLAM	GLAST
x xFF L xx MxxV IM Y PLGix LI GKix D xx L	consensus
⊕++	
YMITVIVGLIIHGGIFLPLIYFVVTRKNPFSFFAGIFQAWITALGTASSAGTL	GLT1
YMTVIVLSGLAIHSIVILPLIYFIVVRKNPFRFAMGMTQALLTALMISSSSATL	EAAC1
YTVTVIVGLLIHAVIVLPLLYFLVTRKNPWFVIGLLQALITALGTSSSSATL	GLAST
Y xTVx GLxIH xxLPLxYFxxV RKNP Fx G QA xTAL SS TL	consensus
⊕ + -- -++ ▼+	
PVTFRCLEDNLGIDKRVTRFVLPVGATINMDGTALYEAVAAIFIAQMNGVILD	GLT1
PVTFRCAEEKNRVDKRI TRFVLPVGATINMDGTALYEAVAAVFIAQLNDMDLS	EAAC1
PITFKCLEENNGVDKRI TRFVLPVGATINMDGTALYEALAAIFIAQVNNFDLN	GLAST
PxTFxCxEx xDKRxTRFVLPVGATINMDGTALYEAXAXFIAQ N L	consensus
-- -	
GGQIVTVSLTATLASIGAASIPSAGLV TMLLILTAVGLPTEDISLLVAVDWLL	GLT1
IGQIITISVTATAASIGAAGVPQAGLV TMVIVLSAVGLPAEDVTLIIAVDWLL	EAAC1
FGQIITISITATAASIGAAGIPQAGLV TMVIVLTSVGLPTDDITLIIAVDWFL	GLAST
GQIxTxSxTATxASIGAA xP AGLV TMxxxLx VGLP xDxxLxxAVDWxL	consensus
-+ + - + - -	
DRMRTSVNVVGD SFGAGIVYHLSKSELDTIDSQHRMHEDIEMTKTQSVYDDTK	GLT1
DRFRTVVNLGDAFGTGIVEKLSKKELEQMDVSSEVNIVNPFALASATLDNED	EAAC1
DRLRRTTNVLGDSL GAGIVEHLSRHELKNRDVEMGNSVIEENEMKKPYQLIAQ	GLAST
DR RT NVxGD xG GIV LSx EL D	consensus
NHRESNSNQCVYAAHNSVVIDECKVTLAANGKSADCSVEEEPWKREK	GLT1
SDTKKSYINGGFAVDKSDTISFTQTSQF	EAAC1
DNEPEKPVADSETKM	GLAST
	consensus

Fig 1.4: Hydropathy plots of the three cloned glutamate uptake carriers. Ordinate = hydropathy index; abscissa = position of amino acids in protein. The analysis was done according to the Kyte-Doolittle method with a window of 11 amino acids. The three first peaks of the plots are aligned to emphasize the similarities. Numbers above the plot indicate the transmembrane domains postulated by the different authors.

GLT1



GLAST



EAAC1

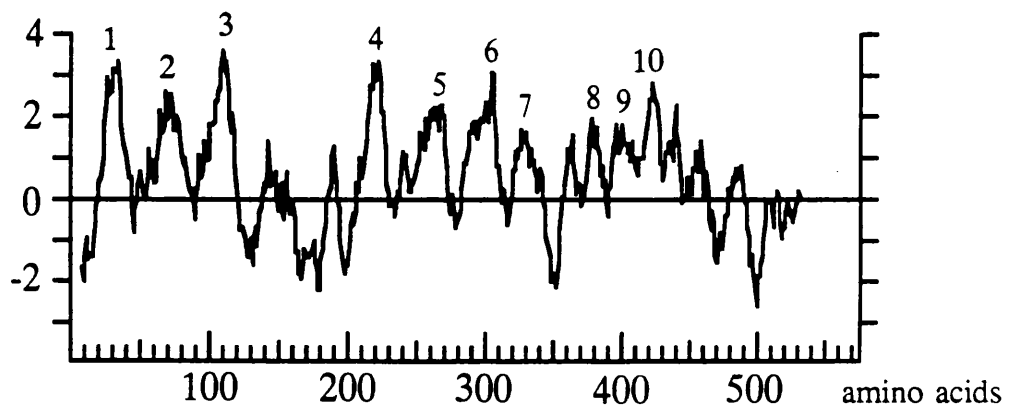


Fig 1.5: Alignment of the sequence of the glutamate uptake carrier GLT-1 with that of the glutamate proton transporter *gltP* from *E. coli*. The first consensus sequence is that of GLT-1 and *gltP* and the second consensus sequence is that of the three cloned glutamate uptake carriers (see Fig 1.3).

granule cells (glutamatergic neurones) but not Purkinje cells (which are GABAergic neurones). The properties of the vesicular uptake of neurotransmitters differ greatly from those observed for the plasma membrane transporter. The affinity of the vesicular carrier for glutamate is relatively low ($K_m = 1.6\text{mM}$; Naito & Ueda, 1985) and it is highly specific for glutamate; even at high concentration, L-aspartate is not transported on the carrier (Naito & Ueda, 1985). The vesicular transporter functions independently of external sodium (Naito & Ueda, 1985) and co-purifies with specific synaptic vesicles markers such as synaptophysin during vesicle isolation (Hell *et al*, 1988) indicating its specific localisation in synaptic vesicles. It is energized by the transport of protons into the vesicle via a Mg^{2+} -ATPase. Consequently, glutamate transport is dependent on ATP and Mg^{2+} , and is inhibited by proton ionophores. Proton accumulation inside the vesicle leads to an increase in the potential difference across the vesicle membrane which in turn drives the transport of glutamate into the vesicle (Maycox *et al*, 1988). In addition, in the absence of chloride ions, vesicular uptake of glutamate is largely reduced (Naito & Ueda, 1985). It is therefore possible that chloride ions are involved in some way in the vesicular transport of glutamate. Burger *et al* (1989) have shown, using a fast isolation method maintaining the proton gradient, that glutamate was concentrated ten-fold in the vesicles. Several agents have been tested for a putative inhibitory action on the uptake of glutamate into synaptic vesicles. Kainate and L-homocysteate were found to be non-competitive inhibitors with apparent K_i values of 1.5 and 4 mM respectively. Taurine, serine, glycine and GABA did not inhibit the uptake of glutamate into synaptic vesicles (Fykse *et al*, 1992).

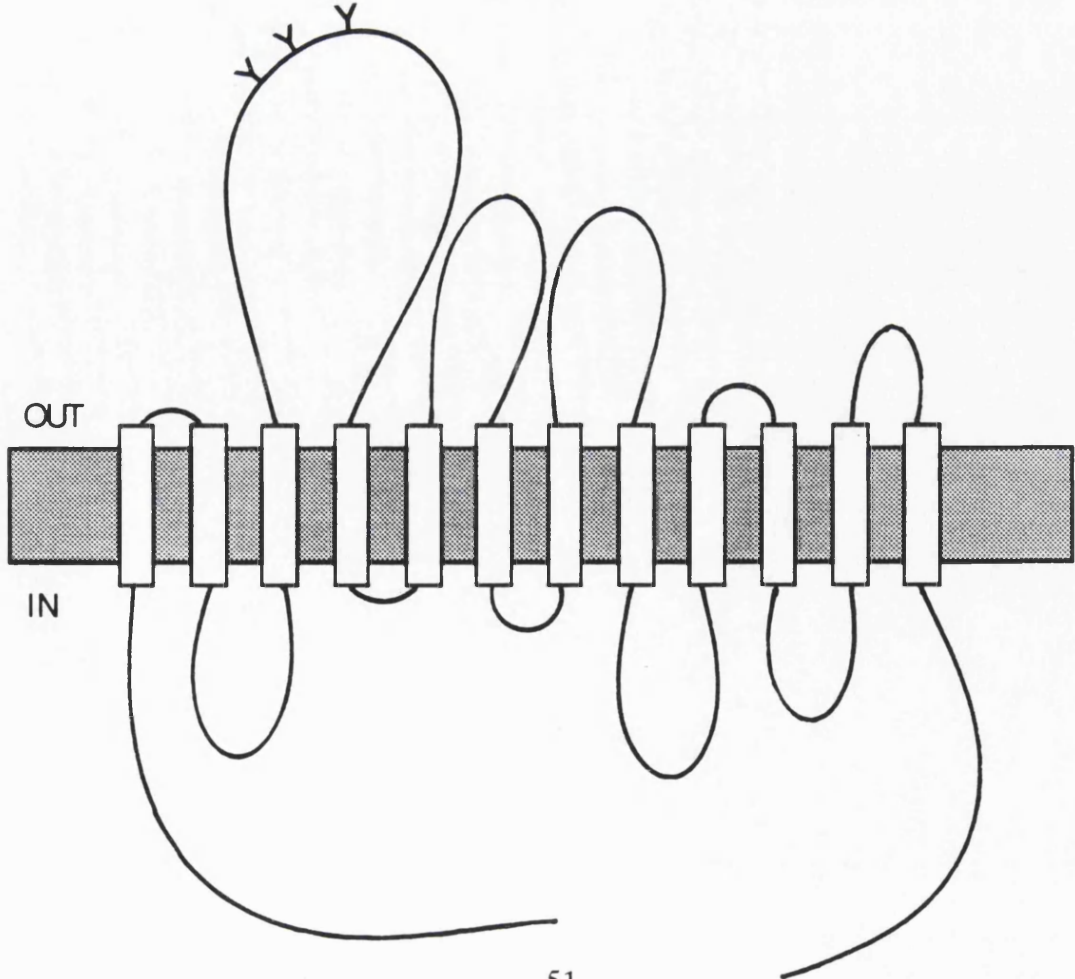
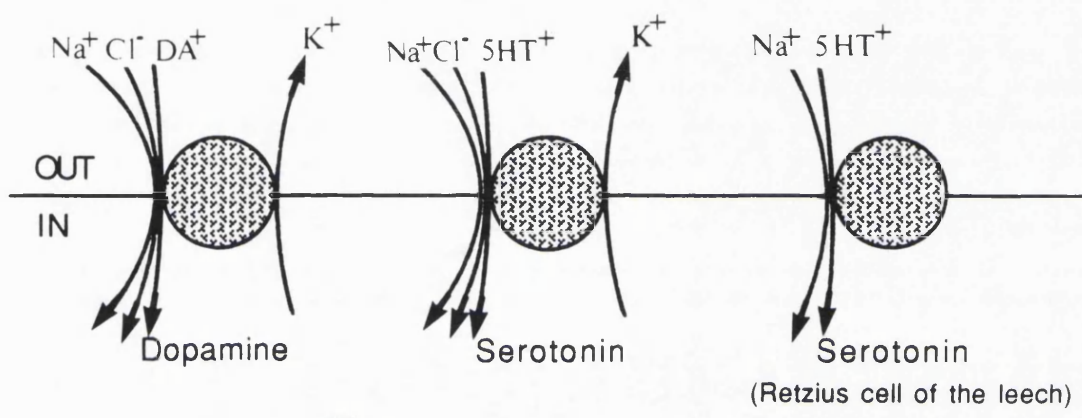
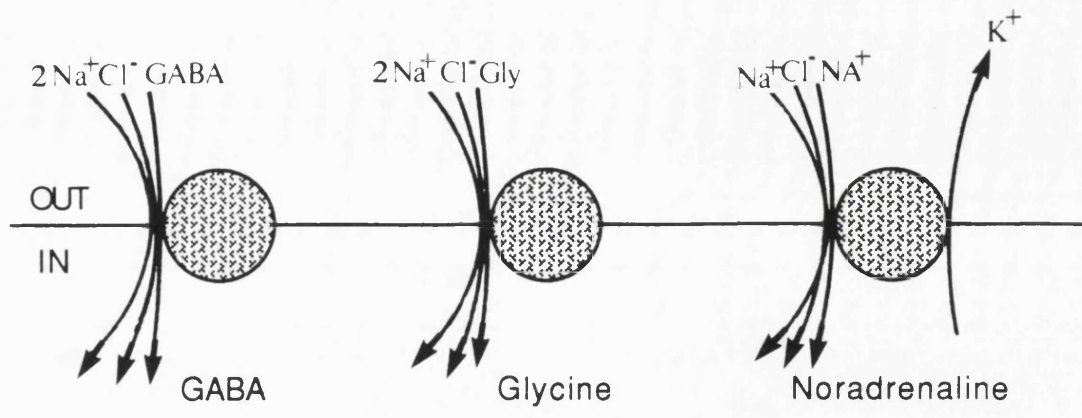
1.7 Other neurotransmitter and amino-acid transporters

Carriers for GABA, glycine, noradrenaline, dopamine and serotonin belong to the growing super-family of amino acid and neurotransmitter transporters that also include transporters for taurine, proline, choline and betaine (for review, see Amara & Arriza, 1993). This family is different from that of the glutamate uptake carriers. However, these two families share several

similarities. These include the strict dependence of the transport on external sodium (Fig 1.6A): all carriers of this large family transport one or several sodium ions into the cell on each cycle of the carrier (Kanner, 1978; Meyer & Cooper, 1982; Keynan *et al*, 1992; Mayor *et al*, 1981; Aragón & Giménez, 1986; Harder & Bonish, 1985; Kuhar & Zarbin, 1978; Rudnick, 1977). The movement of sodium ions into the cell seems to be the major source of energy for accumulation of substrate into the cell against its concentration gradient. Some of the carriers have also been shown to counter-transport one potassium ion on each carrier cycle. These include transporters for noradrenaline, dopamine and serotonin. Interestingly, in the absence of internal potassium, the transport of serotonin can still occur, but with H⁺ being transported out on the carrier in place of potassium (Keyes & Rudnick, 1979). A common feature of the carriers in the GABA carrier family is their dependence on external chloride (Fig 1.6A). A dependence on external (or internal) chloride ions is not found for glutamate transport (Barbour *et al*, 1991).

Recent cloning of several neurotransmitter transporters has revealed the existence of very high sequence and structure similarities between transporters in the GABA carrier family (for review, see Amara & Arriza, 1993). They belong to a large gene family (from which the glutamate uptake carrier is excluded, as described above), and all possess 12 putative transmembrane domains, with both their N- and C-termini on the cytoplasmic side of the cell (Fig 1.6B). Their overall identity ranges from 45 to 65%, with no significant homology with the cloned glutamate transporters. *In situ* hybridizations for each of the cloned transporters of this family have shown that the pattern of expression of the carriers fits well with the localisation of the corresponding transmitter systems, apart from the glycine uptake carrier which is found in parts of the brain where no glycinergic neurones are present. It has been suggested (Smith *et al*, 1992a; Attwell & Bouvier, 1992) that glycine uptake could regulate to a certain extent, the potentiation of NMDA receptors by glycine (see below).

Fig 1.6: Top: Proposed stoichiometries for different neurotransmitter transporters of the GABA transporter family. Bottom: Proposed secondary structure of transporters from this family, bearing 12 putative transmembrane regions with N- and C-termini on the intracellular side of the plasma membrane.



1.8 Release of neurotransmitters

In this section, I review briefly how glutamate, which the glutamate uptake carrier will remove from the extracellular space, is released normally, and how reversed uptake can serve as a release mechanism for glutamate and other transmitters in certain conditions.

1.8.1 Ca²⁺-dependent release

At the synapse, neurotransmitter is stored in synaptic vesicles. The arrival of an action potential causes the opening of voltage-gated calcium channels, a rise of intracellular calcium concentration and the fusion of synaptic vesicles with the plasma membrane, releasing the neurotransmitter into the synaptic cleft. The voltage-gated calcium channels are clustered at the site of release of the neurotransmitter to provide a large local rise of [Ca²⁺] (for review, see Jessel & Kandel, 1993).

1.8.2 Ca²⁺-independent release

In certain conditions, the release of neurotransmitter is calcium-independent (Nicholls, 1989). This phenomenon seems to be due to reversed operation of uptake carriers which has been shown to happen both in physiological and pathological conditions (for review, see Adam-Vizi, 1992).

During anoxia or ischemia, neuronal death is thought to be partially due to a rise in [Glu]_o, generating an excessive entry of calcium ions through NMDA channels (Choi, 1987). Some authors have reported that during anoxia or ischemia, at least part of the glutamate is released in a Ca²⁺-independent manner (Ikeda *et al*, 1989). During these excitotoxic conditions, the ion gradients across the membrane are disrupted ([K⁺]_o rises to about 60mM) and the cells become depolarised (Siesjö, 1990). These changes have been shown to promote the release of glutamate by reversed action of the glutamate uptake carrier (Szatkowski *et al*, 1990).

Schwartz (1987) showed that horizontal cells whole-cell clamped with pipettes containing GABA, sodium and chloride could release GABA when depolarised. This release of GABA was blocked by the uptake blocker, nipecotic

acid. These results are consistent with the release of GABA happening by reversed operation of the GABA uptake carrier. Calcium-independent release of GABA has also been shown to exist in neurones and type-2 astrocytes in culture (Pin & Bockaert, 1989; Gallo *et al*, 1991). In these experiments the release of the neurotransmitter was also dependent on intracellular sodium and blocked in the presence of nipecotic acid. Activation of glutamate receptors present on astrocytes (Clark & Mobbs, 1992) can promote an increase of the sodium concentration inside the cell as well as a depolarization of the cell, and may thereby induce GABA release. This release of GABA by astrocytes could be a protective mechanism against excessive neuronal activity occurring when excessive glutamate release results in $[Glu]_o$ rising significantly in parts of the extracellular space outside the synaptic cleft.

Recently, cloning and localisation of the glycine uptake carrier showed it is expressed in the brain at the sites of glutamatergic synapses (like the hippocampus). This raises the possibility that activity of NMDA receptors is regulated by the glycine uptake carrier controlling the glycine concentration in the extracellular space (Smith *et al*, 1992a; Attwell & Bouvier, 1992). Glycine is a compulsory "co-factor" in the opening of NMDA receptors (see above). A glycine concentration of $3\mu M$ is enough to saturate the glycine site on the NMDA receptor. Given a stoichiometry of the glycine uptake process where one glycine zwitterion is transported into the cell together with two sodium ions and one chloride ion (Kanner & Schuldiner, 1987), the minimum extracellular glycine concentration the transporter is able to maintain is $196nM$ (Attwell & Bouvier, 1992), suggesting a possible regulation of NMDA receptors by glycine uptake. However, autoradiographic studies showed that the localisation of $[^3H]$ -glycine uptake did not correspond to that of NMDA receptors (apart from in the molecular layer of the dentate gyrus) (Fedele & Foster, 1992). Thus, this possible regulation of NMDA receptors by changes in the equilibrium of the glycine uptake carrier still lacks experimental evidence although it is possible to evoke the release of glycine when applying kainate or quisqualate to astrocytes (Levi & Patrizio, 1992), and NMDA receptor responses can be potentiated in slices by the addition of exogenous glycine (Thomson *et al*, 1989).

1.9 Changes of pH during brain stimulation

Recent studies indicate that, during neuronal activity, extracellular and intracellular pH changes occur. In different situations these have been shown to occur in either direction (going more alkaline or more acid) and to be large enough to influence excitatory neurotransmission (Tang *et al*, 1990; Traynelis & Cull-Candy, 1990; Vyklický *et al*, 1990).

1.9.1 Intracellular pH changes

Several activity-dependent intracellular pH changes have been characterised by using either pH-sensitive fluorescent dyes or intracellular pH electrodes. When depolarised by an increase of extracellular potassium concentration, astrocytes from rat cortex have been shown to undergo a large intracellular alkalinization (Chesler & Kraig, 1987; 1989). In glial cells of the leech, these pH changes have been attributed to the activity of the $\text{Na}^+/\text{HCO}_3^-$ co-transporter. The stoichiometry of this transporter varies according to the type of cell: it is thought to transport one Na^+ ion and two HCO_3^- ions in the leech glial cells (Deitmer & Szatkowski, 1990), whereas the transporter expressed by Müller cells of the salamander retina has been shown to transport one sodium ion together with three bicarbonate ions (Newman & Astion, 1991). In neurones, activity-induced acid shifts of pH_i have been reported (for review, see Chesler & Kaila, 1992) and attributed to a net entry of protons through ligand- or voltage-gated channels (Endres *et al*, 1986; Kaila *et al*, 1990) or metabolic CO_2 production (Siesjö, 1985).

1.9.2 Extracellular pH changes

Both extracellular alkaline and acid shifts have been reported. For example, during repetitive stimulation, extracellular acid shifts (Chesler & Kraig, 1987; Davis *et al*, 1987; Sykova & Svoboda, 1990) were recorded from different regions of the brain (preceded by alkaline shifts in certain areas (Kraig *et al*, 1983; Urbanics *et al*, 1978; Mutch & Hansen, 1984; Somjen, 1984)). In the retina of vertebrates and invertebrates, an alkalinization of the extracellular medium during light stimulation has been reported (Coles *et al*, 1988; Borgula *et al*, 1989;

Yamamoto *et al*, 1992). Extracellular alkaline shifts have very often been attributed to H^+ , OH^- , HCO_3^- or NH_4^+ crossing the plasma membrane through ion channels. Indeed, if the intracellular pH of a cell is 7.0 and the extracellular medium has a pH of about 7.3 (values close to the physiological values in the case of mammals), the Nernst potential for H^+ is around -20mV, so there is an electrochemical gradient for H^+ entry (or OH^- and HCO_3^- exit). Experiments on crayfish muscle have shown that $GABA_A$ channels are permeable to bicarbonate ions (Kaila & Voipio, 1987; Kaila *et al*, 1990). Excitatory amino acid transmission has also been found to elicit an extracellular alkalization (Chesler & Chan, 1988; Kraig *et al*, 1983; Rice & Nicholson, 1988). This pH change has been found to be independent of the presence of bicarbonate ions and insensitive to picrotoxin (a blocker of $GABA_A$ channels). The alkaline shift could be induced by stimulation of glutamatergic afferent fibres or by bath application of glutamate or aspartate (Chesler & Rice, 1991; Chen & Chesler, 1992a). These alkaline shifts were insensitive to Mg^{2+} and to Cd^{2+} suggesting that they were not directly related to the opening of voltage-gated Ca^{2+} channels. These pH changes were attributed to proton equivalents going through NMDA or AMPA receptors since the alkalizations were found to be blocked either by CNQX (6-cyano-7-nitroquinoxaline-2,3-dione; a blocker of AMPA/kainate receptors) or D-AP5 (a blocker of NMDA receptors) (Chen & Chesler, 1992b). Alkaline shifts elicited by the application of glutamate were found to be insensitive to picrotoxin (Chen & Chesler, 1992b).

In this thesis (chapter 4), I will show that the glutamate uptake carrier also generates extracellular and intracellular pH changes.

1.10 pH-regulating mechanisms

The pH of the intracellular medium must be maintained within very strict limits for cells to grow and divide. A cell possesses several mechanisms for regulating its intracellular pH. A Na^+/H^+ antiporter is responsible for removing the excess protons generated by the cell's metabolism. Efflux of protons is coupled to the influx of sodium ions in a 1:1 stoichiometry. This antiporter is regulated by the intracellular pH: it is inhibited at more alkaline pH and its

activity increases as the pH falls.

A $\text{Cl}^-/\text{HCO}_3^-$ exchanger is also very important in regulating intracellular pH. HCO_3^- is transported out of the cell in exchange for Cl^- . The activity of this transporter is increased when the intracellular pH of the cell becomes too alkaline. The transport of bicarbonate out of the cell induces the formation of more bicarbonate from OH^- and CO_2 . This formation of HCO_3^- is catalysed by the enzyme carbonic anhydrase which has been shown to be localised in glial cells in the brain (Langley *et al*, 1980). In the proximal tubule of the kidney, a Na^+ -dependent HCO_3^- transporter has also been described (Boron & Boulpaep, 1983). It was later shown to exist in glial cells (Astion & Orkand, 1988; Deitmer & Schlue, 1989) and several other cell types. In the salamander Müller cells used in this study, this transporter is thought to carry one sodium ion into the cell and co-transport three bicarbonate ions (Newman & Astion, 1991) or more likely one Na^+ , one HCO_3^- and one CO_3^{2-} (Aronson, 1989).

1.11 Role of glial cells

1.11.1 K^+ buffering

The membrane potential of glial cells is greater than that of neurones: usually around -90mV. This resting potential is mainly determined by K^+ ions. The extracellular concentration of potassium in resting conditions ranges between 2 and 4mM (Lux & Neher, 1973; Moody *et al*, 1974). This concentration increases during neuronal activity and is returned to resting levels by the action of Na^+/K^+ ATP-ases (Frank *et al*, 1983), activation of K^+/Cl^- co-transporters (Winter-Wolpaw & Martin, 1984), diffusion in the extracellular space or entry to glial cells through K^+ channels (Barres, 1991). The distribution of potassium channels has been thoroughly studied in Müller cells of the salamander retina (Newman, 1984; Brew *et al*, 1986). The main potassium conductance of these cells is located at the endfoot membrane (facing the vitreous in the whole retina). This observation supported the suggestion made by Orkand *et al* (1966) that glial cells could spatially buffer extracellular potassium by taking it up in areas of high concentration and excreting it in areas of low $[\text{K}^+]_o$ (the vitreous humour in the case of Müller cells).

1.11.2 pH regulation

The importance of pH homeostasis in the brain has very often been emphasised. Neuronal and glial activity lead to intracellular and extracellular pH changes (see above). Glial cells have been shown to express several pH-regulating transporters including the Na^+/H^+ exchanger, the $\text{Cl}^-/\text{HCO}_3^-$ exchanger (Kimmelberg, 1981) and the $\text{Na}^+/\text{HCO}_3^-$ co-transporter (Astion & Orkand, 1988). These transporters could be involved in the regulation of interstitial pH. Blocking $\text{Na}^+/\text{HCO}_3^-$ co-transport has been shown to affect the buffering power of the extracellular medium (Deitmer, 1992). Glial cells have also been found to possess most of the carbonic anhydrase present in the brain (Giacobini, 1962) suggesting that glial cells could play an important role in the regulation of extracellular pH in the brain. Indeed, extracellular pH changes occurring in mammalian brain are increased in the presence of acetazolamide (a blocker of carbonic anhydrase) (Kraig *et al*, 1983; Carlini & Ransom, 1986; Sykova, 1989).

1.11.3 Re-uptake of neurotransmitters

Several neurotransmitters have their synaptic action terminated by uptake into glial cells surrounding the site of release. As discussed above, glutamate is one of the neurotransmitters taken up by glial cells. In fact, it has been shown that 90 to 100% of the glutamate applied to sensory ganglia, thalamus or cerebral cortex is taken up into glial cells (Schon & Kelly, 1974; McLennan, 1976). Once in glial cells, glutamate is converted into glutamine by the enzyme glutamine synthase (present in the brain exclusively in astrocytes). Glutamine is then probably released into the extracellular space where it can be taken up again by neurones (Berl *et al*, 1961; Van den Berg & Garfinkel, 1971) and serve as a substrate for further glutamate synthesis by neurones. Astrocytes have also been shown to express GABA uptake carriers. They also contain enzymes for metabolising GABA: GABA transaminase and glutamine synthase. GABA uptake was shown to play an important role in shortening the time course of inhibitory postsynaptic potentials mediated by GABA receptors, and to reduce the activation of GABA_B receptors which inhibit excitatory transmission by action on presynaptic receptors located on excitatory afferent terminals (Thompson &

Gähwiler, 1992; Isaacson *et al*, 1993).

1.11.4 Glutamine synthesis and transport

Glutamine synthase, the enzyme catalysing the synthesis of glutamine from glutamate and ammonium is primarily localised in glial cells (Norenberg & Martinez-Hernandez, 1979). Recent studies have shown that glutamine is more potent than glutamate in stimulating the synthesis of GABA by synaptosomes (Battaglioli & Martin, 1990). Moreover, blocking glutamine synthase provokes an inhibition of the release of GABA and glutamate from the rat striatum (Rothstein & Tabakoff, 1984; Paulsen & Fonnum, 1989) probably by affecting the production of GABA and glutamate from glutamine (Battaglioli & Martin, 1991). These data suggest that glutamate is taken up by glial cells and converted into glutamine which is then transported out of glial cells and taken up by neurones where it serves as a substrate for synthesis of glutamate (in glutamatergic neurones) and GABA (in GABAergic neurones). It was also shown that glutamine production from glutamate was stimulated by the presence of ammonium inside the cells (Waniewski, 1992). This observation is easily explained since glutamine is produced from both glutamate and ammonium.

The mechanism by which glutamine is exported out of glial cells is still unclear. In the cerebrovascular endothelium, glutamine is thought to be transported out into the blood in exchange for neutral amino acids such as histidine, leucine, phenylalanine and tryptophan (James *et al*, 1979; Cangiano *et al*, 1983). Astrocytes also express transporters for neutral amino acids (Speciale *et al*, 1989). Brookes (1992c) has shown that in astrocytes from mouse brain in culture, the efflux of glutamine enhanced the uptake of neutral amino acids such as histidine, leucine, phenylalanine and tryptophan. Moreover, the presence of neutral amino acids in the extracellular medium strengthened the efflux of glutamine from astrocytes. This transport happened in sodium-free solutions but was markedly increased in the presence of sodium ions (Speciale *et al*, 1989; Brookes, 1992a).

1.12 Experiments performed for this thesis

In this thesis, four related studies of the properties of the glutamate uptake carrier in salamander Müller cells were carried out. Using whole-cell recording, the uptake of sulphur-containing analogues of glutamate and aspartate (cysteic acid, cysteine sulphinic acid, homocysteic acid, homocysteine sulphinic acid, S-sulfo-L-cysteine) was studied in order to assess whether an efficient mechanism exists to terminate their possible synaptic action, and to assess whether their extracellular concentration could be kept below neurotoxic levels in the CNS. The analogues were found to be transported on the high affinity glutamate uptake carrier in an electrogenic manner with different affinities. These results are described in chapter 3.

Chapter 4 describes experiments performed to investigate whether pH-changing ions were transported on the glutamate uptake carrier. It is important to determine the stoichiometry of the glutamate uptake carrier since this determines the minimum extracellular glutamate concentration maintainable at equilibrium. For this purpose, both intracellular and extracellular pH measurements were performed. The results of the experiments showed that glutamate uptake was accompanied by an intracellular acidification and an extracellular alkalisation. These pH changes were not found to be due to secondary activation of pH-regulating mechanisms.

Distinguishing between the transport of a proton into the cell or a pH-changing anion (such as OH^- or HCO_3^-) out of the cell as the cause of the above-mentioned pH changes was the purpose of the experiments described in chapter 5. Anion-substitution experiments revealed the transport of a pH-changing anion out of the cell on each cycle of the carrier (OH^- or possibly HCO_3^-). The presence of physiological bicarbonate concentrations inside the cell increased the magnitude of the current generated by the uptake of glutamate. However, inhibiting HCO_3^- production did not abolish the pH changes accompanying glutamate uptake.

Chapter 6 deals with experiments testing the possible modulatory effects of various agents on the magnitude of the current evoked by the transport of glutamate.

Finally, in chapter 7, I discuss the implications of the results obtained, and make some suggestions for future work.

CHAPTER 2

Methods

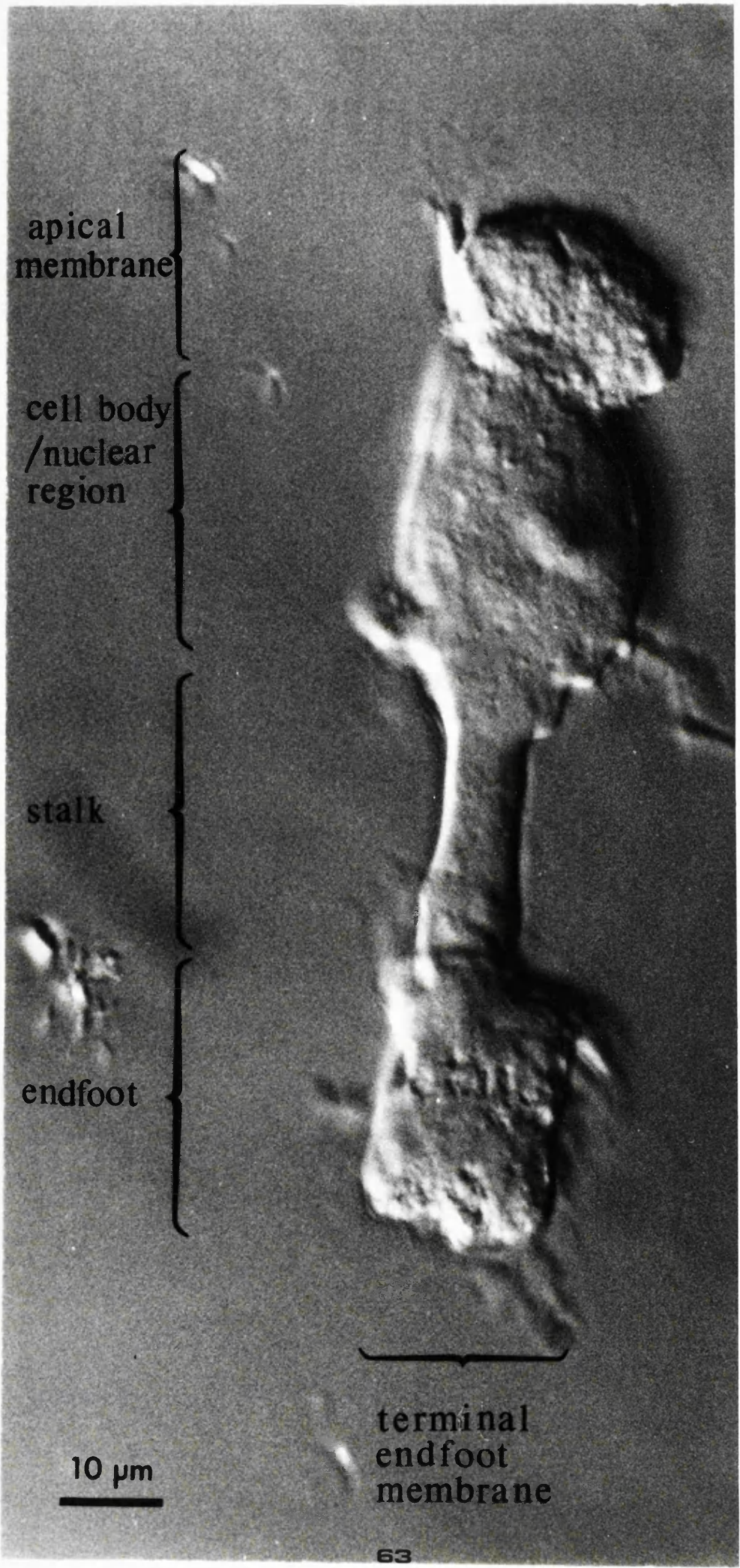
2.1 Cell preparation

Experiments were performed on Müller (glial) cells isolated from retinae of tiger salamanders (*Ambystoma tigrinum*). The animals (25-30 cm long) were decapitated, their brains crushed immediately, and their eyes removed. Excess tissue was trimmed from the eye balls under a dissecting microscope. Each eyeball was then separated in two halves by cutting the sclera slightly anterior to the ora serrata using first a blade and then ophthalmological scissors. The anterior half containing the cornea and the lens was discarded. The second half of the eyeball was then stored in a 30mm petri dish containing solution A (table 2.1) in the refrigerator (5°C) and used within 30 hours. The same process was repeated with the second eye.

To prepare cells, a quarter of a retina was cut from the eyecup. It was then transferred into 2ml of a solution containing (in mM): NaCl 66; KCl 3.7; NaHCO₃ 25; NaH₂PO₄ 10; Na pyruvate 1; DL-cysteine HCl (Sigma) 10 and 10-20 units of papain (Sigma P3125). The retina was then incubated at 34°C for 20 minutes.

After incubation, the retina was rinsed by dropping it four times through 4ml of solution A (table 2.1). The cells were then separated by drawing the retina in and out of a fire polished Pasteur pipette. The suspension of cells was then either plated onto the recording chamber, or, if one of the chemicals used during the experiment was suspected of having an irreversible effect, the cells were plated onto 5-6 13mm diameter glass coverslips. One cell was studied from each coverslip (placed in turn in the recording chamber). The cells were left 10 minutes to settle on the bottom of the dish before being used for the experiment. Typically, cells from one dissociation were viable for 2-3 hours. Müller cells were easily identified from other cells by their morphology (see Fig 2.1). Experiments were performed at room temperature (20 to 30°C).

Fig 2.1 Müller cell from the salamander retina. Cells such as this one were obtained after papain treatment and trituration. In the whole retina, the endfoot of the cell faces the vitreous humour whereas the apical membrane projects between the photoreceptors.



apical
membrane

cell body
/nuclear
region

stalk

endfoot

terminal
endfoot
membrane

10 μm

2.2 Solutions and superfusion

2.2.1 External solutions

In all experiments, the solutions were bath applied. Syringe barrels containing the different solutions were connected to the recording chamber through plastic tubing and a common inlet. The choice of the solution flowing into the chamber was made by opening or closing taps situated on the tubing connecting the syringe to the inlet. The solutions flowed by gravity feed and only one solution was allowed to flow at a time. In most experiments, the flow of solution was continuous throughout the experiment. For external pH experiments (see chapter 4) the solution flow was stopped during pH measurement, to avoid dispersion of the pH gradient. From the recording chamber, solutions were removed by a suction pump through a small tube. To improve the perfusion of the solutions around the cells, these were lifted from the bottom of the dish after going to whole-cell mode and were positioned near the solution inlet. This allowed the solution around the cell to be changed within 1-10 seconds. For experiments where cells were not whole-cell clamped, they were not lifted from the bottom of the dish but a movable inlet was located near the cell. Drugs were added to the external solutions as stated in the appropriate results section. When a vehicle like DMSO was used to dissolve drugs, this was also added to the control solution at the same concentration. When the concentration of the drug added to the external solution was high enough to increase the osmolarity of the bathing medium, choline-Cl was added to the other solutions to balance their osmolarity. The pH of all external solutions (apart from solutions E table 2.1 and H table 2.2) were titrated to 7.4 with NaOH or occasionally NMDG or KOH (as stated in the results sections). The various external solutions used are described in tables 2.1 to 2.2. The most commonly used external solution was solution B (table 2.1). External solutions used on whole-cell clamped cells contained 6mM barium. This divalent cation was added to the solutions to block the inward-rectifying potassium conductance of the cell (Newman, 1985; Brew & Attwell, 1987). Adding barium to the external solution does not affect the current produced by glutamate uptake (Barbour *et al*, 1991). For unclamped Müller cells, barium was not added to the solution: in this case, the large potassium

conductance of the cells (input resistance $\approx 10 \text{ M}\Omega$) will keep the membrane voltage very near the resting potential of the cell and the current evoked by the uptake of glutamate ($\approx 200 \text{ pA}$) will depolarize the cells by only a few millivolts (Mobbs *et al*, 1988).

Arachidonic acid was made up as a stock (5mM) in ethanol. When needed, the stock solution was thawed, sonicated for 5 minutes and the appropriate amount was pipetted into a measuring cylinder. The ethanol was then evaporated by blowing argon onto the arachidonic acid solution in the cylinder and the appropriate quantity of solution B (table 2.1) previously bubbled with argon was then added to the cylinder. Finally, after shaking vigorously, the solution was sonicated for 5 minutes. Argon was used during the preparation of the arachidonic acid solution to avoid contact with oxygen (which can oxidize the fatty acid).

2.2.2 Internal solutions

The solutions used to fill the patch pipette are described in tables 2.3 to 2.6. The standard internal solution was solution J (table 2.3). The pH of all these solutions was titrated to 7.0 using usually KOH and occasionally NMDG (see tables for details). The concentration of free calcium in the internal solutions was calculated using the equilibrium constants for calcium binding to EGTA given by Martell & Smith (1974), allowing for Mg^{2+} binding and pH-dependence of the constants. The values are indicated in the tables.

Solutions L and M have a reduced concentration of Hepes in order to reduce the buffering power of the internal solution and therefore to increase the internal pH changes produced by acid and base fluxes across the cell membrane. Solution N contained the fluorescent pH-sensitive dye BCECF, and also blockers of glutamate metabolism (see Fig 4.9 and section 4.9, chapter 4).

The recipe of internal solutions N-T (tables 2.4 and 2.5), used to test the effect of internal anion substitutions on the magnitude of the current evoked by glutamate, was very simplified compared to the normal internal solution used. This is because some of the substituted anions bind to Na^+ , Mg^{2+} and/or Ca^{2+} with a high affinity. If these cations were present inside the cell, they would

reduce significantly the concentration of free anion in the internal solution. I therefore decided not to include these cations in any of these internal solutions.

2.2.3 Concentration of free glutamate in the superfusion solution

In solution, glutamate and aspartate bind to divalent cations to form soluble complexes. The concentration of glutamate or aspartate available to the glutamate uptake carrier is therefore reduced according to the concentration of the divalent cations present in the external solution. The equilibrium constants (K) for the binding to Mg^{2+} , Ca^{2+} and Ba^{2+} are $79.43M^{-1}$, $26.91M^{-1}$ and $19.05M^{-1}$ respectively with glutamate and $269.15M^{-1}$, $39.81M^{-1}$ and $13.80 M^{-1}$ respectively with aspartate (Martell & Smith, 1974). The fraction of the amino-acid unbound is given approximately by (Barbour *et al*, 1991):

$$\frac{[\text{free amino-acid}]}{[\text{total amino-acid}]} = \frac{1}{(1 + K_{Mg}[Mg] + K_{Ca}[Ca] + K_{Ba}[Ba])}$$

For solutions where $[Ca^{2+}] = 3mM$, $[Mg^{2+}] = 0.5mM$ and $[Ba^{2+}] = 6mM$, the ratio of the free to the total amino-acid concentration is 81% for glutamate and 75% for aspartate. Solutions without barium have 89% of the glutamate and 80% of the aspartate in the unbound form. None of the values quoted in this thesis were corrected for the binding of the amino-acids to divalent cations. The value quoted is always the nominal concentration of applied analogue. None of the conclusions reached in this thesis are critically dependent on the exact concentration of the analogue.

2.3 Recording from cells

2.3.1 Whole-cell patch-clamp recording

The whole-cell patch-clamp technique (Hamill *et al*, 1981) was used in most experiments to study the electrogenic uptake of glutamate, aspartate and their sulphur-containing analogues. Patch pipettes were pulled on a BBCH puller (Mecanex, Geneva) from borosilicate glass with filament (Clark Electromedical,

GC150TF10). The resistance of the pipettes before sealing onto a cell was typically 1-3M Ω when filled with solution J (table 2.3) and bathed in solution B (table 2.1).

The recording chamber, containing the cells, was placed on the fixed stage of a microscope (Ergaval, East Germany, or Microinstruments, Oxford). The headstage of the patch-clamp amplifier was mounted on a micromanipulator (Narishige), itself mounted on a coarse manipulator (Prior). The earth electrode was a silver / silver chloride pellet immersed in the bath solution (during experiments where the composition of the external solution was varied, a 4M NaCl agar bridge was used; see below). The pipette was inserted into a perspex electrode holder (Clark Electromedical) and was positioned against the membrane of the cell and a gentle suction was applied to form a seal between the glass and the cell. The holding voltage was then brought to -40mV and further suction was applied to break the patch of membrane under the tip of the electrode and go into the whole-cell configuration of the patch-clamp. The current flowing across the membrane of the cell was then measured as the voltage drop across a 500M Ω resistance of a current to voltage converter (L/M EPC-7; List Electronics, Germany).

2.3.1 Correction for liquid junction potentials

The internal solution (present in the pipette) and the external solution (from the bath) are of different composition. As a result, a junction potential forms at the tip of the patch pipette. This junction potential is abolished when, after going whole-cell, the internal medium of the cell is dialysed with the pipette solution. The zero current potential set while the pipette was away from the cell is therefore not the actual zero current potential during the course of the experiment. The magnitude of this junction potential was measured by the method of Fenwick *et al* (1982). A 4M NaCl agar bridge as the bath electrode was used to avoid variations in reference electrode potential when changing the composition of the bath solution. The zero current potential was first measured (with the patch-clamp amplifier in current-clamp mode) when a pipette filled with a solution X was bathed in solution X. This external solution X was then

replaced by the normal external solution used during the experiment. The change in zero current, i.e. the junction potential, was then read off the patch-clamp amplifier. The value for each internal solution is indicated in tables 2.3 to 2.6. If the tip potential measured was different to that of solution J (the standard internal solution for which the junction potential is -3mV), the magnitude of the evoked current with that internal solution was normalized using the equation:

$$I_{\text{norm}} = I_{\text{meas}} \times (-43)/(-40 + \text{junct. pot.})$$

where I_{norm} is the normalized value of the magnitude of the glutamate-evoked current, and I_{meas} is the amplitude of the glutamate-evoked current measured during the course of the experiment at an uncorrected voltage of -40mV.

This equation is only valid if used at negative holding potentials where the I-V relationship is a straight line (Barbour *et al*, 1991). Since the measured junction potentials are all small (magnitude < 10mV), this condition holds.

2.3.2 Voltage-clamp quality

The quality of the voltage clamp of Müller cells was assessed for a cell represented as a cable of radius $a=5\mu\text{m}$ and length $L=100\mu\text{m}$. The input resistance of Müller cells is about $10\text{M}\Omega$. This low input resistance is due to a large potassium conductance, 94% of which is located at the endfoot membrane of the cell (Newman, 1984). Assuming a total input resistance of $10\text{M}\Omega$, the resistance of the non-endfoot part of the Müller cell membrane is approximately $167\text{M}\Omega$ while the endfoot membrane resistance (R_{end}) is about $10.6\text{M}\Omega$ (Newman, 1984; Mobbs *et al*, 1988). The current flow across the non-endfoot part of the cell is negligible (because of the high resistance of this part of the cell membrane). The cell can therefore be considered as two resistors in series: the cytoplasmic resistance and the endfoot resistance (R_{end}). All the voltage-clamp experiments were performed in barium-containing solution to block the potassium conductance (Newman, 1985). In barium, Müller cells have an input resistance between 200 and $500\text{M}\Omega$. Thus, two possible experimental conditions are considered here.

Case 1: Potassium conductance unblocked

The cytoplasmic resistance of the cell is proportional to the length of cell considered and inversely proportional to its cross-sectional area (A). The cells were always whole-cell clamped with the electrode on the cell body (roughly the middle of the cell). The cytoplasmic resistivity (ρ) is assumed to be $2\Omega\text{m}$.

Between the electrode and the endfoot, the cytoplasmic resistance is:

$$\text{cytoplasmic resistance} = (\rho \cdot L/2)/A = 1.27 \text{ M}\Omega$$

The endfoot resistance of the cell considered is $10.6 \text{ M}\Omega$ (see above).

The voltage drop between the electrode and the endfoot end of the cell is then given by:

$$1.27 \text{ M}\Omega / (1.27\text{M}\Omega + 10.6\text{M}\Omega)$$

Thus, for a voltage step away from the resting potential, the voltage step at the end of the cell will be 10.7% less than that imposed at the voltage-clamping electrode. In fact, in my experiments, barium was used to block inward rectifier channels, so the voltage non-uniformity will be less than this.

Case 2: Potassium conductance blocked by barium

Here I will consider two possible sources of the cell conductance remaining in the presence of barium.

a- the residual conductance of the cell is due to incomplete block of the inward rectifier channels.

In the presence of barium, the input resistance of the cell is between 200 and $500\text{M}\Omega$. For a cell of input resistance of $200\text{M}\Omega$ with 94% of this conductance being at the endfoot, the voltage drop at the endfoot of the cell ($50\mu\text{m}$ away from the voltage-clamping electrode) calculated as above will be 0.6% less than at the voltage-clamping electrode. It is therefore a good approximation to say that the voltage clamp of the cells was uniform.

b- the residual conductance is uniformly spread over the cell membrane

If the cell is treated as a cable of length $L=100\mu\text{m}$ and radius $a=5\mu\text{m}$, it is possible to calculate the electrical space constant (λ) of the cell. λ is the distance from the patch pipette (where the voltage is applied) at which for an infinite cable, the cell voltage will have dropped to e^{-1} of its value at the pipette. The electrical space constant is given by:

$$\lambda = (a.R_m / 2.\rho)^{1/2}$$

where ρ is the specific cytoplasmic resistance of the cell (assumed to be $2\Omega\text{m}$) and R_m the specific membrane resistance (membrane resistance x membrane area).

The membrane area of the model cell considered is the sum of the areas at the two ends of the cell and along the main shaft of the cell, i.e. $2\pi a^2 + 2\pi aL = 3.30 \times 10^{-9} \text{ m}^2$.

Thus, $R_m = (2 \times 10^8 \Omega) \times (3.3 \times 10^{-9} \text{ m}^2) = 0.66 \Omega\text{m}^2$

and $\lambda = 908 \mu\text{m}$

The cells were always patch clamped at the cell body (roughly the middle of the cell). For an infinite cable, the voltage at a distance $50\mu\text{m}$ away from the voltage clamping electrode would be given by:

$$\text{fractional voltage drop} = V_x / V_o = e^{(-x/\lambda)}$$

where V_x is the voltage at a distance $x=50\mu\text{m}$ from the patch pipette where the voltage V_o is applied, i.e. $V_x / V_o = 0.95$. Thus the voltage at the endfoot is only 5% different to that applied at the electrode. This calculation assumes for simplicity that the voltage drop is exponential, which is not the case since the ends of the cell are sealed. Correcting for this would give even less voltage drop than calculated above.

2.3.3 Series resistance error

If the current flowing through the resistance of the patch pipette is large, then the voltage drop across the series resistance of the tip of the pipette will not

be negligible and the actual voltage across the cell membrane is significantly different from the command voltage. This problem can be reduced by keeping the series resistance low, or by studying smaller cells with smaller currents. Two cases (from this thesis) will be considered.

Case 1: typical size current and typical R_s

$R_s = 2M\Omega$ (series resistance measured when in whole cell mode)

$I = 200pA$ (glutamate uptake current)

Voltage drop: $V = R.I = 2.10^6 \times 200.10^{-12} = 0.4mV$

A typical value of voltage error due to current flowing through the series resistance is only 0.4mV.

Case 2: worst case; cell containing ClO_4^-

In this case, the size of the current evoked by glutamate was greatly increased and a large inward current (independent of the glutamate evoked current) developed as soon as the patch membrane was ruptured.

$R_s = 2M\Omega$ (series resistance)

$I = 600pA$ (glutamate uptake current) + $1nA$ ("leak current")
 $= 1.6nA$

Voltage drop: $V = R.I = 2.10^6 \times 1.6.10^{-9} = 3.2mV$

This worst-case voltage drop is also negligible.

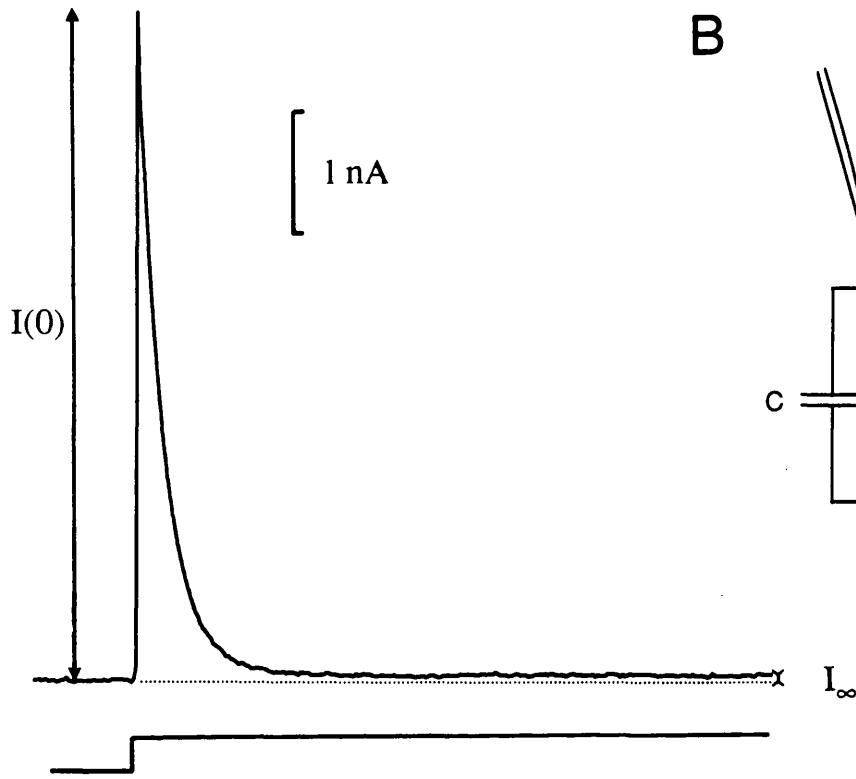
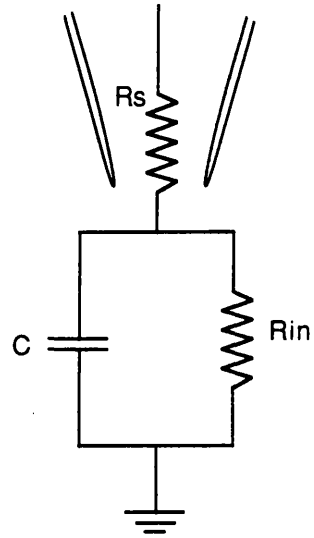
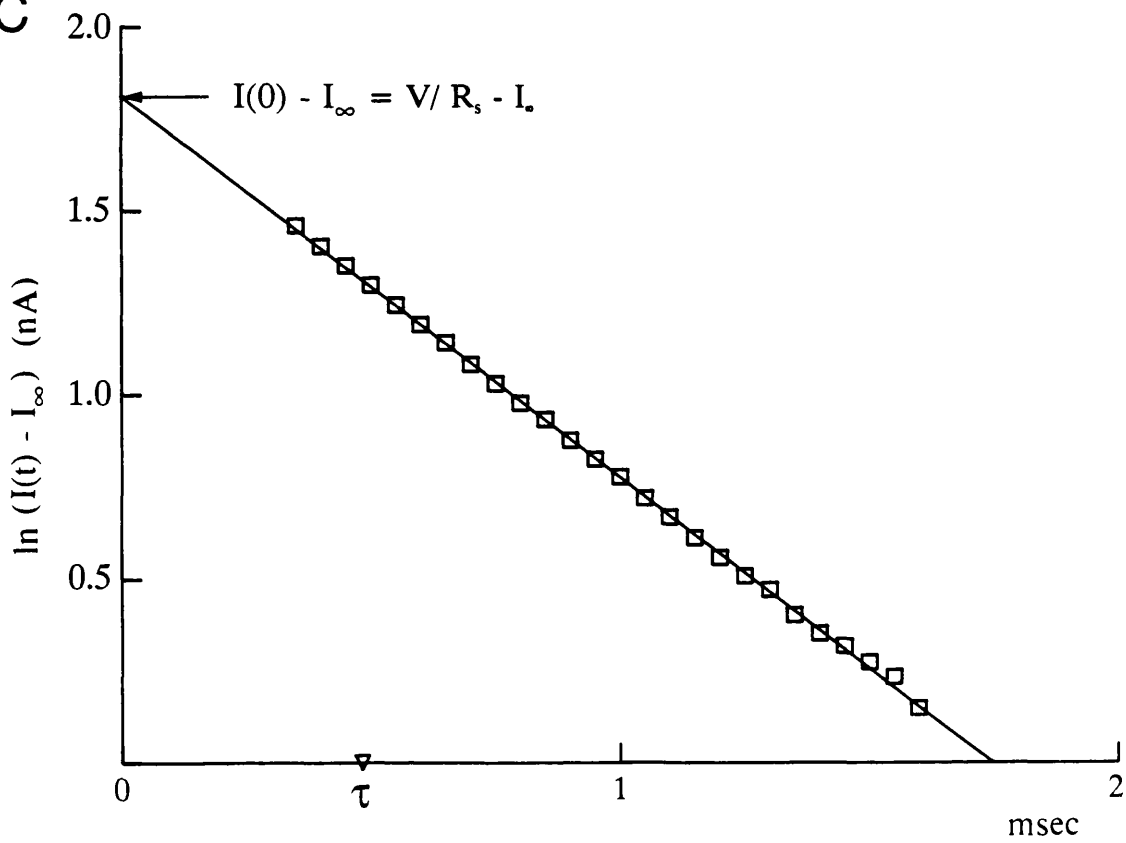
2.3.4 Data acquisition

During the course of the experiment, the data were sent to a chart recorder running continuously as well as stored on magnetic tape (one RACAL store 4DS FM tape recorder or on videotape via via a pulse code modulator attachment).

2.3.5 Data analysis

Data could be analysed either by direct measurement on the chart record or by playing the record back from the tape into a computer (PDP 11/73) via an analogue-to-digital converter. Data were plotted using a Hewlett Packard plotter

Fig 2.2 Capacity transient analysis. A- Current flowing through a whole-cell clamped Müller cell in response to a 10mV voltage step from -43mV. B- Circuit diagram of a whole-cell patch-clamped cell where R_s is the series resistance, R_{in} is the input resistance of the cell and C its membrane capacitance. C- Semilogarithmic plot of $I-I_{\infty}$ (where I_{∞} is the steady state current) against the length of time elapsed after the voltage step. For this cell, the values obtained after analysis were $R_s = 1.8M\Omega$, $R_{in} = 144.5M\Omega$ and $C = 274pF$.

A**B****C**

(model 7470A). The membrane capacitance, series resistance and input resistance were calculated from the analysis of the current response to 10mV voltage pulses. These pulses were applied at the beginning of the recording of each new cell and regularly during the experiment if required. The current transients were later analysed on the computer.

The electric circuit of a whole-cell clamped cell can be represented as in Fig 2.2B. The parameters of this circuit were analysed for each cell using the method described by Tessier-Lavigne *et al*, (1988). In response to a small voltage step (10mV) a current flows through this circuit (Fig 2.2A) with a decay following an exponential form:

$$I(t) = V \cdot (1 + (R_{in}/R_s)e^{-t/\tau}) / (R_{in} + R_s) \quad (1)$$

in which

- t = time after the application of the pulse
- V = amplitude of the step
- τ = time constant of the decay of the transient
- R_{in} = input resistance of the cell
- R_s = series resistance

The time constant of the decay is given by the equation:

$$\tau = C \cdot R_{in} \cdot R_s / (R_{in} + R_s)$$

At $t=0$, the current is $I(0) = V/R_s$. Therefore, R_s can be deduced from this equation. The value of $I(0)$ was obtained by semi-logarithmic extrapolation (see Fig 2.2C).

The current at $t=\infty$ is $I(\infty) = V/(R_{in} + R_s)$ allowing the calculation of R_{in} . The capacitance of the cell can then be calculated from the time constant of the current relaxation:

$$C = \tau (R_{in} + R_s) / R_{in} \cdot R_s$$

2.4 Internal pH measurements

2.4.1 Experimental apparatus

The apparatus used for the fluorescence measurements is described in Fig 2.3. The rest of the set-up was the same as that used for electrical recordings

(see above). The cells were illuminated with light from a Xenon lamp after it had gone through a filter ($440\pm 5\text{nm}$ or $490\pm 5\text{nm}$) and a neutral density filter (N.D.=2). A shutter was available to restrict the illumination time. Emission from the chosen cell was directed to a photomultiplier after going through a diaphragm (to restrict the fluorescence collected to that of only one cell) and a filter ($530\pm 5\text{nm}$). The fluorescence signal from the photomultiplier was then amplified and recorded on video tapes.

The fluorescent dye BCECF was dissolved in the internal solution and introduced into the cell via the patch pipette for most of the experiments. In the case where the cells were not whole-cell clamped, the lipophilic acetoxymethyl (AM) ester form of the dye was used. Cells were preincubated for thirty minutes in a solution (solution A, table 2.1) containing $10\mu\text{M}$ BCECF-AM and $0.2\mu\text{M}$ pluronic acid (Rink *et al*, 1982). Most of the experiments were performed while exciting the dye at 490nm . For this excitation wavelength, the fluorescence of the dye depends strongly on the intracellular pH of the cell. Control experiments were also performed with an excitation wavelength of 440nm which is close to the isosbestic point of the dye at which the dye's fluorescence is insensitive to pH (but will alter if dye is lost from the cell or if the cell moves out of the viewing diaphragm). No change in the amount of emission was recorded from the cell when the dye was excited at 440nm (Fig 2.4) suggesting that the fluorescent changes measured when the dye was excited at 490nm were solely due to changes in the intracellular pH of the cell.

2.4.2 Calibration of BCECF fluorescence with weak acids and bases

The method used for calibrating intracellular pH changes was derived from that of Szatkowski & Thomas (1986) and of Eisner *et al* (1989). A weak base in solution exists in two forms in equilibrium with each other so that



Similarly for a weak acid,



When a weak base is applied to a cell, the assumption is made that its neutral form (B) freely crosses the cell membrane until the concentration of neutral form

is equal inside and outside the cell. Once inside the cell, it will bind protons and produce an alkalization until an equilibrium is reached. Similarly, when a weak acid is applied to the cell, its neutral form HA crosses the membrane and releases a proton until the concentration of the neutral form is (presumably) equal inside and outside the cell.

2.4.3 Calculation of the absolute pH, the buffering power of the cell and the pH changes (from Szatkowski & Thomas (1986) and Eisner *et al* (1989))

The buffering power is defined as (van Slyke, 1922)

$$\beta = \Delta(\text{total added or subtracted protons}) / \Delta\text{pH}_i$$

Thus, the pH change produced in a cell by the application of the base is given by:

$$\Delta\text{pH}_B = [\text{BH}^+]_i / \beta \quad (1)$$

where ΔpH_B is the steady state pH during the application of the base and β is the buffering power of the intracellular medium. The new value of pH obtained during the application of the weak base is therefore:

$$\text{pH}_B = \text{pH}_i + \Delta\text{pH}_B \quad (2)$$

where pH_i is the intracellular pH before applying the base. From the Henderson-Hasselbalch equation,

$$\text{pH}_B = \text{pK}_B + \log ([\text{B}]_i / [\text{BH}^+]_i) \quad (3)$$

where $[\text{B}]_i$ is the concentration of neutral form of the base inside the cell, $[\text{BH}^+]_i$ the concentration of base bound to a proton inside the cell and pK_B is the pK value of the weak base (assumed to be equal inside and outside the cell).

Calculation of the intracellular pH:

Combining equations (1), (2) and (3) gives:

$$pH_i + \Delta pH_B = pK_B - \log ((\beta \cdot \Delta pH_B) / [B]_i) \quad (4)$$

If the pK of the weak base is far from the external pH, then most of the weak base is in the protonated form in the extracellular medium and the concentration of the protonated form can be assumed to be essentially equal to the total external concentration of the base $[B_T]_o$. Therefore, from the Henderson-Hasselbalch equation,

$$pH_o = pK_B + \log ([B]_o / [BH^+]_o) = pK_B + \log ([B]_o / [B_T]_o)$$

$$\text{so } pH_o - pK_B + \log [B_T]_o = \log [B]_o = \log [B]_i \quad (5)$$

Inserting equation (5) into equation (4) gives:

$$pH_i - pH_o = \log ([B_T]_o / \beta \cdot \Delta pH_B) - \Delta pH_B \quad (6)$$

In the case of the application of a weak acid, the analogous equation is:

$$pH_i - pH_o = - \log ([A_T]_o / \beta \cdot \Delta pH_A) + \Delta pH_A \quad (7)$$

Adding equations (6) and (7) leads to:

$$pH_i - pH_o = 0.5 \{ \log ([B_T]_o / [A_T]_o) + \log (\Delta pH_A / \Delta pH_B) + \Delta pH_A - \Delta pH_B \} \quad (8)$$

assuming that β is constant over the range of pH_i changes studied.

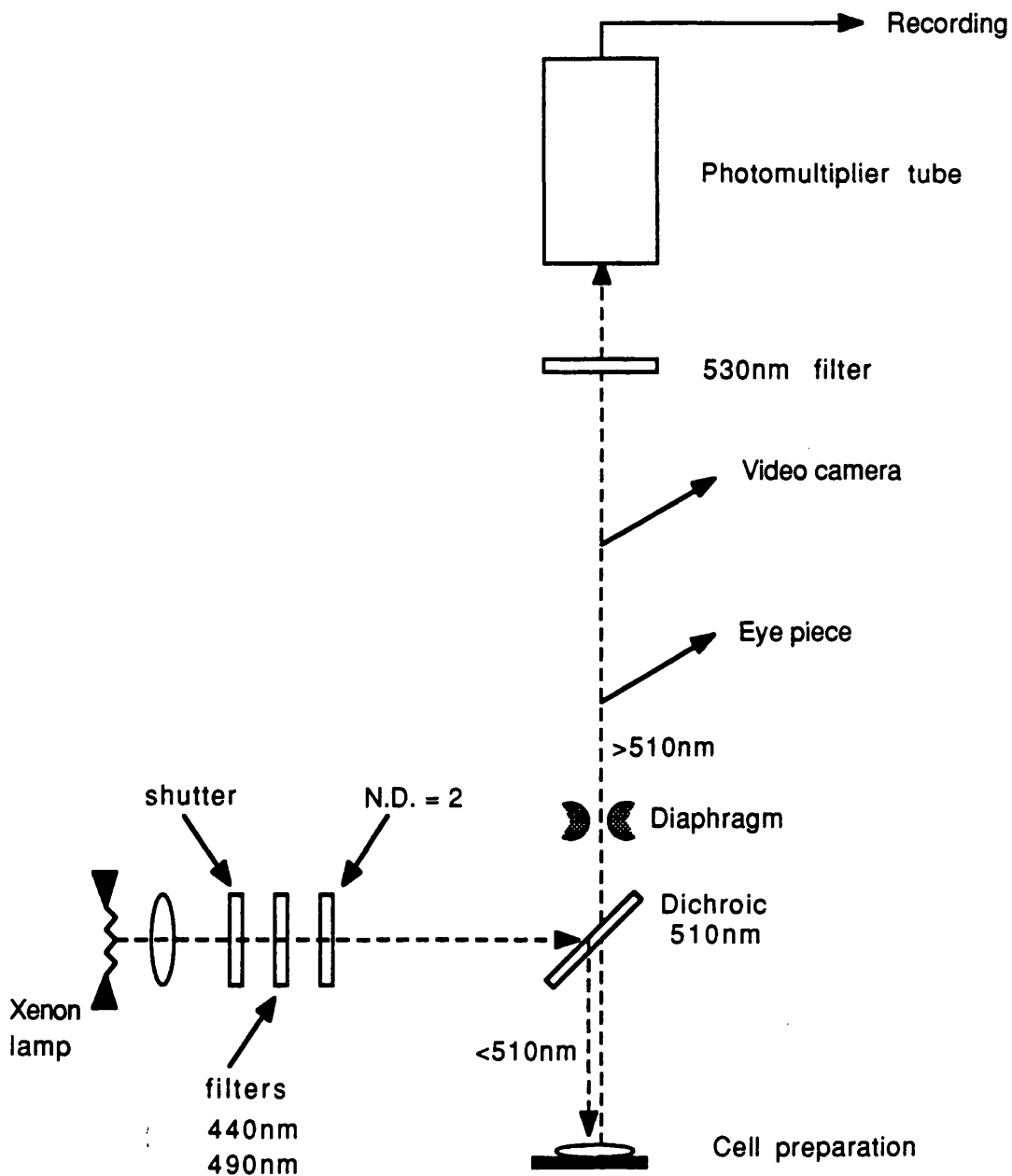
Given that during the experiment, the intracellular pH is close to the pK of the fluorescent dye used to monitor pH (pK for BCECF is 6.98), the fluorescence change is found empirically to be proportional to the pH change (Fig 2.5; Rink *et al*, 1982), i.e.

$$\Delta pH = \alpha \cdot \Delta F \quad (\alpha \text{ being a constant}).$$

Substituting $\alpha \cdot \Delta F$ for ΔpH in equation (8) gives:

$$pH_i - pH_o = 0.5 \{ \log ([B_T]_o / [A_T]_o) + \log (\Delta F_A / \Delta F_B) + \alpha \cdot (\Delta F_A - \Delta F_B) \} \quad (9)$$

Fig 2.3 Apparatus for fluorescence recordings. The light from a xenon lamp is directed through a filter (either 440nm or 490nm) and through a neutral density filter (N.D.=2) that regulate the wavelength and the intensity of the light directed onto a dichroic mirror. The dichroic mirror reflects light of wavelength below 510nm onto the cells. The intensity of the light emitted by the fluorescent dye BCECF (inside the cells) changes according to the cell pH. This emitted fluorescence is collected by a photomultiplier tube after passing through the dichroic mirror and a 530nm filter. In the light path, a diaphragm allows restriction of the collected light to that of only one cell.



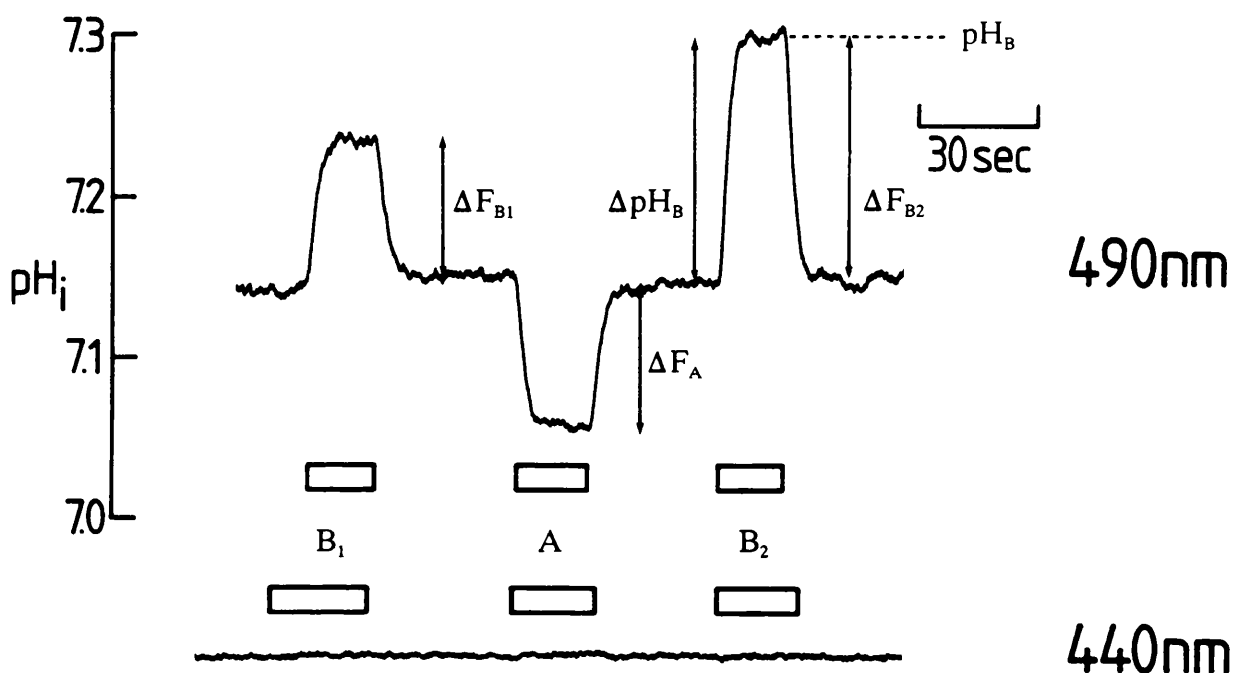


Fig 2.4: Top: Calibration of the fluorescence of BCECF with weak acids and bases. The upper trace shows the fluorescence changes recorded when trimethylamine and acetate were applied to a cell excited with a wavelength of 490nm. B_1 and B_2 indicate the application of 2.5 and 5mM trimethylamine respectively whereas A shows the moment of application of 5mM acetate. Upwards is more alkaline. Different values used for the calculation of the intracellular pH, the buffering power and the value of α (fluorescence change per unit of pH) are indicated on the figure:

ΔF_{B1} and ΔF_{B2} for the calculation of α

ΔF_A for the calculation of pH_i (having calculated α)

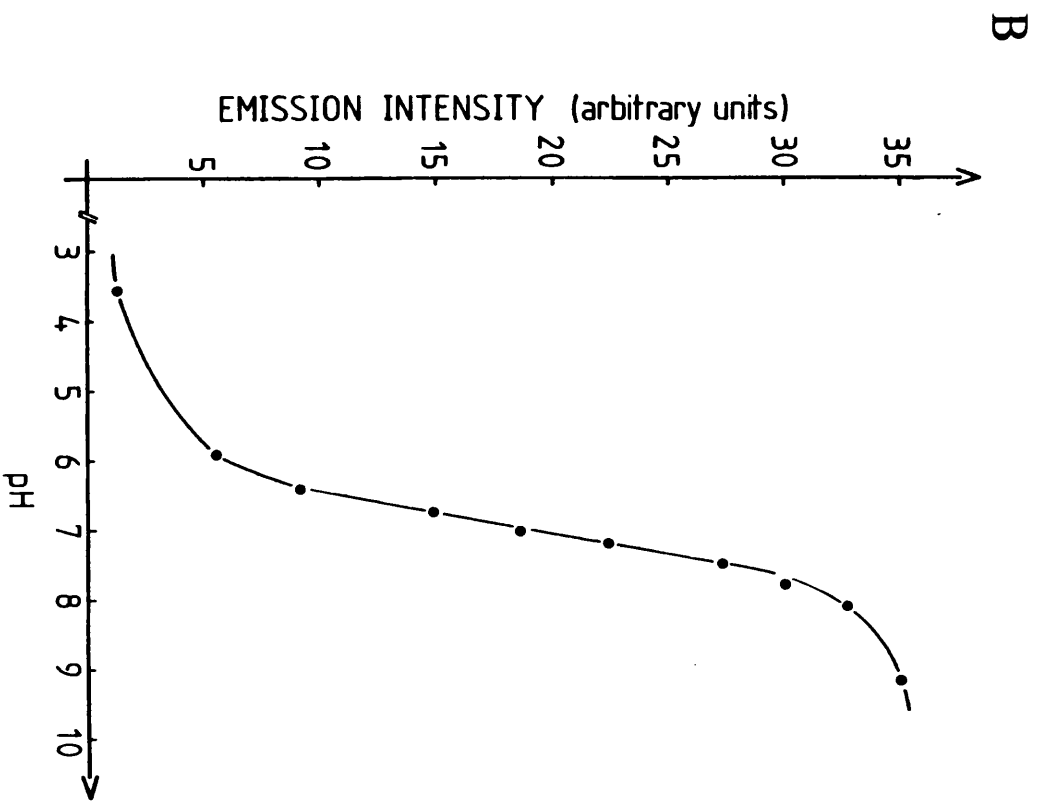
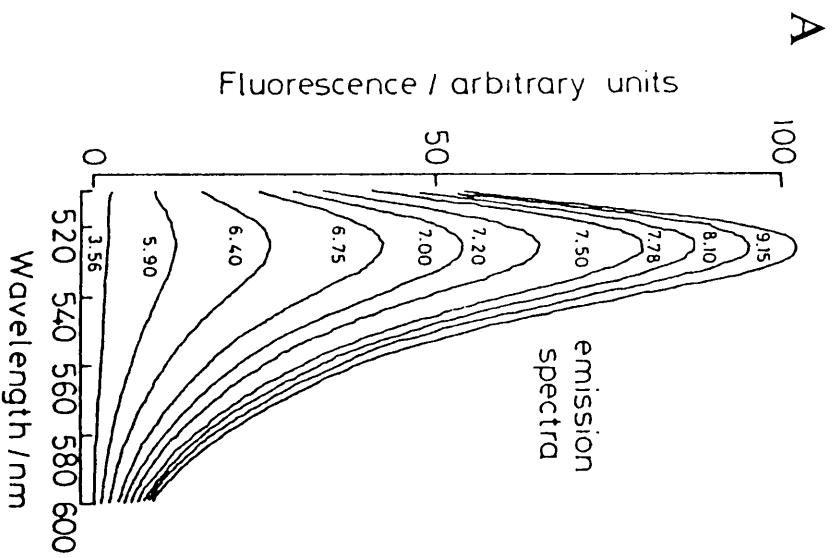
ΔpH_B and pH_B for the calculation of β (having calculated α and pH_i)

Bottom: When the same experiment was performed using an excitation wavelength of 440nm (isosbestic wavelength), no change of fluorescence was detected.

Fig 2.5: Characteristics of the fluorescent dye BCECF.

A- Emission spectra of BCECF at various pH values. Graph taken from Rink *et al*, 1982.

B- Plot of the emission intensity (at 530nm) as a function of pH. Note that the intensity of emission of BCECF changes linearly with pH over a large range (approximately between pH 6.3 and pH 7.8) which includes the physiological range of pH of a cell.



Similarly, equation (6) becomes:

$$pH_i - pH_o = \log ([B_T]_o / \beta \cdot \alpha \cdot \Delta F_B) - \alpha \cdot \Delta F_B \quad (10)$$

If two different concentrations B_1 and B_2 of the weak base are used and give rise to the respective fluorescence changes ΔF_{B1} and ΔF_{B2} (see Fig 2.4), the value of α can be calculated by equating the two values for $pH_i - pH_o$ obtained from equation (10):

$$\alpha = \log ((B_1 \cdot \Delta F_{B2}) / (B_2 \cdot \Delta F_{B1})) / (\Delta F_{B1} - \Delta F_{B2}) \quad (11)$$

If a weak acid is applied (giving fluorescence ΔF_A) and an equal concentration of weak base is applied (giving fluorescence ΔF_B), then from equation (9), the intracellular pH can be calculated as

$$pH_i = 0.5 (\log (\Delta F_A / \Delta F_B) + \alpha (\Delta F_A - \Delta F_B)) + pH_o$$

Calculation of the buffering power:

The total concentration of weak base (B) is given by the equation:

$$B_T = [BH^+]_i + [B]_i \quad \text{or} \quad [BH^+]_i = B_T - [B]_i \quad (12)$$

Combining equations (3) and (12) gives:

$$pH_B = pK_B - \log ((B_T - [B]_i) / [B]_i)$$

$$\text{or} \quad [B]_i = B_T / (1 + 10^{(pK_B - pH_B)}) \quad (13)$$

$$\text{Now, } \beta = [BH^+]_i / \Delta pH_B \quad \text{or} \quad [BH^+]_i = \beta \cdot \Delta pH_B \quad (\text{from (1)}) \quad (14)$$

Substituting (14) into (3) gives:

$$pH_B = pK_B - \log (\beta \cdot \Delta pH_B / [B]_i)$$

$$\text{or} \quad 10^{(pK_B - pH_B)} = (\beta \cdot \Delta pH_B) / [B]_i$$

$$\text{or } [B]_i = (\beta \cdot \Delta \text{pH}_B) / 10^{(\text{pK}_B - \text{pH}_B)} \quad (15)$$

Combining (13) and (15) gives:

$$B_T / (1 + 10^{(\text{pK}_B - \text{pH}_B)}) = (\beta \cdot \Delta \text{pH}_B) / 10^{(\text{pK}_B - \text{pH}_B)}$$

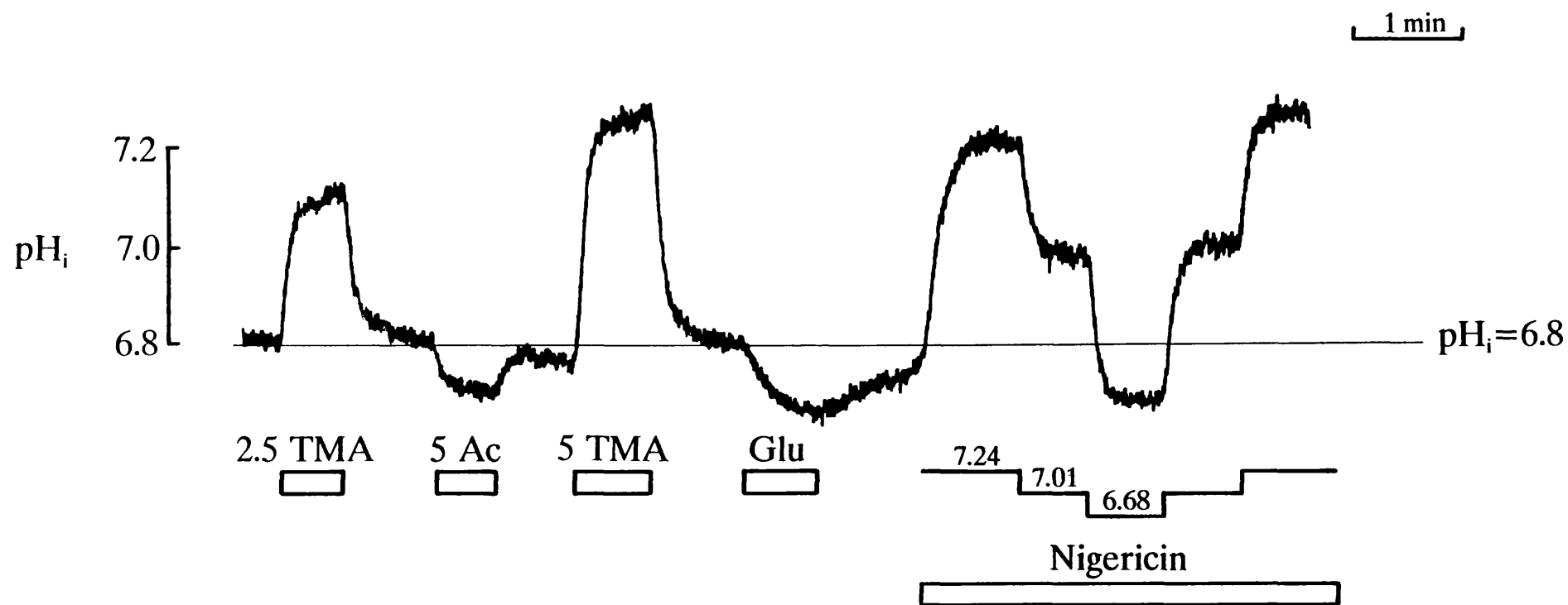
$$\text{or } \beta = B_T \cdot 10^{(\text{pK}_B - \text{pH}_B)} / \{(1 + 10^{(\text{pK}_B - \text{pH}_B)}) \cdot \Delta \text{pH}_B\} \quad (16)$$

The pK of the weak base used (trimethylamine) is $\text{pK}_B = 9.8$. For the measurements of the other values, see Fig 2.4. This method was used in most of the experiments to calibrate the pH changes induced by the application of glutamate or aspartate to the cells (see chapter 4 and 5) because it is not destructive for the cells and therefore allows several cells to be studied in the same dish (unlike calibration with nigericin). In order to confirm the results obtained by this method, the experiment described below was performed.

2.4.4 Calibration of the fluorescence using nigericin

Nigericin is a ionophore which can incorporate into the membrane of cells and exchange K^+ for H^+ . For a high density of ionophores in the membrane, the pH gradient across the cell membrane can thus be equilibrated with the $[\text{K}^+]$ gradient. When a solution containing nigericin and 100mM $[\text{K}^+]$ (equal to the intracellular $[\text{K}^+]$) is applied to a cell, the internal pH of the cell equilibrates with the pH of the nigericin solution. However, incorporating nigericin in the membrane is irreversible and it therefore means that once the cell has been calibrated, no further experiment can be done with it. For this reason, when nigericin was used in an experiment, the cells were plated on 13mm diameter coverslips and only one cell from each coverlip was studied. The accuracy of the weak acid plus weak base calibration method used in this thesis was tested by comparing it with the nigericin method. Müller cells were whole-cell patch-clamped using a BCECF-containing internal (solution L, table 2.3) and the fluorescence of the dye was first of all calibrated as described above, followed by a second calibration using nigericin-containing solutions. As shown in Fig 2.6, the two calibration methods gave very similar results.

Fig 2.6: Calibration of the fluorescence of BCECF with nigericin compared to that with weak acids and bases. Left: fluorescence of a cell containing BCECF calibrated with weak acids and bases. The intracellular pH calculated was 6.799. Right: same cell subsequently calibrated with three nigericin-containing solutions of different pH. The values calculated for the intracellular pH was 6.80. These two methods did not give significantly different results ($n=6;p>0.9$). Upwards is more alkaline.

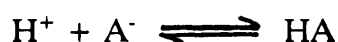


In several cases, calibration of the cells' pH was checked with the nigericin method to make sure that a drug used during the experiment had no effect on the fluorescence of BCECF (see chapter 4 for details).

2.4.5 Calculation of the contribution of BCECF to the buffering power of the intracellular medium

The calibration method used (see above) allowed for the calculation of the buffering power (β) of the intracellular medium of the cell. The mean value obtained for β was 19.8 ± 4.6 mM per pH unit (mean \pm sem; n=45). The pH-sensitive fluorescent dye, having a pK value of 6.98, could increase the buffering power of the cell (although its concentration is very low: $98\mu\text{M}$). The following calculation assesses this.

For a solution of a weak acid AH and its salt A⁻, the equilibrium between the two forms can be expressed as:



Let B be the total concentration of buffer in the solution: $B = [\text{A}^-] + [\text{AH}]$ and C be the total concentration of acid: $C = [\text{H}^+] + [\text{AH}]$.

Then, $[\text{A}^-] = [\text{H}^+] + B - C$

At equilibrium,

$$[\text{H}^+] = K \cdot [\text{AH}] / [\text{A}^-] \quad (1)$$

where K is the dissociation constant.

$$\text{or } [\text{H}^+] = K \cdot (C - [\text{H}^+]) / \{[\text{H}^+] + B - C\} \quad (2)$$

$$\text{or } [\text{H}^+]^2 + B \cdot [\text{H}^+] - C \cdot [\text{H}^+] = K \cdot C - K \cdot [\text{H}^+] \quad (3)$$

Assuming that $B \gg [\text{H}^+]$ and that $B \gg K$, the equation can be simplified to:

$$B \cdot [\text{H}^+] - C \cdot [\text{H}^+] = K \cdot C$$

$$\text{or } C = B \cdot [\text{H}^+] / (K + [\text{H}^+]) \quad (4)$$

and the amount of acid dC which must be added to the solution to produce an increase of $[\text{H}^+]$ by $d[\text{H}^+]$ is given by:

$$dC / dH = B \cdot K / (K + [\text{H}^+])^2 \quad (5)$$

Now, the buffering power is $\beta = -dC / dpH = -(dC / dH) / dpH / dH$

Since $dpH / dH = d(-\log_{10}H) / dH = -1 / 2.303 H$, we find

$$\beta = 2.303BK[H^+] / (K + [H^+])^2 \quad (8)$$

The concentration of BCECF (tested for its buffering power) was $98\mu\text{M}$, its pK is 6.98 (therefore, K is $1.05 \cdot 10^{-7}\text{M}$) and the intracellular pH of the cells was 7.0 (thus, $[H^+] = 10^{-7}\text{M}$).

The buffering of the intracellular medium due to the presence of BCECF is $\beta = 0.056\text{mM}$, a value totally negligible when compared to the calculated total buffering power of the cell (20mM , see above).

2.5 External pH measurements

2.5.1 pH-sensitive electrodes

Electrodes were pulled from borosilicate glass containing a filament (Clark Electromedical, GC150TF10) on a BBCH puller (Mecanex, Geneva).

Silanizing technique:

The ion-sensing resin is dissolved in a water immiscible solvent. It is therefore necessary to make the glass at the tip of the electrode hydrophobic to allow a tight contact between the organic electrolyte and the glass at the tip of the electrode. This is done by exchanging the H of the hydroxyl groups at the surface of the glass for silicon atoms. The glass becomes therefore very hydrophobic. If this process is not done correctly, the liquid ion-sensing resin can be easily displaced by the aqueous solution surrounding the electrode.

The tip of the electrode was dipped into a solution of hexamethyldisilazane (Fluka) 10% in 1-chloro-naphtalene (Fluka) for approximately 20 seconds. The same process was repeated for all the other electrodes. In order to evaporate the solvent (1-chloro-naphtalene) and make the glass at the tip of the electrode hydrophobic, the electrodes were baked in an oven at 90°C for at least two hours. After this treatment, the electrodes were back filled by injecting a small amount of Hydrogen Ionophore I - Cocktail A (Fluka) from a plastic capillary and a cat's whisker was used to direct the

ionophore down to the electrode tip. The solution used to fill the electrode above the resin was solution A, table 2.1, chosen because it is a well-buffered solution. When blockers such as amiloride (section 4.6) were used in the course of the experiment, the pH electrode was calibrated both in the presence and in the absence of the drug.

2.5.2 Electrical apparatus

The pH electrode was connected to a dual electrometer (World Precision Instruments, model FD223) of very high input resistance ($10^{15}\Omega$). A bath electrode (Ag wire) was connected to the other channel of the electrometer. Measures of the change of voltage across the resin of the pH electrode (with the change of voltage measured in the bath) were recorded by the electrometer and stored on a tape recorder and a chart recorder.

2.5.3 Calibration of the pH microelectrode

A typical calibration of a pH microelectrode is shown in Fig. 2.7. The electrode was bathed successively in a solution of high buffering power at pH 6.5 (solution E, table 2.1) and a solution of high buffering power at pH 7.4 (solution B, table 2.1) until stabilisation of the electrode voltage. The voltage response of the electrode to this pH change was as predicted by the Nernst equation for protons, confirming its high selectivity against other ions.

2.5.4 Calculation of the pH at various times during the experiment, and of the corresponding $[H^+]$ change.

Having calibrated the electrode voltage (in mV) in terms of pH, it was possible to calculate the pH of the solution around the cell before activation of the glutamate uptake carrier. Similarly, the pH after 12 seconds was calculated. These two values were converted into changes in the concentration of free protons ($[H^+] = 10^{-pH}$) and, finally, the concentration of total added protons (correcting for the buffering power and assuming that the volume in which the pH changes is fixed, e.g. if the cell membrane and the electrode form a closed compartment) was calculated as in section 2.4.5:

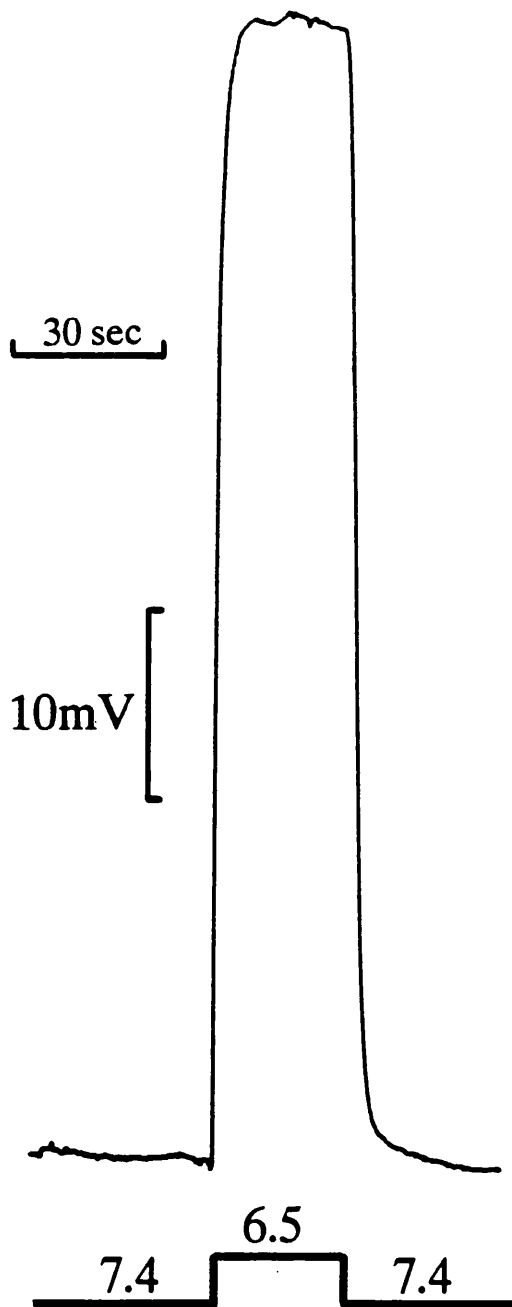


Fig 2.7: Calibration of a pH electrode. The trace shows the response of a pH-sensitive electrode to the successive application of solutions of different pH. For this electrode the total deflection was 60 mV, which is close to the theoretical Nernstian prediction. Upwards is more acid.

$$\Delta C = (\Delta[H^+] \cdot B \cdot K) / (K + [H^+])^2$$

where ΔC is the real change of proton concentration in 12 seconds, ΔH is the change of free proton concentration, B is the concentration of buffer (Hepes) in the external solution, K is a constant (equal to $10^{-pK \text{ of Hepes}}$), and H is the mean value of the free proton concentration before activation of glutamate uptake and after 12 seconds of activation.

2.6 Measurements of external ClO_4^- concentrations

2.6.1 Experimental apparatus

The same electrical apparatus as for the measurements of external pH were used during these experiments (see section 2.5.2).

2.6.2 Anion-sensitive electrode

The first part of the process of preparing anion-sensitive electrodes follows exactly that of the pH-sensitive electrode (see section 2.5.1). The liquid ion-sensitive resin used to fill the tip of the pipette was nominally a chloride-sensitive resin (Chloride Ionophore I - Cocktail A, Fluka). The back filling solution used was 100mM NaCl chosen for its fixed concentration of Cl^- ions. Such an electrode could detect micromolar levels of SCN^- or ClO_4^- (Fig 2.8) even in the presence of 126mM Cl^- (present in solution B, table 2.1 for example).

2.6.3 Calibration of the electrode and calculation of the change in $[\text{ClO}_4^-]$

The first calibrations of the response of the anion-sensitive electrode to low concentrations of ClO_4^- were performed in Cl^- -free external solutions (solution I, table 2.2), because I expected the presence of Cl^- to decrease the sensitivity to ClO_4^- . However, when these calibrations were then compared to calibrations of the same electrodes in a Cl^- -containing solution (solution B, table 2.1), there were no significant differences (probably because the resin is so much more sensitive to ClO_4^- than to Cl^-). Normal external solutions containing Cl^- were therefore used.

The anion-sensitive electrode was calibrated at the beginning and/or at the

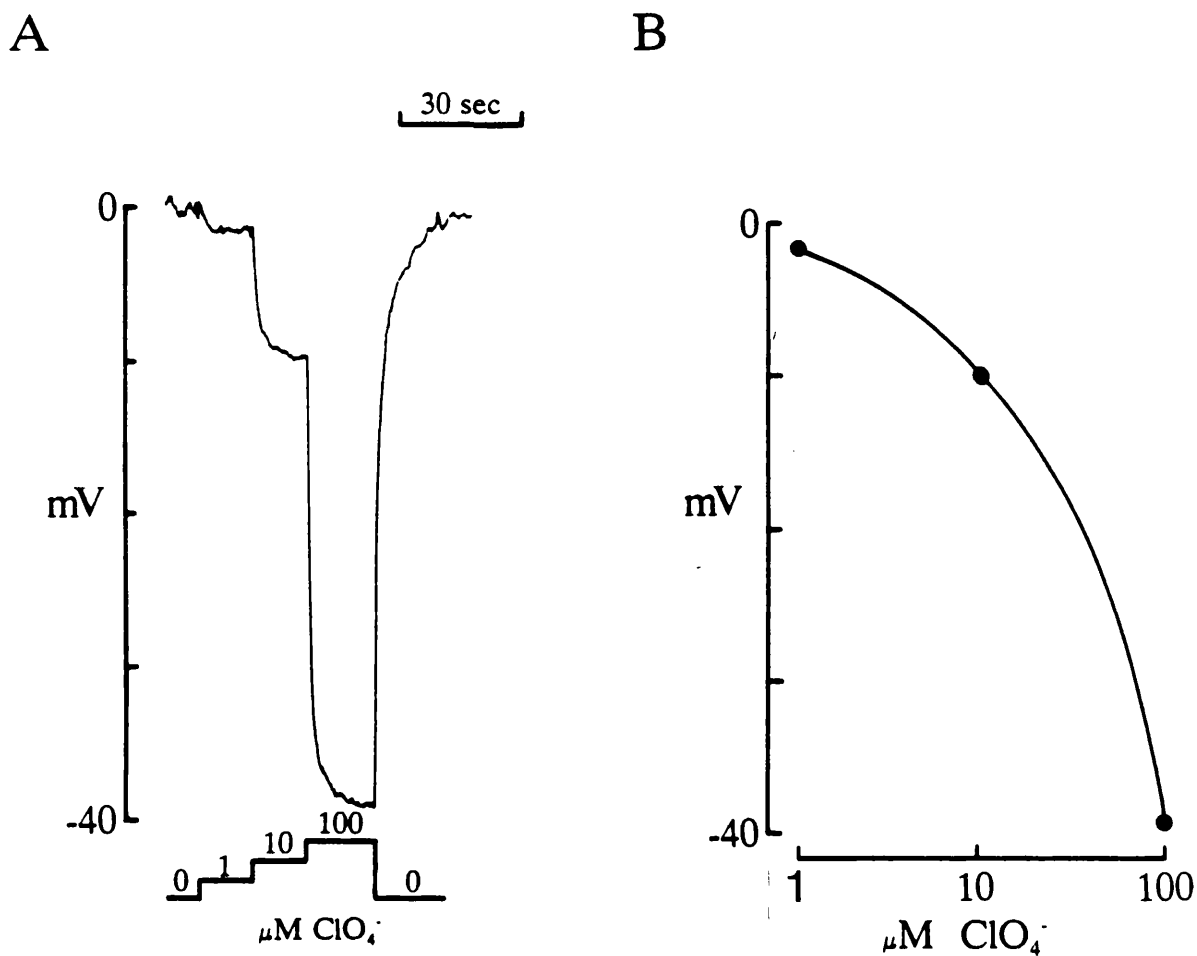


Fig 2.8: Calibration of an anion-sensitive electrode. A: Response of a typical anion-sensitive electrode to the bath application of external solution (solution B, table 2.1) containing 1, 10 and 100 μM ClO_4^- . B: Plot of the change of voltage of the anion-sensitive electrode, against the concentration of ClO_4^- applied. This curve was subsequently used to convert the potential difference measured by the electrode into a change in the external concentration of ClO_4^- around the cell during the rest of the experiment.

end of each cell studied. This was done by running solutions containing three different concentrations of ClO_4^- (1, 10 and $100\mu\text{M}$) through the experimental bath. A typical result from such a calibration is shown in Fig. 2.8. From the voltage deflections obtained when the different solutions were applied, a curve was drawn to relate the voltage change (in mV) to the concentration of ClO_4^- . This curve was subsequently used to convert the deflections obtained during the experiment into a ClO_4^- concentration change.

2.7 Diffusion of a substance from the patch pipette into the cell

Several of the experiments described in chapter 6 involved having to introduce certain proteins or peptides into the cell via the patch pipette. The time needed for the pipette solution and the cell internal medium to equilibrate was determined using the calculations detailed below.

The diffusion flux of a molecule (J , in moles per sec) is given by:

$$J = -D.A.dC/dx \quad (1)$$

where D is the diffusion coefficient of the substance (m^2/sec ; roughly inversely proportional to the cube root of the molecular weight for spherical macromolecules), A is the area available for diffusion and C is the concentration of the substance at point x .

For a localized barrier at the end of the pipette,

$$J = DA (C_{\text{pipette}} - C_{\text{cell}}) / w \quad (2)$$

where w is the width of the barrier.

For a cell of volume V , the amount of substance in the cell is $V.C_{\text{cell}}$ and J tends to increase this amount, therefore:

$$J = d(V.C_{\text{cell}}) / dt \quad (3)$$

From equations (2) and (3):

$$V.dC_{\text{cell}} / dt = DA. (C_{\text{pipette}} - C_{\text{cell}}) / w \quad (4)$$

Now the series resistance at the end of the pipette is:

$$R_s = \rho.w / A$$

where ρ is the resistivity of the pipette solution $\approx 0.8 \Omega\text{m}$ for 100mM solutions.

$$\text{so } A / w = \rho / R_s \quad (5)$$

Inserting (4) into (3) gives:

$$V \cdot dC_{\text{cell}} / dt = D \cdot \rho \cdot (C_{\text{pipette}} - C_{\text{cell}}) / R_s \quad (6)$$

C_{pipette} is constant, so

$$V \cdot d(C_{\text{cell}} - C_{\text{pipette}}) / dt = - (\rho D / R_s) \cdot (C_{\text{cell}} - C_{\text{pipette}})$$

$$\text{or } d(C_{\text{cell}} - C_{\text{pipette}}) / dt = - (C_{\text{cell}} - C_{\text{pipette}}) / \tau \quad (7)$$

where $\tau = (V \cdot R_s) / (\rho \cdot D)$

$$\text{The equation is of the form } dy/dt = -y / \tau \text{ or } dy / y = -dt / \tau \quad (8)$$

$$\text{where } y = C_{\text{cell}} - C_{\text{pipette}} \quad (9)$$

Integrating equation (8) gives:

$$\int dy / y = - \int dt / \tau$$

$$\text{or } \ln y \text{ (at time } t) - \ln y \text{ (at time } 0) = -(t-0)/\tau$$

$$\text{or } \ln (y(t) / y(0)) = -t / \tau$$

$$\text{or } y(t) / y(0) = e^{-t/\tau}$$

$$\text{or } y(t) = y(0) \cdot e^{-t/\tau} \quad (10)$$

Substituting (9) into (10) gives:

$$C_{\text{cell}}(t) - C_{\text{pipette}} = (C_{\text{cell}}(0) - C_{\text{pipette}}) \cdot e^{-t/\tau}$$

At time zero, $C_{\text{cell}} = 0$

Therefore, $C_{\text{cell}}(t) = C_{\text{pipette}} \cdot (1 - e^{-t/\tau})$

The concentration rises to its steady state concentration, C_{pipette} , with an exponential time course of time constant $\tau = V \cdot R_s / \rho \cdot D$

The final concentration in the cell is equal to that in the pipette.

Case 1: PKA catalytic subunit

Mol. Wt. = 40862 therefore $D \approx 7.23 \cdot 10^{-11} \text{ m}^2 \text{ s}^{-1}$ (see below)

$R_s = 3 \text{ M}\Omega$

$V = 10^{-14} \text{ m}^3$ (estimated volume of a Müller cell)

$\rho = 0.8 \text{ }\Omega\text{m}$

$\tau = V \cdot R_s / \rho \cdot D \approx 9 \text{ minutes}$

Thus, at least 25 minutes were left in whole-cell mode before examining the

glutamate uptake current in the presence of internal PKA catalytic subunit.

Case 2: peptide inhibitor of PKA

The peptide inhibitor used in chapter 6 to block the activity of cAMP-dependent protein kinase has the following sequence:

NH₂-Thr-Tyr-Ala-Asp-Phe-Ile-Ala-Ser-Gly-Arg-Thr-Gly-Arg-Arg-Arg-Ala-Ile-His-Asp-COOH

Mol.Wt. \approx 2400 therefore $D \approx 18.6 \cdot 10^{-11} \text{ m}^2 \text{ s}^{-1}$ (see below)

$$R_s = 3 \text{ M}\Omega$$

$$V = 10^{-14} \text{ m}^3$$

$$\rho = 0.8 \text{ }\Omega\text{m}$$

$$\tau = V \cdot R_s / \rho \cdot D \approx 3.4 \text{ minutes}$$

Thus, at least 13 minutes were allowed in whole-cell mode for the peptide to enter the cell before measuring the glutamate uptake current in the presence of the peptide.

An estimate of the diffusion coefficient of the molecules was calculated knowing that the diffusion coefficient is inversely proportional to the cube root of the molecular weight, taking β -Lactoglobulin as the reference molecule (Mol. Wt. = 37100; $D = 7.48 \cdot 10^{-11} \text{ m}^2 \text{ s}^{-1}$).

Table 2.1
Extracellular solutions A-E

solution: **A** storage and washing
 B standard external solution
 C potassium-free external solution
 D sodium-free external solution
 E Pipes buffered external solution

	A	B	C	D	E
KCl	2.5	2.5	0	2.5	2.5
NaCl	104.5	104.5	104.5	0	104.5
MgCl ₂	0.5	0.5	0.5	0.5	0.5
CaCl ₂	3	3	3	3	3
Hepes	5	5	5	5	0
D-Glucose	15	15	15	15	15
BaCl ₂	0	6	6	6	6
Choline-Cl	0	0	0	104.5	0
Pipes	0	0	0	0	5
pH	7.4	7.4	7.4	7.4	6.5
adjusted with	NaOH	NaOH	NaOH	NMDG*	NaOH

* NMDG is N-methyl-D-glucamine

All concentrations are in mM.

Table 2.2
Extracellular solutions F-I

solution: F external solution of low buffering power
 G sodium-free solution of low buffering power
 H external solution for calibration with nigericin
 I gluconate external for calibration of anion electrodes

	F	G	H	I
KCl	2.5	2.5	105	0
NaCl	104.5	0	0	0
MgCl ₂	0.5	0.5	0.5	0
CaCl ₂	3	3	1.5	0
Hepes	0.05	5	5	5
D-Glucose	15	15	15	15
BaCl ₂	6	6	6	0
Choline-Cl	0	104.5	0	0
Nigericin	0	0	0.001	0
K-gluconate	0	0	0	2.5
Na-gluconate	0	0	0	104.5
Mg-gluconate ₂	0	0	0	0.5
Ca-gluconate ₂	0	0	0	3
pH	7.4	7.4	7.24; 7.01 and 6.68	7.4
adjusted with	NaOH	NMDG*	KOH	NaOH

* NMDG is N-methyl-D-glucamine

All concentrations are in mM.

Table 2.3
Internal solutions J-M

solution:	J	standard internal solution
	K	potassium-free internal solution
	L	BCECF-containing solution
	M	BCECF-containing solution with metabolic poisons

	J	K	L	M
KCl	95	0	95	95
Choline-Cl	0	95	0	0
K ₂ EGTA	5	0	5	5
Na ₂ EGTA	0	5	0	0
NaCl	5	0	5	5
Na ₂ ATP	5	0	5	5
MgATP	0	5	0	0
Hepes	5	5	0.5	0.5
CaCl ₂	1	1	1	1
MgCl ₂	7	2	7	7
BCECF	0	0	0.1	0.1
Na-malonate	0	0	0	0.2
Na-oxalomalate	0	0	0	1.5
Aminooxyacetic acid	0	0	0	5
Methionine sulfoximine	0	0	0	2
Albizziin	0	0	0	1
Iodoacetate	0	0	0	0.5
N-ethylmaleimide	0	0	0	0.3
Pyridoxal-5-phosphate	0	0	0	0.1
Rotenone	0	0	0	0.01
pH	7.0	7.0	7.0	7.0
adjusted with	KOH	NMDG*	KOH	KOH
Free [Ca ²⁺] @ 23°C	77nM	77nM	77nM	77nM
Tip potential (in mV)	-3	+1	-3	-3

* NMDG is N-methyl-D-glucamine

All concentrations are in mM.

Table 2.4
Internal solutions N-Q

solution:	N	control internal for anion substitutions
	O	Br ⁻ -containing internal solution
	P	I ⁻ -containing internal solution
	Q	IO ₃ ⁻ -containing internal solution

	N	O	P	Q
KCL	112	0	0	0
KBr	0	112	0	0
KI	0	0	112	0
KIO ₃	0	0	0	112
K ₂ EGTA	5	5	5	5
K ₂ ATP	5	5	5	5
Hepes	5	5	5	5
pH	7.0	7.0	7.0	7.0
adjusted with	KOH	KOH	KOH	KOH
Free [Ca ²⁺] @ 23°C	<1nM	<1nM	<1nM	<1nM
Tip potential (in mV)	-7	-4	-5	-11

All concentrations are in mM.

Table 2.5
Internal solutions R-V

solution:	R	NO ₃ ⁻ -containing internal solution
	S	ClO ₄ ⁻ -containing internal solution
	T	SCN ⁻ -containing internal solution
	U	control internal for HCO ₃ ⁻ -containing solution
	V	HCO ₃ ⁻ -containing internal solution*

	R	S	T	U	V
KCl	0	0	0	95	95
KNO ₃	112	0	0	0	0
KClO ₄	0	112	0	0	0
KSCN	0	0	112	0	0
K ₂ EGTA	5	5	5	5	5
K ₂ ATP	5	5	5	0	0
Hepes	5	5	5	5	5
MgATP	0	0	0	5	5
CaCl ₂	0	0	0	1	1
MgCl ₂	0	0	0	2	2
NaHCO ₃	0	0	0	0	10
NaCl	0	0	0	10	0
Acetazolamide	0	0	0	1	1
pH	7.0	7.0	7.0	7.0	7.0
adjusted with	KOH	KOH	KOH	KOH	KOH
Free [Ca ²⁺] @ 23°C	<1nM	<1nM	<1nM	77nM	77nM
Tip potential (in mV)	-8	-4	-6	-3	-3

All concentrations are in mM.

* solution V was permanently bubbled with 5% CO₂.

Table 2.6
Internal solutions W- Ω

solution:	W	potassium-free ClO ₄ ⁻ -containing solution
	X	potassium-free NO ₃ ⁻ -containing solution
	Y	high-sodium ClO ₄ ⁻ -containing solution
	Z	5mM ascorbate internal
	Ω	control for 5mM ascorbate internal

	W	X	Y	Z	Ω
HClO ₄	112	0	0	0	0
HNO ₃	0	112	0	0	0
NMDG (free base)	112	112	0	0	0
NMDG ₂ EGTA	5	5	0	0	0
KClO ₄	0	0	82	0	0
NaClO ₄	0	0	30	0	0
KCl	0	0	0	95	95
MgATP	0	0	0	5	5
CaCl ₂	0	0	0	1	1
MgCl ₂	0	0	0	2	2
NaCl	0	0	0	5	10
Hepes	5	5	5	5	5
K ₂ EGTA	5	5	5	5	5
Thiourea	0	0	0	10	10
Na-ascorbate	0	0	0	5	0
pH	7.0	7.0	7.0	7.0	7.0
adjusted with	NMDG*	NMDG*	KOH	KOH	KOH
Free [Ca ²⁺] @ 23°C	<1nM	<1nM	<1nM	77nM	77nM
Tip potential (in mV)	+2	-7	-4	-3	-3

* NMDG is N-methyl-D-glutamine

All concentrations are in mM.

CHAPTER 3

Electrogenic Uptake of Sulphur-containing Analogues of Glutamate and Aspartate

3.1 Introduction

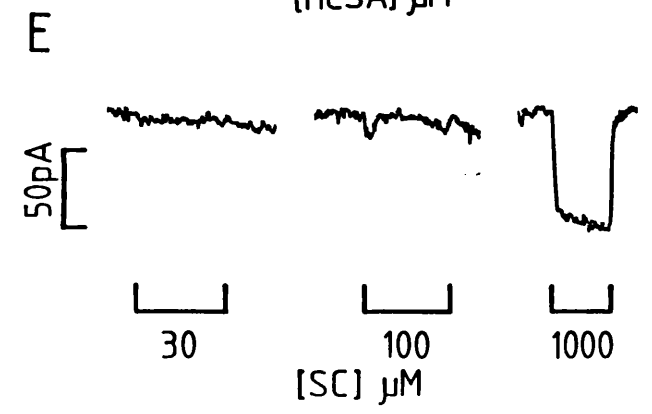
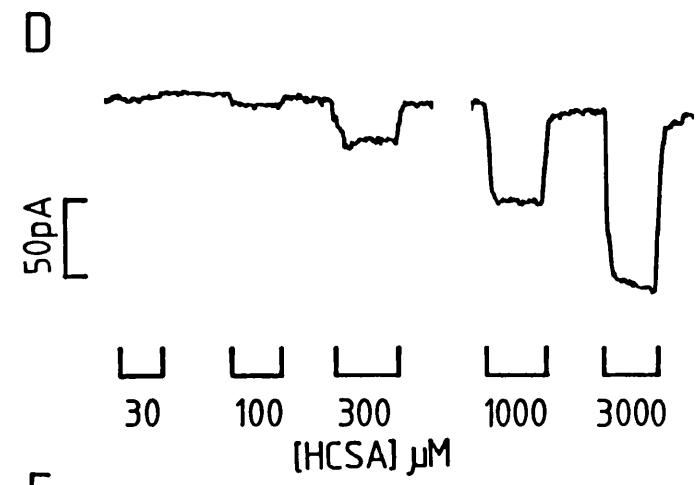
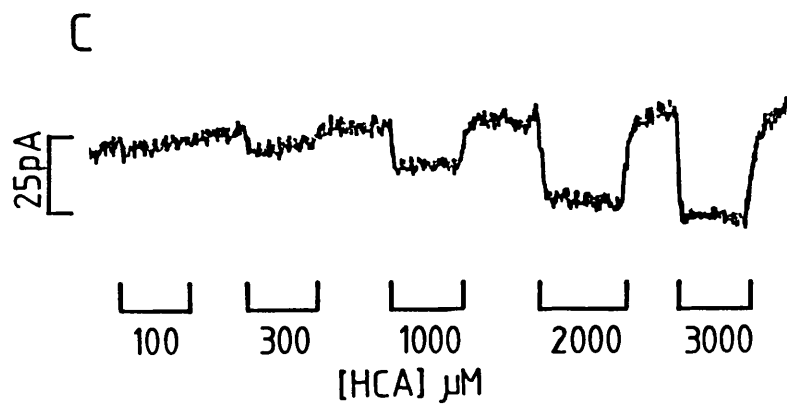
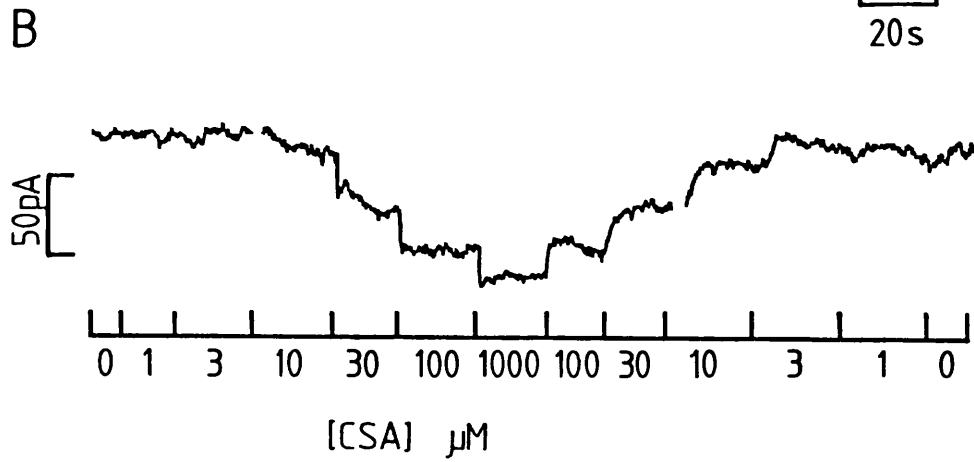
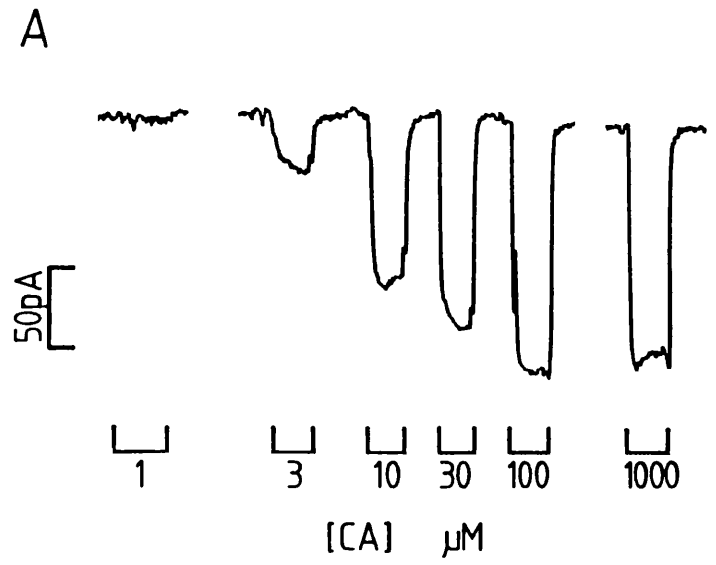
This chapter describes the currents evoked in Müller cells by sulphur-containing analogues of glutamate and aspartate. The aim of these experiments was to determine whether these analogues are transported on the glutamate uptake carrier and to determine the characteristics of their transport (V_{max} and K_m values). This is important because these sulphur-containing analogues have been proposed as neurotransmitter candidates (Mewett *et al*, 1983) and some of them (HCA and SC) may have a neurodegenerative action (Olney *et al*, 1975; Ohmori *et al*, 1972).

3.2 Dose-dependence of currents evoked by sulphur-containing amino-acids

The effect of applying sulphur-containing analogues of glutamate (homocysteic acid and homocysteine sulphinic acid) and aspartate (cysteic acid and cysteine sulphinic acid) as well as S-sulfo-L-cysteine was tested on Müller cells voltage-clamped to around -43mV. Solutions containing different concentrations of each analogue were applied sequentially to the cell by bath perfusion (in solution B, table 2.1). All of these sulphur-containing analogues generated an inward membrane current. Evidence presented below indicates that this current was generated by the analogues being transported on the glutamate uptake carrier. Note that since glutamate-gated channels are absent from salamander Müller cells (Brew & Attwell, 1987), the analogues cannot have evoked a current by opening such channels.

To assess the possible neurotoxic or neurotransmitter role of the sulphur-containing analogues, it is important to know their affinity for the uptake carrier. Fig 3.1A shows the effect of increasing doses of L-cysteate (CA) on the membrane current of a cell. CA at a dose of $1\mu\text{M}$ did not induce any detectable

Fig 3.1 Effect of different doses of L-cysteic acid (CA) (A), L-cysteinesulphinic acid (CSA) (B), L-homocysteic acid (HCA) (C), L-homocysteinesulphinic acid (HCSA) (D) and S-sulpho-L-cysteine (SC) (E) on the membrane current of five different Müller cells voltage clamped to -43mV. Drug concentrations given beneath each trace. Inward current shown downward. In all four cells studied with 100 and 1000 μ M SC, no convincing current was produced by 100 μ M of the drug.



current. Doses from $3\mu\text{M}$ to $100\mu\text{M}$ induced inward membrane currents of increasing magnitude. Above $100\mu\text{M}$, the response to the application of CA was not increased further.

Similar results were obtained with L-cysteine sulphinic acid (CSA), L-homocysteic acid (HCA), L-homocysteine sulphinic acid (HCSA) and S-sulpho-L-cysteine (SC) (Fig 3.1B-E), but the doses of amino acid required to evoke a half-maximum current varied greatly from micromolar levels (for CSA) to millimolar concentrations (for HCA and HCSA). One millimolar SC routinely evoked a response whereas a concentration of $100\mu\text{M}$ did not produce any convincing detectable current. Higher doses were not tested.

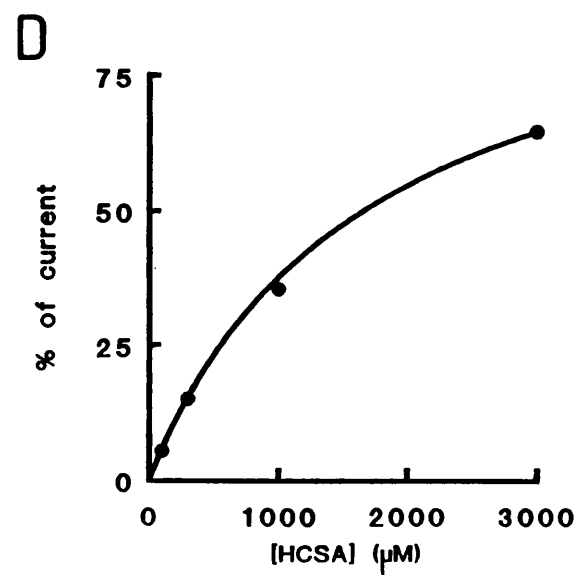
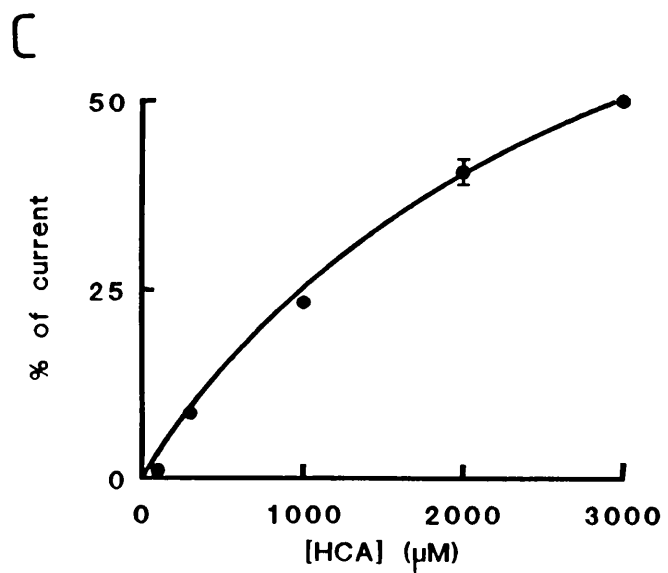
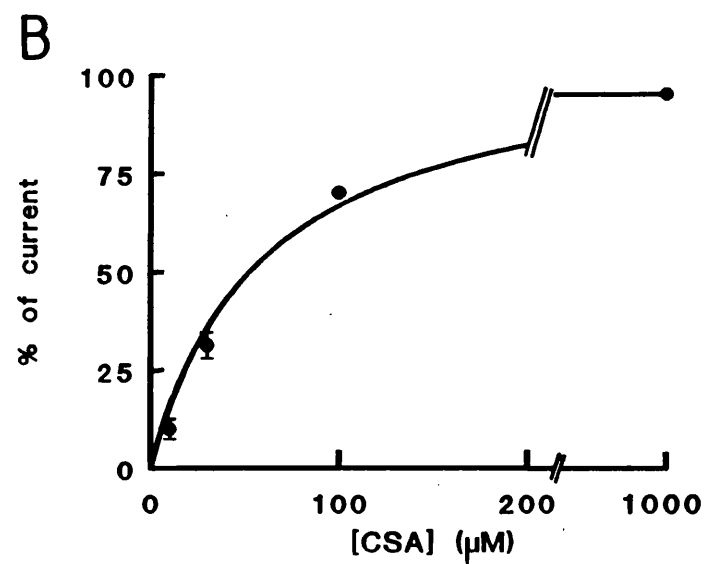
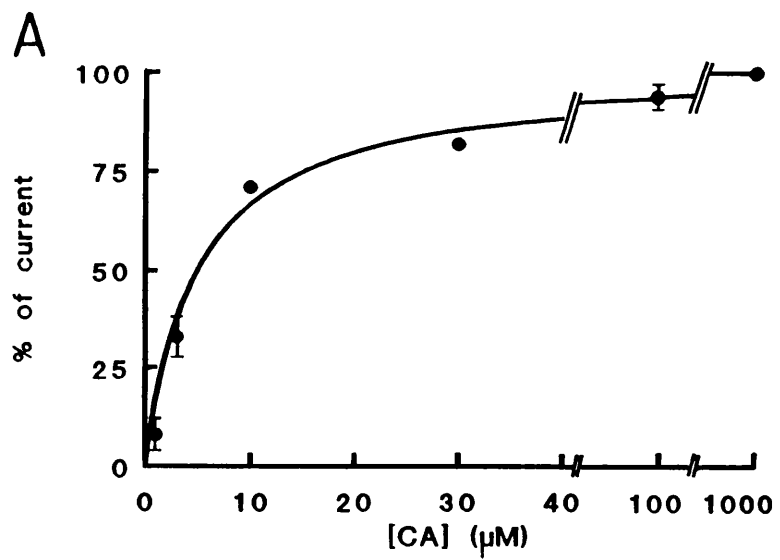
Fig 3.2A-D shows mean dose-response curves from 5 cells (except for HCSA for which 6 cells were studied) all held at -43mV . The dose response-curves of all the sulphur-containing analogues studied were well fitted by a Michaelis-Menten equation:

$$V = \frac{V_{\max} \times c}{c + K_m}$$

where V is the current evoked by the analogue applied at concentration c , V_{\max} is the current evoked by a saturating dose of the analogue and K_m is the concentration that evokes a half-maximal response. This is consistent with one molecule of amino-acid being transported per cycle of the carrier as has been found for the uptake of L-glutamate and D-aspartate (Brew & Attwell, 1987; Barbour *et al*, 1991).

For all the analogues, except S-sulpho-L-cysteine, values of V_{\max} (relative to the V_{\max} value for L-glutamate obtained from the same cell) and K_m were estimated using Eadie-Hofstee plots of the data (i.e. plots of V against V/c). The K_m values obtained for CA, CSA, HCA and HCSA were 6, 60, 2950 and $1650\mu\text{M}$ respectively. The V_{\max} values relative to the V_{\max} for L-glutamate were 0.64 ± 0.07 , 0.37 ± 0.02 , 0.21 ± 0.02 and 0.41 ± 0.03 .

Fig 3.2 Dose-response curves for the action of CA (A), CSA (B), HCA (C) and HCSA (D) on the membrane current of Müller cells. Five cells studied for each analogue, except for HCSA for which six cells were studied. Points show mean current \pm sem. Smooth curves were fitted by Eadie-Hofstee analysis and have the form $V/V_{\max} = c/(c+K_m)$, where c is the drug concentration and K_m was $6\mu\text{M}$ for CA, $60\mu\text{M}$ for CSA, $2950\mu\text{M}$ for HCA and $1650\mu\text{M}$ for HCSA. The values for V_{\max} obtained from Eadie-Hofstee plots were defined to be 100% for these graphs: V_{\max} values were different for each drug (see table 7.1).



3.3 Voltage-dependence of the current evoked by sulphur-containing amino-acids

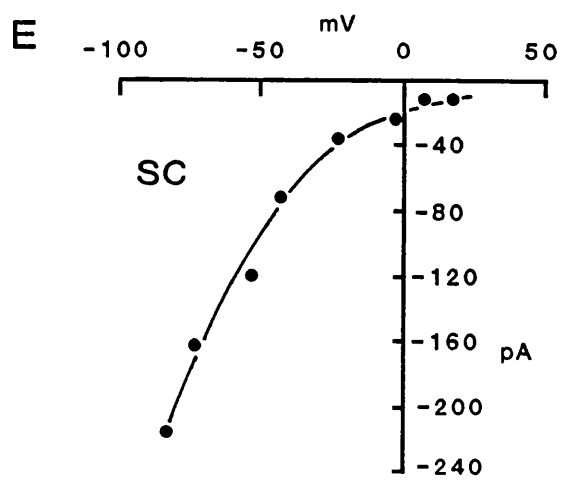
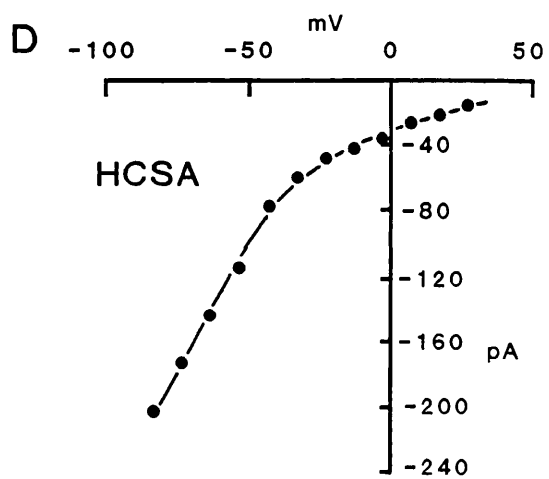
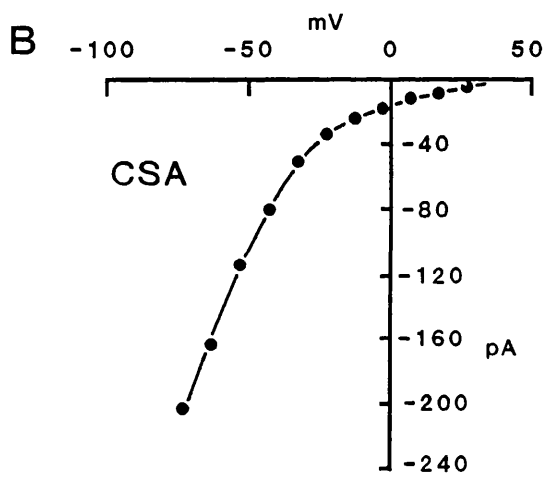
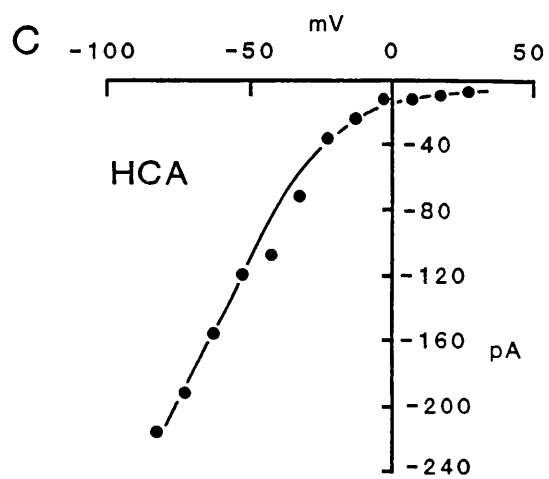
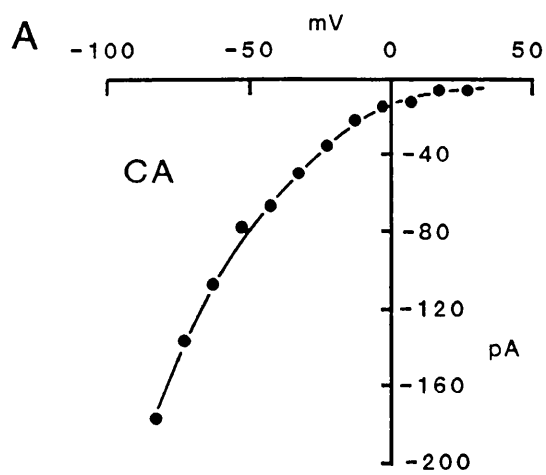
Whether the sulphur-containing amino-acids are acting on ion channels or on the glutamate uptake carrier can be distinguished by examining the voltage-dependence of the current they evoke (Brew & Attwell, 1987). Fig 3.3A shows the size of the inward current evoked by bath application (solution B, table 2.1) of $10\mu\text{M}$ CA plotted against the voltage at which the cell was held. The evoked current, large at -85mV (the resting potential for these cells), became smaller at more positive potentials but did not become outward, even at voltages as positive as $+30\text{mV}$. Instead, the currents remained inward and simply decreased asymptotically towards zero. Similar results were obtained using $100\mu\text{M}$ CSA, 3mM HCA, 3mM HCSA and 1mM SC (Fig 3.3B-E).

These curves are not consistent with the activation of well-known types of glutamate-gated channels, which would show a reversal potential around 0mV (Hablitz & Langmoen, 1982; Mayer & Westbrook, 1984). On the contrary, the I-V relations are similar to those reported for the uptake of glutamate and aspartate (Brew & Attwell, 1987; Barbour *et al*, 1991). This behaviour is thought to be due to the carrier transporting a net positive charge into the cell on each cycle, so that a positive potential slows the rate of uptake.

3.4 Sodium-dependence of the sulphur-containing amino-acid uptake current

It has been reported that the glutamate uptake is completely abolished when external sodium is replaced by choline (Kanner and Sharon, 1978a; Brew & Attwell, 1987). To investigate the sodium-dependence of the currents evoked by sulphur-containing analogues, the amino-acids were applied to the cell by perfusion in a sodium-free solution (solution D, table 2.1), in between applications in sodium-containing solutions (solution B, table 2.1). Fig 3.4A shows the absence of current when the drug is applied in a sodium-free solution whereas the previous and the following application of the same drug in a sodium-containing solution evoked a large current. For simplicity, an outward shift of baseline current, of about 40pA , observed when external sodium was removed, has been omitted from the traces. Similar results were obtained for $100\mu\text{M}$ CSA,

Fig 3.3 Voltage dependence of the current evoked in Müller cells (a different cell for each drug) by 10 μ M CA (A), 100 μ M CSA (B), 3mM HCA (C), 3mM HCSA (D) and 1mM SC (E). Similar results were obtained in four other cells for each analogue.



3mM HCA, 1mM HCSA and 1mM SC (Fig 3.4B-E). Thus, as has been found for the uptake of L-glutamate, the current evoked by the sulphur-containing amino-acids is absolutely dependent on the presence of external sodium.

These data are consistent with the current evoked by the sulphur-containing amino-acids reflecting their uptake on the glutamate uptake carrier. They are not consistent with the current being generated by their action on glutamate receptors of the AMPA/kainate type: these channels let sodium and potassium through, and would generate an outward potassium current when the analogue was applied in a sodium-free external solution.

3.5 Dependence of the current on intracellular potassium

Barbour *et al* (1988, 1991) have previously reported that glutamate uptake is abolished by removal of intracellular potassium. To determine the internal potassium dependence of the current evoked by the sulphur-containing analogues, recordings were made using pipettes containing either 105 or 0mM KCl (solution J or K, table 2.3). The different sulphur-containing analogues were applied by bath perfusion. Potassium was removed from the extracellular solution (solution C, table 2.1) to prevent it from leaking into the cell and preventing the complete removal of potassium inside the cell (Barbour *et al*, 1988).

When the cells were whole-cell clamped at -43mV using internal solutions containing no potassium, the inward membrane current evoked by the agonists rapidly decreased almost to zero. This is shown in Fig 3.5A for the current evoked by 30 μ M CA at different times after patch rupture. The amplitude of the evoked current declined rapidly with time reflecting the decrease of intracellular concentration of K⁺ (diffusing out of the cell into the pipette). The decline of the current typically reached a steady state 3-4 minutes after patch rupture. Similar results were obtained when 100 μ M CSA, 3mM HCA, 3mM HCSA and 1mM SC were applied. This decline was not observed when the cells were whole-cell clamped using an intracellular solution containing 100mM K⁺, suggesting that intracellular potassium activates the current evoked by the sulphur-containing analogues.

Fig 3.5B shows typical data obtained when the sulphur-containing

Fig 3.4 Sodium dependence of the current evoked in Müller cells (a different cell for each drug, clamped at -43mV) by 100 μ M CA (A), 100 μ M CSA (B), 3mM HCA (C), 1mM HCSA (D) and 1mM SC (E). Each panel shows a response to the drug in ordinary barium-Ringer solution containing 107mM Na⁺ ions, followed by a lack of response to the drug when all the external sodium ions were removed, followed by a return to control solution. Drug timing shown above each record. Oscillations in current at the start of some applications are due to the superfusion solution swirling around the cell, causing the cell not to be exposed to a constant drug concentration until several seconds after the drug solution was turned on.

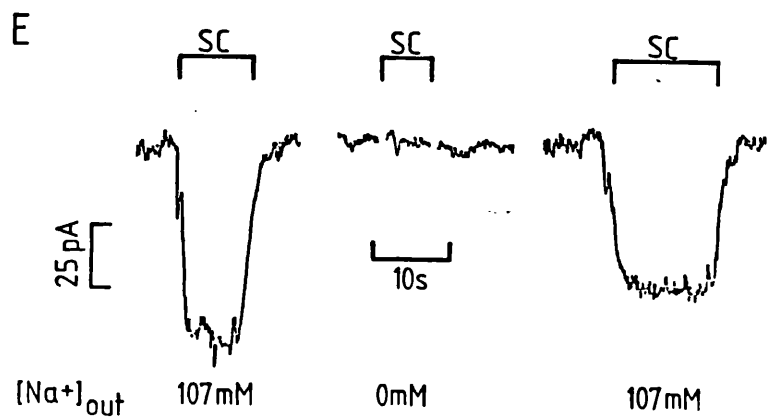
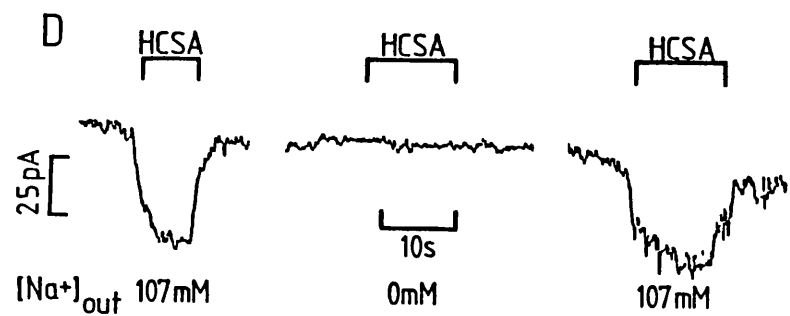
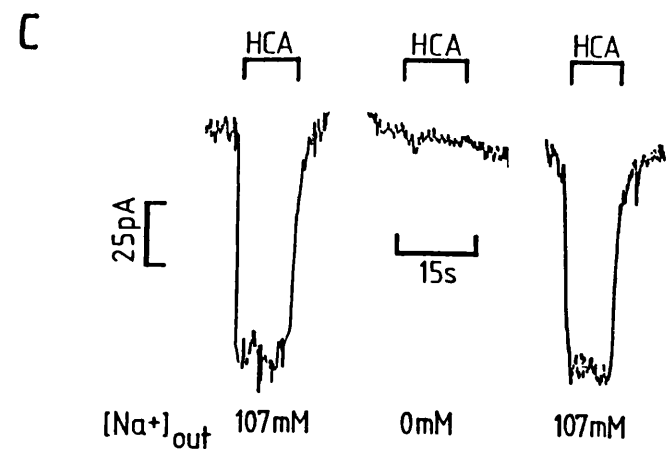
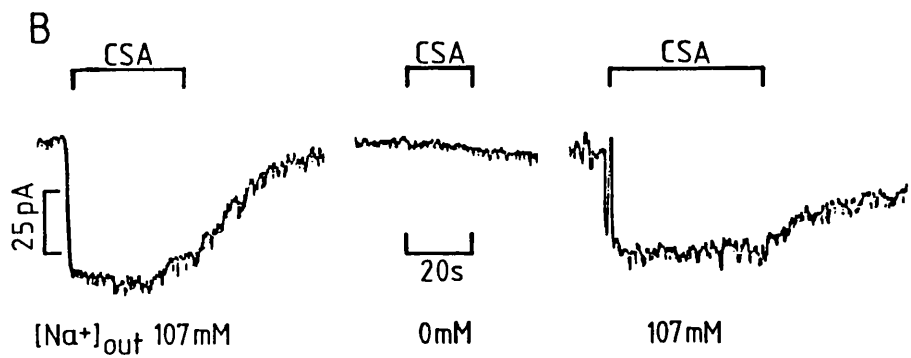
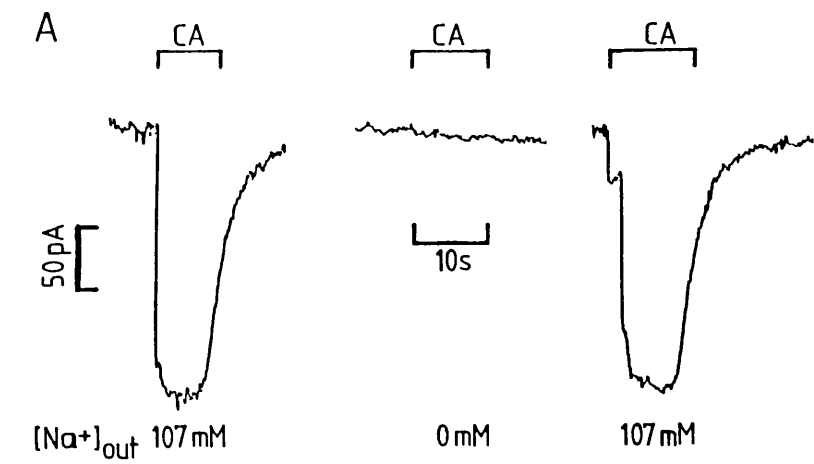
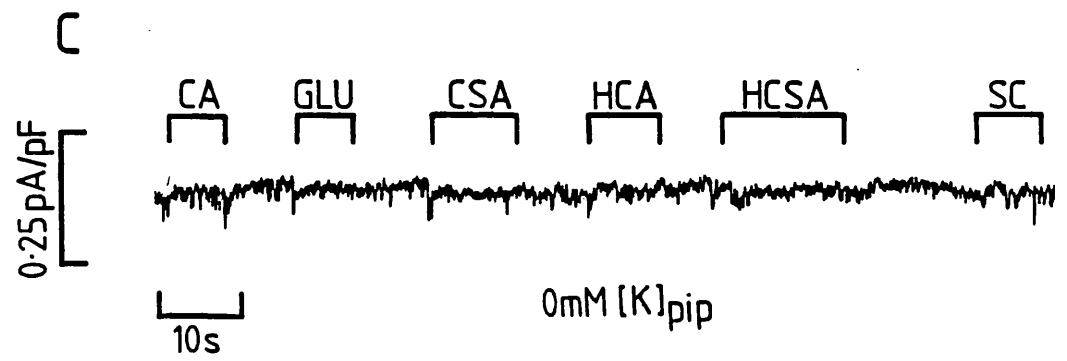
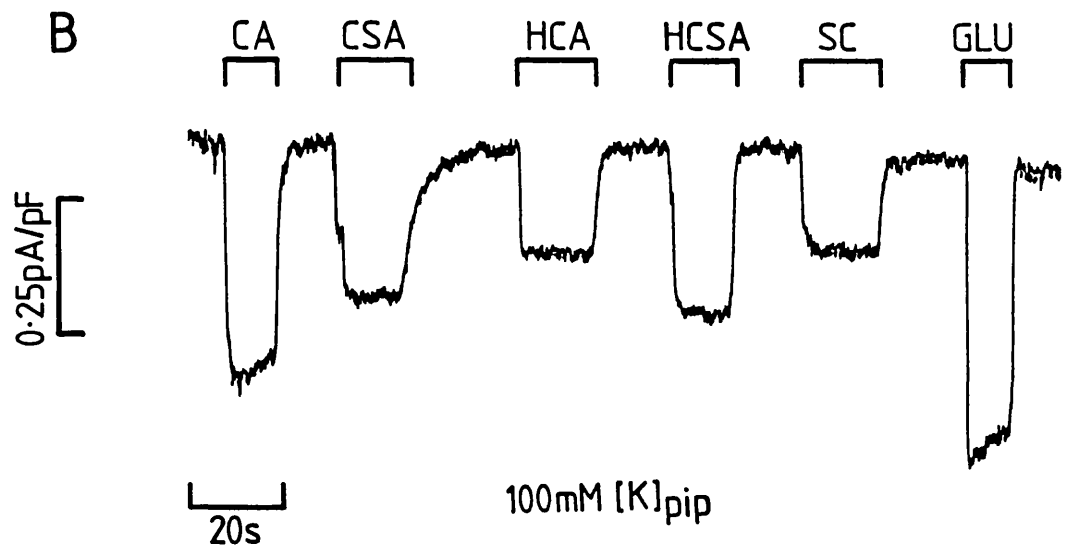
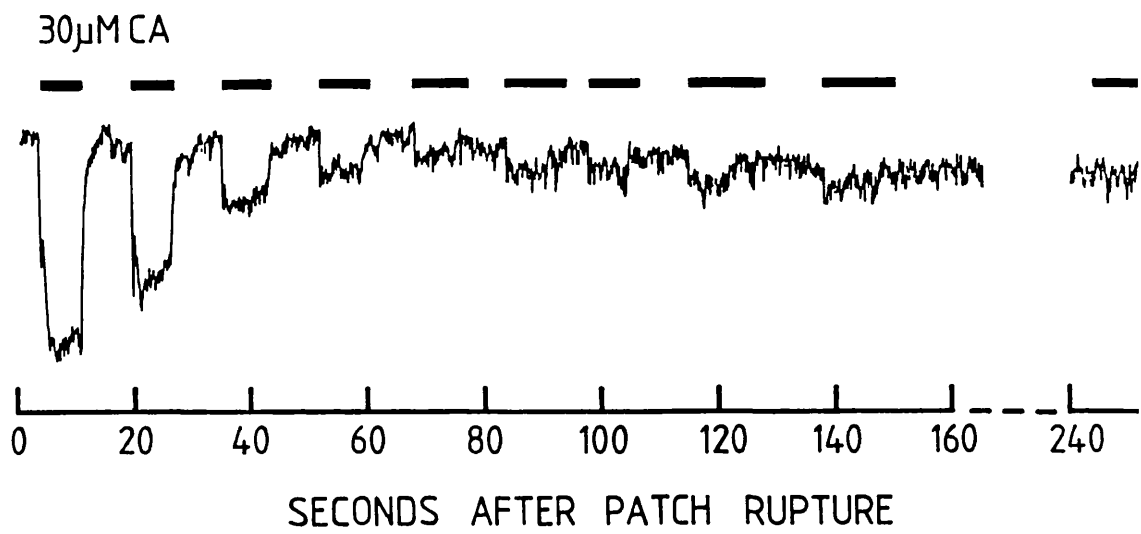


Fig 3.5 A- repeated application of CA to a cell clamped to approximately -43mV with an electrode containing no potassium, at different times after rupturing the membrane patch under the electrode and passing to whole-cell mode. The CA-evoked current declines greatly as the potassium initially in the cell diffuses out to the patch electrode. Timing of CA application shown by bars above record. B and C, currents evoked in two different Müller cells by 30 μ M CA, 100 μ M CSA, 3mM HCA, 3mM HCSA, 1mM SC and 30 μ M L-glutamate (Glu). Cells were whole-cell clamped to -43mV with pipettes containing 105mM (B) or 0mM (C) potassium. Records shown were obtained 7 min after passing to whole-cell mode (i.e. after the exchange of pipette and cell contents was complete). Currents have been normalized by cell capacitance to take account of differences in cell membrane area.



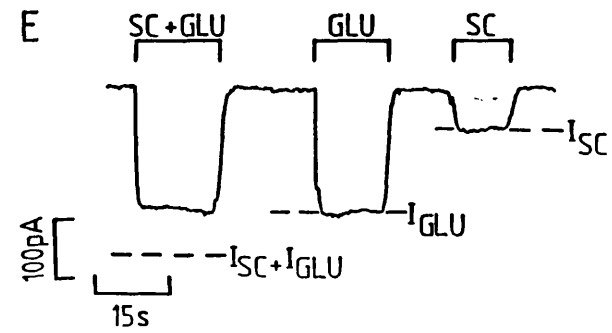
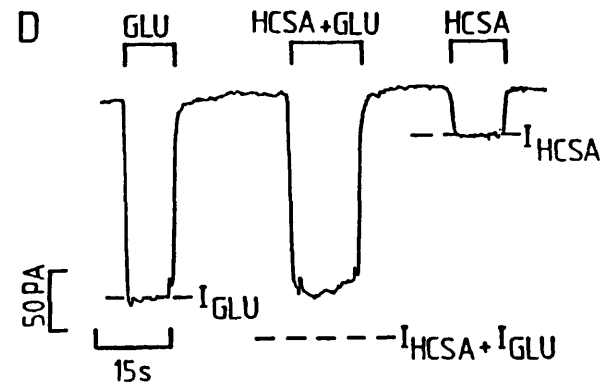
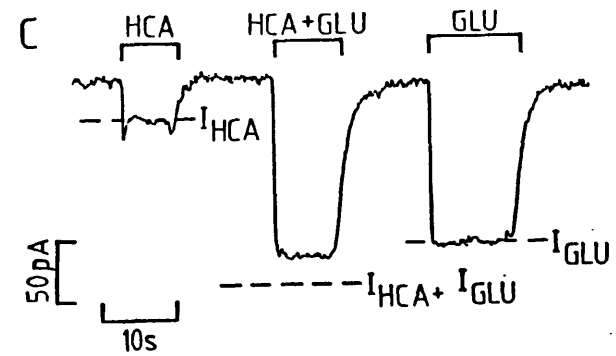
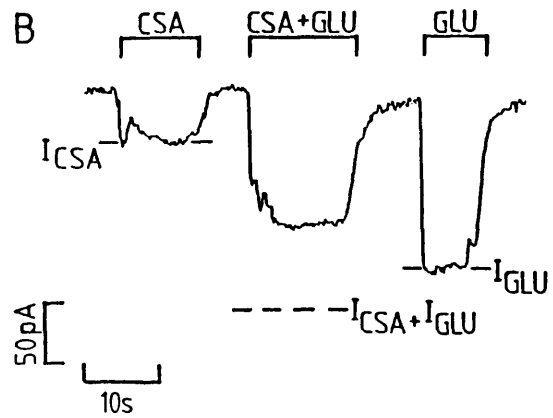
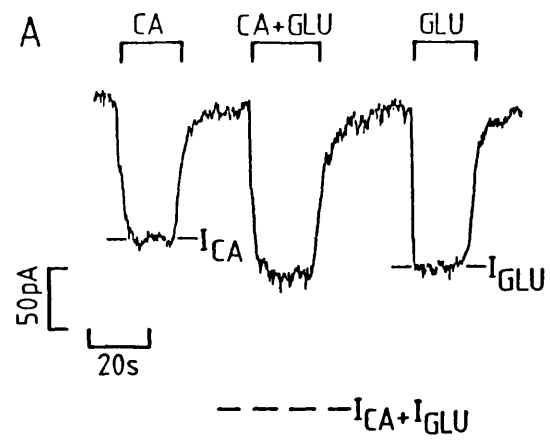
analogues were applied to a cell whole cell clamped using an internal solution containing 105mM K⁺ and Fig 3.5C shows a cell where the internal solution contained no potassium. The current magnitude was measured 7 minutes after patch rupture (whether the cells were whole cell clamped using an internal solution containing 105 or 0mM potassium) to allow for complete exchange of the solutions between the pipette and the cell, and was normalised by the cell capacitance to compensate for cells being of different sizes. The currents evoked by the analogues when the cells were whole-cell clamped using a solution containing no potassium were much smaller than those seen with potassium in the pipette although they were still significantly different from zero. In five cells recorded with 0mM [K⁺]_{pipette}, the mean currents (at -43mV, normalised by the cell capacitance) evoked by 30μM CA, 100μM CSA, 3mM HCA, 3mM HCSA and 1mM SC were on average 5.1±2.9 (mean ± sd), 3.7±2.4, 7.4±4.4, 4.0±2.2 and 6.5±4.1% of the corresponding current produced with 100mM [K⁺]_{pipette}.

The reduction of the evoked current when potassium is removed from the patch pipette is similar to that observed for the uptake of glutamate and is again consistent with the currents evoked by the sulphur-containing amino-acids reflecting their transport on the glutamate uptake carrier. The current remaining with no potassium in the pipette may be due either to non-complete removal of intracellular potassium (perhaps because it leaks slowly out of cellular organelles) or to the carrier working at a greatly reduced rate in a potassium-independent manner.

3.6 Lack of summation of currents produced by glutamate and the sulphur-containing analogues

To investigate whether L-glutamate and the sulphur-containing amino-acids are transported on the same carrier or on separate carriers (as suggested by Parsons & Rainbow, 1984), I compared the currents evoked separately by 30μM glutamate and the sulphur-containing analogues with the current evoked by the simultaneous application of glutamate and one of the amino-acids. If the transport is by separate carriers, one would expect the current evoked by simultaneous application of glutamate and one of the sulphur-containing

Fig 3.6 Competition of glutamate and sulphur-containing analogues for activation of electrogenic glutamate uptake carrier. Each panel shows the current evoked at -43mV by 30 μ M L-glutamate alone, the current evoked by one sulphur-containing analogue alone, and the current produced by application of glutamate and the sulphur-containing analogue together. Dashed lines through the traces show the currents produced by glutamate alone and by the sulphur-containing analogue alone, and also the sum of these two currents (i.e. the current which would be produced by co-application of glutamate and its sulphur analogue if they acted on different carriers). The latter current is always larger (more inward) than the actual current produced by co-application of glutamate and each sulphur-containing analogue. Sulphur-containing analogues used were: 3 μ M CA (A), 50 μ M CSA (B), 2mM HCA (C), 1mM HCSA (D) and 1mM SC (E).



analogues to be the sum of the currents evoked by the two drugs applied separately.

Fig 3.6A shows the current induced by $3\mu\text{M}$ CA, by $30\mu\text{M}$ glutamate and by the simultaneous application of the two drugs. $3\mu\text{M}$ CA and $30\mu\text{M}$ glutamate evoked currents of similar amplitude. The dashed line shows the amplitude of the sum of two currents. The simultaneous application of the two drugs evoked a much smaller current than the sum of the currents evoked by the two drugs alone. Similar results were obtained with $50\mu\text{M}$ CSA, 2mM HCA, 1mM HCSA and 1mM SC (Fig 3.6B-E).

These data rule out the possibility that the sulphur-containing analogues act solely on an uptake carrier independent of that for glutamate.

3.7 Conclusion

The data presented in this chapter are consistent with the sulphur-containing amino-acids being taken up into Müller cells by the electrogenic sodium- and potassium-dependent glutamate uptake carrier. The implication of the K_m and V_{max} values, found for the uptake for each sulphur-containing amino-acid, for their possible neurotransmitter and neurotoxic action, are considered in the discussion.

CHAPTER 4

Changes of pH induced during glutamate uptake into glial cells

4.1 Introduction

The glutamate uptake carrier is known to be powered by the co-transport of an excess of sodium ions into the cell and is also thought to counter-transport one potassium ion out of the cell, but there is still controversy over whether the carrier transports a proton into the cell on each of its cycles (see introduction, section 1.6.1). The object of the experiments described in this chapter was to investigate the possibility of the transport of a pH-changing ion on the glutamate uptake carrier (either a proton into the cell or a pH-changing anion out of the cell).

4.2 External pH changes induced during L-glutamate and D-aspartate uptake

I first investigated extracellular pH changes associated with glutamate uptake. Müller cells were bathed in a Ringer of low buffering power (50 μ M Hepes instead of the usual 5mM; solution F, table 2.2) so that any pH changes produced by the uptake carrier transporting a pH-changing ion would be increased. The pH changes were recorded just outside the cell using a pH-sensitive electrode positioned close to the cell membrane (see methods). The cells were initially whole-cell clamped at a positive potential (+7mV or +17mV). At this potential, the glutamate transporter is largely inhibited (Brew & Attwell, 1987). In the presence of 100 μ M L-glutamate, stepping the voltage from its original value to a negative value (-70mV to -85mV, at which the current evoked by glutamate uptake is large) evoked an alkalinization of the extracellular solution, shown in Fig 4.1A. Stepping the voltage negative in a similar manner but in the absence of external glutamate did not evoke any pH change: see Fig 4.3 below. The pH of the bathing solution returned to its original level as soon as the cell's membrane potential was returned to its initial positive value. Activating the uptake carrier by changing the voltage in a non-flowing solution containing glutamate, instead of by superfusing a glutamate-containing solution,

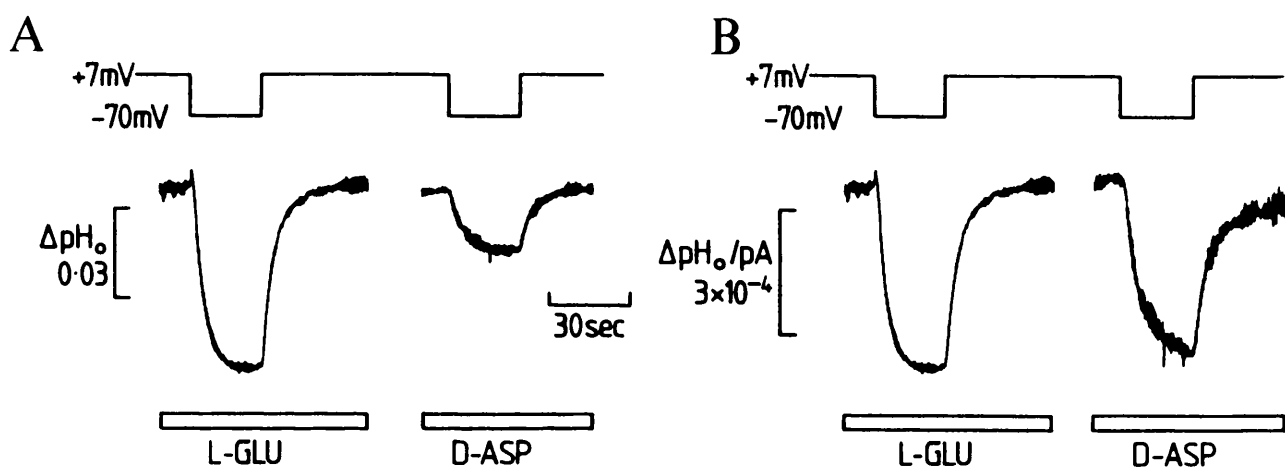


Fig 4.1: A- Extracellular pH changes (alkaline downwards) monitored when stepping the membrane voltage of a Müller cell from a positive potential (+7mV), where the activity of the uptake carrier is very small, to -70mV, where it is large, in the presence of L-glutamate (100 μ M) or D-aspartate (100 μ M). B- The same pH changes after normalisation by the increase in uptake current evoked by the voltage step in the presence of glutamate or aspartate (162 pA in L-glutamate and 54pA in D-aspartate).

prevents the external pH gradient generated by uptake being dissipated by the solution flow.

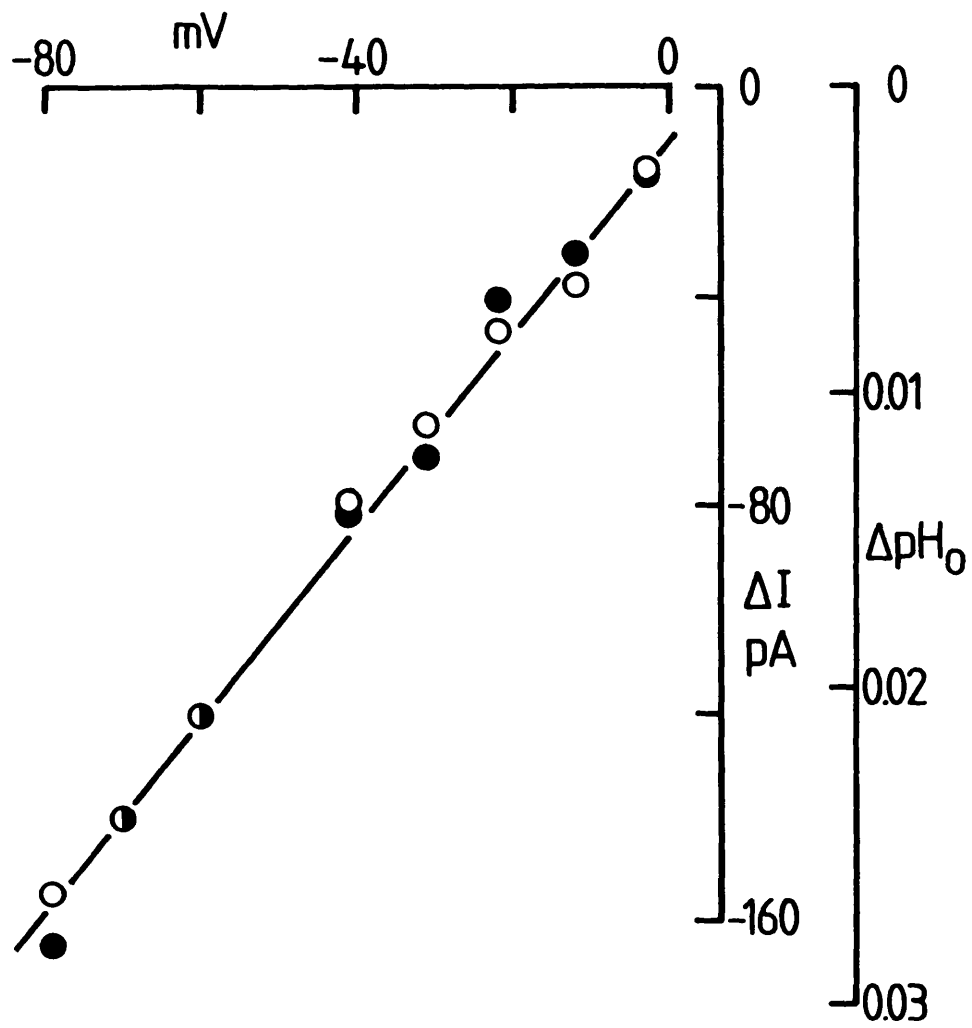
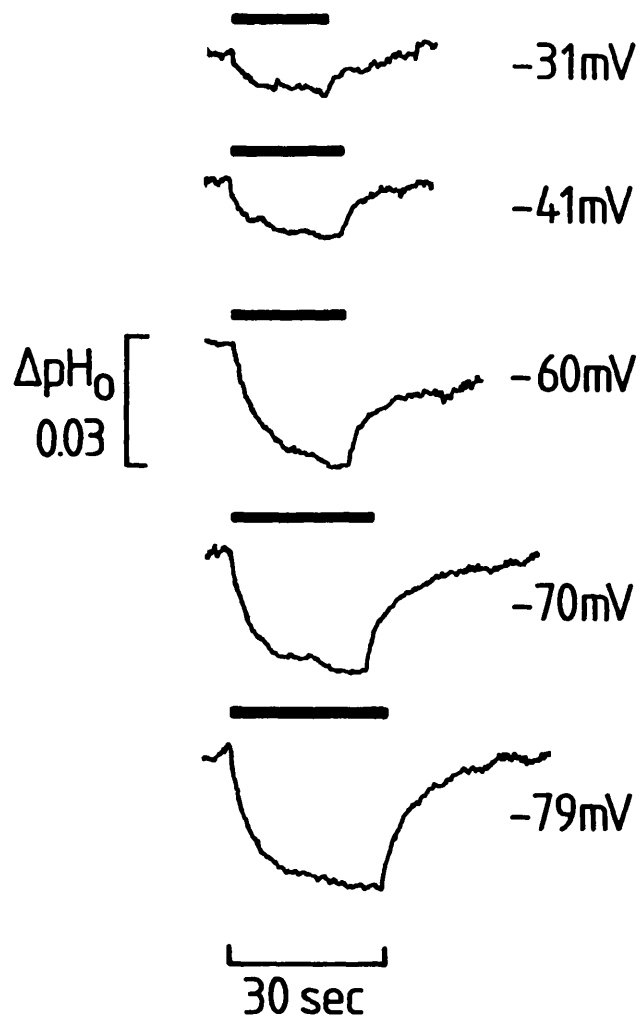
Stepping the voltage in the same way but in the presence of 100 μ M D-aspartate (which can also be transported on the glutamate uptake carrier but with a lower K_m and V_{max} ; Barbour *et al*, 1991) also made the extracellular solution go more alkaline (Fig 4.1A). As shown in Fig 4.1B, the alkalinizations evoked by L-glutamate and D-aspartate were of similar size when normalised by the increase in amplitude of the glutamate and aspartate uptake currents evoked by polarising from +7mV to -70mV (162 and 54pA for glutamate and aspartate respectively, calculated as the uptake current at -70mV minus that at +7mV). Note that for small pH changes like those in Fig 4.1, the change in extracellular $[H^+]$ is approximately proportional to the change in pH, so the fact that the pH change is proportional to the uptake current for glutamate and aspartate implies that the $[H^+]$ change is also proportional to the uptake current. These data are consistent with the notion that the stoichiometry of the uptake process is the same whether the carrier transports glutamate or aspartate. They also imply that the pH change does not result from metabolism of L-glutamate within the cell, because D-aspartate is not metabolised. In 16 cells, the ratio of the extracellular proton concentration changes (normalised by uptake current) evoked by D-aspartate and L-glutamate was 0.91 ± 0.08 (mean \pm s.e.m).

4.3 Voltage-dependence of the pH_o change

The voltage-dependence of the extracellular pH change was studied by stepping the voltage from a positive holding potential to various (more negative) potentials in the presence of 100 μ M glutamate. Fig 4.2A shows the alkalinization of the extracellular solution outside a Müller cell when the voltage was stepped from +7mV to -31, -41, -60, -70 and -79mV. The amplitude of the alkalinization was increased as the voltage step was increased. Fig 4.2B is a plot of the extracellular pH change measured 12 sec after starting the voltage step from a value of +7mV (closed circles), and of the corresponding increase in the amount of glutamate uptake current (open circles, measured relative to its value at +7mV) as a function of the test potential. The voltage-dependencies of these

Fig 4.2: Voltage dependence of the extracellular alkalinization. Müller cells were held at +7mV (where glutamate uptake is largely inhibited) in the presence of 100 μ M L-glutamate. The holding voltage was then stepped successively to various test potential to activate various amount of glutamate uptake.

A- Changes of external pH (alkaline downwards) monitored when stepping the voltage to various test potentials (indicated next to the pH trace). B- Plot of the extracellular alkalinization (\bullet) and of the increase in uptake current on polarizing from the holding potential to the test potential (\circ). For small pH changes, as here, $\Delta[H^+]_o$ is approximately proportional to ΔpH_o . Thus, $\Delta[H^+]_o$ is proportional to the uptake current flowing. Note that the uptake current plotted here is not the absolute size of the current, but its magnitude minus the magnitude at +7mV. This accounts for the apparent extrapolated reversal potential of +7mV for the current plotted here, instead of a gradual reduction of current towards zero at positive potentials (Brew & Attwell, 1987).



two quantities superimpose. Thus, the $[H^+]_o$ change is proportional to the amplitude of the glutamate uptake current flowing in the cell. Similar results were obtained in 3 cells.

4.4 Sodium-dependence of the pH_o change

The glutamate uptake carrier is known to be powered by sodium ions being transported into the cell on each cycle of the carrier. As a result, when external sodium is completely replaced by choline, glutamate uptake is completely abolished (Kanner & Sharon, 1978a; Brew & Attwell, 1987). It was therefore important to study the sodium-dependence of the extracellular pH change. For that purpose, the experiment of Fig 4.1 was repeated in either sodium-free solution (sodium totally replaced by choline; solution D, table 2.1) or in the control solution containing sodium (solution B, table 2.1). Fig 4.3A shows the pH change monitored by a pH electrode outside the cell when the holding voltage was stepped from +17mV to -83mV in the presence of 100 μ M L-glutamate. Note that no pH change was observed when the voltage was stepped in the absence of L-glutamate. Fig 4.3B shows the same experiment carried out on the same cell but in a solution lacking sodium. Stepping the voltage in the absence or in the presence of L-glutamate did not evoke any extracellular alkalinization.

The sodium-dependence of the extracellular pH change is consistent with it being due to the activity of the glutamate uptake carrier.

4.5 Changes of extracellular pH evoked during glutamate uptake when using patch pipettes of different series resistance

The glutamate uptake carrier transports an excess of sodium ions into the cell on each cycle (see introduction, section 1.6.1). It is possible, therefore, that the extracellular pH change observed when activating the uptake carrier is not due to a pH-changing ion being transported on the uptake carrier but is due to the secondary activation of a pH-regulating mechanism (for example Na^+/H^+ exchange or Na^+/HCO_3^- co-transport) following an increase of intracellular sodium concentration generated by glutamate uptake. To investigate this

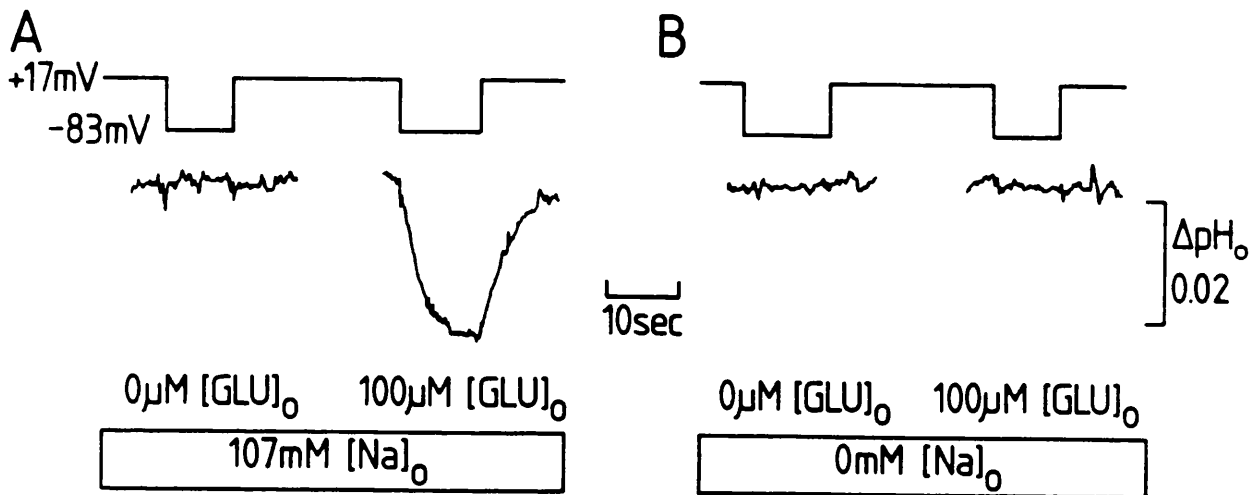


Fig 4.3: Dependence of the external pH change on external sodium. A- Müller cells were held at +17mV (where the uptake carrier is poorly activated) and the holding voltage was stepped negative first of all in the absence of glutamate in a bathing solution containing the normal concentration of sodium (107mM), and then in a solution containing 100 μ M L-glutamate. Stepping the voltage to -83mV in the absence of glutamate did not evoke any extracellular pH change. In contrast, stepping the voltage in the presence of 100 μ M glutamate evoked an extra inward current (not shown) due to glutamate uptake, accompanied by an external alkalinization. B- The same procedure was then performed in an external bathing solution lacking sodium (replaced by choline). Stepping the voltage in these conditions did not evoke any pH change whether glutamate was present or absent.

Fig 4.4: Concentration of internal Na⁺ during glutamate uptake.

Na⁺ influx occurs when glutamate uptake is activated (probably 2 Na⁺ ions are transported into the cell on each cycle of the carrier). These ions either accumulate inside the cell or diffuse into the patch pipette. Now, in general,

$$d[\text{Na}^+]_i/dt = (\text{Influx} - \text{Efflux})/\text{cell volume}$$

Volume: The volume of the cell is typically $V=10^{-14} \text{ m}^3$.

Influx: This depends on the current. Let us assume a current of 200pA. The uptake current is generated because (probably) one net positive charge is transported into the cell on each cycle of the carrier (see chapter 7). 200 pA corresponds to $2 \cdot 10^{-10}/96500$ mole of charge per second. If the carrier transports 2 Na⁺ ions into the cell per cycle and the volume of the cell is $V= 10^{-14}\text{m}^3$, the sodium influx is

$$\begin{aligned} \text{Influx} &= (4 \cdot 10^{-10}/96500) \text{ mole per second} \\ &= 4.15 \times 10^{-15} \text{ mole per second} \\ &= I \end{aligned}$$

Efflux: The efflux to the patch pipette is proportional to the diffusion coefficient of sodium, D, and the area of the diffusion barrier at the end of the pipette, A, and inversely proportional to the length of the diffusive barrier, Δx. For simplicity, transmembrane efflux on the Na⁺/K⁺ pump or other membrane carriers and channels is ignored.

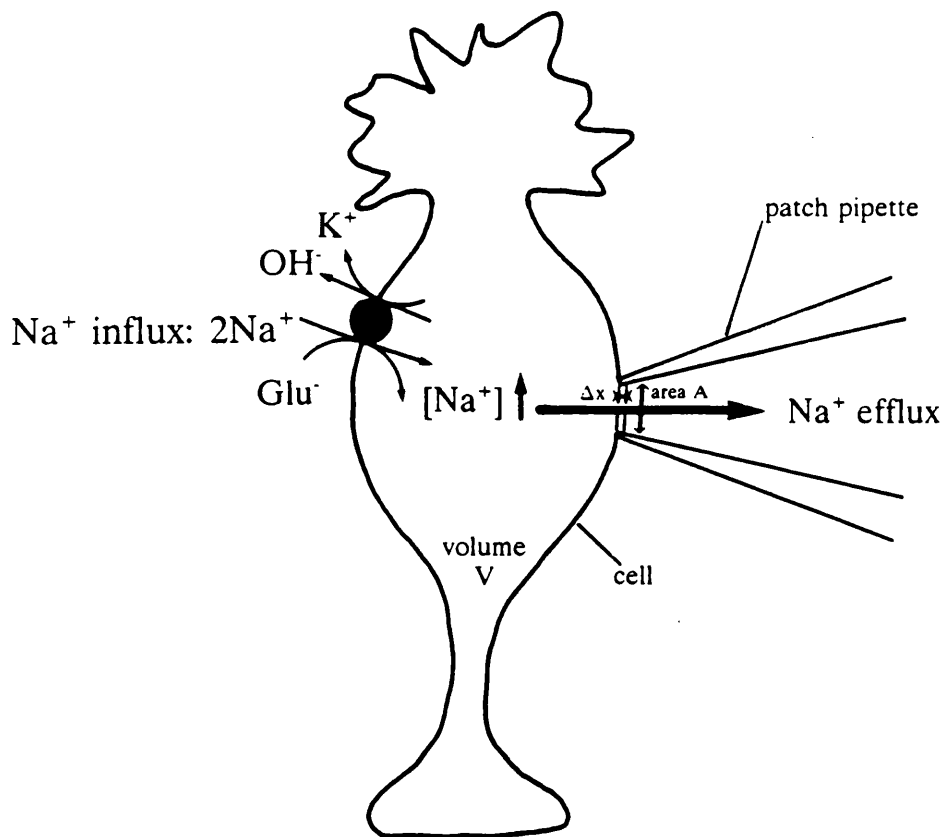
$$\text{Efflux} = DA (\text{Na}^+_i - \text{Na}^+_{\text{pipette}})/ \Delta x \text{ (the pipette sodium concentration is 15mM).}$$

An expression for A/Δx can be obtained from the series resistance of the pipette. $R_s = (\rho \cdot \Delta x)/A$; where ρ is the resistivity of the pipette solution.

Therefore, $A/\Delta x = \rho/R_s$ and $V \cdot d[\text{Na}^+]_i/dt = I - \{D\rho \cdot ([\text{Na}^+]_i - [\text{Na}^+]_{\text{pipette}})/R_s\}$

Thus, the steady state $[\text{Na}^+]_i$ reached (when $d[\text{Na}^+]_i/dt = 0$) is

$$[\text{Na}^+]_{i\infty} = (I \cdot R_s)/(D\rho) + \text{Na}^+_{\text{pipette}}$$



and the time constant with which this is reached is

$$\tau = (R_s \cdot V) / (D \cdot \rho)$$

Now, $D_{\text{NaCl}} = 1.5 \cdot 10^{-9} \text{ m}^2 \text{ s}^{-1}$; $R_s = 2 \text{ M}\Omega$; and $\rho = 0.8 \text{ }\Omega \text{ m}$ for 100 mM KCl , so

$$[\text{Na}^+]_{i\infty} = (I \cdot R_s) / (D \rho) + \text{Na}^+_{\text{pipette}} = (4.15 \cdot 10^{-15} \times 2 \cdot 10^6) / (1.5 \cdot 10^{-9} \times 0.8) + 15$$

$$= 21.9 \text{ mole} \cdot \text{m}^{-3} = 21.9 \text{ mM} \text{ and}$$

$$\tau = (R_s \cdot V) / (D \cdot \rho) = (2 \cdot 10^6 \times 10^{-14}) / (1.5 \cdot 10^{-9} \times 0.8) = 17 \text{ seconds}$$

or if $R_s = 30 \text{ M}\Omega$, $[\text{Na}^+]_{i\infty} = (I \cdot R_s) / (D \rho) + \text{Na}^+_{\text{pipette}} = 119 \text{ mole} \cdot \text{m}^{-3} = 119 \text{ mM}$

$$\text{and } \tau = (R_s \cdot V) / (D \cdot \rho) = (30 \cdot 10^6 \times 10^{-14}) / (1.5 \cdot 10^{-9} \times 0.8)$$

$$\approx 4 \text{ minutes}$$

In practise, such a large calculated rise in $[\text{Na}^+]_i$ would have to be accompanied by a fall in $[\text{K}^+]_i$ for osmotic reasons.

Fig 4.5: Dependence on electrode series resistance of the external $[H^+]_o$ change (calculated from equation section 2.5.4 as the total effective transmembrane proton flux needed to generate the observed $[H^+]_o$ change, given the buffering power at the initial value of pH). The $[H^+]_o$ change was normalised by the ratio of the glutamate uptake current/ $\sqrt{\text{cell capacitance}}$ (see below for why this normalisation is used). Regression line is not significantly different from horizontal ($p > 0.10$; test of independence between two values), while the theory below predicts a straight line through the origin.

Theoretical prediction for $[H^+]_o$ change if it is generated by a rise in $[Na^+]_i$ activating Na^+/H^+ exchange.

On the hypothesis that Na^+/H^+ exchange generates the pH_o change, the fact that doubling the glutamate uptake current doubles the pH_o change (Fig 4.2) implies that the proton flux on the Na^+/H^+ exchanger is proportional to the change in $[Na^+]_i$ produced by uptake, i.e. Proton flux $\propto \Delta[Na^+]_i$.

Now, the predicted $\Delta[Na^+]_i$ produced by uptake is proportional to the uptake current $\times R_s$ (see legend to Fig. 4.4).

Thus, $\Delta[Na^+]_i \propto I_{Glu} \times R_s$

and so Proton flux $\propto I_{Glu} \times R_s$.

In a spherical cell of radius a , the $\Delta[H^+]_o$ generated by a proton flux on the Na^+/H^+ exchanger is proportional to: (proton flux)/ a (see equation 5, section 7.2.4).

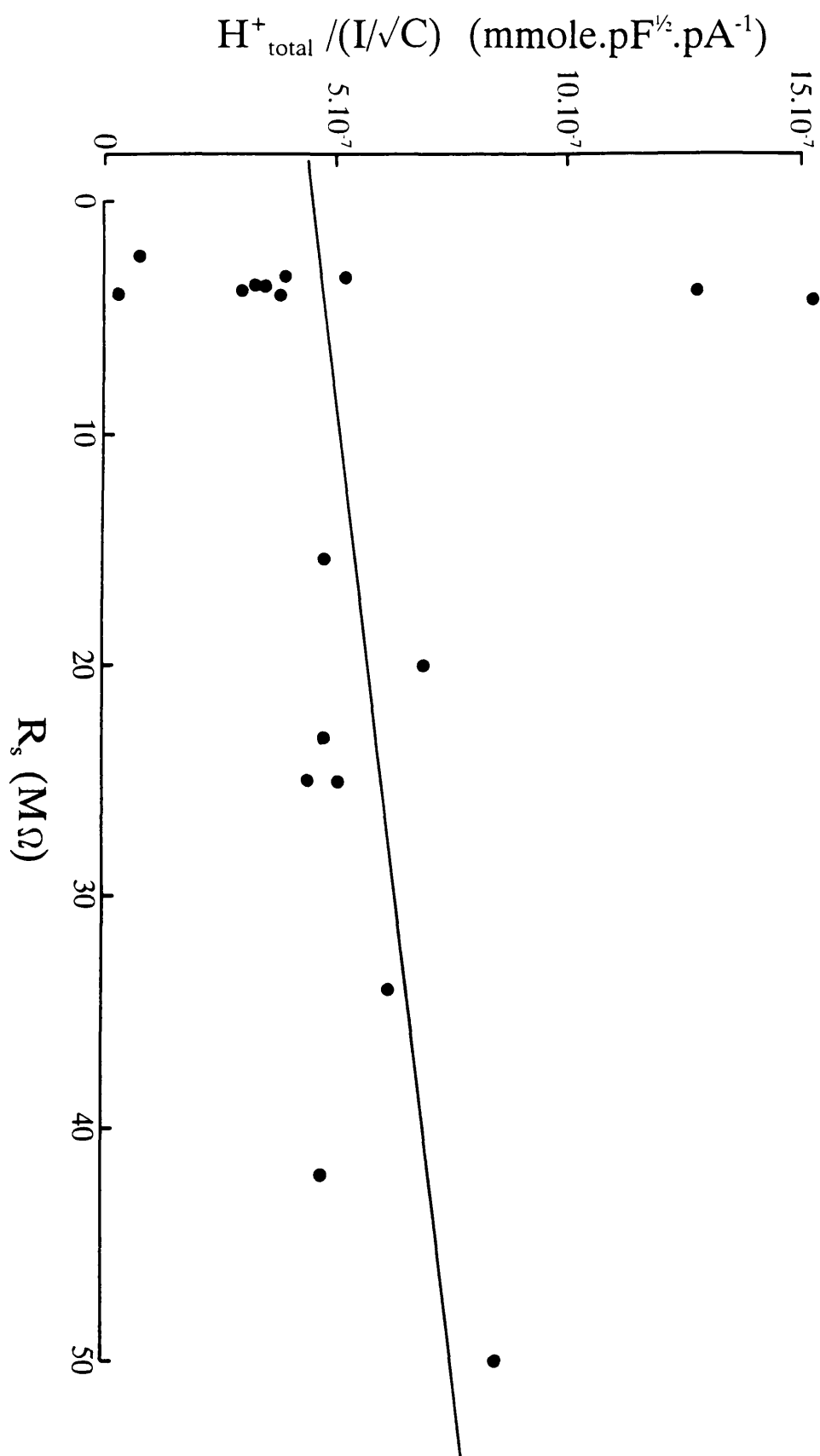
Thus, $\Delta[H^+]_o \propto (\text{Proton flux}/a) \propto (I_{Glu} \times R_s)/a$

Now, a is proportional to \sqrt{C} , where C is the cell capacitance

so $\Delta[H^+]_o \propto (I_{Glu} \times R_s)/\sqrt{C}$

and $\Delta[H^+]_o/(I_{Glu}/\sqrt{C}) \propto R_s$

Thus, a plot of $\Delta[H^+]_o/(I_{Glu}/\sqrt{C})$ against R_s should be a straight line through the origin.



possibility, Müller cells were whole-cell clamped using patch pipettes of different series resistance. The series resistance was varied by systematically altering the heat settings at which the electrodes were pulled. Pipettes of low series resistance (typically $2\text{M}\Omega$) allow the cell to be very thoroughly perfused, therefore the intracellular sodium concentration does not rise significantly. In contrast, patch pipettes of high R_s (up to $50\text{M}\Omega$) favour an increase of intracellular sodium concentration by reducing diffusion into the patch pipette (calculations on this point are given in the legend to Fig 4.4).

Fig 4.5 shows the size of the pH_o change measured outside 18 different cells divided by the amplitude of the uptake current in each cell as a function of the series resistance of the patch pipette used to whole-cell clamp the cell. If a rise in $[\text{Na}^+]_i$ was responsible for generating the pH_o change indirectly, the normalised $[\text{H}^+]_o$ change is predicted to be proportional to series resistance (i.e. the graph should be a straight line through the origin: see Fig legend 4.5). In fact, there was no significant difference in size of pH_o response in cells whole-cell clamped with pipettes of small and large series resistance. This result suggests that the extracellular pH change measured during glutamate uptake is not due to secondary activation of a pH-regulating mechanism sensitive to an increase of intracellular sodium concentration.

4.6 Effect of amiloride on the pH_o change evoked by glutamate uptake

Blocking the pH-regulating mechanisms provides an alternative way to check that extracellular pH changes were not due to the glutamate uptake carrier raising $[\text{Na}^+]_i$. For this purpose, Müller cells were voltage-clamped at $+17\text{mV}$ and bathed in a low buffer solution (solution F, table 2.2) containing $100\mu\text{M}$ L-glutamate with or without 1mM amiloride, which blocks Na^+/H^+ exchange by 90% (Putnam *et al*, 1986). As shown in Fig 4.6, stepping the voltage to activate the glutamate uptake carrier produced an extracellular alkalinization, and the amplitude of this pH change was not significantly different in the presence of 1mM amiloride. In 5 cells, the ratio of the extracellular pH change (divided by the size of the uptake current) in the presence and the absence of 1mM amiloride was 0.953 ± 0.042 (mean \pm sem). This implies that the extracellular

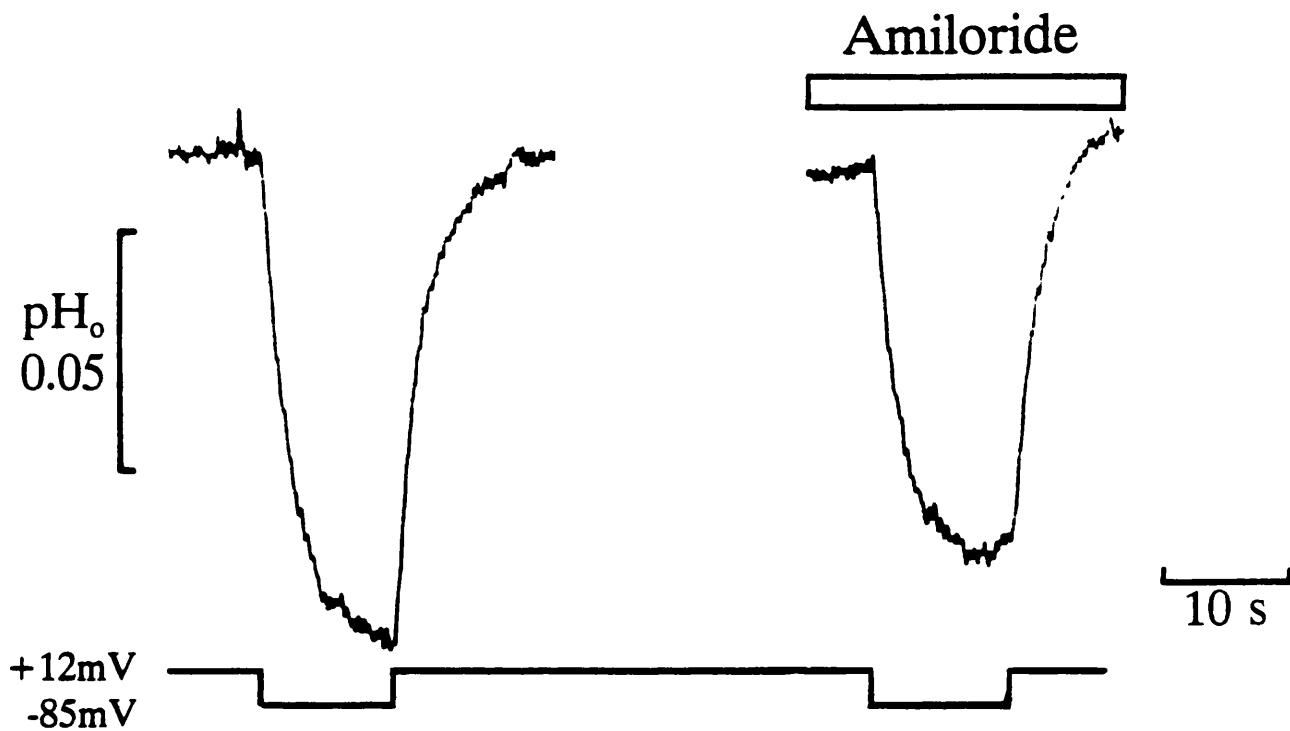


Fig 4.6: Lack of amiloride-sensitivity to the extracellular alkalinization. The first panel shows the extracellular alkalinization evoked by a cell when the holding voltage was stepped from +17mV to -67mV in a low buffer solution containing 100 μ M L-glutamate. The other panel shows the external pH change evoked by the same cell when stepping the voltage from +17mV to -67mV in the presence of 100 μ M L-glutamate and 1mM amiloride (blocker of the Na⁺/H⁺ antiporter). The ratio of the pH change normalized by the amplitude of the uptake current (to compensate for slight rundown of the uptake current with time) in the presence and in the absence of amiloride was 0.953 ± 0.042 (mean \pm sem; n=5). This value is not significantly different from 1 (Student test; $p > 0.1$).

pH change observed is not due to a secondary activation of the Na^+/H^+ antiporter by a raised $[\text{Na}^+]_i$.

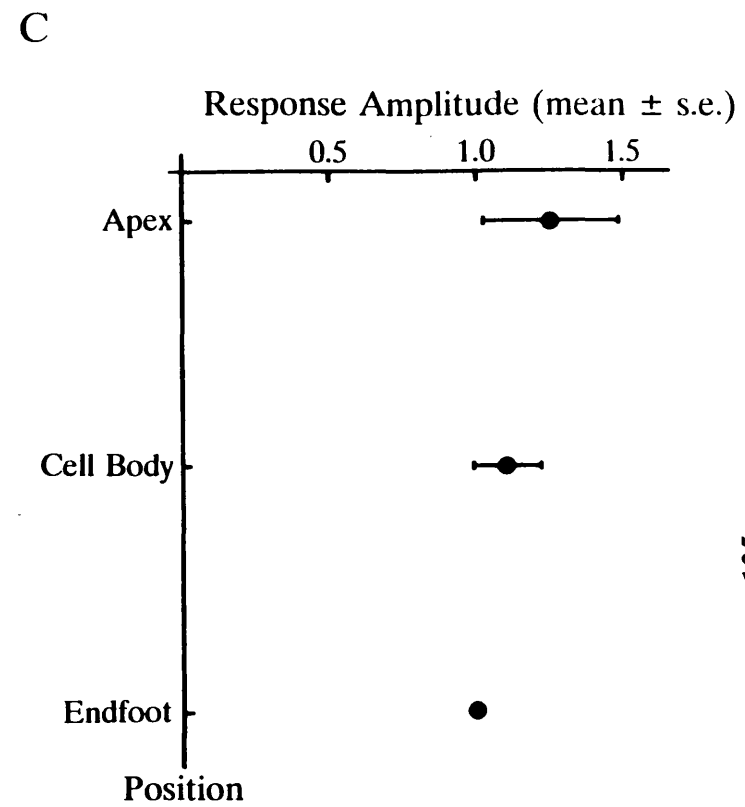
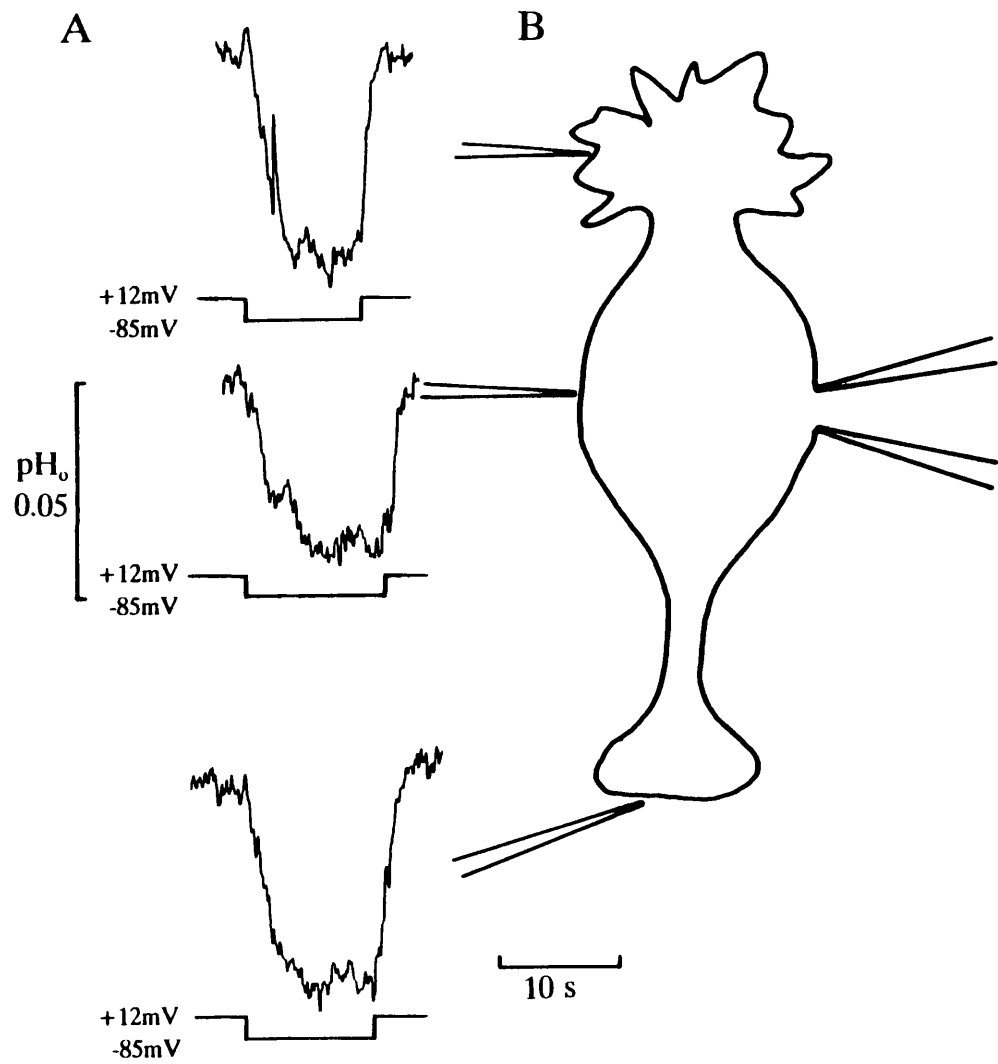
4.7 Measurements of the extracellular pH changes at different parts of the cell

It was not possible to perform a similar experiment as the above using DIDS or harmaline to block the $\text{Na}^+/\text{HCO}_3^-$ co-transporter, since both these drugs affected the pH electrode. A different approach to further control for this possibility was therefore used.

It is known that the Müller cells' $\text{Na}^+/\text{HCO}_3^-$ co-transporter is concentrated at the endfoot of the cell (Newman & Astion, 1991). An experiment to measure the glutamate-evoked extracellular alkalinization at different parts of the cell was therefore performed, to assess the possibility that a secondary activation of the sodium/bicarbonate co-transporter might be the origin of the extracellular alkalinization. For this experiment, Müller cells were whole-cell clamped at +17mV and the pH-sensitive electrode was positioned outside various parts of the cell, keeping the distance between the cell membrane and the tip of the electrode as constant as possible (measured during the experiment on a TV monitor attached to a camera viewing the preparation via the microscope). Fig 4.7 shows the pH_o changes recorded from a typical cell when the holding voltage was stepped to -67mV in low buffer solution containing 100 μM L-glutamate (solution F, table 2.2). In 8 cells, the pH_o change values normalised to the pH change at the endfoot were 1, 1.102 ± 0.103 and 1.254 ± 0.215 (mean \pm sem) for the endfoot (vitreal part), the cell body and the apical membrane respectively.

In Müller cells 60% of the total number of $\text{Na}^+/\text{HCO}_3^-$ transporters are located at the endfoot which is in contact with the vitreous humour (Newman & Astion, 1991). This non-uniformity does not match the spatial distribution of the pH_o change produced by glutamate uptake. This strongly suggests that the observed extracellular alkalinization is not due to secondary activation of the $\text{Na}^+/\text{HCO}_3^-$ co-transporter by uptake raising $[\text{Na}^+]_i$.

Fig 4.7: Mapping of the external pH change. Müller cells were whole-cell clamped at +17mV and bathed in a low buffer solution containing 100 μ M L-glutamate. The pH electrode was successively positioned at different parts of the cell and the holding voltage was stepped to -67mV to activate the glutamate uptake carrier. The figure shows typical recordings of extracellular alkalinization at the different parts of the cell. The pH measurements at the different parts of the cell were made in a random order and several measurements were made for the same cell at the same position. In 8 cells, the pH changes (normalised to the value of the pH change at the endfoot) had relative amplitudes (mean \pm sem) of 1, 1.102 \pm 0.103 and 1.254 \pm 0.215 at the endfoot, the cell body and the apical membrane respectively.



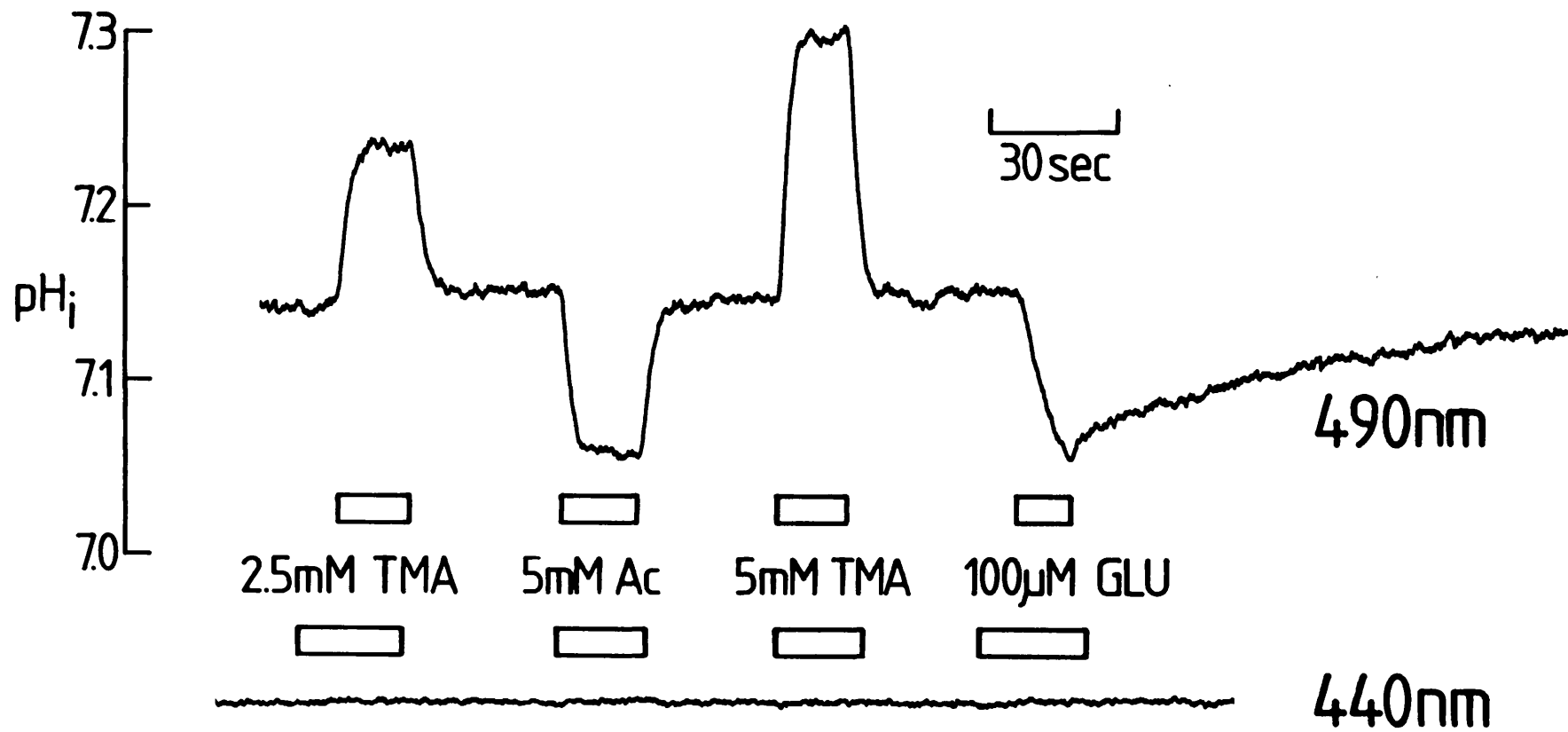
4.8 Internal pH changes induced during L-glutamate uptake

If the glutamate uptake carrier transports a pH-changing ion, then it should generate a pH change inside the cell of the opposite sign to that generated outside the cell. To test this, Müller cells were whole-cell clamped using an internal solution containing BCECF, a pH-sensitive fluorescent dye (solution L, table 2.3). With excitation at 490nm wavelength, BCECF fluorescence is increased at more alkaline pH values (see Methods). Fig 4.8 top shows 490nm fluorescence of a cell loaded with BCECF and clamped at -43mV during the application of the weak base trimethylamine (TMA, which makes the cell alkaline and increases the fluorescence) and of the weak acid acetate (Ac, which acidifies the cell and decreases the fluorescence). Two concentrations of TMA and one of Ac were applied to calibrate the fluorescence trace in terms of pH (Eisner *et al*, 1989). This calibration method gave results similar to calibration with nigericin (see Methods), and was preferred because nigericin kills all the cells in the experimental chamber (not just the one being studied).

After the calibration solutions in fig 4.8 top, 100 μ M glutamate was applied and generated a decrease of fluorescence, corresponding to an acidification of about 0.1 pH units. After removing glutamate, the pH recovered slowly. The dye BCECF has an isosbestic wavelength of around 440nm (see Methods). Fig 4.8 bottom shows (in the same cell) that neither the weak acid and base nor glutamate generated a change of the fluorescence excited at 440nm wavelength.

In 45 cells, the mean pH change evoked by 20 seconds of 100 μ M L-glutamate was 0.23 ± 0.04 (mean \pm sem). The calibration method used allows one to calculate the buffering power of the cells. The mean value (\pm s.e.m) calculated for 50 cells was 19.8 ± 4.6 mM/pH unit. If one H⁺ were transported into the cell (or one OH⁻ out of the cell) for each elementary charge of uptake current flowing into the cell (e.g. 1 H⁺ or OH⁻ moved per carrier cycle) then, for a typical uptake current of 200pA (at -43mV) flowing for $t = 20$ seconds into a cell of typical volume $V = 10^{-14}$ m³ and buffering power $\beta = 20$ mM/pH unit, a pH change of $t(I/F)/(\beta V) = 0.2$ units is predicted (where F is the Faraday). This is similar to the observed mean value of 0.23 units. By contrast, if the pH change

Fig 4.8: Internal pH of Müller cells monitored with BCECF ($96\mu\text{M}$) included in the internal solution and loaded into the cells through the patch pipette. Variations of intracellular pH were recorded as fluorescence changes monitored at 530 nm when the dye was excited at 490 nm (see methods chapter). Applying a weak base (trimethylamine, TMA, 2.5mM or 5mM) or weak acid (acetate, Ac, 5mM) made the intracellular pH of the cell go alkaline or acid respectively (seen as increases or decreases of the amount of fluorescence). Applying L-glutamate ($100\mu\text{M}$) evoked an intracellular acidification. The same experiments performed with the dye excited at 440nm (near the isosbestic wavelength) did not show any change of fluorescence evoked by TMA, Ac or glutamate. This record was obtained immediately after the 490 nm record, and after this 440 nm record was obtained, another 490 nm response to glutamate was recorded which was similar to the response shown in the top of this figure.



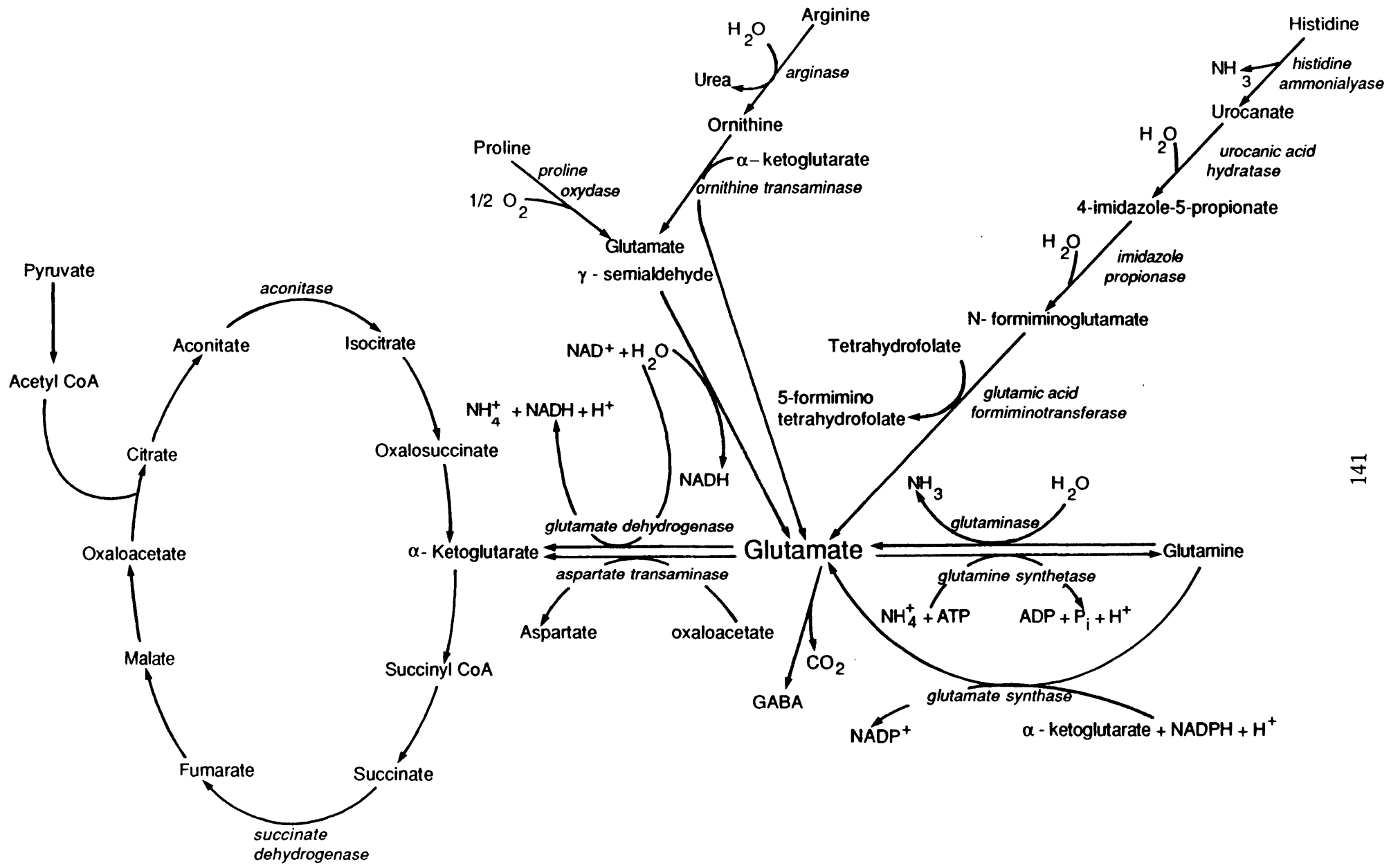
were produced by HCO_3^- ions being transported out of the cell on the uptake carrier, approximately 9 HCO_3^- would have to be transported per carrier cycle to generate the same pH change (because the pK' value of HCO_3^- is 6.1 so most of the transported bicarbonate ions will not leave a proton in the cell or bind one at the outside of the cell).

4.9 Is the intracellular pH change evoked by L-glutamate due to metabolism?

L-glutamate, being a metabolisable agonist, could produce an intracellular acidification by being metabolised inside the cell. Fig 4.9 shows the different metabolic pathways involving glutamate. Several of them could be responsible for the intracellular acidification detected when L-glutamate uptake is activated. To investigate this possibility, I first of all compared the pH change evoked by glutamate and by the uptake of a non-metabolised analogue of glutamate. D-aspartate is known to be transported on the glutamate uptake carrier, although the affinity for its transport is higher than that of L-glutamate (Barbour *et al*, 1991). Moreover, D-aspartate is not metabolised and therefore cannot produce a metabolic pH change. Fig 4.10 shows uptake currents and pH changes produced in the same cell by $100\mu\text{M}$ L-glutamate and D-aspartate. D-aspartate was applied at a more negative potential (-63mV) than L-glutamate (-43mV) to increase its uptake current: the V_{max} (actually I_{max} for a voltage clamp experiment) of aspartate uptake is about one quarter of that for L-glutamate (Barbour *et al*, 1991). Both D-aspartate and L-glutamate evoked an intracellular acidification. The pH change evoked by D-aspartate (like the uptake current) was smaller than that evoked by L-glutamate. However, the intracellular acidification per pA of uptake current was not significantly different for the two agonists (ratio D-aspartate/L-glutamate = 0.98 ± 0.1 (mean \pm sem) in 20 cells). This strongly suggests that the acidification accompanying the uptake of L-glutamate is not due to its metabolism inside the cell secondary to its uptake.

To verify this point further, experiments were performed where Müller cells were whole-cell clamped with either of two different internal (pipette) solutions, one containing metabolic poisons, and the other being the control solution lacking the poisons. The metabolic poisons used were (see methods for

Fig 4.9: This diagram shows the metabolic pathways by which L-glutamate can be metabolised. Several of them produce or consume protons and therefore could be responsible for an intracellular pH change following L-glutamate uptake.



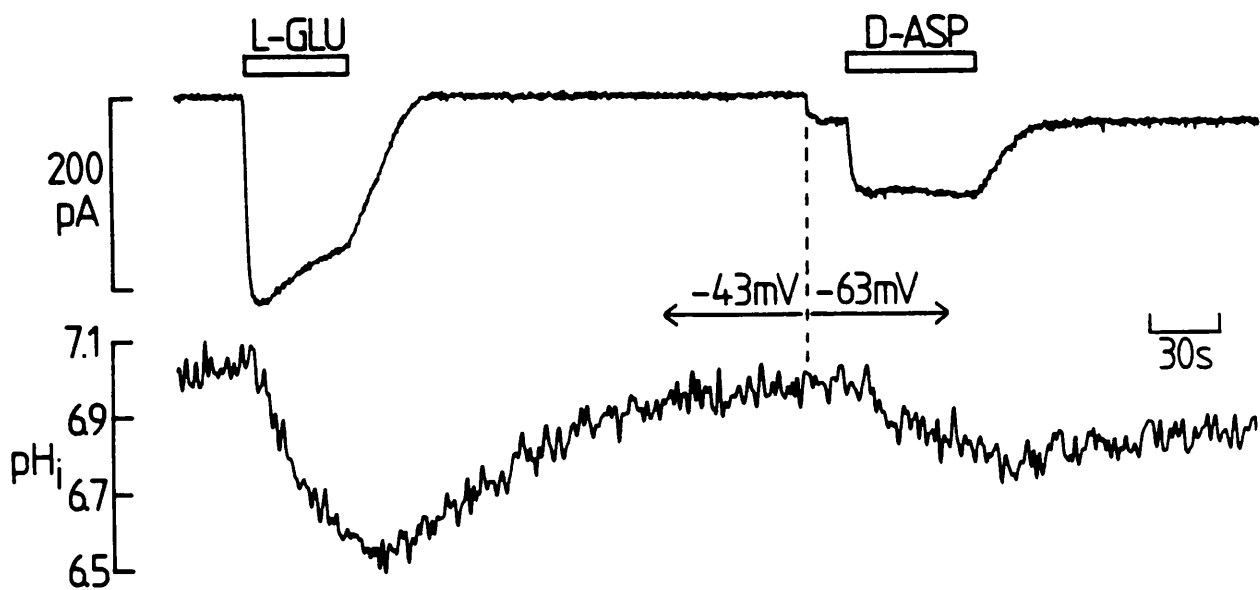


Fig 4.10: Intracellular acidification induced during L-glutamate and D-aspartate uptake. Top trace shows the inward current generated by L-glutamate (left) and D-aspartate (right) uptake into Müller cells. Bottom trace shows the drop in the fluorescence emission at 530nm of the BCECF excited at 490nm indicating an acidification of the intracellular pH. The current evoked by D-aspartate was smaller than that evoked by L-glutamate but so was the internal pH change.

details of the concentrations: solution M, table 2.3):

Na-malonate (blocks the Krebs cycle)

Na-oxalomalate (blocks the Krebs cycle)

aminooxyacetic acid (blocks glutamate transaminase)

methionine sulphoximine (blocks glutamine synthetase)

albizziin (blocks glutaminase)

iodoacetate (blocks glyceraldehyde 3-phosphate dehydrogenase)

N-ethylmaleimide (blocks mitochondrial glutamate transport)

pyridoxal-5-phosphate (blocks glutamate dehydrogenase)

rotenone (blocks mitochondrial electron transport and thus prevents ATP formation).

For both internal solutions, 7 minutes was allowed after going to whole-cell mode to allow equilibration of the pipette solution with the cell cytoplasm. L-glutamate ($100\mu\text{M}$) and D-aspartate ($100\mu\text{M}$) were applied successively to the cells and the ratios of the evoked pH changes per pA of uptake current were calculated.

In the 21 cells containing metabolic poisons, the ratio $(\text{pH}_{\text{asp}}/I_{\text{asp}})/(\text{pH}_{\text{glu}}/I_{\text{glu}})$ was 1.01 ± 0.12 (mean \pm sem), similar to the value of 0.98 ± 0.10 quoted above for the control cells. These results rule out the possibility of the observed intracellular acidification being due to metabolism. Possibly little or no metabolic contribution to the pH change is observed because cytoplasmic enzymes are dialysed into the pipette when very large electrodes ($2\text{M}\Omega$ series resistance for these experiments) are used.

4.10 Sodium dependence of the pH_i change

It has been shown previously that glutamate uptake is dependent on external sodium (Peterson & Raghupathy, 1972; Kanner & Sharon, 1978a; Brew & Attwell, 1987). It was therefore important to study the sodium-dependence of the intracellular pH change induced by L-glutamate and D-aspartate. L-glutamate was applied to the cells by bath perfusion in a sodium-free solution (sodium completely replaced by choline; solution D, table 2.1) in between applications in sodium-containing solutions. In the absence of external sodium, the uptake

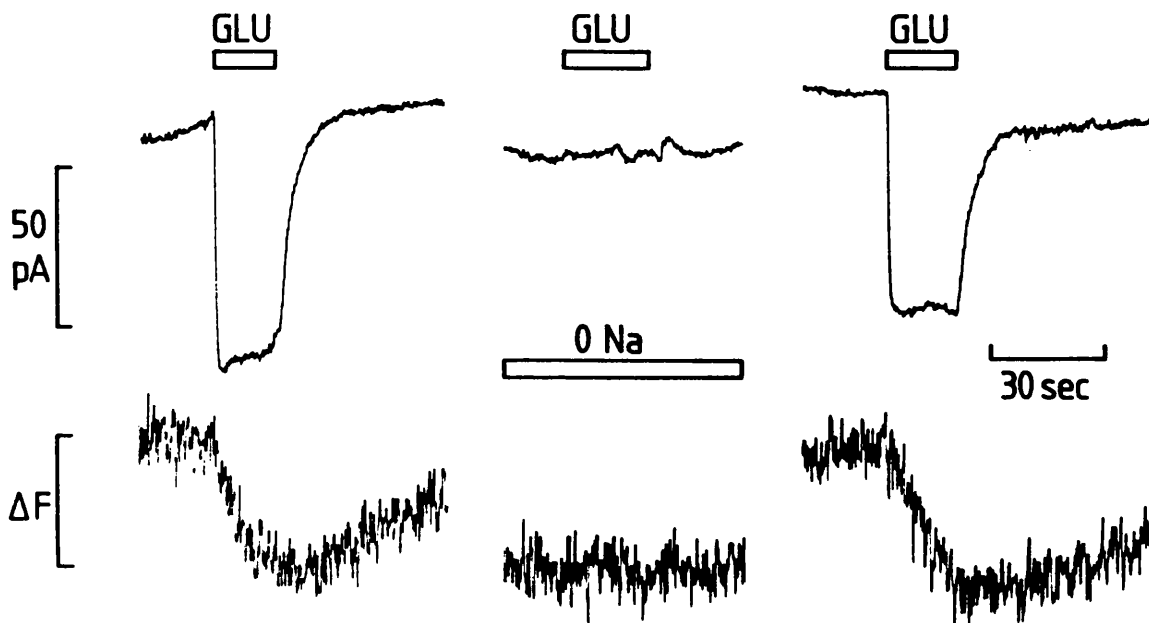


Fig 4.11: Dependence of the intracellular acidification on external sodium. Top traces show the inward membrane current generated by glutamate uptake in the presence of extracellular sodium ions (far left and far right). Application of the same dose of glutamate in the absence of external sodium ions (middle trace) did not evoke any membrane current. Bottom traces are the changes in fluorescence emission indicating an acidification (acidification is downwards) of the intracellular medium accompanying the uptake of glutamate (far left and far right traces) and the lack of a change of fluorescence emission (middle trace) in the absence of external sodium ions. The fluorescence was not calibrated in terms of pH changes for this cell.

current evoked by L-glutamate was totally abolished and so was the intracellular acidification (Fig 4.11). Thus, like the uptake of glutamate, the intracellular pH change is dependent on external sodium. This result further supports the idea that the intracellular acidification reflects the activity of the glutamate uptake carrier.

4.11 Amiloride sensitivity of the internal pH acidification

As for the external pH change, it was important to check that the intracellular acidification of the cell accompanying L-glutamate and D-aspartate uptake was not due to secondary activation of a pH-regulating transporter caused by sodium transport on the uptake carrier raising the $[Na^+]$ inside the cell. For this purpose, experiments were first performed to compare the intracellular pH change in the presence and in the absence of amiloride (1mM), a blocker of the Na^+/H^+ transporter. This dose of amiloride blocks Na^+/H^+ exchange by 90% (Putnam *et al*, 1986). Fig 4.12 shows the intracellular acidification of a typical cell when L-glutamate (100 μ M) was applied to the cell first in the control conditions and then in the presence of 1mM amiloride. The fluorescence changes (proportional to pH changes) are normalised by the size of the uptake current (divided by cell capacitance), to compensate for a slight rundown of the uptake current over time. In 5 cells, the ratio of the change of fluorescence (normalised by uptake current) in the presence of amiloride and in the absence of the blocker was:

$$(F/I)_{+ \text{ amiloride}} / (F/I)_{\phi \text{ amiloride}} = 0.95 \pm 0.04 \text{ (mean } \pm \text{ sem).}$$

Thus, amiloride did not significantly reduce the glutamate-evoked pH change. To check that amiloride did not affect the BCECF dye, the fluorescence of some cells was calibrated in the presence and the absence of amiloride with the nigericin method (see Methods chapter). No effect of the blocker on the calibration of the pH sensitive dye was detected.

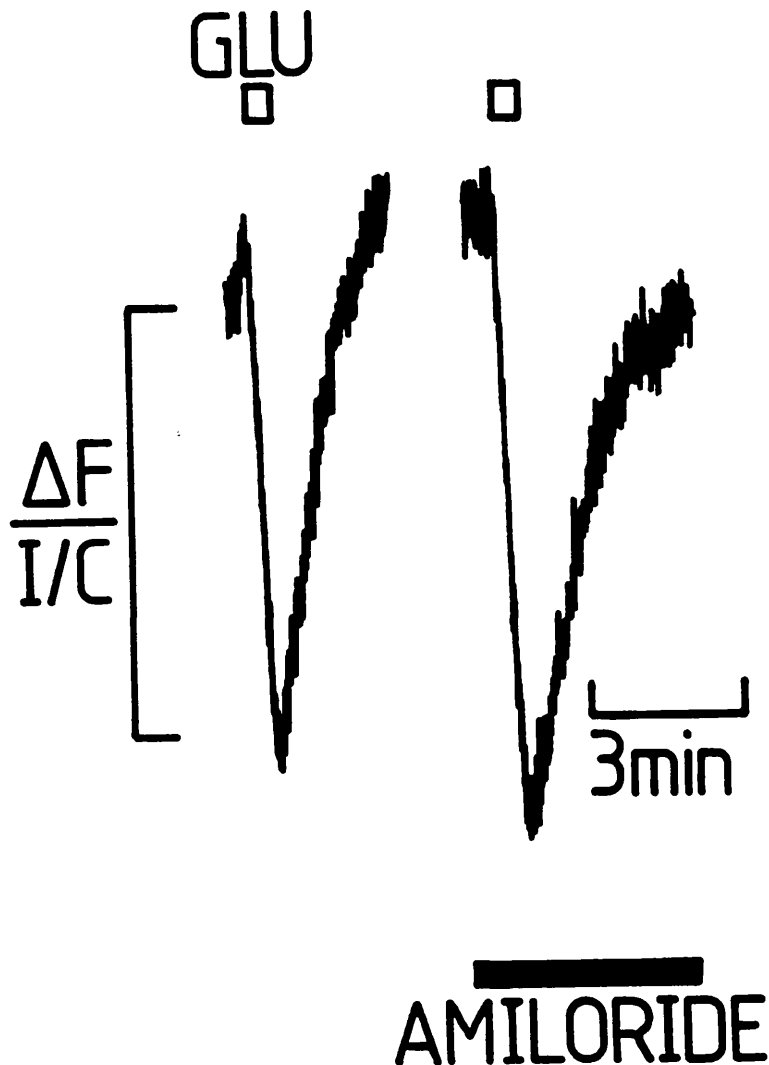


Fig 4.12: Sensitivity of the intracellular acidification to the presence of amiloride, a blocker of the Na^+/H^+ antiporter. Left: Fluorescence change (divided by the current/capacitance) evoked by the application of glutamate to a cell whole-cell clamped with an internal solution containing BCECF. A drop in the fluorescence indicates the acidification of the intracellular medium of the cell. Right: Application of the same dose of glutamate to the cell in the presence of amiloride (in the extracellular medium) produced a similar drop in the amount of fluorescence (divided by the current/capacitance).

4.12 Effect of DIDS on the internal pH change induced during glutamate uptake

DIDS and harmaline are blockers of the $\text{Na}^+/\text{HCO}_3^-$ transporter. DIDS, a stilbene, blocks the co-transporter by binding covalently to its anion site (Aronson, 1989; Grassl & Aronson, 1986) whereas harmaline binds to the cation site. DIDS also partially blocks glutamate uptake, reducing the uptake current by $49 \pm 7\%$ in 5 cells (Fig 4.13), probably by binding to the anion-binding site on the carrier which is characterised in chapter 5. Despite this reduction of the uptake current, DIDS was used in these experiments since harmaline affected the fluorescence of the pH-sensitive dye BCECF. L-glutamate ($100\mu\text{M}$) was applied to Müller cells whole-cell clamped at -43mV either in the presence or in the absence of $500\mu\text{M}$ DIDS in the bathing solution (solution B, table 2.1). This dose of DIDS reduces $\text{Na}^+/\text{HCO}_3^-$ transport by 95% (Newmann & Astion, 1991). In 7 cells, the ratio of the glutamate-evoked intracellular acidification (normalised by uptake current) in the presence and in the absence of the blocker was:

$(\text{pH}/I)_{+ \text{DIDS}} / (\text{pH}/I)_{\phi \text{DIDS}} = 1.11 \pm 0.10$ (mean \pm sem). Thus, blocking the $\text{Na}^+/\text{HCO}_3^-$ cotransporter does not reduce the intracellular acidification generated per pA of uptake current. This strongly supports the idea that transport of a pH-changing ion on the glutamate uptake carrier (rather than the activation of a pH-regulating carrier secondary to the transport of Na^+ into the cell) generates the observed pH changes.

4.13 Intracellular pH changes in unclamped cells

Some intracellular pH measurements were performed on intact, unclamped, undialysed cells. The cells were loaded with the acetoxymethyl ester form of BCECF (see Methods section 2.4.1 for details). L-glutamate ($30\mu\text{M}$) or D-aspartate ($30\mu\text{M}$) were applied to the cells by superfusion in a Ringer solution lacking barium (solution A, table 2.1). Leaving the cells' K^+ conductance unblocked by barium ensures that the uptake current (of about 200pA) only depolarises the cells a few millivolts from their resting potential of -90mV : the input resistance of cells without barium present is about $10\text{M}\Omega$ (Mobbs *et al*, 1988). The fluorescence of BCECF was recorded as for the experiments

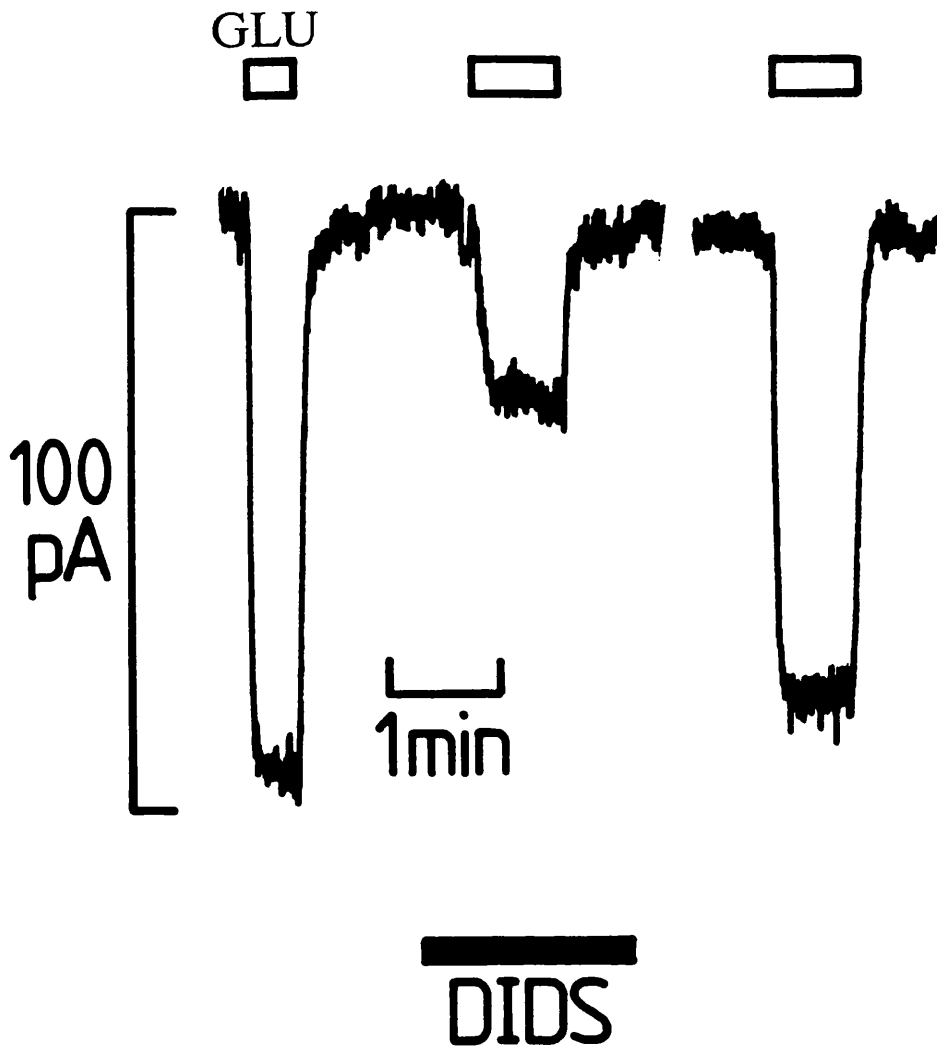


Fig 4.13: Effect of DIDS on the glutamate uptake current. Left: L-glutamate ($30\mu\text{M}$) applied to the cells in the absence of DIDS generated a large inward membrane current. Middle: application of the same dose of glutamate in the presence of DIDS ($500\mu\text{M}$) evoked a smaller current. Right: Recovery of the inward current reflecting uptake of glutamate into the cell in the absence of DIDS. DIDS is known to block the $\text{Na}^+/\text{HCO}_3^-$ co-transporter by binding covalently to the transporter on its anion site. It is therefore likely that DIDS partially blocks the glutamate uptake carrier by occupying an anion binding site on the carrier (see chapter 5).

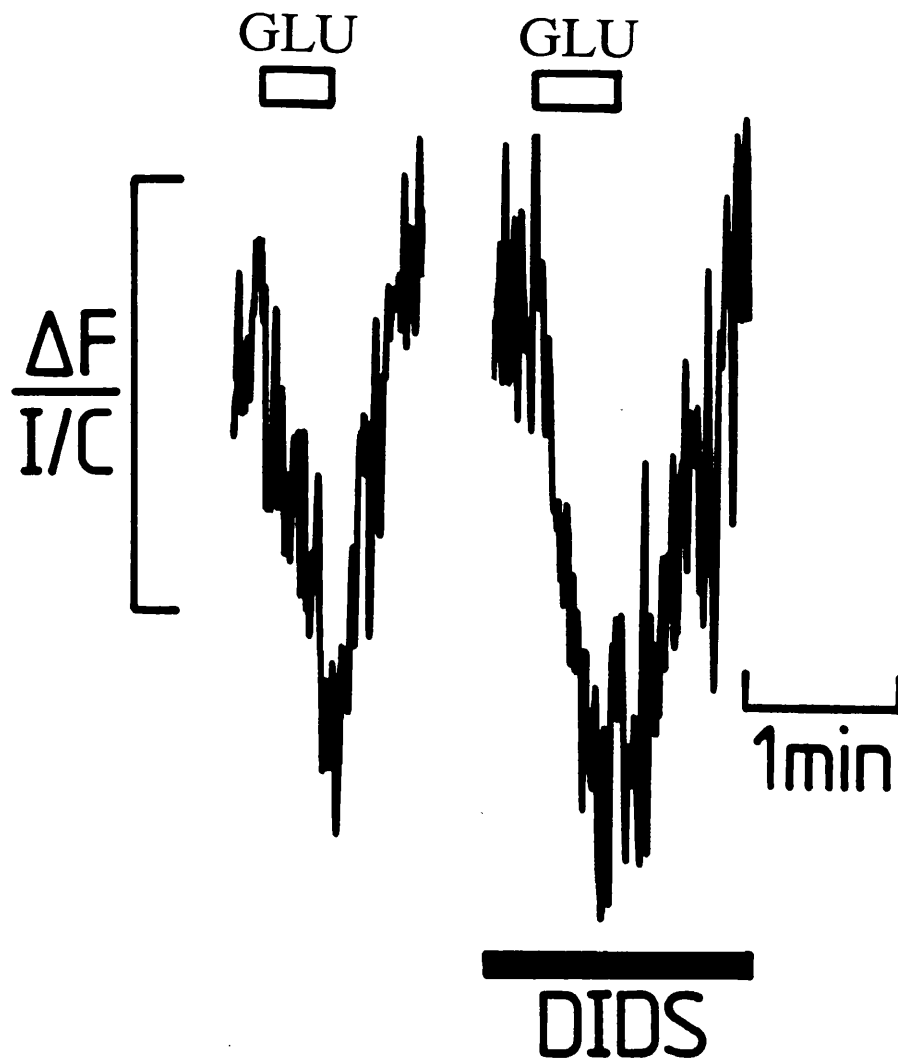


Fig 4.14: Lack of DIDS sensitivity to the intracellular acidification. Application of L-glutamate ($100\mu\text{M}$) to the cells in the absence of DIDS evoked a drop in the fluorescence of BCECF from the cell (left). Right trace shows the change in the fluorescence generated by the application of glutamate in the presence of DIDS. Fluorescence from this particular cell was not calibrated in terms of pH changes, but the fluorescence change was normalised by the current/capacitance to compensate for the inhibition of the glutamate uptake current produced by DIDS.

described above (see Methods, section 2.4). Application of L-glutamate or D-aspartate evoked a fluorescence decrease (Fig 4.15) as for whole-cell clamped Müller cells, showing that the glutamate-evoked intracellular acidification is not an artefact resulting from whole-cell clamping. These pH changes occur when the cells still have all their physiological contents.

4.14 Pharmacology of the pH change in unclamped cells

An important characteristic of the glutamate uptake carrier is that it does not transport the glutamate analogues N-methyl-D-aspartate (NMDA), kainate and α -amino-3-hydroxy-5-methyl-4-isoxazole-4-yl-propionate (AMPA), used to classify glutamate-gated channels, nor the glutamate metabotropic agonist *trans*-1S,3R-1-amino-cyclopentyl-1,3-dicarboxylate (*trans*-ACPD). Fig 4.15 shows an experiment performed on unclamped Müller cells to verify that the intracellular acidification induced when L-glutamate was applied to the cell was not evoked by these other glutamate analogues. NMDA ($30\mu\text{M}$), kainate ($30\mu\text{M}$), AMPA ($30\mu\text{M}$), quisqualate ($30\mu\text{M}$) and *trans*-ACPD ($30\mu\text{M}$) were applied successively to the cells in a barium-free Ringer solution (solution A, table 2.1). None of these agonists evoked any significant intracellular acidification (quantitative data are given in figure 4.15 legend). However, D-aspartate ($30\mu\text{M}$) as well as L-glutamate ($30\mu\text{M}$) both evoked an intracellular pH change as described above. This experiment confirms that the pH change shows the pharmacology of the glutamate uptake carrier.

4.15 Conclusion

The experiments described above strongly suggest that the glutamate uptake carrier transports a pH-changing ion. The observed pH changes could be due to a proton being transported into the cell, but the same results would be obtained if a pH-changing anion were transported out. The experiments described in this chapter do not allow a distinction between these two possibilities. A possible uptake stoichiometry based on these data therefore, is that one glutamate ion is transported into the cell together with two sodium ions; one potassium ion is transported out of the cell; and either a proton is

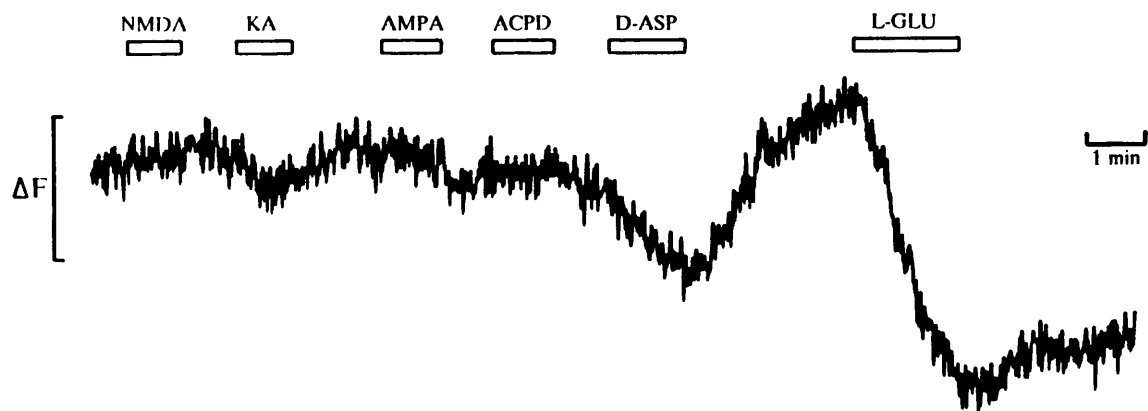


Fig 4.15 Pharmacology of the intracellular acidification in unclamped Müller cells. Data from a Müller cell loaded with BCECF-AM (see methods). No significant fluorescence changes were recorded when the cell was perfused with NMDA, kainate, AMPA or *trans*-ACPD (blockers of glutamate-gated channels and metabotropic glutamate receptors). In contrast, application of D-aspartate or L-glutamate at the same dose ($30\mu\text{M}$) produced an acidification of the intracellular medium of the cell (shown downwards). Fluorescence from this particular cell was not calibrated in terms of pH.

transported into the cell or a pH-changing anion (such as hydroxide or bicarbonate) is transported out (Fig 5.2). These two possibilities would produce the same sign of uptake current (one net positive charge being transported into the cell on each cycle of the carrier), and would both result in an intracellular acidification and extracellular alkalinization. The experiments described in the following chapter were performed to distinguish between the two possibilities.

CHAPTER 5

Effect of internal anions on the glutamate uptake carrier

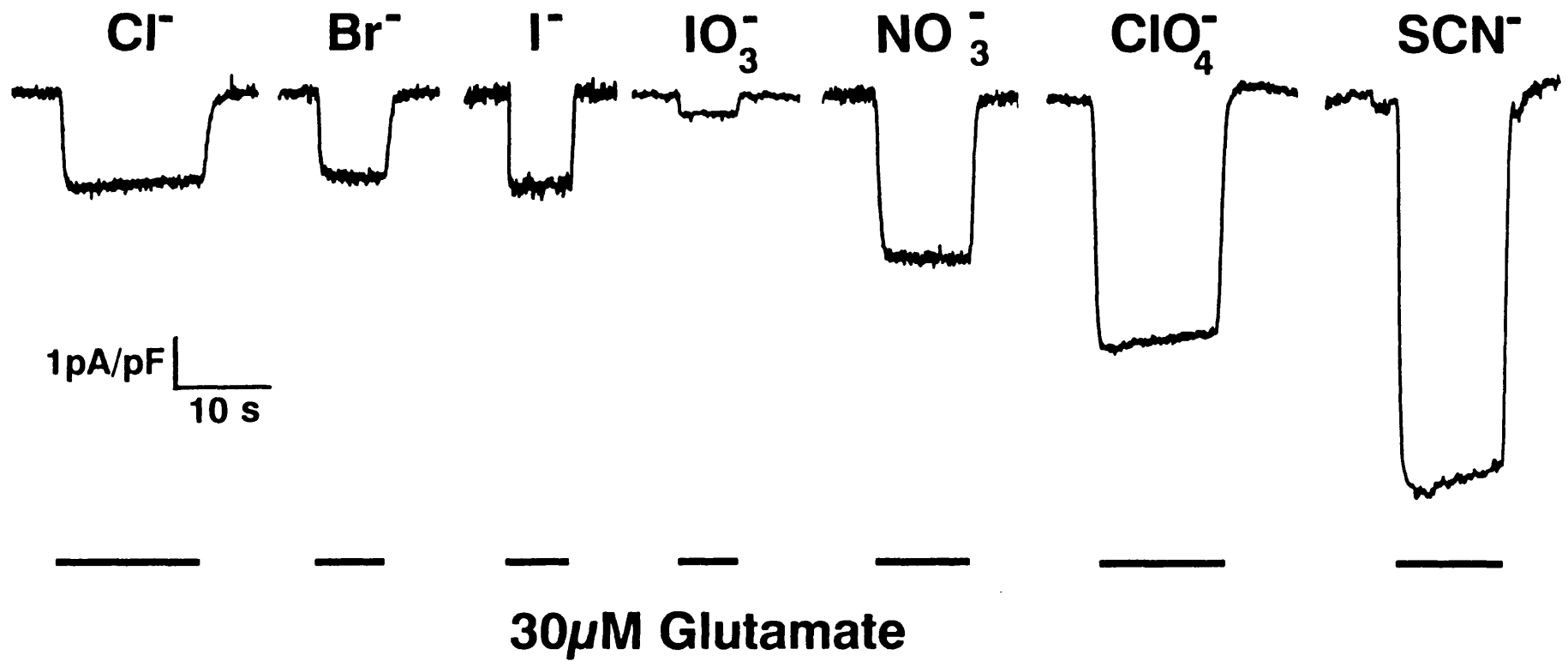
5.1 Introduction

The aim of the experiments described in this chapter was to investigate whether pH changes monitored during the uptake of glutamate and aspartate were due to a proton being transported into the cell, or due to a pH-changing anion such as hydroxyl or bicarbonate being transported out of the cell, on the glutamate uptake transporter.

5.2 Substitutions of anions in the intracellular solution: effect on the amplitude of the glutamate uptake current

If the pH changes monitored during glutamate uptake are due to a pH-changing anion being transported out of the cell, it implies that the carrier has an internal anion binding site. I investigated this possibility by studying the effect of completely replacing the internal Cl^- used normally in my pipette solution with various other anions. The idea was that these anions might be able to compete with the physiologically transported anion for binding to the carrier, and could therefore affect the amplitude of the current generated by glutamate uptake if they were transported at a different rate to the normally transported anion. Internal solutions were prepared by totally replacing the internal Cl^- with Br^- , I^- , IO_3^- , NO_3^- , ClO_4^- or SCN^- (for composition, see tables 2.4 and 2.5). Müller cells were whole-cell clamped using one of these internal solutions and the current generated by glutamate uptake was measured. Fig 5.1 shows typical currents evoked by $30\mu\text{M}$ L-glutamate in cells filled with different anions and held at -43mV . Replacing Cl^- by Br^- or I^- did not produce any significant change of the amplitude of the uptake current (normalized by the capacitance of the cell to compensate for the cells being of different size and membrane area: Barbour *et al*, 1991). Similarly, Barbour *et al* (1991) found that replacing Cl^- by the large anion gluconate had no effect on the uptake current. In contrast, replacing Cl^- by NO_3^- , ClO_4^- or SCN^- greatly increased the evoked current. On the other hand,

Fig 5.1: The effect on the amplitude of the glutamate uptake current of a complete replacement of Cl⁻ ions by various other anions in the internal solution. This figure shows the amplitude of the glutamate uptake current (normalised by the cell capacitance) for cells whole-cell clamped with internal solutions where Cl⁻ was the main anion (left trace) or in which all chloride ions were replaced by various anions (indicated above each current trace). Glutamate (30μM) application is indicated by a black bar underneath each current trace.



replacing Cl^- by IO_3^- reduced the current evoked by $30\mu\text{M}$ glutamate. Uptake currents (normalized by cell capacitance) with Cl^- , Br^- , I^- , IO_3^- , NO_3^- , ClO_4^- and SCN^- had the ratio 1, 1.4 ± 0.3 (mean \pm s.e.m.; 8 cell pairs), 0.9 ± 0.2 (3), 0.38 ± 0.1 (7), 2.4 ± 0.3 (18), 2.8 ± 0.4 (10) and 4.1 ± 0.5 (5). These results suggest that the glutamate uptake carrier possesses an internal anion binding site.

5.3 External pH changes accompanying glutamate uptake when internal Cl^- is replaced with NO_3^- or ClO_4^-

There are two ways in which binding of an intracellular anion might affect the rate of glutamate uptake, as shown in Fig 5.2. First, there may be a site to which anions bind and (e.g. allosterically) regulate the rate of glutamate uptake without being transported themselves (Fig 5.2A). In this case, the pH changes produced by uptake may reflect either the transport of a proton into the cell or the counter-transport of a pH-changing anion on the uptake carrier. In this case, the increase in uptake current produced by internal NO_3^- , ClO_4^- and SCN^- should produce a corresponding increase in the change of extracellular $[\text{H}^+]$ generated by the uptake carrier. Alternatively, if the carrier transports a pH-changing anion out of the cell (Fig 5.2B), NO_3^- , ClO_4^- and SCN^- could increase the rate of uptake and the uptake current by competing for transport (at a higher rate) on this site (in contrast, IO_3^- would have to bind well but be transported more slowly than the normally transported anion). In this case, since NO_3^- , ClO_4^- and SCN^- are the salts of strong acids (and will not produce a pH change when transported) one would expect the increased uptake current produced by these anions to be associated with a decrease in the external $[\text{H}^+]$ change produced by uptake (and the ratio of $[\text{H}^+]$ change to uptake current to be even further decreased).

To see which of these possibilities occurs, I measured how the external $[\text{H}^+]$ change was altered when internal Cl^- was replaced by NO_3^- , ClO_4^- (solutions R or S, table 2.5). Cells were held initially at $+17\text{mV}$ (a voltage at which glutamate uptake is largely inhibited; Brew & Attwell, 1987) and the extracellular pH change evoked on stepping the voltage to -67mV was measured, first of all in a bathing solution lacking glutamate (solution F, table 2.2) and then in a

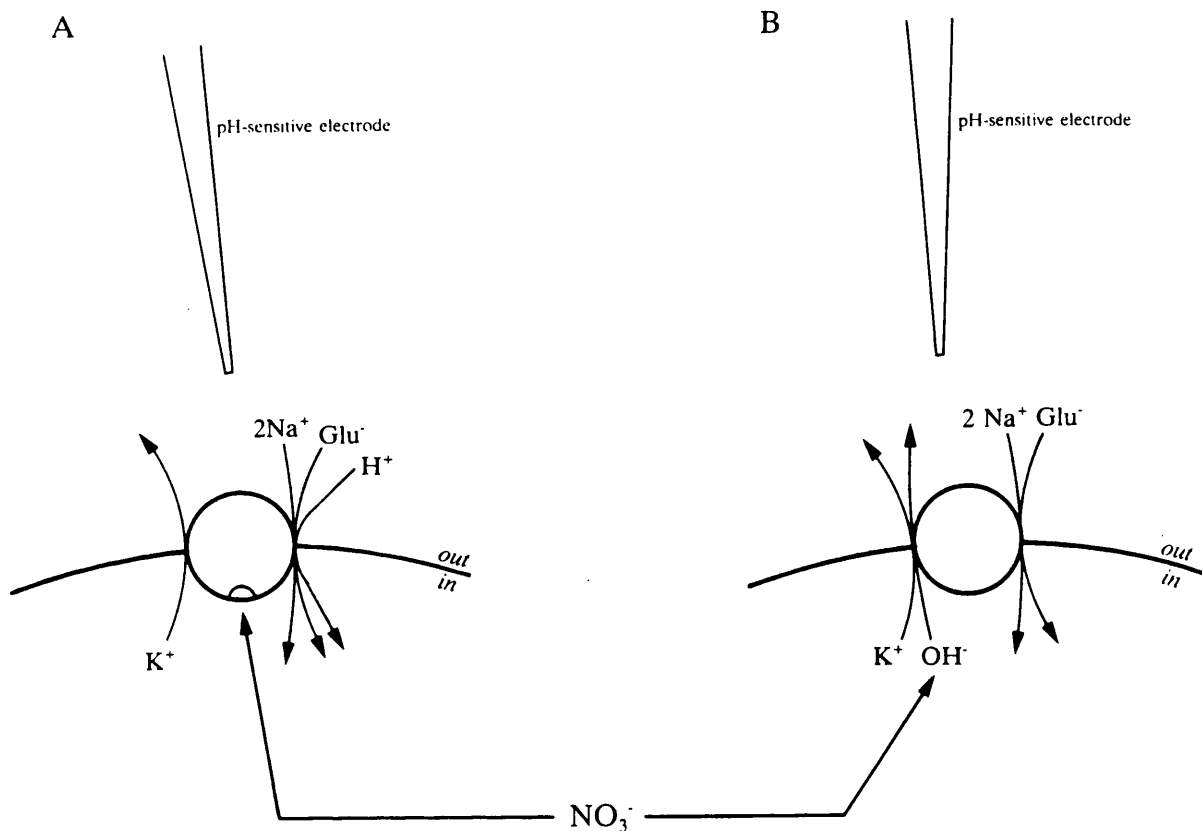


Fig 5.2: Two possible explanations for the effect of NO_3^- , ClO_4^- or SCN^- present inside the cell on the amplitude of the current generated by glutamate uptake. A- These anions are able to act as a (for example allosteric) modulator of the carrier, somehow speeding it up without changing its stoichiometry; the uptake-evoked pH changes may be produced by H^+ entry on the carrier as shown here or by a pH-changing anion transported out. B- These anions compete with a physiologically transported anion and speed up the transport because they are transported faster. The amplitude of the current is correspondingly increased.

solution containing $100\mu\text{M}$ L-glutamate (solution F, table 2.2). Only when L-glutamate (or D-aspartate) was in the bath could a pH change be measured (as already shown in Fig 4.3). The pH change was smaller with NO_3^- or ClO_4^- in the cell than with Cl^- inside (0.035 ± 0.02 pH unit (mean \pm sem) with a NO_3^- internal and 0.041 ± 0.01 pH unit with a ClO_4^- internal compared to 0.049 ± 0.02 with a Cl^- internal solution). Fig 5.3 (top) shows the extracellular alkalization measured outside two typical cells containing Cl^- or NO_3^- , when stepping the voltage from +17 to -67mV. The bottom part of the figure shows the same pH changes after normalising by the amount of uptake current (divided by the capacitance of the cell). In 5 cell pairs, the normalised ΔpH_o was 0.035 ± 0.005 pH units per pA/pF with Cl^- and 0.007 ± 0.002 pH units per pA/pF with NO_3^- inside (mean \pm sem). Similarly, for 5 cell pairs whole-cell clamped using a internal solution containing either Cl^- or ClO_4^- , the normalised extracellular pH change (in the same units) was 0.032 ± 0.006 and 0.011 ± 0.001 respectively (mean \pm sem). These results suggest that anions such as NO_3^- , ClO_4^- or SCN^- can compete with a physiologically transported pH-changing anion for transport out of the cell on the uptake carrier.

5.4 Efflux of ClO_4^- during glutamate uptake

Direct evidence for the transport of anions out of the cell on the uptake carrier was obtained by developing an anion-sensitive electrode that could detect low concentrations of ClO_4^- or SCN^- (see methods chapter, section 2.6). Müller cells were whole-cell clamped to -43mV using an internal solution containing either Cl^- or ClO_4^- as the main anion. Fig 5.4 shows the current evoked by the application of $30\mu\text{M}$ L-glutamate and the response of an anion-sensitive electrode just outside two different cells containing ClO_4^- (A) or Cl^- (B). Although both cells showed an inward current reflecting the uptake of L-glutamate, the anion-sensitive electrode only showed a response outside the cell containing ClO_4^- . A 5mV deflection of the electrode voltage corresponded (for that electrode) to a $6.8\mu\text{M}$ rise of the extracellular ClO_4^- concentration when ClO_4^- was present inside the cell. The rise in $[\text{ClO}_4^-]$ evoked by glutamate, outside cells containing ClO_4^- , was reproduced for 27 cells. The glutamate-evoked efflux of

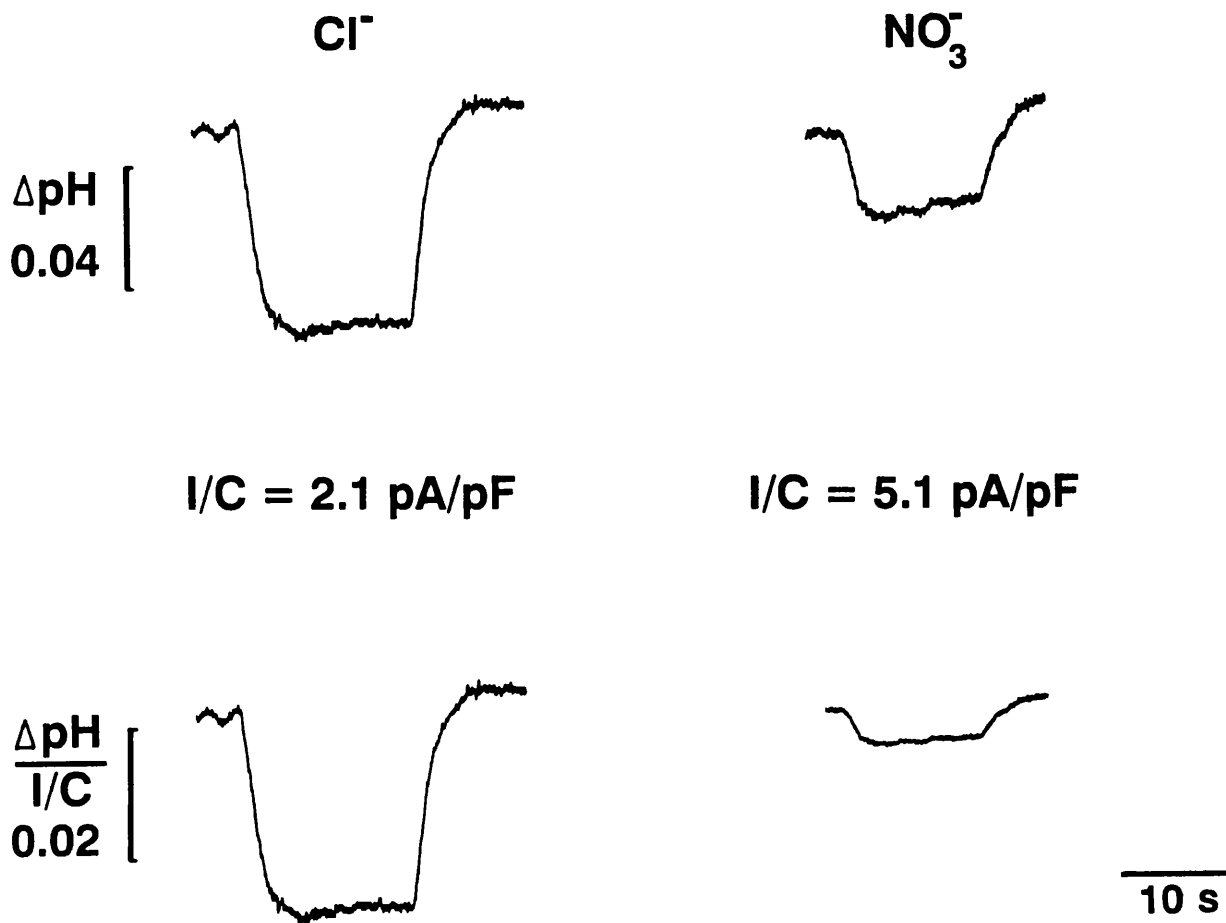


Fig 5.3: The extracellular pH change induced when glutamate uptake was activated by stepping the voltage from +17mV (at which the glutamate uptake carrier is largely inhibited) to -67mV (where the current induced by glutamate uptake is large) in the presence of 100 μ M L-glutamate. Top: pH_o changes obtained from a typical cell containing Cl⁻ (left) or NO₃⁻ (right). Bottom: the pH_o changes normalised by the size of the current/capacitance (I/C was 2.1pA/pF for the Cl⁻-containing cell and 5.1pA/pF for the NO₃⁻-containing cell). The extracellular pH change monitored was much smaller when the cell contained NO₃⁻ than Cl⁻ (about 2 times smaller in absolute terms, and 5 times smaller when normalised by the size of the uptake current divided by the capacitance).

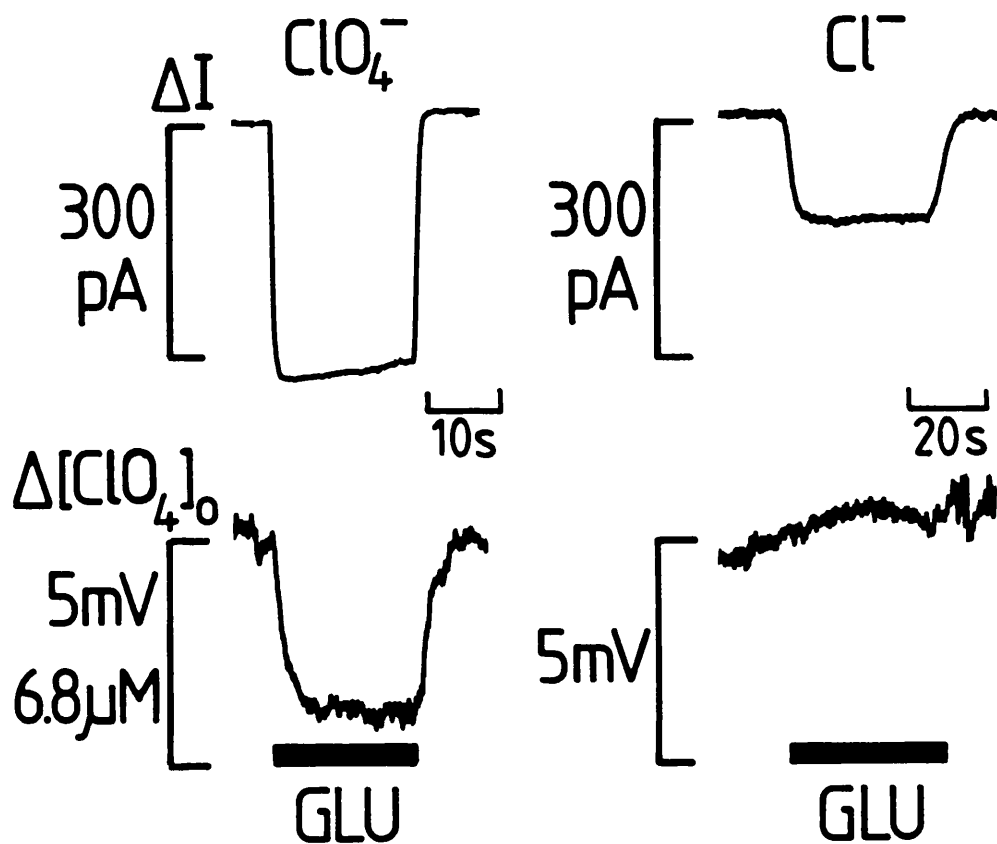


Fig 5.4: Efflux of ClO_4^- during glutamate uptake. The left panel at the top shows the inward current evoked by the application of $30\mu\text{M}$ L-glutamate to a Müller cell whole-cell clamped to -43mV . The bottom of the same panel shows the associated increase of ClO_4^- concentration measured just outside the cell with a perchlorate-sensitive electrode (an increase in the concentration of ClO_4^- is shown downwards). The right panel of the figure shows the results obtained in a cell whole-cell clamped with an internal solution containing Cl^- as the main anion. The current evoked by the application of the same dose of L-glutamate is smaller (top) and the anion-sensitive electrode does not detect any change in the ClO_4^- concentration outside the cell.

ClO_4^- was superimposed on a sustained efflux of the anion (measured as a sustained change of ion-sensitive electrode voltage when the electrode was moved up to the cell). This efflux may occur through anion channels or carriers: it was not blocked by the application of the Cl^- channel blocker anthracene-9-carboxylic acid (9AC) in the bath solution (see section 5.11).

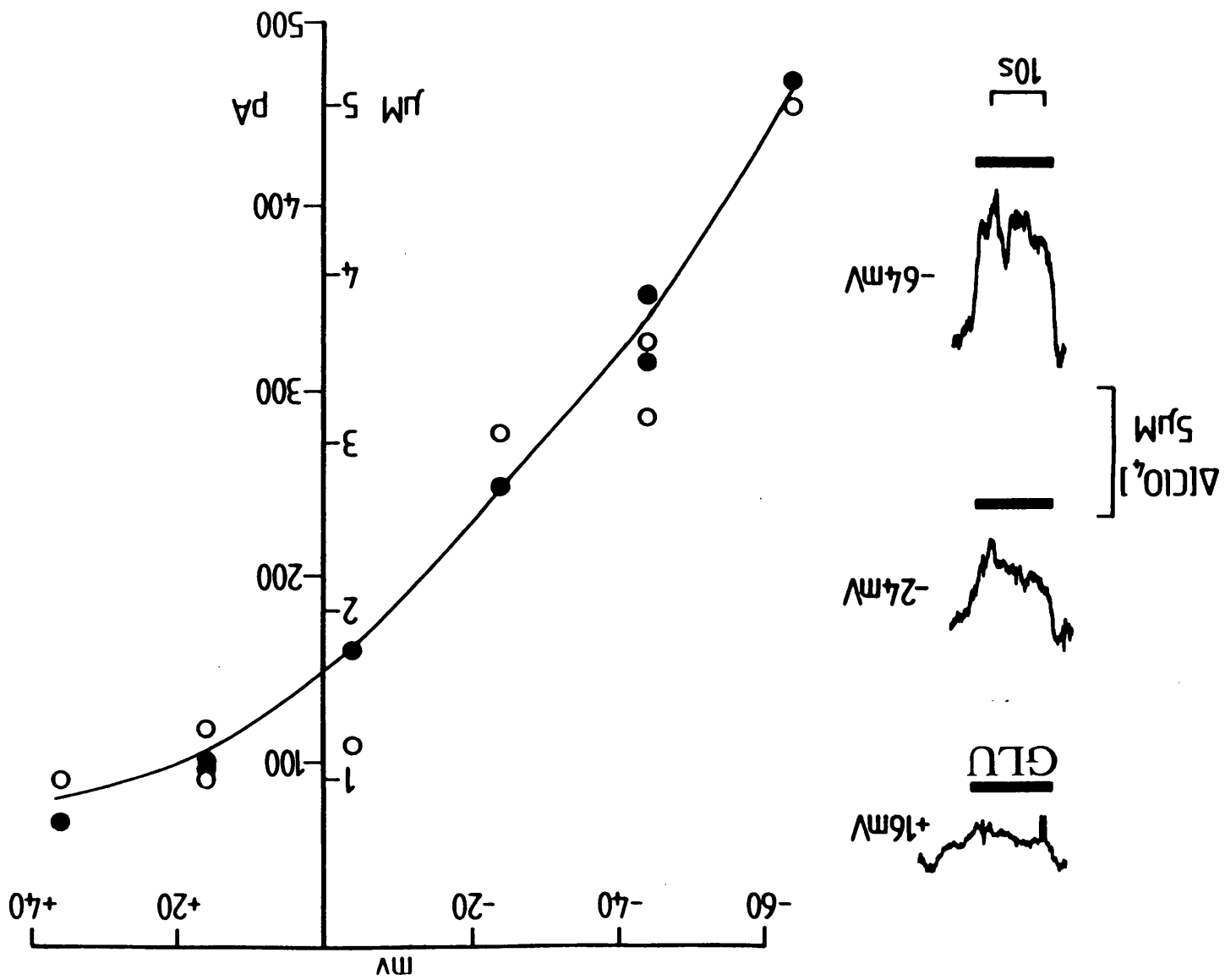
5.5 Voltage-dependence of the ClO_4^- efflux

To confirm that the glutamate-evoked ClO_4^- efflux was via the uptake carrier, its voltage-dependence was studied. L-glutamate ($30\mu\text{M}$) was applied to Müller cells, whole-cell clamped using a ClO_4^- -containing solution (solution S, table 2.5), held at various voltages. Fig 5.5 shows the amplitude of the uptake current and the increase of extracellular concentration of ClO_4^- evoked by glutamate as a function of the holding voltage. The amount of ClO_4^- coming out of the cell increased as the cell was hyperpolarised, in proportion to the increase of uptake current across the cell membrane. Similar results were obtained from 5 cells. These results are consistent with the hypothesis that ClO_4^- ions can be transported out of the cell on the glutamate uptake carrier.

5.6 Dependence of the ClO_4^- efflux on external sodium

For further comparison with the properties of glutamate uptake, the dependence of the efflux of ClO_4^- on the presence of sodium ions in the extracellular solution was investigated. Müller cells were clamped to -43mV with pipettes containing ClO_4^- , and $30\mu\text{M}$ L-glutamate was applied successively in Na^+ -containing and Na^+ -free solutions. In 5 cells, an efflux of ClO_4^- was detected by an extracellular anion-sensitive electrode when glutamate uptake was activated by bath application of the agonist in the presence of sodium (Fig 5.6B), but not in the absence of external sodium (Fig 5.6A) which completely blocks glutamate uptake carrier (Kanner & Sharon, 1978a; Brew & Attwell, 1987). No uptake current was evoked when glutamate was applied in the absence of sodium. These results showing that the efflux of ClO_4^- , like the uptake of glutamate, depends strictly on the presence of external sodium ions, support the hypothesis that the ClO_4^- anions are transported out of the cell on the glutamate uptake carrier.

Fig 5.5: Voltage-dependence of the uptake-evoked anion efflux. An anion-sensitive electrode was used to detect the rise in $[\text{ClO}_4^-]$ (shown downwards) outside cells clamped with electrodes containing ClO_4^- as the main anion. The left pannel represents specimen records of $[\text{ClO}_4^-]_o$ change at +16, -24 and -64 mV. Right: dependence on voltage of the glutamate-evoked uptake current (\bullet) and the rise in $[\text{ClO}_4^-]$ outside the same cell (\circ). The current and ClO_4^- data have been arbitrarily scaled to superimpose as well as possible over the whole voltage range.



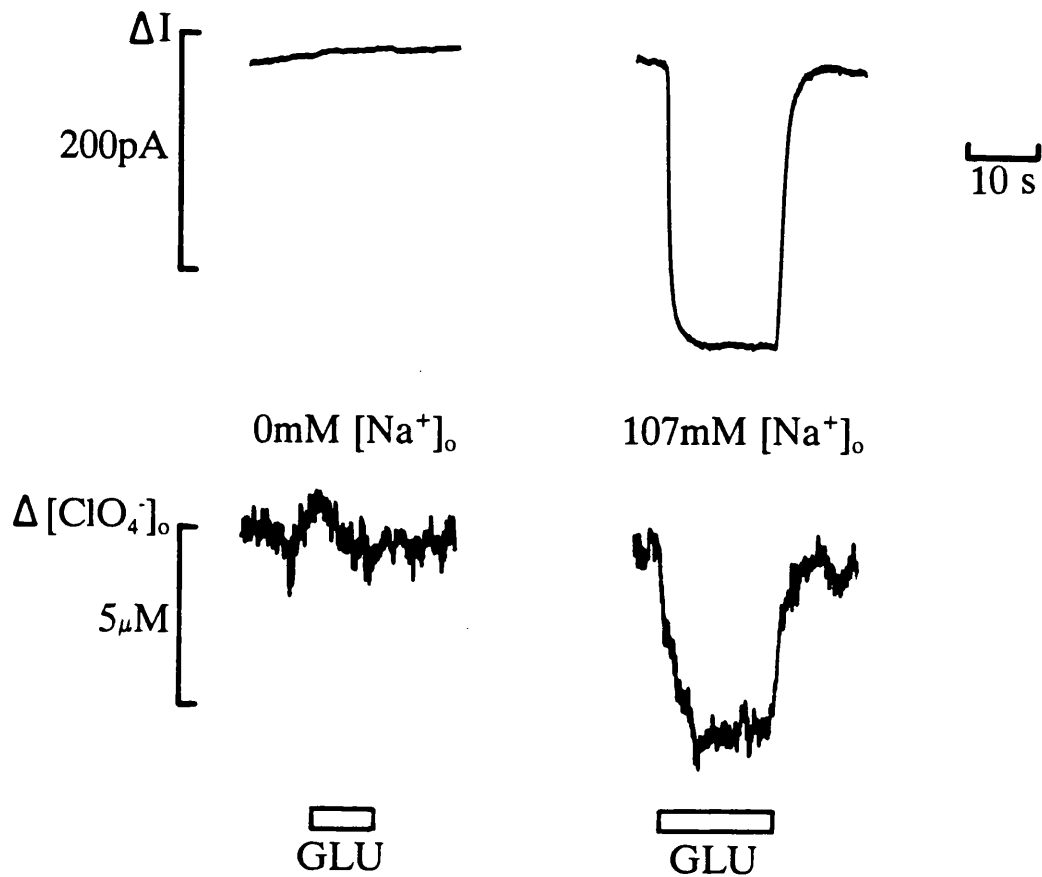


Fig 5.6: Dependence of the efflux of ClO_4^- on external sodium. Applying L-glutamate ($30\mu\text{M}$) to a Müller cell whole-cell clamped to -43mV (with an internal solution containing ClO_4^-) in the absence of external sodium did not evoke any membrane current (top trace) nor any rise of $[\text{ClO}_4^-]_o$ (bottom trace, rise in concentration shown downwards; measured with an anion-sensitive electrode positioned just outside the cell). Subsequent application of glutamate in an external solution containing sodium produced an inward membrane current as well as a rise of $[\text{ClO}_4^-]_o$.

5.7 Dependence of the uptake current on internal potassium when ClO_4^- or NO_3^- is present inside the cell

The glutamate uptake current has been shown to be dependent on the presence of internal potassium ions, probably because the uptake carrier transports a K^+ ion out of the cell (Barbour *et al.*, 1988). It was of interest to determine whether this requirement for internal K^+ still held with ClO_4^- or NO_3^- inside the cell. For example, these anions might act by altering the stoichiometry of the uptake carrier, so that it no longer needs to transport a K^+ : this would double the observed uptake current for a given rate of glutamate uptake.

To test this, cells containing ClO_4^- (or NO_3^-) were studied alternating between cells clamped (at -43mV) with an intracellular solution containing the normal concentration of potassium ions (solution S or R, table 2.5) and cells clamped with a solution lacking potassium (replaced by NMDG- ClO_4^- or NMDG- NO_3^- ; solution W or X, table 2.6). The extracellular solution contained no potassium (solution C, table 2.1), in order to prevent K^+ leakage into the cell raising the intracellular $[\text{K}^+]$ (Barbour *et al.*, 1988). Müller cells with internal solutions lacking potassium showed a much smaller inward current when perfused with glutamate than did cells containing potassium. Measurements of the current (and of the capacitance) were made 7 minutes after patch rupture to allow for essentially complete exchange of the cell and pipette solutions. For NMDG- NO_3^- -containing cells, the amplitude of the uptake current, in response to the application of $30\mu\text{M}$ L-glutamate (normalised by the capacitance of the cell) was reduced to $35 \pm 6\%$ of the control value with K- NO_3 in the cell (5 cell pairs). For cells whole-cell clamped using a NMDG- ClO_4^- -containing solution, the amount of uptake current was reduced to $34 \pm 18\%$ of the value with K- ClO_4 in the cell (15 cell pairs, Fig 5.7). For comparison, with Cl^- in the cell, omitting K^+ from the internal solution reduces the uptake current to only 4% of its value with K^+ present (Barbour *et al.*, 1991). The larger residual current with ClO_4^- or NO_3^- in the cell may be the result of a higher affinity for internal K^+ in the presence of these ions (implying that $[\text{K}^+]_i$ has to be lowered further to inhibit uptake): a precedent for this possibility is the higher affinity for K^+ seen when D-aspartate is used instead of L-glutamate as a substrate for the uptake carrier

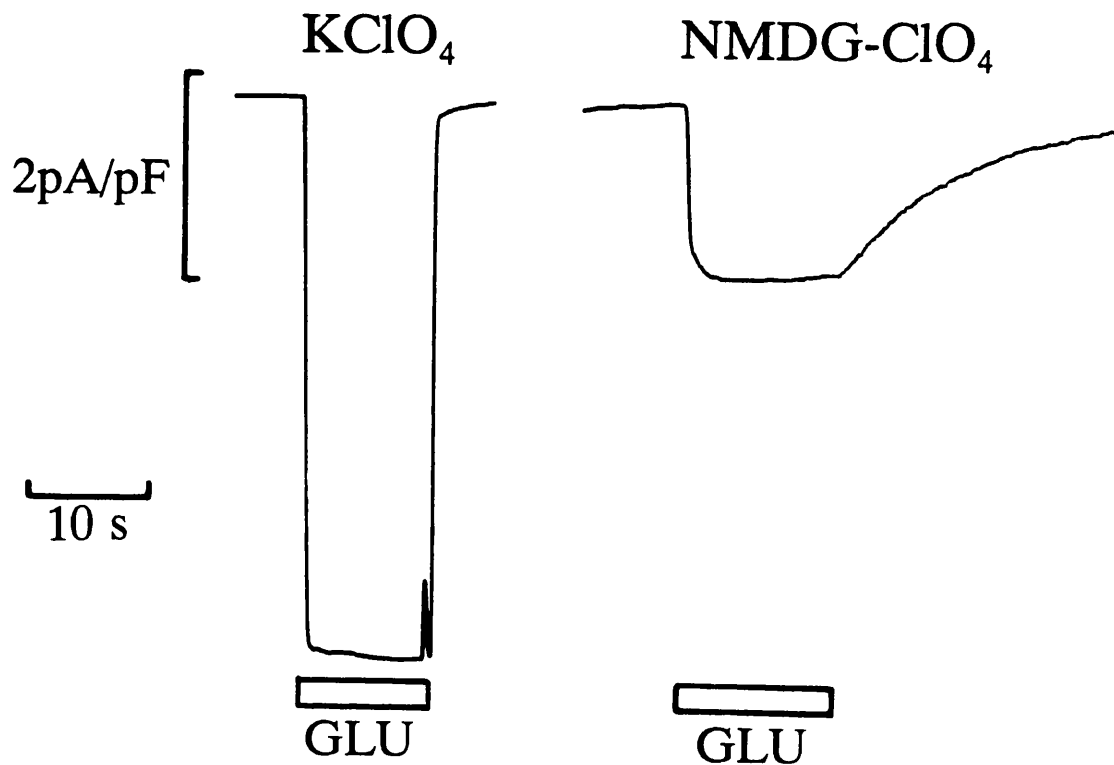


Fig 5.7: Dependence of the glutamate-evoked current on intracellular potassium, when ClO_4^- is present inside the cell. Typical data from Müller cells whole-cell clamped using either a KClO_4 internal (left panel; solution S, table 2.5) or a solution where KClO_4 has been replaced by NMDG-ClO_4 (right panel; solution W, table 2.6). The current evoked by the application of L-glutamate ($30\mu\text{M}$) was monitored 7 minutes after patch rupture and divided by the capacitance of the cell to compensate for cells being of different sizes. Similar results were obtained in 15 cell pairs.

(Szatkowski *et al.*, 1991). Alternatively, the larger residual current may be the result of a poor perfusion of the cells in these particular experiments, since the series resistance obtained for the electrodes was typically between 6 and 10 M Ω (as compared with the 1-2M Ω obtained in the experiments of Barbour *et al.* (1988) on cells containing Cl⁻). Whatever the cause of the less complete suppression of uptake produced by internal K⁺ removal, these results show that the uptake current is strongly dependent on internal K⁺ even when it has been potentiated two or three times by NO₃⁻ or ClO₄⁻.

5.8 Pharmacology of the efflux of ClO₄⁻

The pharmacology of the current and ClO₄⁻ efflux evoked by L-glutamate and its analogues was investigated in cells whole-cell clamped to -43mV with an internal solution containing ClO₄⁻. Fig 5.8 shows the current and the ClO₄⁻ efflux evoked in a cell by the successive application of L-glutamate (30 μ M), D-aspartate (30 μ M), N-methyl-D-aspartate (NMDA, 30 μ M), kainate (30 μ M) and quisqualate (30 μ M). The pharmacology of the evoked current was that of the uptake carrier, in that the agonists activating glutamate-gated channels and the metabotropic receptor did not evoke any current nor any ClO₄⁻ efflux. Similar results were obtained in 5 cells. Interestingly, the presence of ClO₄⁻ inside the cell increased the size of the D-aspartate response relative to that for L-glutamate (cf. with the currents in Fig 4.8 evoked with Cl⁻ inside), suggesting an increase in the relative V_{max} of uptake for D-aspartate: this was not investigated further.

5.9 Measurement of the efflux of ClO₄⁻ when the cells were whole-cell clamped with a solution containing a high concentration of sodium

I considered the possibility that the efflux of ClO₄⁻ evoked by glutamate might not be due to ClO₄⁻ moving on the uptake carrier itself, but due to the uptake carrier transporting Na⁺ into the cell, raising [Na⁺]_i and thus activating an efflux of ClO₄⁻ on a Na⁺-dependent carrier (like the Na⁺/HCO₃⁻ co-transporter). This was tested by comparing two sets of cells. One set of cells was whole-cell clamped using the usual ClO₄⁻ internal (solution S, table 2.5). The other set was whole-cell clamped using a solution containing a raised

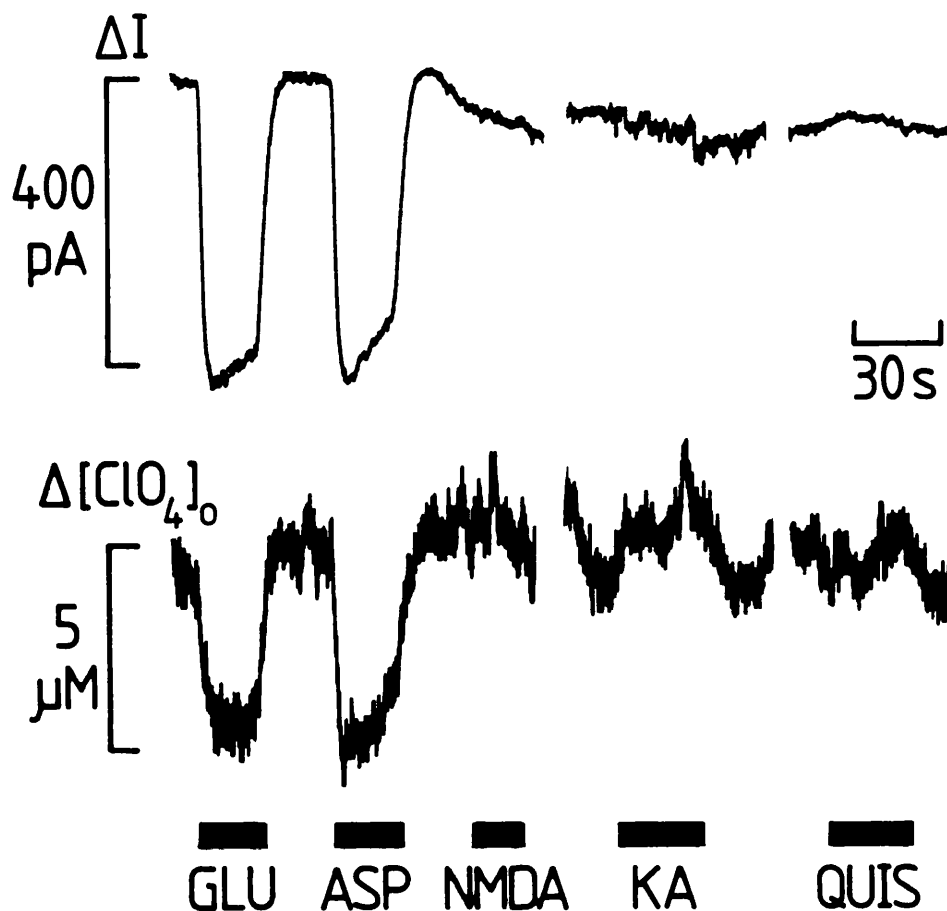


Fig 5.8: Pharmacology of the rise of $[\text{ClO}_4^-]$ outside a Müller cell whole-cell clamped with a solution containing ClO_4^- (solution S, table 2.5). Top: current evoked at -43mV by the application of the various glutamate analogues. Bottom: the associated increase in $[\text{ClO}_4^-]_o$ (increase shown downwards) produced by ClO_4^- efflux, measured with an anion-sensitive electrode positioned just outside the cell. L-glutamate (GLU, $30\mu\text{M}$) and D-aspartate (ASP, $30\mu\text{M}$) both evoked a large inward current accompanied by an efflux of ClO_4^- . In contrast, the agonists which activate glutamate-gated ion channels and metabotropic receptors, NMDA ($30\mu\text{M}$), kainate ($30\mu\text{M}$) and quisqualate ($30\mu\text{M}$) did not evoke any current nor any efflux of ClO_4^- . Note that internal ClO_4^- appears to increase the V_{max} of uptake for aspartate relative to that for glutamate (see text).

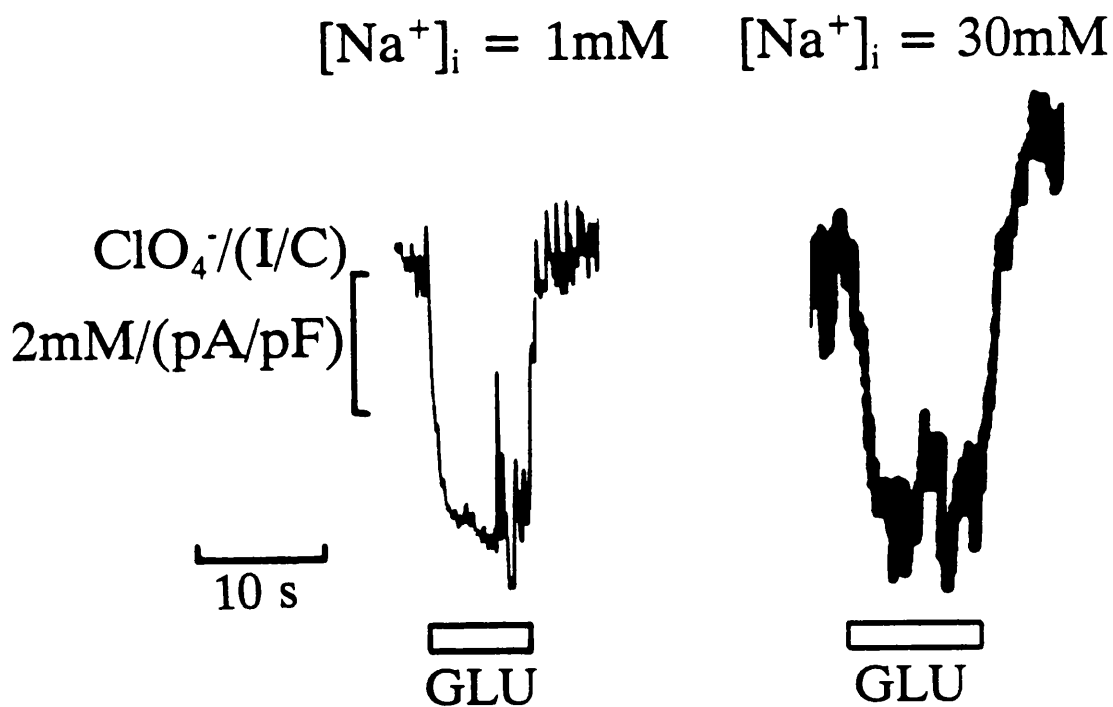


Fig 5.9: Dependence of the rise of $[\text{ClO}_4^-]_o$ during glutamate uptake on the intracellular sodium concentration. Left trace shows the rise of $[\text{ClO}_4^-]_o$ (bottom; increase shown downwards) induced by the application of $30\mu\text{M}$ glutamate to a Müller cell whole-cell clamped with a sodium-free internal solution. Right trace shows the same experiment performed on another cell that was whole-cell clamped using an internal solution containing 30mM Na^+ . C- shows the $[\text{ClO}_4^-]_o$ changes normalised by the uptake current (divided by the cell capacitance) for the two cells.

concentration (30mM) of sodium (solution Y, table 2.6). A given sodium influx during glutamate uptake will produce a smaller fractional rise of $[\text{Na}^+]_i$ in the latter solution than in the former. Fig 5.9 shows the rises in $[\text{ClO}_4^-]_o$ outside specimen cells studied with each of these solutions. In 5 cell pairs, the $[\text{ClO}_4^-]_o$ rise normalised by the size of the uptake current (divided by the capacitance of the cell) in cells with high sodium internal solution was not smaller than the rise in cells with zero sodium internal solution (the ratio cells with high $[\text{Na}^+]_{\text{pipette}}$ / cells with zero $[\text{Na}^+]_{\text{pipette}}$ was 1.90 ± 0.75 ; mean \pm sem). These results suggest that any rise of internal sodium concentration during glutamate uptake does not lead secondarily to the efflux of ClO_4^- observed.

5.10 Harmaline sensitivity of the ClO_4^- efflux

The possible involvement of the $\text{Na}^+/\text{HCO}_3^-$ co-transporter in generating the ClO_4^- efflux was further investigated using the blocker harmaline, 2mM of which inhibits $\text{Na}^+/\text{HCO}_3^-$ transport by 70% (Newman & Astion, 1991). This was used instead of DIDS or DNDS to block $\text{Na}^+/\text{HCO}_3^-$ co-transport since the latter blockers were found to affect the anion-sensitive electrode. Müller cells were whole-cell clamped at -43mV using a ClO_4^- internal solution, and glutamate (30 μM) was applied to the cell successively in the presence and in the absence of harmaline (2mM), while monitoring the rise of $[\text{ClO}_4^-]_o$ with an anion-sensitive electrode positioned just outside the cell. The ClO_4^- -sensitive electrode was calibrated both in the presence and in the absence of the blocker (see methods). In 5 cells, the ratio of the efflux of ClO_4^- monitored in the presence of harmaline to the efflux in the absence of the blocker was 1.29 ± 0.39 (mean \pm sem) (Fig 5.10). These results show that the efflux of ClO_4^- evoked by glutamate can not be blocked by inhibiting the $\text{Na}^+/\text{HCO}_3^-$ co-transporter, and so does not reflect ClO_4^- transport in place of HCO_3^- transport on the $\text{Na}^+/\text{HCO}_3^-$ carrier.

5.11 Measurements of the continuous efflux of ClO_4^- in the presence of 9AC

As mentioned earlier, even in the absence of glutamate, it was possible to detect a non-zero $[\text{ClO}_4^-]$ just outside cells clamped with electrodes containing ClO_4^- . The efflux of ClO_4^- induced by bath application of glutamate was

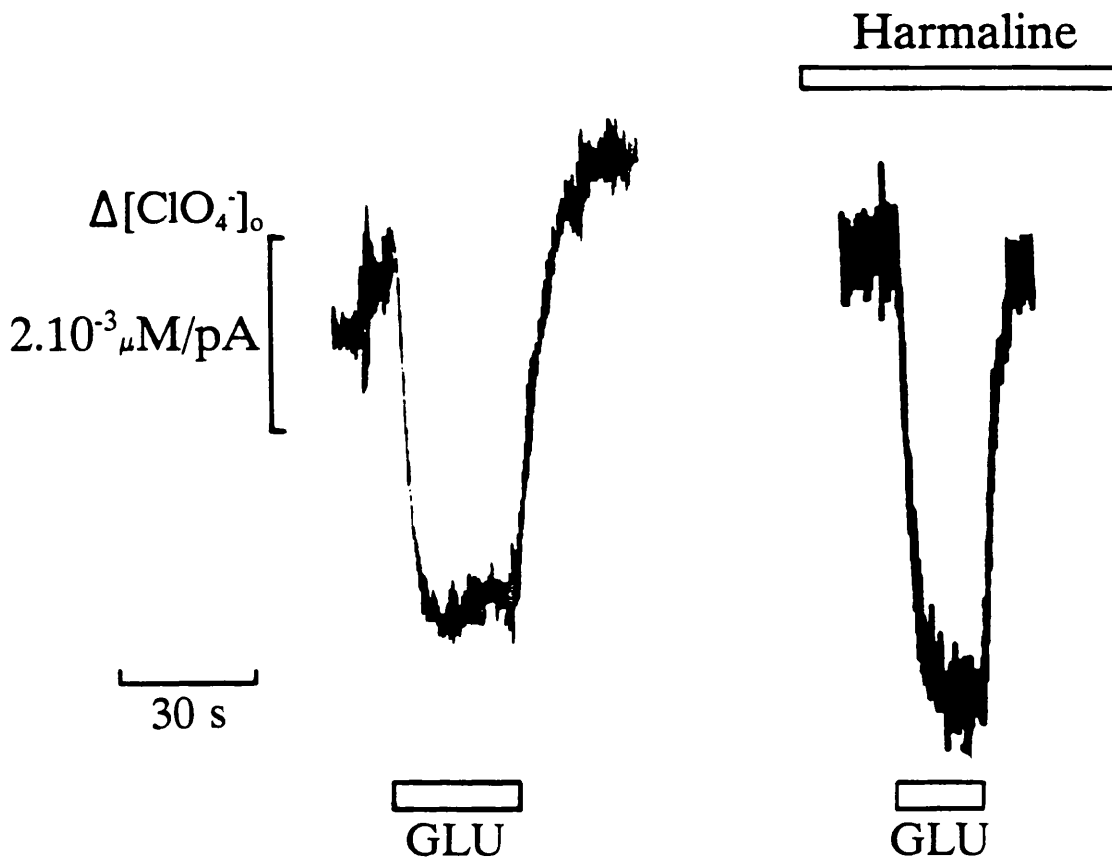


Fig 5.10: Sensitivity of the glutamate evoked ClO_4^- efflux to harmaline (2mM), a blocker of $\text{Na}^+/\text{HCO}_3^-$ co-transport. Left trace shows the rise in $[\text{ClO}_4^-]_o$ evoked by the application of glutamate to a Müller cell containing KClO_4 (increase shown downwards) measured with an anion-sensitive electrode positioned just outside the cell, in the absence of harmaline. B- same experiment performed on the same cell but with external solutions containing 2mM harmaline to block the $\text{Na}^+/\text{HCO}_3^-$ co-transporter. The rise in $[\text{ClO}_4^-]_o$ was not affected by the blocker.

superimposed on a continuous efflux of the anion. I investigated the possibility that this leakage of ClO_4^- out of the cell occurred through Cl^- channels, by using a blocker of those channels: anthracene-9-carboxylic acid (9AC) (solution S, table 2.5 with $400\mu\text{M}$ 9AC added from a 2M stock in DMSO). This dose of 9AC was shown to block essentially 100% of the chloride membrane conductance of rat skeletal muscle (Palade & Barchi, 1977). In 4 cell pairs, the presence of 9AC did not block the continuous efflux of the anion seen in the absence of glutamate. It is therefore likely that the glutamate-independent efflux of ClO_4^- is due to the transport of the anion through 9AC-insensitive anion channels or through anion carriers. This was not investigated further.

5.12 Summary of the chapter so far

The experiments described above strongly suggest that the pH changes accompanying glutamate uptake (described in chapter 4) are due to the transport of a pH-changing anion out of the cell rather than the transport of a proton into the cell (see discussion, section 7.2.4). Two anions are major candidates for generating the pH changes seen during glutamate uptake: OH^- and HCO_3^- . The following experiments were performed in order to try to distinguish between these two possible anions.

5.13 Effect of intracellular bicarbonate on the amplitude of the uptake current

A possible transport of the anion bicarbonate out of the cell on the uptake carrier was first tested by comparing the effect of using HCO_3^- -containing and nominally HCO_3^- -free internal solutions on the amplitude of the current evoked by glutamate. Müller cells were studied alternately, whole-cell clamping half of them with a nominally HCO_3^- -free internal solution (solution U, table 2.5), and the other half with a solution containing 10mM Na- HCO_3 and which was bubbled with 5% CO_2 until put in the electrode (solution V, table 2.5). In the nominally HCO_3^- -free solution, the concentration of HCO_3^- and CO_2 were found, with a blood gas analyser, to be 400 and $50\mu\text{M}$ respectively. Both solutions also contained acetazolamide (1mM) to block carbonic anhydrase: this was to minimize formation of HCO_3^- from CO_2 generated by metabolism in the

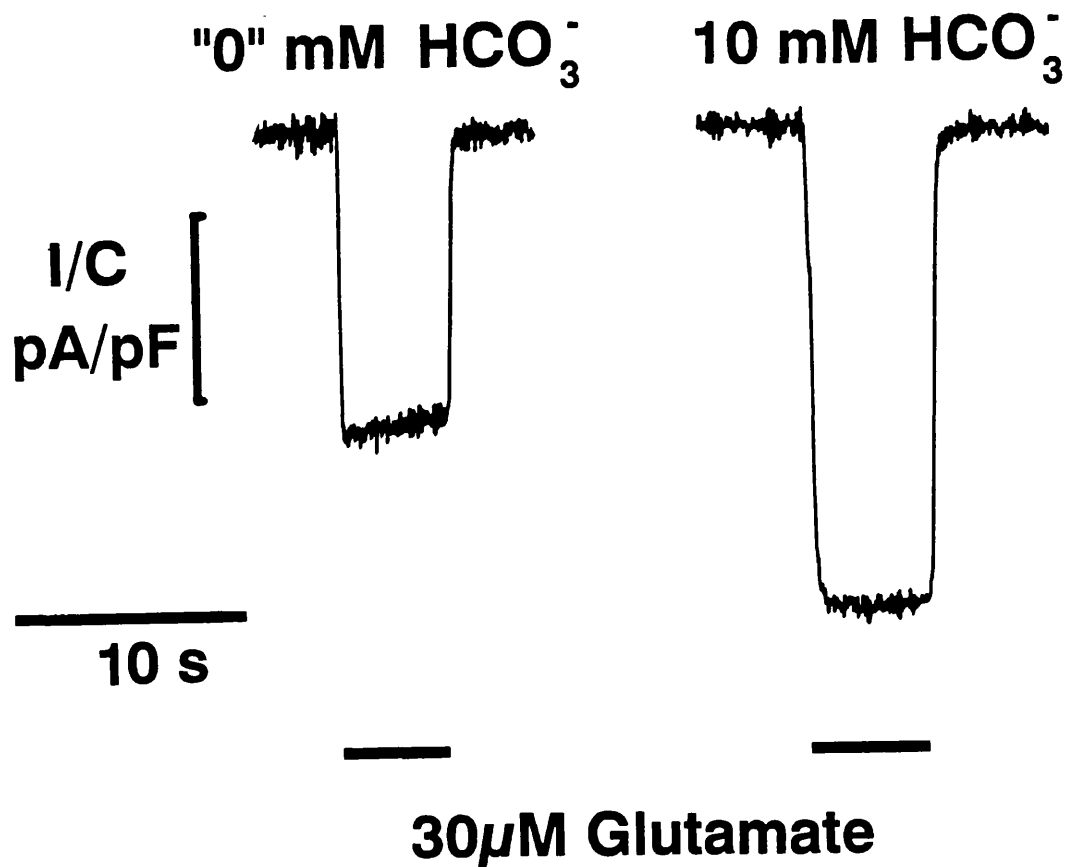


Fig 5.11: Uptake currents evoked at -43mV in two cells clamped with pipettes containing nominally zero (actually 400μM; left) or 10mM HCO₃⁻ (solutions U and V, table 2.5 respectively). Data are normalised by the cell capacitance to compensate for differences in cell surface area. Data were selected to be typical of the mean currents seen with and without added HCO₃⁻.

cells studied with the nominally HCO_3^- -free solution, and to avoid depletion of HCO_3^- (forming CO_2) in cells with HCO_3^- -containing solution. The pH of both solutions was adjusted to 7.0. L-glutamate ($30\mu\text{M}$) was applied to the cells by bath perfusion. In 10 cell pairs held at -43mV , the presence of 10mM HCO_3^- increased the amplitude of the uptake current by $39\pm 18\%$ (Fig 5.11). These results suggest that HCO_3^- could be transported out of the cell on the glutamate uptake carrier on at least a fraction of carrier cycles.

5.14 Internal pH changes with and without 10mM internal HCO_3^-

The 39% increase of uptake current produced by adding HCO_3^- to the internal solution (see preceding section) might result from OH^- being transported on the uptake carrier in the absence of added HCO_3^- , but HCO_3^- being transported on 28% ($39\% / \{100\% + 39\%\}$) of carrier cycles when internal HCO_3^- is present (with OH^- still being transported on 72% of carrier cycles). If so, this would reduce the effective loss of alkali from the cell per uptake current because, whereas each transported OH^- is equivalent to adding a proton to the cell, each transported HCO_3^- is equivalent to adding only 0.11 of a proton (because the pK of HCO_3^- is 6.1). Thus, the predicted acid load with added HCO_3^- is:

$$\begin{aligned} \text{Acid load}_{\text{HCO}_3^-} &= \text{Acid load}_{\phi\text{HCO}_3^-} + 0.11 \times 0.39 \times \text{Acid load}_{\phi\text{HCO}_3^-} \\ &= 1.04 \times \text{Acid load}_{\phi\text{HCO}_3^-} \end{aligned}$$

Since the uptake current is increased by 39%, the ratio acid load/uptake current with added HCO_3^- is predicted to be $1.04/1.39 = 0.75$ of its value without added HCO_3^- . To test this, the experiment described in the previous section was repeated, but measuring glutamate-evoked intracellular pH changes at the same time as the uptake current. The resulting values of effective acid load / (uptake current/capacitance) (with acid load calculated as $\Delta\text{pH} \times$ buffering power for each cell) were $2.7 \pm 1.4 \text{ mM}/(\text{pA}/\text{pF})$ (mean \pm sd) with no added HCO_3^- and $1.4 \pm 0.7 \text{ mM}/(\text{pA}/\text{pF})$ with added HCO_3^- . Despite the scatter of the data, the smaller acid load per uptake current with added HCO_3^- is consistent with mainly OH^- being transported in the absence of HCO_3^- , but some HCO_3^- also being transported when it is present inside the cell.

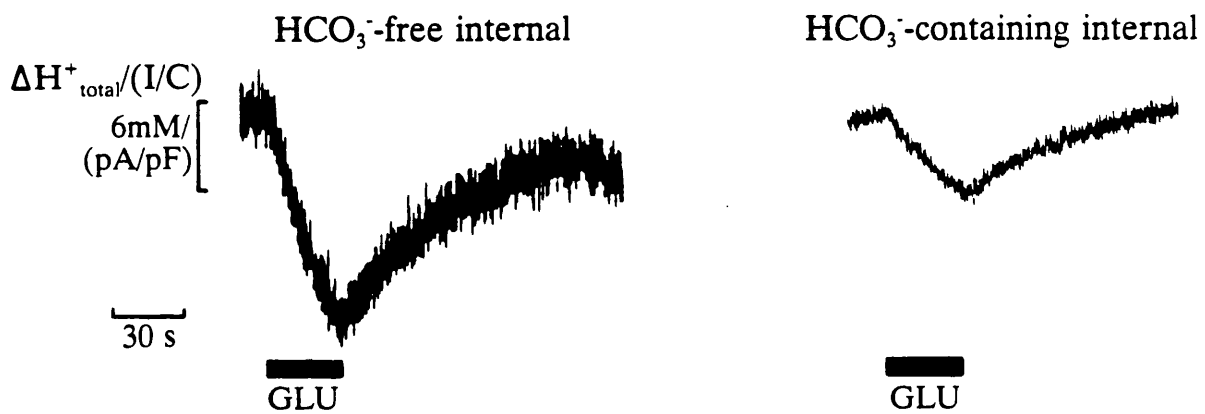


Fig 5.12: Changes of intracellular pH evoked by glutamate when the cell is whole-cell clamped with an internal solution containing added HCO₃⁻. Left: total effective transmembrane proton flux needed to generate the observed [H⁺]_i change. The [H⁺]_i change was normalised by the current/capacitance to compensate for cells being of different size. These cells were chosen to represent the average values of $\Delta[H^+]_i/(I/C)$.

5.15 Effect of depleting the intracellular bicarbonate concentration on the amplitude of the uptake current

I considered the possibility that even with no added internal HCO_3^- , the presence of a trace level of HCO_3^- could account for the uptake observed, without postulating any OH^- transport. One approach to demonstrating an obligatory transport of HCO_3^- out of the cell on the glutamate uptake carrier is to deplete HCO_3^- from the internal solution. This was attempted by bubbling the internal solution with oxygen (100%). Müller cells were whole-cell clamped with such an internal solution (solution J, table 2.3) and compared to cells containing the control solution which was not so bubbled (solution J, table 2.3). The current evoked by the application of $30\mu\text{M}$ glutamate was recorded (and normalised by the capacitance of the cell). In 3 cell pairs, the ratio of the current in the cells with nominally HCO_3^- -free solution to the current in the cells with the normal solution was 0.99 ± 0.04 (mean \pm sem). This result might suggest that HCO_3^- is not an obligatory ion for transport by the carrier, provided that the O_2 bubbling procedure does indeed remove $\text{CO}_2/\text{HCO}_3^-$ from the solution.

5.16 Effect of external acetazolamide on the extracellular pH change evoked during glutamate uptake

If HCO_3^- is transported on the uptake carrier, it can only generate a pH change by reacting with H^+ to form H_2CO_3 and thus CO_2 and H_2O . The second part of this reaction (and hence the pH change) is catalysed by carbonic anhydrase. To further investigate the possible transport of HCO_3^- ions, I tested the effect of acetazolamide, a blocker of carbonic anhydrase, on the extracellular pH changes evoked during glutamate uptake (initially for cells with no added bicarbonate in the internal solution). In other preparations (Kaila *et al*, 1990), inhibiting carbonic anhydrase greatly reduces pH changes produced by the transport of HCO_3^- across the membrane. The extracellular pH change was monitored as described in chapter 4 using a pH electrode positioned just outside the cell. The uptake of glutamate was activated by stepping the voltage from a positive value (+7mV, where the uptake is largely reduced) to a more negative value (-88mV, at which the current evoked by the uptake of glutamate is large)

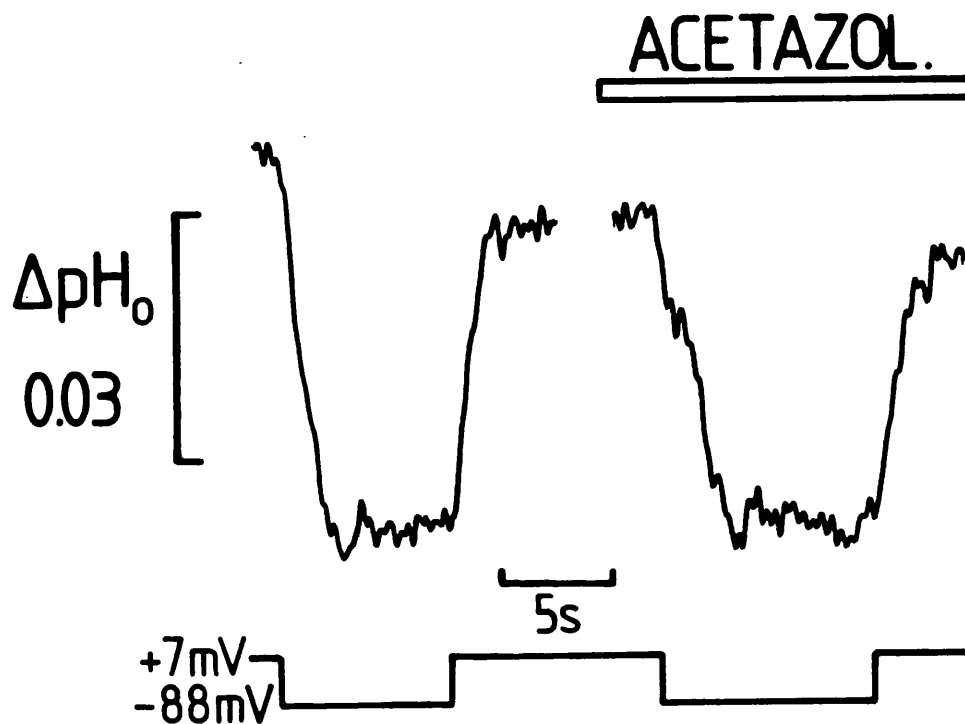


Fig 5.13: The effect of acetazolamide (a carbonic anhydrase inhibitor) on the extracellular pH change evoked during glutamate uptake. Stepping the voltage to -88mV (bottom trace) in the absence of external acetazolamide evoked an alkalinization of the external medium (top trace). The same voltage step performed when the external solution contained 100 μ M acetazolamide evoked a similar extracellular pH change.

in the presence of $100\mu\text{M}$ L-glutamate, in a solution of low buffering power (solution F, table 2.2). This procedure was performed in the absence and in the presence of $1\mu\text{M}$ acetazolamide in the extracellular solution (a dose which blocks extracellular pH changes produced by HCO_3^- movement across the membrane in other preparations; Kaila *et al*, 1990). The cells were kept on coverslips, and only one cell was studied per coverslip in order to be able to monitor the extracellular pH change of each cell before acetazolamide had ever been applied. In 4 cells, the ratio of the extracellular pH change (normalised by the size of the uptake current to compensate for slight run-down during the experiment) in the presence of acetazolamide ($1\mu\text{M}$) compare to in the absence of the blocker was 1.05 ± 0.15 (mean \pm sem; Fig 5.13). Thus, blocking carbonic anhydrase does not reduce the size of the extracellular pH change. The concentration of acetazolamide used during the experiment did not affect the buffering power of the external solution. This suggests that with no added HCO_3^- inside the cell, the majority of the pH change produced by glutamate uptake is not produced by the transport of HCO_3^- , ruling out an obligatory transport of HCO_3^- and suggesting that OH^- is transported.

5.17 Effect of acetazolamide outside on the internal pH change induced by glutamate uptake

The effect of acetazolamide ($100\mu\text{M}$) applied externally on the intracellular acidification was also investigated. In other preparations (Kaila *et al*, 1990), this dose of acetazolamide reduces by 60% the intracellular pH change produced by HCO_3^- movement across the membrane. Müller cells were again plated onto coverslips and only one cell from each coverslip was studied (see above). L-glutamate ($100\mu\text{M}$) was applied to the cells whole-cell clamped at -43mV using a nominally HCO_3^- -free internal solution (solution U, table 2.5 to which metabolic blockers were added). In the presence of acetazolamide, the pH change was 0.88 ± 0.07 (mean \pm s.d.; Fig 5.14) of its value in the control solution (solution B, table 2.1), again suggesting that (with no added HCO_3^-) the majority of the pH change is not produced by HCO_3^- transport and HCO_3^- transport is not obligatory.

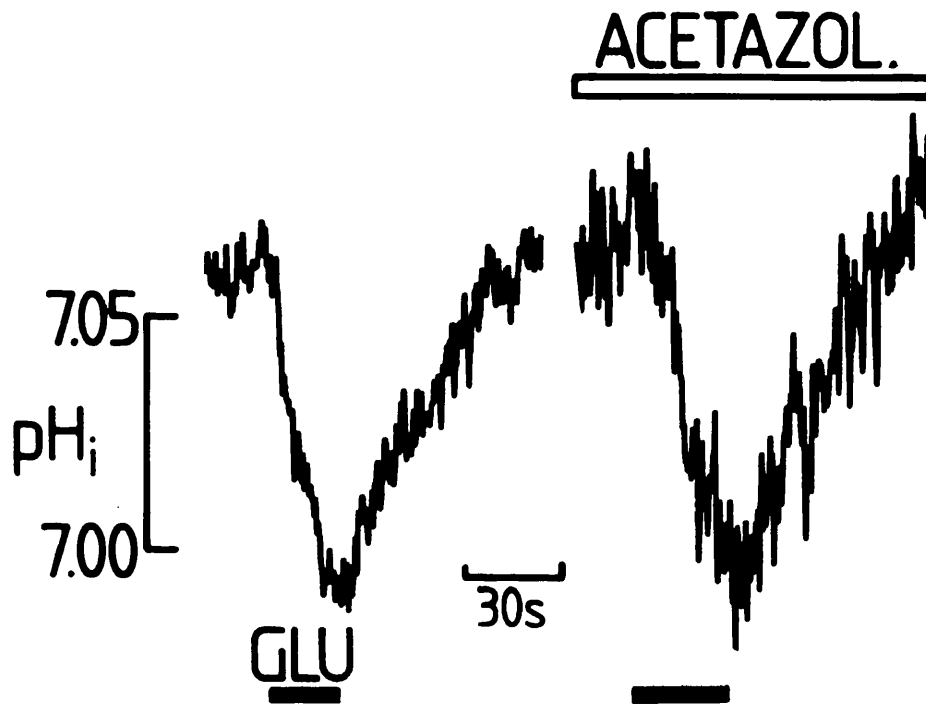


Fig 5.14: Lack of effect on the intracellular acidification of acetazolamide (a carbonic anhydrase inhibitor). Data from a Müller cell whole-cell clamped with a internal solution containing BCECF (pH-sensitive fluorescent dye). L-glutamate ($100\mu\text{M}$) was successively applied to the cells in the absence (left panel) and in the presence (right panel) of acetazolamide ($100\mu\text{M}$). The intracellular pH change seen in the presence of acetazolamide was similar to that seen without acetazolamide.

5.18 Conclusion

The experiments presented in this chapter suggest that a pH-changing anion is transported out of the cell on the glutamate uptake carrier (instead of a proton being transported in). In the absence of added intracellular bicarbonate, this pH-changing anion is more likely to be a hydroxyl than a bicarbonate ion for several reasons. First of all, experiments using acetazolamide to block carbonic anhydrase do not abolish the pH changes monitored inside and outside the cell during glutamate uptake (in contrast with the results obtained by Kaila *et al* (1990) on the pH changes generated by HCO_3^- moving through GABA channels). Moreover, for experiments with nominally HCO_3^- -free internal solutions and a carbonic anhydrase blocker present (as well as metabolic blockers to avoid production of CO_2 by the cell), calculations suggest that the cell would use up all its endogenous bicarbonate within 2 seconds (see discussion, section 7.2.4) and would not be able to produce it at a sufficient rate to maintain the observed uptake current. Therefore, the transport of a HCO_3^- ion cannot be obligatory. In contrast, calculations suggest that the dissociation of water can generate enough hydroxyl ions to provide one OH^- per unitary charge transported (see discussion, section 7.2.4). However, the possibility that some bicarbonate can be transported out on the glutamate uptake carrier is suggested by the results shown in Fig 5.11, which show a larger uptake current in the more physiological condition when bicarbonate is present inside the cell at a concentration of about 10mM. I therefore propose the stoichiometry for glutamate transport shown in Fig 5.15, where one glutamate ion is transported into the cell with two sodium ions and one potassium ion is counter-transported together with one hydroxyl ion or a bicarbonate ion.

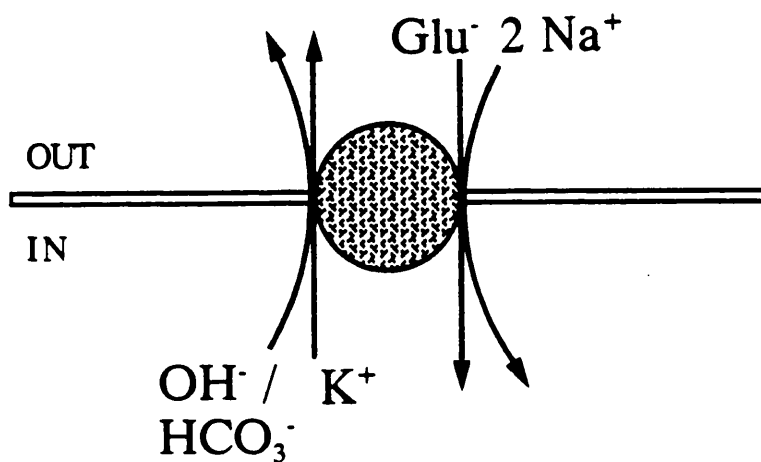


Fig 5.15: The proposed stoichiometry for the glutamate uptake carrier. On each cycle of the carrier, one glutamate ion comes in with two sodium ions and one potassium ion leaves the cell together with one hydroxide or bicarbonate (perhaps on 1/3 of carrier cycles as suggested by the data in Fig 5.13). As a result of this stoichiometry, one net positive charge enters the cell per cycle of the carrier, producing an inward current. Moreover, the anion leaving the cell produces an extracellular alkalization and an intracellular acidification (as described in chapter 4).

Chapter 6

Modulation of the rate of glutamate uptake

6.1 Introduction

This chapter describes experiments to investigate how the rate of glutamate uptake might be modulated. The effects of ATP and adenosine on the magnitude of the glutamate uptake current were tested, since there are receptors of poorly understood function for these compounds expressed in glial cells. The effect of ascorbate was tested since, as discussed below, there is reason to believe it might modulate the uptake rate. The effect of annexin I (a calcium-dependent lipid-binding protein) on the inhibitory action of arachidonic acid on uptake was also investigated for reasons described in detail below. The cloning and sequencing of rat and rabbit glutamate uptake carriers have revealed putative c-AMP-dependent protein kinase (PKA) phosphorylation sites as well as several putative sites for phosphorylation by protein kinase C (PKC) (see introduction, section 1.6.5). The possibility that glutamate uptake might be modulated by phosphorylation by these protein kinases was therefore investigated.

6.2 Effect of ascorbate on the amplitude of the glutamate-evoked current

Since ascorbate has been suggested to be transported out of the cell on the glutamate uptake carrier (Grünewald & Fillenz, 1984), it was of interest to study the effect of ascorbate either inside the cell or outside the cell on the amplitude of the current generated by glutamate uptake. Na-ascorbate was added to the external solution (solution B, table 2.1) at a concentration of 1mM, together with thiourea (10mM) to prevent oxidation. The control solution had 1mM NaCl (instead of Na-ascorbate) and 10mM thiourea added to it. The cells were whole-cell clamped at -43mV and glutamate (30 μ M) was applied successively in the absence and the presence of external ascorbate. The ratio of the amplitude of the uptake current in the absence and in the presence of ascorbate (1mM) was 1.04 ± 0.14 (mean \pm sem; n=7). This value is not

significantly different from 1. Thus, 1mM extracellular ascorbate has no effect on the glutamate uptake carrier. The free ascorbate level in the CSF is 200-500 μ M (Cammack *et al*, 1991).

Experiments were also performed to investigate the effect of internal ascorbate on the glutamate uptake carrier. Cells were whole-cell clamped to -43mV, alternating between the control internal solution (solution Ω , table 2.6) and an internal solution containing 5mM ascorbate (solution Z, table 2.6). Glutamate (30 μ M) was applied to the cells and the evoked current was monitored (and normalised by the capacitance of the cell to compensate for cells being of different sizes). The mean value was 0.89 ± 0.4 pA/pF (mean \pm sem; n=5) for cells containing no ascorbate and 0.90 ± 0.3 pA/pF (mean \pm sem; n=5) for cells containing ascorbate. These two values are not significantly different. Thus, the presence of ascorbate (5mM) inside the cells has no effect on the glutamate uptake carrier in whole-cell clamped salamander Müller cells.

6.3 Effect of external ATP on the inward current evoked by glutamate uptake

Whether glutamate uptake is modulated by external ATP was investigated by applying glutamate (30 μ M) to Müller cells clamped at -43mV, first of all in an ATP-free external medium (solution B, table 2.1) and then in the same external solution containing 100 μ M ATP. The cells were whole-cell clamped at -43mV. After 2 minutes in ATP, the amplitude of the uptake current (normalised by the cell capacitance to compensate for a slight decrease in cell surface area with time (Barbour *et al*, 1991)) was $95 \pm 6\%$ of the control value (mean \pm sem; n=4). After 9 minutes in ATP-containing solution, the magnitude of the current/capacitance was $99.5 \pm 17\%$ of the control value (mean \pm sem; n=4). These values are not significantly different from unity. It was therefore concluded that external ATP does not modulate the uptake carrier, at least under whole-cell clamp conditions.

6.4 Effect of external adenosine on the glutamate-evoked current

The effect of external adenosine was investigated in a similar manner. Glutamate (30 μ M) was applied at -43mV first of all in control solution (solution

B, table 2.1) and then in the same solution containing adenosine ($100\mu\text{M}$). After 2 minutes in adenosine, the amplitude of the current evoked by the uptake of glutamate was $99 \pm 2\%$ of the control value (mean \pm sem; $n=7$). After 10 minutes in adenosine, the magnitude of the uptake current was $96 \pm 4\%$ of the control amplitude (mean \pm sem; $n=7$). These values are not significantly different from the control values. These results strongly suggest that external adenosine does not affect the glutamate uptake carrier, at least under whole-cell clamp conditions.

6.5 Effect of external annexin I on the the glutamate uptake carrier

Brain damage in anoxia or ischemia results from the extracellular glutamate concentration rising too high (for review, see Choi, 1988). Arachidonic acid is released in brain anoxia (Rehncroa *et al*, 1982) and inhibits glutamate uptake (Silverstein *et al*, 1986; Barbour *et al*, 1989), possibly contributing to the rise in extracellular glutamate concentration to neurotoxic levels. Annexin I (a calcium-dependent lipid-binding protein) (for review, see Crompton *et al*, 1988) has been suggested to have a neuroprotective role when injected into the rat brain 30-60 minutes after induction of ischemia (Relton *et al*, 1991; Black *et al*, 1992). It seems possible, therefore, that annexin I might exert its protective action by binding arachidonic acid and preventing its inhibition of glutamate uptake.

6.5.1 Effect of external annexin I on the amplitude of the glutamate-evoked current

Annexin I on its own might be expected to stimulate glutamate uptake by binding any free arachidonic acid present in the cell membrane and decreasing the inhibitory effect that arachidonic acid has on uptake, just as albumen does (Volterra *et al*, 1992). The effect of annexin I on the magnitude of the current evoked by $30\mu\text{M}$ glutamate was investigated on cells whole-cell clamped at -43mV . Usually, the cells were split into two groups, one of them being in solution containing annexin I isolated from bovine lung (at a concentration of 1mg per ml ; annexin I was a gift of S. Moss). For some cells, the annexin I was

perfused onto the cell after recording from the cell in control solution (solution B, table 2.1). The amplitude of the current evoked by the application of glutamate ($30\mu\text{M}$) (divided by the capacitance to compensate for cells being of different sizes) was $0.88 \pm 0.11\text{pA/pF}$ (mean \pm sd; $n=6$) for control cells whereas the value for cells in contact with annexin I was $0.73 \pm 0.11\text{pA/pF}$ (mean \pm sd; $n=6$). These values are not significantly different (Student t test; $p>0.50$). Annexin I was therefore found not to have any effect on the uptake of glutamate.

6.5.2 Effect of external annexin I on the inhibition of the glutamate uptake carrier by arachidonic acid

As annexin I is a calcium-dependent lipid-binding protein, and is thus expected to bind arachidonic acid, it was interesting to test whether it affected the inhibition of glutamate uptake produced by arachidonic acid (see introduction para 1.6.3). After monitoring the inward current evoked by the application of glutamate ($30\mu\text{M}$) in a control solution (solution B, table 2.1), a solution containing $10\mu\text{M}$ arachidonic acid (in solution B, table 2.1) was applied. The same concentration of glutamate was then applied to the cells. In the control cells, the amplitude of the current (normalised by the capacitance of the cell to compensate for any loss of cell membrane area) after 5 minutes of exposure to arachidonic acid was $54.5 \pm 5\%$ of the pre-arachidonic acid control value. For cells in contact with annexin I, the corresponding value was $52.7 \pm 10\%$ of the control value. These two values are not significantly different. Thus, annexin I did not have any effect on the inhibition of glutamate uptake by arachidonic acid.

6.6 Effect of PKA catalytic subunit and of a peptide inhibitor of PKA present inside the cell on the amplitude of the glutamate evoked current

PKA comprises two subunits: the catalytic subunit which is responsible for phosphorylation of the substrate, and the regulatory subunit which binds to the catalytic subunit to block its action. The regulatory subunit has a binding site for cAMP. The binding of cAMP to the regulatory subunit triggers the release of the

catalytic subunit which becomes free to phosphorylate substrates.

6.6.1 Protein kinase A catalytic subunit

The first approach taken to investigate the possible effect of PKA on glutamate uptake was to whole-cell clamp cells, alternating between two different internal solutions: a control internal solution (solution J, table 2.3) and the same solution containing PKA catalytic subunit ($0.5\mu\text{M}$, from Sigma). As the PKA catalytic subunit is a large molecule, cells were kept, and glutamate uptake was monitored, for 25 minutes after going whole-cell to allow the catalytic subunit of PKA to diffuse from the patch pipette into the cell (see methods, section 2.7). At the start of the experiment, the magnitude of the uptake current (divided by the capacitance) was 0.58 ± 0.1 pA/pF (mean \pm sem; $n=5$) for the control cells and 0.58 ± 0.07 pA/pF (mean \pm sem; $n=5$) for cells whole-cell clamped with the PKA catalytic subunit internal solution. The ratio of the amplitude of the evoked current (divided by the capacitance of the cell) 25 minutes after going whole-cell to the value just after going whole-cell was 0.82 ± 0.06 pA/pF (mean \pm sem; $n=5$) for control cells and 0.92 ± 0.15 pA/pF (mean \pm sem; $n=5$) for the cells containing PKA catalytic subunits. These values are not significantly different, suggesting that either the glutamate uptake carrier is not affected by phosphorylation by PKA, or that it is already fully phosphorylated in the conditions used for these experiments and that addition of catalytic subunits for PKA cannot affect the phosphorylation state of the carrier.

6.6.2 Peptide inhibitor of protein kinase A

The second approach was to try to inhibit a putative PKA activity that might already be present in the cell. This experiment was performed using a peptide inhibitor of the PKA catalytic subunit (given by E. Mandley). This peptide is able to bind to the catalytic subunit and block its activity. For this reason, the concentration of the peptide inhibitor used should ideally be equal to that of the PKA protein (since the stoichiometry of the inhibition is 1:1). However, the concentration of PKA in salamander Müller cells is unknown and the concentration of inhibitor was chosen to be greater than the PKA

concentration in *Xenopus* oocytes (250nM - 1 μ M). The lyophilized peptide inhibitor (10 μ g) was solubilised in 1ml of the normal internal solution (solution J, table 2.3) giving a final concentration of inhibitor of approximately 4 μ M. Different cells were whole-cell clamped to -43mV, using alternately the control internal solution and the internal solution containing the peptide inhibitor. The amplitude of the current generated by glutamate uptake (30 μ M glutamate) was monitored regularly over 15 minutes to allow for diffusion of the peptide from the patch pipette into the cell (see methods section 2.7). At the start of the experiment, the amplitude of the uptake current (normalised by the capacitance of the cell) was 0.93 ± 0.12 pA/pF (mean \pm sem; n=5) for control cells whereas for cells whole-cell clamped with an internal solution containing PKA peptide inhibitor, the corresponding value was 1.02 ± 0.15 pA/pF (mean \pm sem; n=5). These two values are not significantly different. Comparing the magnitude of the current (divided by the capacitance of the cell) 15 minutes after going whole cell to that just after going whole cell gave a ratio of 0.88 ± 0.06 (mean \pm sem; n=5) for the control cells whereas the cells with the peptide inhibitor had a corresponding ratio of 0.97 ± 0.07 (mean \pm sem; n=5). Once again these two values are not significantly different. These experiments suggest that PKA does not affect the glutamate uptake carrier in whole-cell clamped salamander Müller cells.

6.7 Effect of TPA, an activator of protein kinase C, on the amplitude of the inward current evoked by glutamate uptake

To test the effect of activating protein kinase C on glutamate uptake, cells were dissociated and plated onto several coverslips. The external solution was then replaced by either normal external solution (solution B, table 2.1) to which 100nM DMSO was added or by the same solution supplemented with 100nM phorbol 12-O-tetradecanoylphorbol-13-acetate (TPA, also known as PMA, in DMSO). The cells were whole-cell clamped to -43mV and the current generated by glutamate uptake was monitored in the presence or the absence of TPA according to the conditions in which the cells were kept up to the time of recording. The amplitude of the current (divided by the capacitance of the cell)

was 1.45 ± 0.08 pA/pF (mean \pm sem) for control cells whereas the corresponding value was 1.35 ± 0.48 pA/pF (mean \pm sem) for cells kept in 100nM TPA. These two values are not significantly different. However, the values of the amplitude of the uptake current were a lot more scattered for cells kept in 100nM TPA. A possible explanation for this is shown in Fig 6.1, which is a plot of the amplitude of the uptake current (normalised by the capacitance of the cell) against the length of time for which the cells were left in the control solution or in the solution containing TPA before being whole-cell clamped. Each point represents only one cell, which weakens the statistical value of the data, but the analysis is potentially interesting: the uptake current in cells not exposed to TPA is roughly constant, while that for the cells in TPA declines slowly. Phorbol esters are known to have two separate effects on protein kinase C activity: they initially activate protein kinase C in a Ca^{2+} in a phospholipid-independent manner, and they also in the longer term severely reduce PKC enzymatic activity through post-transcriptional down-regulation (Isakov *et al*, 1990). The results shown in Fig 6.1 could therefore reflect, at early times, a rapid TPA-induced phosphorylation of the glutamate uptake carrier (or of another protein which modulates the carrier's activity) by PKC leading to an increase in the activity of the carrier, followed at late times by a decrease in the enzymatic activity of PKC with a consequent decrease of the phosphorylation state of the carrier (or of the putative modulatory protein) and thus a diminution of its activity. Further experiments are needed to check the reliability of the data trends in Fig 6.1.

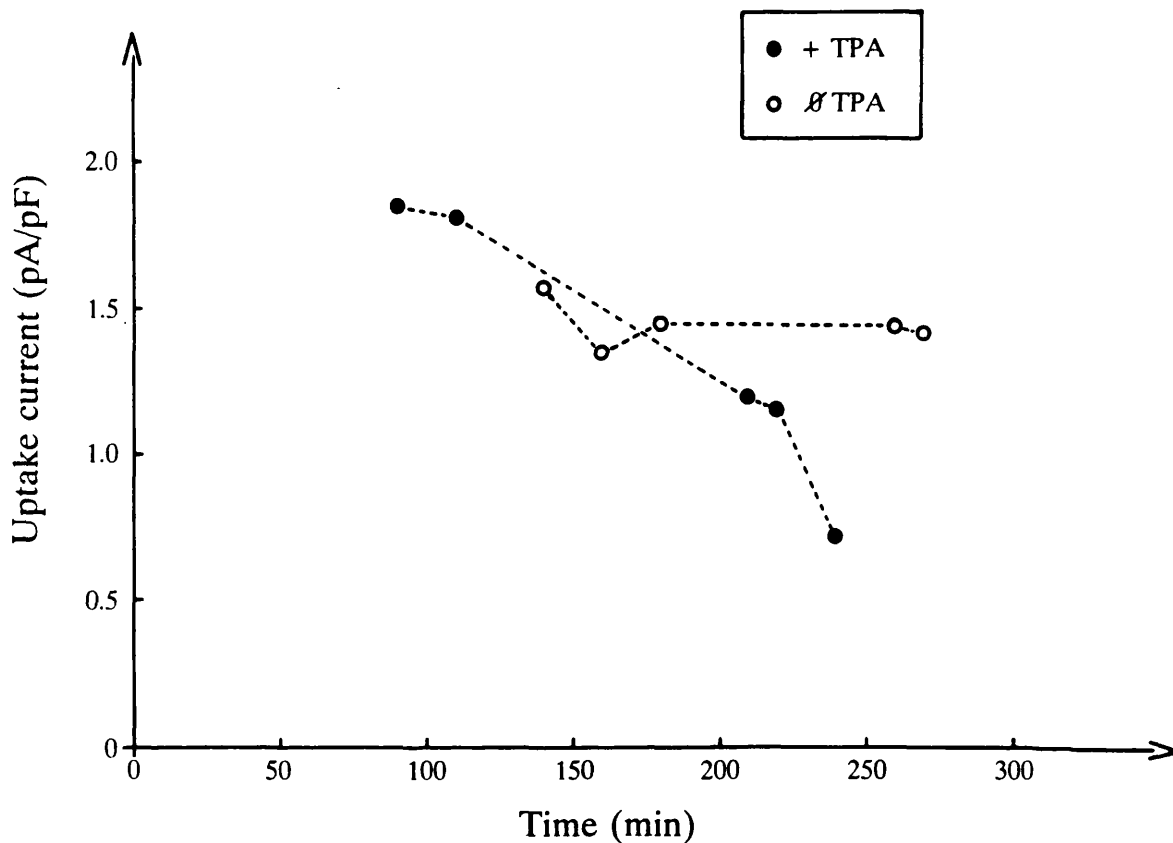


Fig 6.1: Effect of prolonged application of TPA on the magnitude of the glutamate uptake current. Open circles show the magnitude of the uptake current (generated by the application of $30\mu\text{M}$ glutamate) normalised by the capacitance of the cell, for cells kept in normal external solution after retinal dissociation. Closed circles show the value obtained for cells kept in the presence of TPA after retinal dissociation. Each circle represents one cell and all ten cells were from the same dissociation.

Chapter 7

Discussion

In this chapter, I will discuss the implications of the results presented in the preceding chapters.

7.1 Electrogenic uptake of sulphur-containing analogues of glutamate and aspartate

In chapter 3, it was shown that application of sulphur-containing analogues of glutamate and aspartate to whole-cell clamped Müller cells evoked inward currents. The ionic-dependence and voltage-dependence of these currents and how they interacted with the glutamate uptake current were described. In this section, I will consider the possibility that sulphur-containing analogues of glutamate and aspartate are transported on a carrier different to the glutamate uptake carrier. I will then discuss the excitotoxic action of the sulphur analogues and relate it to their rate of uptake and to their ability to activate NMDA receptors. Finally, I will postulate possible ways in which sulphur-containing analogues could be released from cells in physiological and pathological conditions.

7.1.1 Sulphur-containing amino-acids activate the electrogenic glutamate uptake carrier

The currents evoked by the application of cysteic acid (CA), cysteine sulphinic acid (CSA), homocysteic acid (HCA), homocysteine sulphinic acid (HCSA) and S-sulpho-L-cysteine (SC) showed a strict dependence on external sodium and internal potassium, just as glutamate uptake does. The dependence of the currents on membrane potential was also found to be very similar to that of the current produced by glutamate uptake: the current was large when the cell was held at negative membrane potentials and became smaller at more positive potentials. At no potentials did the current show any sign of reversal (potentials

tested up to +30mV). The currents evoked by these analogues did not sum with that produced by the uptake of glutamate. These results are consistent with the currents being produced by the transport of sulphur-containing analogues of glutamate and aspartate on the glutamate uptake carrier. Some transport of sulphur-containing analogues on a different carrier cannot be ruled out, but this carrier would have to have characteristics very similar to the glutamate uptake carrier. In what follows, it will therefore be assumed, for simplicity, that there is only one carrier that transports all the sulphur-containing analogues of glutamate and aspartate as well as glutamate and aspartate themselves. The stoichiometry of the transport is postulated to be the same as that for glutamate: two sodium ions transported into the cell with one molecule of glutamate analogue, and one potassium ion and one hydroxyl (or one bicarbonate; see below) are counter-transported.

7.1.2 Inhibition of HCA transport with β -p-chlorophenylglutamate

The results expressed above are consistent with the findings of Wilson & Pastuszko (1986), based on radiotracing experiments, that CA and CSA are transported on the same carrier as glutamate and aspartate. Some authors however, have suggested that CA and CSA are transported on a carrier different from that on which glutamate itself is transported (Parsons & Rainbow, 1984). Moreover, HCA was suggested to be transported on a low affinity carrier, different from the high affinity glutamate uptake carrier (Cox *et al*, 1977). Davies *et al* (1985) also proposed that HCA was transported on a carrier different from that of glutamate, whereas the results from chapter 3 are consistent with low affinity transport of homocysteic acid on the high affinity glutamate transporter. Davies *et al* based their conclusion on the following observation: β -p-chlorophenylglutamate inhibited the uptake of [3 H]-HCA, but did not affect the uptake of [3 H]-glutamate. However, these authors used a glutamate concentration (500 μ M) far above the concentration needed to saturate uptake and a concentration of HCA (75 μ M) very much lower than the K_m for the activation of HCA uptake (determined as around 3mM in the experiments described in chapter 3). The selective inhibition of HCA uptake by β -p-

chlorophenylglutamate can be explained by considering the equations for competitive inhibition of binding to the uptake site as follows.

Suppose that both glutamate and HCA are taken up by the same carrier, with rates of uptake in the absence of inhibitor given by, for glutamate:

$$V_{\text{Glu}} = V_{\text{max, Glu}} \times [\text{Glu}] / \{[\text{Glu}] + K_{\text{M, Glu}}\}$$

and for HCA:

$$V_{\text{HCA}} = V_{\text{max, HCA}} \times [\text{HCA}] / \{[\text{HCA}] + K_{\text{M, HCA}}\}$$

where V_{max} is the maximum uptake rate at a saturating level of substrate, and K_{M} is the substrate concentration giving a half-maximal uptake rate. In the presence of inhibitor (β -p-chlorophenylglutamate) at concentration I and with K_{M} value K_{I} , these equations become (for competitive inhibition):

$$V_{\text{Glu}} = V_{\text{max, Glu}} \times [\text{Glu}] / \{[\text{Glu}] + K_{\text{M, Glu}} (1 + I/K_{\text{I}})\}$$

$$V_{\text{HCA}} = V_{\text{max, HCA}} \times [\text{HCA}] / \{[\text{HCA}] + K_{\text{M, HCA}} (1 + I/K_{\text{I}})\}$$

Now, in the experiments of Davies *et al*, $[\text{Glu}]$ was much higher than $K_{\text{M, Glu}}$ while $[\text{HCA}]$ was much smaller than $K_{\text{M, HCA}}$, so (providing I is not $\gg K_{\text{I}}$) the last two equations become approximately:

$$V_{\text{Glu}} = V_{\text{max, Glu}}$$

and
$$V_{\text{HCA}} = V_{\text{max, HCA}} \times [\text{HCA}] / \{K_{\text{M, HCA}} (1 + I/K_{\text{I}})\}$$

Thus, the rate of glutamate uptake is saturated at its maximal value and is unaffected by the presence of inhibitor, while HCA uptake is reduced by the inhibitor. If the glutamate concentration used had been lower (i.e. non-saturating), then the inhibitor would have had an effect. The results of Davies *et al* (1985) are therefore compatible with the transport of the two substances (glutamate and HCA) on the same carrier. Indeed, later studies confirmed that homocysteate uptake into cultured neurones and glial cells was not selectively blocked by β -p-chlorophenylglutamate (Griffiths *et al*, 1992).

7.1.3 Termination of postulated neurotransmitter action

Several of the sulphur-containing analogues of glutamate and aspartate

have been proposed as neurotransmitter candidates (see introduction section 1.2). One of the characteristics required for such a role is the presence of a potent mechanism for removal of the substance from the extracellular solution. The K_m values for the uptake of CA and CSA (table 7.1) indicate a high affinity transport process. These findings therefore support their putative role as neurotransmitters. However, for HCA, HCSA and SC, the K_m for the activation of the glutamate uptake carrier was very high (implying low affinity transport on the high affinity glutamate carrier). Therefore, unless another means exists for quickly removing the analogue from the extracellular medium (such as electroneutral high affinity transport or breakdown by an extracellular enzyme), the results described here seriously undermine the notion of these three analogues being fast acting neurotransmitters.

7.1.4 Excitotoxic actions of the sulphur-containing amino-acids

The excitotoxic effect of glutamate is thought to be mainly due to an excessive activation of NMDA receptors by the neurotransmitter, leading to a massive influx of calcium (and sodium) into neurones (Meldrum & Garthwaite, 1990). Sulphur-containing analogues of glutamate and aspartate have been found to activate NMDA receptors with different potencies (Patneau & Mayer, 1990). Comparing the potency of these analogues to activate NMDA receptors, their K_m for uptake, and their known neurotoxic action was therefore interesting. The aim of the following analysis was to explain what factors determine the neurotoxicity or otherwise of different glutamate analogues.

In the situation considered, I assumed that the analogues are released into the extracellular space at a rate low enough not to saturate uptake into cells (and that the analogues are not released via reversed action of the glutamate uptake carrier). For simplicity, the extracellular space is treated as a single compartment. At equilibrium, the release of analogues will be balanced by their removal from the extracellular medium by uptake, thus:

$$\text{Release rate} = V_{\max} \cdot c / (K_m + c) = V_{\max} \cdot c / K_m \text{ for } c \ll K_m \quad (1)$$

$$\text{or } c = \text{Release rate} \cdot K_m / V_{\max} \quad (2)$$

where c is the extracellular concentration of the analogue, K_m is the Michaelis-Menten constant for the transport of the analogue considered and V_{max} the maximum uptake rate of the analogue. The current flowing through NMDA-type channels opened by the binding of different analogues of glutamate and aspartate is proportional to $(c/K_{NMDA})^{1.4}$ (Patneau & Mayer, 1990) if $c \ll K_{NMDA}$, where K_{NMDA} is the concentration of the analogue which evokes a half-maximum current through the NMDA channels. Thus, the current through NMDA channels is proportional to (from equation (2):

$$\{[\text{Release rate} \cdot K_m / V_{max}] / K_{NMDA}\}^{1.4} \quad (3)$$

If we assume that a certain threshold amount of current or calcium influx through NMDA channels is needed to generate excitotoxicity, then equation (3) predicts that the minimum release of analogue needed to produce this current is :

$$\text{release rate needed for excitotoxicity} \propto K_{NMDA} [V_{max}/K_m] \quad (4)$$

Therefore, an analogue will be more excitotoxic for a low K_{NMDA} or a low rate of uptake (V_{max}/K_m), since less release will then be needed to produce the fractional activation of NMDA receptor needed for excitotoxicity. A useful parameter describing this is the excitotoxic index defined by:

$$\text{excitotoxic index} = [1/K_{NMDA}] / [V_{max}/K_m] \quad (5)$$

The excitotoxic index of each analogue is inversely proportional to the release rate needed for the analogue to induce excitotoxic damage. Table 7.1 shows the values of this index derived from the values of K_{NMDA} for each of the analogues studied here (from Patneau & Mayer, 1990) and from the values of K_m and V_{max} (from chapter 3 of this thesis). For SC, an estimate of V_{max}/K_m was calculated from the current generated by the application of 1mM of the analogue by assuming that 1mM was well below the K_M for SC, since only that dose evoked

	NMDA channels	Glu uptake			Excitotoxic index
	$K_{\text{NMDA}} (\mu\text{M})$	$K_{\text{m}} (\mu\text{M})$	V_{max}	$V_{\text{max}}/K_{\text{m}} (\mu\text{M}^{-1})$	$[1/K_{\text{NMDA}}]/[V_{\text{max}}/K_{\text{M}}]$
	(from Patneau & Mayer)	(from this thesis)			
Glu	2.3	15	1	0.067	6.52
Asp	16.9	4	0.25	0.063	0.95
CA	302.0	6	0.64	0.107	0.031
CSA	43.0	60	0.37	0.0065	3.58
HCA	12.9	2950	0.21	0.00007	1107.0
HCSA	29.9	1650	0.41	0.00025	134.0
SC	8.2	---	---	0.00015	833.0

Table 7.1: Excitotoxic index values of glutamate, aspartate and their sulphur-containing analogues. V_{max} values were normalised to the value for glutamate. For SC, individual values of K_{M} and V_{max} were not obtained, but their ratio was estimated from the response to 1mM SC - the lowest dose tested which produced a response.

a current (higher doses were not tested). The order suggested by the excitotoxic index, for the potency to induce excitotoxic damage, is as follows:

$$\text{HCA} > \text{SC} > \text{HCSA} > \text{Glu} > \text{CSA} > \text{Asp} > \text{CA}$$

The particular values for Asp and HCA are interesting. These two analogues have a similar EC_{50} value for opening NMDA channels, which suggests equal potential for causing excitotoxic damage. However, HCA is poorly taken up by the carrier compared to aspartate. As a result, the excitotoxic index for HCA is very much higher than that for aspartate.

The order of potency for the excitotoxicity of the analogues is similar to that found by Pullan *et al* (1987) who generated retinal excitotoxicity by superfusing glutamate analogues. Their order of potency was as follow:

$$\text{HCA} > \text{SC} > \text{HCSA} > \text{Glu} = \text{CSA} = \text{CA}$$

However, the values shown in table 7.1 predict that HCA is 170 times ($1107/6.52$) more toxic than glutamate and 36000 times ($1107/0.031$) more toxic than CA whereas Pullan *et al* only found a fivefold difference in the toxicity of these analogues. Several reasons can explain these discrepancies. First of all, if the analogues are perfused onto the slice as in Pullan *et al*'s experiments instead of being released from neurones as assumed in the calculation above, the concentration of analogue depends on the uptake rate (as expressed by equation (2)) but also on the diffusion of the analogue into the slice. As a result, the concentration of the analogue will depend more weakly on the rate of uptake of the analogue than is expressed by equation (2). This will reduce differences in the excitotoxic potential of the various analogues. Secondly, it is likely that excitotoxic damage occurs when extracellular concentration of analogue is not very small compared to the K_M of uptake, while in the calculation above I assumed $c \ll K_M$. Moreover, the experiments described in chapter 3 were performed on cells whole-cell clamped to -43mV . In physiological conditions, the resting potential of glial cells is around -90mV . This may affect the ratio of V_{max} of the different analogues (for example, $V_{\text{max, Asp}}/V_{\text{max, Glu}}$ is $1/5$ at -40mV but $1/3$ at -80mV ; Barbour *et al*, 1991). Lastly, excitotoxicity may not just reflect the activation of NMDA receptors (Meldrum & Garthwaite, 1990).

7.1.5 Mechanism of release of sulphur-containing amino-acids

Because of their charges, the sulphur-containing analogues of glutamate and aspartate are probably prevented from crossing the blood-brain barrier, like glutamate and aspartate are. However, during neurodegenerative disorders such as sulphite oxidase or cystathionine synthase deficiency (see introduction, section 1.2), homocysteic acid and S-sulpho-L-cysteine are found in high concentrations in the extracellular space of the brain. It is possible, therefore, that these analogues are released by neurones or glial cells. They could be released by conventional calcium-dependent vesicular release (after depolarisation of neurones) or, as shown for glutamate, by reversed operation of the glutamate transporter (Szatkowski *et al*, 1990), or by hetero-exchange on the carrier with uptake of a glutamate anion being followed by release of a sulphur analogue anion. Either of the last two modes of release would invalidate the calculation presented above of relative excitotoxic potential of the different analogues.

7.2 **Stoichiometry of the glutamate uptake carrier**

In this paragraph, I will discuss the evidence for the transport of each type of ions on the glutamate uptake carrier and, based partly on the results in chapters 4 and 5, will reach the conclusion that glutamate is transported into the cell with two sodium ions and that one potassium ion is counter-transported together with a hydroxyl ion (or possibly a bicarbonate).

7.2.1 Glutamate

The dependence of high affinity glutamate uptake on the concentration of glutamate obeys a Michaelis-Menten equation with a K_m value for glutamate between 2 and 50 μ M (Hertz, 1979; Erecińska, 1987; Pines *et al*, 1992). This indicates that one glutamate is transported into the cell on each carrier cycle. As the uptake process evokes an inward membrane current when cells are whole-cell clamped and over 99% of glutamate is negatively charged at physiological pH, other ions must also be transported on the carrier.

7.2.2 Sodium

Several experiments led to the conviction that the glutamate uptake carrier was a sodium co-transporter: (1) glutamate uptake was found to be strictly dependent on external sodium (Roskoski, 1978); (2) glutamate can stimulate [^3H]-sodium uptake (Stallcup *et al*, 1979; Baetge *et al*, 1979; Kimelberg *et al*, 1989); (3) glutamate uptake is inhibited by high internal sodium concentrations (Barbour *et al*, 1991).

Erecińska *et al* (1983) investigated the sodium-dependence of the equilibrium $[\text{D-asp}]_i/[\text{D-asp}]_o$ in rat brain synaptosomes and found that it was consistent with the transport of two sodium ions into the cell with each aspartate (or glutamate) anion. Stallcup *et al* (1979) and Baetge *et al* (1979) also suggested that two sodium ions were transported with each glutamate from the dependence of uptake rate on $[\text{Na}^+]_o$. Electrophysiological studies of the uptake of glutamate also shown a sigmoid dependence of uptake current on the extracellular sodium concentration, suggesting that at least two sodium ions (or possibly three) were transported on the carrier with each glutamate (Brew & Attwell, 1987; Schwartz & Tachibana, 1990). Sodium co-transport down its electrochemical gradient is thought to be the major source of energy for the glutamate uptake carrier (see below). On thermodynamic grounds, one can calculate that at least two sodium ions must be co-transported with each glutamate to provide the accumulative power that radiotracing experiments have shown for the carrier.

7.2.3 Potassium

There are several lines of evidence suggesting that potassium is counter-transported on the glutamate uptake carrier. In synaptosomes, a potassium gradient with $[\text{K}]_i > [\text{K}]_o$ was found to stimulate glutamate uptake (Kanner & Sharon, 1978a, b). Moreover, raising external potassium inhibits glutamate uptake (Peterson & Raghupathy, 1972) and stimulates glutamate efflux (Kanner & Marva, 1982). These results were difficult to interpret with confidence since altering the potassium gradient changes the membrane potential, which could explain these observations without any transport of potassium on the carrier. However, more recently, electrophysiological experiments have shown the same

dependence of glutamate uptake on intracellular (whole-cell pipette) potassium even when the membrane potential is held constant (Barbour *et al*, 1988). This potassium-dependence followed Michaelis-Menten kinetics, suggesting that one potassium ion was transported out on the carrier. Arguing against the counter-transport of potassium were results obtained by Schwartz & Tachibana (1990). They did not find any dependence on pipette potassium concentration for the uptake of aspartate in whole-cell clamped salamander Müller cells (the same preparation as Barbour *et al*). These discrepancies can be explained because Schwartz & Tachibana (1990) were only able to lower the intracellular potassium concentration from 90mM to 9mM (due to the size of patch pipette used to whole-cell clamp the cells). The affinity of the glutamate uptake carrier for potassium is around 4mM when aspartate is transported (as against 15mM when L-glutamate is transported by the carrier). It follows that the internal concentration of potassium has to be lowered much more to significantly reduce D-aspartate uptake than to reduce L-glutamate uptake. Direct evidence of the transport of potassium on the glutamate uptake carrier has now been obtained by Amato *et al* (1993a) by measurement of potassium coming out of the cell with a K^+ -sensitive electrode when glutamate uptake is activated.

7.2.4 pH-changing ions

Several authors have suggested that protons were transported on the glutamate uptake carrier. Nelson *et al* (1983) showed that in the absence of sodium and potassium gradients, glutamate uptake could be stimulated by a proton gradient ($pH_o < pH_i$) in membrane vesicles isolated from renal brush border. It was not possible, however, to rule out a possible effect of the proton gradient on the membrane potential. Erecińska *et al* (1983) found that D-aspartate uptake in rat brain synaptosomes was associated with an extracellular alkalinisation, but did not check whether this was a direct effect of uptake, or an indirect one resulting from Na^+ entry on the carrier raising $[Na^+]_i$ and affecting the operation of pH regulating carriers like Na^+/H^+ exchange or Na^+/HCO_3^- co-transport. On the other hand, Schwartz & Tachibana found that D-aspartate uptake into salamander Müller cells did not produce any acidification of the

intracellular medium (monitored by fluorescence of the pH-sensitive fluorescent dye BCECF loaded into the cell in the membrane permeant acetoxymethylester form). However, in Schwartz & Tachibana's experiments, the membrane current generated by glutamate uptake was not monitored. There was therefore no evidence that the cells were taking glutamate up. Experiments performed in this thesis show that glutamate uptake is associated with an intracellular acidification and an extracellular alkalinization and that these do not result from secondary activation of pH-regulating carriers (chapter 4). Further experiments showed that these pH changes were due to a pH-changing anion, presumably OH^- or HCO_3^- , being transported out of the cell on the carrier (chapter 5). Interestingly, the recent cloning of three different glutamate carriers has revealed significant homologies with prokaryotic transporters known to co-transport pH-changing ions (Storck *et al*, 1992; Pines *et al*, 1992; Kanai & Hediger, 1992). These include the sodium-independent glutamate-proton transporter *glpP* in *E. coli* (Tolner *et al*, 1992) and the sodium-proton-glutamate transporter *glpT* from *B. stearothermophilus* (de Vrij *et al*, 1989). It is uncertain whether *glpP* and *glpT* actually transport a proton, or whether they transport an OH^- or HCO_3^- ion in the other direction, as I have postulated for the glutamate uptake carrier in salamander glial cells.

Could bicarbonate be the main anion transported?

It is obviously interesting to determine whether the pH-changing anion transported is OH^- or HCO_3^- . My experiments were done in solutions without added HCO_3^- . Furthermore, blocking carbonic anhydrase did not abolish the pH changes associated with glutamate uptake, whereas blocking carbonic anhydrase greatly reduces pH changes due to bicarbonate movement in other preparations (Kaila *et al*, 1990). Thus, OH^- might be the favoured candidate for the transported anion. The following calculations reinforce this idea.

The CO_2 and HCO_3^- concentrations measured in the nominally bicarbonate-free internal solution (solution J, table 2.3 with metabolic blockers) were $50\mu\text{M}$ and $400\mu\text{M}$ respectively. If one bicarbonate ion is transported out on the carrier, the efflux would be (for a typical 200pA current) $(2 \times 10^{-10} / 96500)$

= 2×10^{-15} bicarbonate ion per second. A cell of typical volume 10^{-14} m^3 (10^{-11} litre) contains, if $[\text{HCO}_3^-] = 400 \mu\text{M}$, $(10^{-11}) \times (4 \times 10^{-4}) = 4 \times 10^{-15}$ moles of bicarbonate. If bicarbonate is transported out of the cell at a rate of $2 \times 10^{-15} \text{ mol s}^{-1}$, all the bicarbonate would be lost in 2 seconds, yet glutamate uptake can be maintained for minutes. If carbonic anhydrase is blocked (and metabolic blockers are present in the cell to inhibit further CO_2 production), the cell has two sources of HCO_3^- :

- (1) reaction of water with CO_2
- (2) diffusion of HCO_3^- from the patch pipette

With carbonic anhydrase blocked, the rate constant of production of HCO_3^- from CO_2 is 0.037 s^{-1} (Edsall & Wyman, 1958). From the $50 \mu\text{M}$ CO_2 measured in my solutions (see above), HCO_3^- would therefore be produced at a rate of $(5 \times 10^{-5}) \times 0.037 \times 10^{-11} = 1.9 \times 10^{-17} \text{ mol s}^{-1}$. Diffusion of HCO_3^- from the pipette (of series resistance $3 \text{ M}\Omega$) would bring in $2.1 \times 10^{-16} \text{ mol s}^{-1}$ (see legend to fig 4.4 for a detailed calculation). These values add up to only 2.3×10^{-16} moles/s (only 11% of the 2×10^{-15} moles/s which would be needed if one HCO_3^- moved per carrier cycle). It is therefore concluded that HCO_3^- transport is not obligatory for the operation of the glutamate uptake carrier.

In contrast, dissociation of water (concentration 56M) at a rate constant of $2.5 \times 10^{-5} \text{ s}^{-1}$ (Eigen & De Maeyer, 1958) generates (in a cell of volume 2×10^{-11} litre) $56 \times (2 \times 10^{-11}) \times (2.5 \times 10^{-5}) = 2.8 \times 10^{-14} \text{ mol s}^{-1}$ of hydroxyl ions, while the glutamate uptake carrier can transport (for a typical current of 200 pA) only $2 \times 10^{-10} / 96500 = 2 \times 10^{-15}$ hydroxyl ions per second (assuming that one OH^- is transported per cycle of the carrier). It is therefore plausible that hydroxyl ions are the main counter-transported anions, even though it is not possible to rule out some HCO_3^- transport. Indeed, experiments presented in chapter 5 (Fig 5.11) of this thesis suggest that HCO_3^- ions can also be transported on the carrier and may be transported in physiological conditions where the concentration of bicarbonate is around 10mM .

How many hydroxyl ions are transported per carrier cycle?

In section 4.8 I showed that the intracellular pH change produced by

uptake was roughly consistent with one OH⁻ leaving the cell per carrier cycle. A further estimate of the stoichiometry of hydroxyl transport can be obtained from the experiments in chapter 5 measuring ClO₄⁻ efflux by comparing the measured and expected accumulation of ClO₄⁻ outside the cell.

The efflux, J, of perchlorate across the surface membrane is given by the equation:

$$J = I/F \quad (1)$$

where I is the current generated by glutamate uptake and F is the Faraday, assuming that one ClO₄⁻ moves (and by extension one OH⁻) per elementary charge of uptake current. This ClO₄⁻ will diffuse out from the cell in the external solution. Treating the cell as a sphere, the rate of ClO₄⁻ diffusion across a concentric sphere of radius r in the external solution is:

$$\text{rate of ClO}_4^- \text{ diffusion} = -4\pi r^2 D dc/dr \quad (2)$$

where c is the concentration of ClO₄⁻ and D is the diffusion coefficient for ClO₄⁻ (2x10⁻⁹ m² s⁻¹). This must be equal to the ClO₄⁻ flux across the cell membrane. Thus,

$$I/F = -4\pi r^2 D dc/dr \quad (3)$$

$$\text{or} \quad \int dc = -\int (dr.I)/(4\pi r^2.D.F) \quad (4)$$

Integrating the equation from a (the radius of the cell) to infinity gives (because the concentration at infinity is zero):

$$c_a = I/(4\pi.a.D.F) \quad (5)$$

If the uptake current is 300pA (with ClO₄⁻ inside), and if one ClO₄⁻ is transported in 64% (1.8/2.8 from fig 5.1) of the carrier cycles, then the concentration of ClO₄⁻ expected just outside the cell is:

$$c_a = (0.64 \times I)/(4\pi.a.D.F) = 7.6\mu\text{M}$$

The concentration of perchlorate measured by the electrode with ClO₄⁻ present inside the cell was around 6μM, very close to the calculated value. It can be concluded tentatively that the glutamate uptake carrier has one internal anion binding site and that in physiological conditions, one hydroxyl (or one bicarbonate) is transported out per cycle of the carrier.

7.2.5 Most likely stoichiometry

The first order dependence of glutamate uptake on external glutamate and internal potassium concentration suggests that one of each of these ions are transported on the carrier per cycle. Evidence reviewed above suggest that two sodium ions are co-transported with each glutamate and that one hydroxyl (or possibly bicarbonate) is counter-transported per carrier cycle. As a result of this stoichiometry, one net positive charge is transported into the cell on each cycle of the carrier. No other charged ions seem to be transported, in particular Cl^- is not transported (Barbour *et al*, 1991).

7.3 **Accumulative power of the carrier**

The accumulative power of the carrier depends exclusively on its stoichiometry. At equilibrium (no net transport of glutamate across the cell membrane), the minimum extracellular glutamate concentration that the uptake carrier can maintain is given by (from equating the free energy change of one carrier cycle to zero):

$$[\text{Glu}^-]_o = [\text{Glu}^-]_i \left(\frac{[\text{Na}^+]_i}{[\text{Na}^+]_o} \right)^2 \left(\frac{[\text{K}^+]_o}{[\text{K}^+]_i} \right) \left(\frac{[\text{OH}^-]_o}{[\text{OH}^-]_i} \right) e^{VF/RT} \quad (1)$$

In physiological conditions (at 37°C), $[\text{Na}^+]_i = 25\text{mM}$ (Ballanyi *et al*, 1987), $[\text{Na}^+]_o = 145\text{mM}$, $[\text{K}^+]_o = 2.5\text{mM}$, $[\text{K}^+]_i = 145\text{mM}$, $[\text{OH}^-]_o = 251\text{nM}$, $[\text{OH}^-]_i = 100\text{nM}$ and $V = -80\text{mV}$. The value of the internal glutamate concentration is less certain and ranges from 0.1mM to 5mM in glial cells and around 15mM in neurones when measured by immunochemical methods (Marc *et al*, 1990; Ottersen, 1989). Values obtained from biochemical measurements range from 5 to 20mM in cultured glial cells or neurones and whole brain (Schousboe *et al*, 1975; Berger *et al*, 1977; Kvamme *et al*, 1985; Lehmann & Hansson, 1987; Levi & Patrizio, 1992). Because glutamate seems to be taken up more into glial cells than into neurones (see below) (Schon & Kelly, 1974; McLennan, 1976) an intermediate value of $[\text{Glu}^-]_i = 3\text{mM}$ was chosen for the following calculation. For the values given above, the minimum extracellular glutamate concentration the carrier can maintain is predicted by equation (2) to be approximately $[\text{Glu}^-]_o$

= $0.2\mu\text{M}$. This concentration is at the bottom of the dose-response curve for most glutamate receptors (Forsythe & Clements, 1990; Sather *et al*, 1992; Schoepp *et al*, 1990).

7.4 Function of hydroxyl counter-transport

A carrier with a stoichiometry of one glutamate and two sodium ions transported into the cell and one potassium ion counter transported (i.e. no OH^- transport) could lower extracellular glutamate concentrations (at equilibrium) to only $1.5\mu\text{M}$ (from a calculation similar to that above). The glutamate uptake carrier present in salamander Müller cells can lower extracellular glutamate concentrations to 200nM (previous section). Transport of a hydroxyl ion out of the cell thus increases the accumulative power of the carrier.

Changes of pH due to the transport of hydroxyl ions out of the cell on the carrier may play an important role in intracellular signalling or as a messenger between neurones and glial cells (see below). Certainly, changes of pH in physiological or pathological conditions will affect the rate of uptake of glutamate (see below). The optimum extracellular pH for the salamander uptake carrier is 7.3 (Barbour *et al*, unpublished observations). The physiological pH of the extracellular medium is around 7.4 for mammals and 7.6 for amphibians. Any decrease of this extracellular pH (for example when acid containing neurotransmitter vesicles are released into the extracellular space) will have the effect of stimulating glutamate uptake. Transport of hydroxyl ions may also contribute to a reduction of osmotic changes as glutamate and sodium are transported into the cell.

7.5 How similar are amphibian and mammalian glutamate uptake transporters?

As some parts of this discussion deal with glutamate uptake in mammalian systems, it is important to stress the similarities between mammalian and amphibian glutamate uptake (studied in this thesis).

Sarantis & Attwell (1990) have investigated electrogenic glutamate uptake in Müller cells of the rabbit retina. The uptake process was strictly dependent on

external sodium and on intracellular potassium. The proposed stoichiometry was with one glutamate and three sodium being transported into the cell while one potassium ion was transported out. There was no direct evidence for the transport of three sodium ions (as opposed to two) but since the carrier was electrogenic, it was necessary to postulate that three sodium ions were transported into the cell in order to account for the inward current observed (the transport of pH changing ions was not investigated in that study). All studies of glutamate uptake carriers in mammalian cells show a strict dependence on external sodium, although some authors have reported first order Michaelis-Menten kinetics (rather than a sigmoid $[Na]_o$ -dependence) for the transport of sodium in cultured astrocytes (e.g. Drejer *et al*, 1982; Kimelberg *et al*, 1989). However, in these experiments, the cells were not whole-cell clamped and depolarization of the astrocytes (by activation of glutamate gated channels) cannot be ruled out. This depolarisation would reduce uptake when the external sodium concentration was high, and thus might convert a sigmoid dependence on external sodium into a more first order Michaelis-Menten dependence. Most of the studies from mammalian synaptosomes have also suggested that mammalian uptake carriers counter-transport potassium ions (Kanner & Sharon, 1978 a, b; Roskoski, 1979).

More recently, the cloning of three different mammalian uptake carriers (see introduction section 1.6.5) emphasized the similarities between the different carriers. These were all found to be strictly dependent on external sodium. GLT-1 (Pines *et al*, 1992) was also found to be dependent on internal potassium and EAAC1 (Kanai & Hediger, 1992) was inhibited by extracellular potassium. It is interesting to note that Kanai & Hediger's clone (EAAC1) generates an intracellular acidification (personal communication) but this property has not yet been reported for the other cloned transporters. Tanaka (1993) found that Glu-1, when expressed in oocytes, take up glutamate in a chloride-dependent manner (uptake was reduced when external chloride was replaced by acetate). However, since the oocytes were not voltage clamped and given that oocytes can have a large chloride conductance (Dascal, 1987), it is not possible to rule out a possible indirect effect in which removing external chloride depolarises the membrane

potential and inhibits uptake.

7.6 Neuronal vs glial glutamate uptake

There is some controversy over the relative importance of glial and neuronal glutamate uptake carriers. Intuitively, uptake carriers located on the presynaptic terminal of a glutamatergic synapse would be at the ideal place to quickly lower the extracellular glutamate concentration after depolarisation-evoked release. However, several experiments suggest that most of the glutamate released by neurones is taken up by glial cells. [³H]-glutamate when applied to the nervous system ends up mainly (90%) in glial cells (Schon & Kelly, 1974; McLennan, 1976). Moreover, inhibiting glutamine synthase (the enzyme responsible for the conversion of glutamate into glutamine, located mainly in glial cells in the brain (Norenberg & Martinez-Hernandez, 1979)) reduces the calcium-dependent release of glutamate from rat striatal slices *in vitro* (Rothstein & Tabakoff, 1984) and from rat striatum *in vivo* (Paulsen & Fonnum, 1989). These results suggest that the conversion of glutamate to glutamine in glia (followed by movement of glutamine back to neurones) is required to maintain the pools of releasable glutamate in nerve terminals and that uptake of glutamate into glial cells is the major pathway for removal of extracellular glutamate after being released by neurones.

7.7 Glutamate uptake is associated with intra- and extracellular pH changes

7.7.1 Likely pH changes observed *in vivo* due to glutamate uptake

Assessing the amplitude of the pH changes produced by glutamate uptake is important if one wishes to postulate an effect on cells such as variation of enzyme activity or modulation of neuronal excitability (see below). In physiological conditions, the pH of the cells and of the extracellular fluid are buffered by CO₂/HCO₃⁻ which should result in a higher buffering power than would pertain in the experiments carried out with Hepes as a buffer, which are presented in chapters 4 and 5. An estimate of the uptake-evoked pH changes that will occur *in vivo* can be made as follows. Addition of CO₂/HCO₃⁻ to the

cells will increase their buffering power by 23mM. The buffering power of unclamped cells was measured to be around 16mM (in the experimental conditions described in chapter 4). The presence of bicarbonate would therefore increase the buffering power by a factor of 2.4 and would decrease the pH change by the same factor. The typical pH change of 0.1 pH unit monitored in the experiments described in chapter 4 would thus correspond to an *in vivo* pH change of 0.04 pH unit. A corresponding alkalization will occur in the extracellular space. However, extracellular pH changes will occur *in vivo* in a restricted space around each cell (in contrast to the experiments on dissociated cells which are surrounded by a large volume of extracellular fluid) and in a solution of buffering power of 55mM (calculated from the concentration of bicarbonate (24 mM) in the extracellular space). Typically, the extracellular volume is 1/4 of the intracellular space, which would lead to the pH_o change being four fold larger than the pH_i change. The 55mM buffering power (15% higher than the intracellular buffering power) will slightly reduce this pH change. Overall, in the case described above, the corresponding extracellular pH change would therefore be 0.14 pH unit. In the retina, where glutamate is released continuously in the dark, or in the brain when glutamate is released massively for example during an epileptic seizure, the internal and extracellular pH changes could thus be significant and may play an important signalling role (see below). Recently, Amato *et al* (1993b) have shown that glutamate uptake can evoke significant pH changes in rat hippocampal slices.

7.7.2 How do uptake-evoked pH changes affect cells?

Extracellular and intracellular pH shifts occur in the central nervous system during stimulation (for review, see Chesler & Kaila, 1992) and are large enough to influence excitatory synaptic transmission. Traynelis & Cull-Candy (1990, 1991) showed that NMDA receptors from cerebellar neurones were inhibited by a rise of $[H^+]_o$, with 50% of the inhibition occurring close to physiological pH (around 7.3). This inhibition seemed to be via a decrease in the opening probability of the channel and a reduction in the proportion of long bursts of opening. In contrast, AMPA or kainate channels were unaffected by

similar changes in extracellular pH. These results were confirmed by Tang *et al* (1990) and by Vyklický *et al* (1990) on rat and mouse hippocampal neurones. Similarly, a decrease of extracellular pH blocks sodium conductance in frog node of Ranvier (Hille, 1992). As a result, neurones become less excitable. The mechanism for this action of protons on voltage-gated sodium channels is still not clear. It could result from a decrease in single channel conductance by protons titrating several groups facing the pore of the channel or by titrating one essential group within the pore. Alternatively, protons could alter the gating kinetics, leading to less channels opening for the same depolarisation. Sigworth (1980) showed that an increase in proton concentration affects the gating mechanism and the single channel conductance of voltage-gated sodium channels at the node of Ranvier. Voltage-gated calcium channels are also inhibited by a rise in proton concentration (Iijima *et al*, 1986). In contrast, GABA-gated chloride channels of crayfish muscle fibres were found to be inhibited by an increase of extracellular pH (Pasternack *et al*, 1992). These modulations of voltage- and ligand-gated channels by protons all lead to an increase of excitability at higher pH_o .

Several metabolic enzymes are likely to be affected by the intracellular pH changes calculated above. For example, phosphofructokinase, the enzyme catalysing the rate limiting step of glycolysis is very sensitive to pH. If the pH of the cell increases from 7.1 to 7.2, the activity of the enzyme phosphofructokinase increases nearly 20 fold. Glutamate dehydrogenase, the enzyme responsible for the formation of α -ketoglutarate and $NADPH + H^+$ from glutamate was found to be stimulated by a decrease of internal pH in *Clostridium symbiosum* (Syed & Engel, 1990). These authors suggested that the enzyme could exist in two forms: a high activity form found mainly at acidic pH and a low activity state predominant at higher pH.

Glutamine synthase (see introduction section 1.11.4) is also modulated by intracellular pH changes. A shift from 7.4 to 7.8 in the extracellular pH (supposed to induce an alkalization of the internal medium when a CO_2 /bicarbonate solution is used (Kimmelberg *et al*, 1986)) produced a 3.4 fold increase in the intracellular glutamine concentration in mouse cultured astrocytes

(Brookes, 1992b). The acidification of the intracellular medium of the cell associated with glutamate uptake would therefore be expected to reduce the activity of glutamine synthase.

Gap junctions are channels mediating cell-to-cell coupling. They allow the movement of ions and small molecules from one cell to the other without leakage into the extracellular space. Spray *et al* (1981) have shown that gap junctional conductance was greatly increased by alkalinizations of the order of 0.10 pH units. The intracellular acidification associated with glutamate uptake would therefore have the opposite effect and tend to induce the closure of gap junctions. Gap junctions between glial cells normally serve to potentiate the clearing of K⁺ from the extracellular space by "spatial buffering" (Mobbs *et al*, 1988).

Intracellular acidification as well as external alkalinization evoked by glutamate uptake may therefore be involved in the modulation of neuronal excitability and alteration of glial cell metabolism, and may represent a novel second messenger action of glutamate.

7.8 Modulation of glutamate uptake

7.8.1 Effect of ascorbate on glutamate uptake

Several groups have suggested that ascorbate might be transported out of the cell by the glutamate uptake carrier (Grünewald & Fillenz, 1984; Cammack *et al*, 1991). Indeed, application of L-glutamate to synaptosomes from rat brain or injection into the brain induces the efflux of ascorbate (Grünewald & Fillenz, 1984; O'Neill *et al*, 1984; Cammack *et al*, 1991) measured by voltammetry (Ghasemzadeh *et al*, 1991). The efflux of ascorbate from synaptosomes can also be evoked by applying D- or L-aspartate or by raising the extracellular potassium level to 60mM (Grünewald & Fillenz, 1984; O'Neill *et al*, 1984). Moreover, removing extracellular sodium decreases the ascorbate efflux induced by the application of glutamate (Grünewald & Fillenz, 1984). The efflux of ascorbate was abolished in the presence of glutamate uptake inhibitor D,L-threo β -hydroxy-aspartic acid and approximately halved by SITS (which had been suggested to selectively block glial uptake (Waniewski & Martin, 1983)). Furosemide (an

inhibitor of Cl⁻-coupled transport) was also a potent inhibitor of glutamate-induced ascorbate efflux (Wilson & Dixon, 1989; Cammack *et al*, 1991). In contrast, antagonists of glutamate receptors had no effect on the glutamate-evoked ascorbate efflux (Grünewald & Fillenz, 1984). Finally, lesions of corticostriatal pathways inhibited ascorbate efflux evoked by glutamate in the striatum (O'Neill *et al*, 1984). These results led to the suggestion that the glutamate uptake carrier might counter-transport ascorbate. However, experiments described in chapter 6 show that adding ascorbate to the internal solution did not affect the amplitude of the glutamate-evoked current in salamander Müller cells. Furthermore, the presence of ascorbate outside the cell did not inhibit the uptake current as would be expected if ascorbate is transported out of the cell on the carrier. Moreover, furosemide does not affect glutamate uptake into salamander Müller cells (Ballerini, Edwards & Attwell, unpublished observations) while it was shown to inhibit glutamate-evoked ascorbate efflux. These results argue against the transport of ascorbate on the glutamate uptake carrier and are consistent with the following results obtained by others. Firstly, measurement of both the efflux of ascorbate evoked by the application of glutamate and the amount of [³H]-glutamate taken up by synaptosomes from rat brain showed that much less ascorbate was released than [³H]-glutamate taken up (Grünewald & Fillenz, 1984). Secondly, ascorbate was not able to evoke the release of [³H]-glutamate from pre-loaded synaptosomes and the presence of 5mM ascorbate in the incubation medium did not affect the uptake of [³H]-glutamate into synaptosomes (Grünewald & Fillenz, 1984). These apparent contradictions can be explained if, as seems likely, glutamate and ascorbate are transported on two different carriers. The uptake of glutamate is accompanied by an increase in intracellular sodium concentration (and in high input resistance synaptosomes a depolarisation) that might activate reversed ascorbate transport. Indeed, Na⁺-dependent ascorbate transport has been described in rat and mouse astrocytes in culture. This uptake mechanism was not significantly affected by extracellular Cl⁻ removal, but was blocked by furosemide, SITS and DIDS (Wilson & Dixon, 1989).

7.8.2 Effect of activating or inhibiting cAMP-dependent protein kinase

The recently cloned glutamate uptake carriers show a conserved putative site for phosphorylation by cAMP-dependent protein kinase (PKA). However, results presented in chapter 6 show that neither the presence of catalytic subunits of PKA in the internal solution nor a peptide inhibitor of PKA affected the amplitude of the current generated by glutamate uptake. These results can be explained in several different ways. First of all, the glutamate uptake carriers cloned to date are all from mammals and the amphibian glutamate uptake carrier may not contain this putative phosphorylation site for PKA. An alternative explanation is that this site is actually located outside the cell, as suggested by Kanai & Hediger (1992) in their representation of the carrier. Finally, if this putative site exists in salamander Müller cells' carriers, it may not be accessible to PKA due to the tertiary structure of the protein. Experiments similar to those presented in chapter 6 and others (such as labelling of phosphorylation sites with ^{32}P) would have to be performed on cells expressing one of the cloned cDNAs to test these hypotheses. Elucidation of the crystal structure of the protein would also be useful in investigating the accessibility of the site to PKA.

7.8.3 Effect of activating protein kinase C

Protein kinase C (PKC) has previously been found to activate glutamate uptake into glial cells in culture (Casado *et al*, 1991). However, the effect of the phorbol ester TPA (activator of PKC) was studied for only 10 minutes. The results presented in chapter 6 suggested tentatively that PKC might initially activate glutamate uptake in salamander Müller cells but following prolonged exposure might then down-regulate the level of PKC expression in the cells. Several experiments have to be performed to confirm the preliminary results presented in chapter 6. More cells will be studied to reproduce the results already obtained and to increase the level of significance of the data. If the effect of TPA is confirmed, cells will be studied after several hours of contact with TPA, using an internal solution containing PKC. The aim of this experiment would be to restore the potentiation of glutamate uptake in these cells and show

conclusively that the decline in glutamate-evoked current is related to the loss of PKC activity in the cells. Presumably, a receptor-linked mechanism exists to up- or down-regulate the activity of the carrier via PKC. Since trans-ACPD receptors linked to phospholipase C have been shown to be expressed by these cells (Keirstead & Miller, 1992), this could be a pathway for the up-regulation of the carrier. According to this model, phospholipase C induces the synthesis of IP₃ and diacylglycerol; IP₃ stimulates the release of calcium from internal stores and PKC becomes activated by the presence of diacylglycerol and the elevation of calcium concentration.

7.8.4 Effect of annexin I on the inhibition of glutamate uptake by arachidonic acid

Annexin I has been proposed to protect against neuronal injury during anoxia or ischaemia (Relton *et al*, 1991). Since annexins bind to arachidonic acid (Edwards & Crumpton, 1991), exogenously applied annexin I could act by binding arachidonic acid and preventing it having neurotoxic actions such as potentiating the current passing through NMDA channels (thought to be one of the major ion channels involved in neuronal damage; see introduction, section 1.1.1) and inhibiting glutamate uptake (Chan *et al*, 1983; Barbour *et al*, 1989). Results presented in chapter 6 showed that adding annexin I to the incubation medium of cells affected neither the magnitude of the current generated by glutamate uptake, nor the inhibition of glutamate uptake by arachidonic acid. Thus, although it remains possible that annexin I modulates NMDA receptor activity by binding arachidonic acid, it does not appear to influence the activity of glutamate uptake carrier.

7.9 **Role of glutamate uptake in neurotoxicity and pathology**

In anoxia or ischaemia, because of the lack of oxygen available for cell metabolism, the intracellular ATP concentration falls sharply (aerobic metabolism is switched to anaerobic metabolism). This leads to a rise of [K⁺]_o following the subsequent failure of operation of the Na⁺/K⁺ pump. In the first two minutes, [K⁺]_o rises slowly to around 10mM (and the extracellular space is

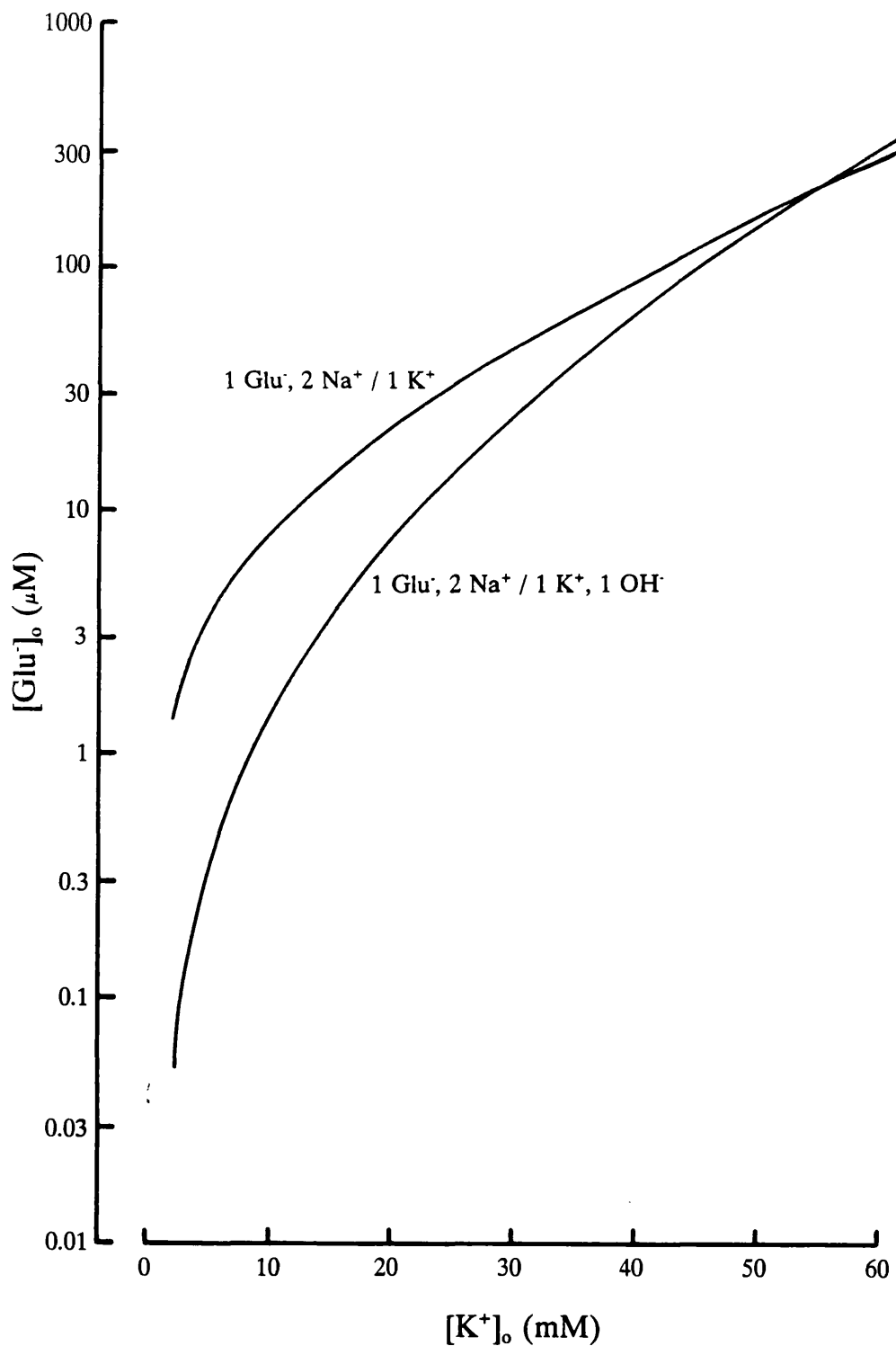
slightly acidified (Hansen, 1985)). $[K^+]_o$ then rises sharply to around 50mM while $[Na^+]_o$, $[Cl^-]_o$ and $[Ca^{2+}]_o$ drop (Hansen, 1985). As a result of the increase of $[K^+]_o$, neurones and glial cells become depolarised and more glutamate is released into the synaptic cleft. This increase of glutamate concentration has been measured by micro-dialysis (Benveniste *et al*, 1984; Hagberg *et al*, 1985; Graham *et al*, 1990), and is thought to be responsible for the neuronal death occurring in anoxia or ischaemia (see introduction, section 1.4). It is not prevented by uptake of the neurotransmitter for several reasons (Brew & Attwell, 1987; Barbour *et al*, 1991). First of all, the increase of $[K^+]_o$ inhibits the release of counter-transported K^+ by the carrier (the K_m for K^+ binding outside Müller cells of the salamander retina is approximately 100mM (Barbour *et al*, 1991)). Second, the depolarisation of the cells due to the rise in $[K^+]_o$ will inhibit the glutamate uptake carrier (see introduction, section 1.6.1). Lastly, the decrease in $[Na^+]_o$ will also contribute to the inhibition of the uptake process. Fig 7.1 shows the minimum extracellular glutamate concentration the carrier can maintain (at equilibrium) when the extracellular potassium concentration rises, calculated from equation (2) section 7.3. If the extracellular potassium concentration rises to 50mM, the carrier will only be able to lower the extracellular glutamate concentration to 150 μ M. The increase of glutamate concentration in anoxia and ischaemia could arise from an increase in vesicular release from presynaptic terminals following their depolarisation. However, Sanchez-Prieto & Gonzalez (1988) have shown that a drop in the ATP level inhibits vesicular release, making this possibility unlikely. A second possibility, revealed by recent studies on glial cells (Szatkowski *et al*, 1991), and by the graph in Fig 7.1, is that the increase of extracellular glutamate concentration in pathological conditions could be due to reversed operation of the glutamate uptake carrier. When the extracellular potassium concentration rises, glutamate will be released until $[Glu]_o$ rises to the new equilibrium level predicted in Fig 7.1.

7.10 Suggestions for future work

As suggested by the results obtained by Kanai & Hediger (1992) on the stoichiometry of their cloned transporter (see introduction, section 1.6.5), the

Fig 7.1: Minimum extracellular glutamate concentration the glutamate uptake carrier can maintain in pathological conditions.

Two different stoichiometries for the carrier were investigated. Equation (2) of section 7.3 was used to determine the extracellular glutamate concentration at equilibrium for various extracellular potassium concentrations. The intracellular glutamate concentration was taken as 3mM (see section 7.3), the ratio $[\text{OH}^-]_o/[\text{OH}^-]_i$ was assumed to remain constant at 2.51, the membrane potential, V_M , was assumed to be equal to V_K and the extracellular sodium concentration was taken as $147.5 - [\text{K}^+]_o$ so that $[\text{Na}^+]_o$ falls by the same amount as $[\text{K}^+]_o$ rises. The intracellular sodium concentration was assumed to rise by 1/4 of the amount that $[\text{Na}^+]_o$ falls (since it is in a volume four times bigger) and the intracellular potassium concentration was assumed to fall by 1/4 of the amount that $[\text{K}^+]_o$ rises. So: $\text{Na}_i = 145 + [(\text{K}_o - 2.5)/4]$; $\text{K}_i = 145 - [(\text{K}_o - 2.5)/4]$ and $\text{Na}_o = 145 - (\text{K}_o - 2.5)$.



mammalian neuronal glutamate transporter seems to bear very similar properties to those of the salamander Müller cell carrier. It would be interesting to confirm the transport of a pH-changing ion on the glutamate uptake carrier from acutely dissociated mammalian astrocytes and neurones. It would be better to study neuronal glutamate uptake in neurones that do not express glutamate receptors. Otherwise, these experiments would have to be carried out in the presence of CNQX and APV (glutamate-gated channel antagonists; see introduction, section 1.1).

Studies of cloned glutamate carriers at the molecular level should also provide insight into functional domains within the molecule. In particular, directed mutagenesis studies should allow designation of those residues of the carriers essential for their function and for the binding of the different ions. An obvious start would be the mutation of charged residues (conserved amongst the three cloned carriers) located close to the transmembrane regions or within the transmembrane regions. However, binding of cations could also occur by electronic interaction with aromatic residues such as phenylalanine or tyrosine (as was shown for the blockade of potassium channels by tetraethylammonium (Heginbotham & MacKinnon, 1992)).

Proline residues have been shown to be absent from transmembrane regions of most membrane spanning proteins since they induce a bend in the α -helices that are the usual secondary structures of transmembrane segments. This observation does not hold for transporters, and transmembrane proline residues have been suspected to play an important role in the transporter function (Brandl & Deber, 1986). However, experiments in which the proline residues were replaced by other amino acids could simply lead to the complete inhibition of the transporter function and therefore be very difficult to interpret in terms of which essential step of the carrier operation is affected.

Further experiments could involve the use of specific (glial or neuronal) antibodies against glutamate carriers. These could prove informative in determining the location of glutamate uptake carriers at an ultrastructural level. For example, they would allow one to address the question of the existence of neuronal glutamate carriers on the pre- or postsynaptic membrane. Alternatively,

neuronal glutamate uptake carriers might only be expressed on the cell body. Electron microscopic location of gold-coupled antibodies to the glutamate uptake carrier would be the most reliable way of solving this open debate.

Another potentially fruitful area of research would be to pursue the search for a modulatory pathway of glutamate uptake. It seems likely that glutamate uptake is constitutively inhibited in physiological conditions for at least two reasons. First of all, for the same concentration of applied glutamate, pH changes monitored in unclamped Müller cells are smaller than those monitored from whole-cell clamped cells (chapter 4). Moreover, the glutamate-evoked current is smaller in Müller cells recorded with perforated patches than those obtained with the same dose of glutamate when the cell accidentally enters whole-cell configuration (Barbara Miller, personal communication). It is possible that a small molecule (washed from the cell very quickly when entering whole-cell configuration) permanently down-regulates the glutamate uptake carrier.

REFERENCES

- Abe, T., Sugihara, H., Nawa, H., Shigemoto, R., Mizuno, N. & Nakanishi, S.** (1992) Molecular characterization of a novel metabotropic glutamate receptor mGluR5 coupled to inositol phosphate/ Ca^{2+} signal transduction. *J. Biol. Chem.*, 267: 13361-13368.
- Adam-Vizi, V.** (1992) External Ca^{2+} -independent release of neurotransmitters. *J. Neurochem.*, 58: 395-405.
- Aizenman, E., Lipton, S.A. & Loring, R.H.** (1989) Selective modulation of NMDA responses by reduction and oxidation. *Neuron*, 2: 1257-1263.
- Aizenman, E., Hartnett, K.A. & Reynolds, I.J.** (1990) Oxygen free radicals regulate NMDA receptor function via a redox modulatory site. *Neuron*, 5: 841-846.
- Alexander, G.E. & Crutcher, M.D.** (1990) Functional architecture of basal ganglia circuits: neuronal substrates of parallel processing. *Trends Neurosci.*, 13: 266-271.
- Amara, S.G. & Arriza, J.L.** (1993) Neurotransmitter transporters: three distinct gene families. *Current opinion Neurobiol.*, 3: 337-344.
- Amato, A., Adams, D. & Attwell, D.** (1993) Detection of K^{+} transported out of isolated salamander glial cells on the glutamate uptake carrier. *J. Physiol.*, UCL meeting, 27P.
- Amato, A., Ballerini, L. & Attwell, D.** (1993b) Intracellular pH changes produced by glutamate uptake in rat hippocampal slices. submitted.
- Andersen, P., Sundberg, S.H., Sveen, O. & Wigström, H.** (1977) Specific long-lasting potentiation of synaptic transmission in hippocampal slices. *Nature*, 266:

736-737.

Aragón, M.C. & Giménez, C. (1986) Efflux and exchange of glycine by synaptic plasma membrane vesicles derived from rat brain. *Biochim. Biophys. Acta*, 855: 257-264.

Aronson, P.S. (1989) The renal proximal tubule: a model for diversity of anion exchangers and stilbene-sensitive anion transporters. *Ann. Rev. Physiol.*, 51: 419-441.

Ascher, P., Bregestovski, P. & Nowak, L. (1988) N-methyl-D-aspartate-activated channels of mouse central neurones in magnesium-free solutions. *J. Physiol.*, 399: 207-226.

Astion, M.L. & Orkand, R.K. (1988) Electrogenic $\text{Na}^+/\text{HCO}_3^-$ cotransport in neuroglia. *Glia*, 1: 355-357.

Attwell, D. & Bouvier, M. (1992) Cloners quick on the uptake. *Current Biology*, 2: 541-543.

Baetge, E.E., Bulloch, K. & Stallcup, W.B. (1979) A comparison of glutamate transport in cloned cell lines from the central nervous system. *Brain Res.* 167: 210-214.

Balcar, V.J. & Johnston, G.A.R. (1972) The structural specificity of the high affinity uptake of L-glutamate and L-aspartate by rat brain slices. *J. Neurochem.*, 19: 2657-2666.

Ballanyi, K., Grafe, P. & ten Bruggencate, G. (1987) Ion activities and potassium uptake mechanisms of glial cells in guinea-pig olfactory cortex slices. *J. Physiol.*, 382: 159-174.

Barbour, B., Brew, H. & Attwell, D. (1988) Electrogenic glutamate uptake in glial cells is activated by intracellular potassium. *Nature* 335: 433-435.

Barbour, B., Szatkowski, M., Ingledeu, N. & Attwell, D. (1989) Arachidonic acid induces a prolonged inhibition of glutamate uptake into glial cells. *Nature*, 342: 918-920.

Barbour, B., Brew, H. & Attwell, D. (1991) Electrogenic uptake of glutamate and aspartate into glial cells isolated from the salamander (*Ambystoma*) retina. *J. Physiol.* 436: 169-193.

Barbour, B., Magnus, C., Szatkowski, M., Gray, P.T.A. & Attwell, D. (1993) Changes in NAD(P)H fluorescence and membrane current produced by glutamate uptake into salamander Müller cells. *J. Physiol.*, 466: 573-597.

Barres, B.A. (1991) New roles for glia. *J. Neurosci.*, 11: 3685-3694.

Bashir, Z.I., Bortolotto, Z.A., Davies, C.H., Berretta, N., Irving, A.J., Seal, A.J., Henley, J.M., Jane, D.E., Watkins, J.C. & Collingridge, G.L. (1993) Induction of LTP in the hippocampus needs synaptic activation of glutamate metabotropic receptors. *Nature*, 363: 347-350.

Battaglioli, G. & Martin, D.L. (1990) Stimulation of synaptosomal γ -aminobutyric acid synthesis by glutamate and glutamine. *J. Neurochem.*, 54: 1179-1187.

Battaglioli, G. & Martin, D.L. (1991) GABA synthesis in brain slices is dependent on glutamine produced in astrocytes. *Neurochem. Res.*, 16: 151-156.

Battaglioli, G., Martin, D.L., Plummer, J. & Messer, A. (1993) Synaptosomal glutamate uptake declines progressively in the spinal cord of a mutant mouse with motor neurone disease. *J. Neurochem.*, 60: 1567-1569.

Beal, M.F., Kowall, N.W., Ellison, D.W., Mazurek, M.F., Swartz, K.J. & Martin, J.B. (1986) Replication of the neurochemical characteristics of Huntington's disease by quinolinic acid. *Nature*, 321: 168-171.

Ben-Ari, Y., Cherubini, E. & Krnjevic, K. (1988) Changes in voltage dependence of NMDA currents during development. *Neurosci. Lett.*, 94: 88-92.

Bennett, J.P.Jr., Logan, W.J. & Snyder, S.H. (1973) Amino acids as central nervous transmitters: the influence of ions, amino acid analogues, and ontogeny on transport systems for L-glutamic and L-aspartic acids and glycine into central nervous synaptosomes of the rat. *J. Neurochem.*, 21: 1533-1550.

Benveniste, H., Drejer, J., Schousboe, A. & Diemer, N.H. (1984) Elevation of the extracellular concentrations of glutamate and aspartate in rat hippocampus during transient cerebral ischaemia monitored by intracerebral microdialysis. *J. Neurochem.*, 43: 1369-1374.

Berger, S.J., Carter, J.G. & Lowry, O.H. (1977) The distribution of glycine, GABA, glutamate and aspartate in rabbit spinal cord, cerebellum and hippocampus. *J. Neurochem.*, 28: 149-158.

Berl, S., Lajtha, A. & Waelsch, H. (1961) Amino acid and protein metabolism-IV cerebral compartments of glutamic acid metabolism. *J. Neurochem.*, 7: 186-197.

Black, M.D., Carey, F., Crossman, A.R., Relton, J.K. & Rothwell, N.J. (1992) Lipocortin-1 inhibits NMDA receptor-mediated neuronal damage in the striatum of the rat. *Brain Res.*, 585: 135-140.

Bliss, T.V.P. & Lømo, T. (1973) Long-lasting potentiation of synaptic transmission in the dentate area of the anaesthetized rabbit following stimulation of the perforant path. *J. Physiol.*, 232: 331-356.

Bliss, T.V.P. & Gardner-Medwin, A.R. (1973) Long-lasting potentiation of synaptic transmission in the dentate area of the unanaesthetized rabbit following stimulation of the perforant path. *J. Physiol.*, 232: 357-374.

Bliss, T.V.P. & Collingridge, G.L. (1993) A synaptic model of memory: long-term potentiation in the hippocampus. *Nature*, 361: 31-39.

Borgula, G.A., Karwoski, C.J. & Steinberg, R.H. (1989) Light-evoked changes in extracellular pH in frog retina. *Vision Res.*, 29: 1069-1077.

Bormann, J. (1989) Memantine is a potent blocker of N-methyl-D-aspartate (NMDA) receptor channels. *Eur. J. Pharmacol.*, 166: 591-592.

Boron, W.F. & Boulpaep, E.L. (1983) Intracellular pH regulation in the renal proximal tubule of the salamander. Basolateral HCO_3^- transport. *J. Gen. Physiol.*, 81: 53-94.

Bortolotto, Z.A. & Collingridge, G.L. (1993) Characterisation of LTP induced by the activation of glutamate metabotropic receptors in area CA1 of the hippocampus. *Neuropharmacology*, 32: 1-9.

Bowe, M.A. & Nadler, J.V. (1990) Developmental increase in the sensitivity to magnesium of NMDA receptors on CA1 hippocampal pyramidal cells. *Dev. Brain Res.*, 56: 55-61.

Brandl, C.J. & Deber, C.M. (1986) Hypothesis about the function of membrane-buried proline residues in transport proteins. *Proc. Natl. Acad. Sci. USA*, 83: 917-921.

Brew, H., Gray, P.T.A., Mobbs, P. & Attwell, D. (1986) Endfeet of retinal glial cells have higher densities of ion channels that mediate K^+ buffering. *Nature*, 324: 466-468.

Brew, H. & Attwell, D. (1987) Electrogenic glutamate uptake is a major current carrier in the membrane of axolotl retinal glial cells. *Nature* 327: 707-709.

Bridges, R.J., Stanley, M.S., Anderson, M.W., Cotman, C.W. & Chamberlin, A.R. (1991) Conformationally defined neurotransmitter analogues. Selective inhibition of glutamate uptake by one pyrrolidine-2,4-dicarboxylate diastereomer. *J. Med. Chem.*, 34: 717-725.

Brookes, N. (1992a) Regulation of the glutamine content of astrocytes by cAMP and hydrocortisone: effect of pH. *Neurosci. Lett.*, 147: 139-142.

Brookes, N. (1992b) Effect of pH on glutamine content derived from exogenous glutamate in astrocytes. *J. Neurochem.* 59: 1017-1023.

Brookes, N. (1992c) Effect of intracellular glutamine on the uptake of large neutral amino-acids in astrocytes: concentrative Na⁺-independent transport exhibits metastability. *J. Neurochem.* 59: 227-235.

Burger, P.M., Mehl, E., Cameron, P.L., Maycox, P.R., Baumert, M., Lottspeich, F., De Camilli, P. & Jahn, R. (1989) Synaptic vesicles immunisolated from rat cerebral cortex contain high levels of glutamate. *Neuron* 3: 715-720.

Cammack, J., Ghasemzadeh, B. & Adams, R.N. (1991) The pharmacological profile of glutamate-evoked ascorbic acid efflux measured by in vivo electrochemistry. *Brain Res.*, 565: 17-22.

Cangiano, C., Cardelli-Cangiano, P., James, J.H., Rossi-Fanelli, F., Patrizi, M.A., Brackett, K.A., Storm, R. & Fischer, J.E. (1983) Brain microvessels take up large neutral amino acids in exchange for glutamine: cooperative role of Na⁺-dependent and Na⁺-independent systems. *J. Biol. Chem.*, 258: 8949-8954.

Carlini, W.G. & Ransom, B.R. (1986) Regional variation in stimulated

extracellular pH transients in the mammalian CNS. Soc. Neurosci. Abstr. 12: 452.

Casado, M., Zafra, F., Aragón, C. & Giménez, C. (1991) Activation of high-affinity uptake of glutamate by phorbol esters in primary glial cell cultures. J. Neurochem., 57: 1185-1190.

Chan, P.H., Kerlan, R. & Fishman, R.A. (1983) Reductions of γ -aminobutyric acid and glutamate uptake and $(\text{Na}^+ + \text{K}^+)\text{-ATPase}$ activity in brain slices and synaptosomes by arachidonic acid. J. Neurochem., 40: 309-316.

Chen, J.C.T. & Chesler, M. (1992a) Modulation of extracellular pH by glutamate and GABA in rat hippocampal slices. J. Neurophysiol., 67: 29-36.

Chen, J.C.T. & Chesler, M. (1992b) Extracellular alkaline shifts in rat hippocampal slice are mediated by NMDA and non-NMDA receptors. J. Neurophysiol., 68: 342-344.

Chesler, M. & Chan, C.Y. (1988) Stimulus-induced extracellular pH transients in the *in vitro* turtle cerebellum. Neuroscience, 27: 941-948.

Chesler, M. & Kaila, K. (1992) Modulation of pH by neuronal activity. Trends in Neurosci., 15: 396-402.

Chesler, M. & Kraig, R.P. (1987) Intracellular pH of astrocytes increases rapidly with cortical stimulation. Am. J. Physiol., 253: R666-R670.

Chesler, M. & Kraig, R.P. (1989) Intracellular pH transients of mammalian astrocytes. J. Neurosci., 9: 2011-2019.

Chesler, M. & Rice, M.E. (1991) Extracellular alkaline-acid pH shifts evoked by iontophoresis of glutamate and aspartate in turtle cerebellum. Neuroscience, 41: 257-267.

Choi, D.W. (1985) Glutamate neurotoxicity in cortical cell culture is calcium-dependent. *Neurosci. Lett.*, 58: 293-297.

Choi, D.W. (1987) Ionic dependence of glutamate neurotoxicity. *J. Neurosci.*, 7: 369-379.

Choi, D.W. (1988) Glutamate neurotoxicity and diseases of the central nervous system. *Neuron*, 1: 623-634.

Clark, B. & Mobbs, P. (1992) Transmitter-operated channels in rabbit retinal astrocytes studied *in situ* by whole-cell patch clamping. *J. Neurosci.*, 12: 664-673.

Coles, J.A., Giovannini, P. & Thomas, R.C. (1988) Changes in extracellular pH induced by light stimulation in slices of honeybee drone retina. *J. Physiol.*, 398: 59P.

Cotman, C.W., Flatman, J.A., Ganong, A.H. & Perkins, M.N. (1986) Effects of excitatory amino acid antagonists on evoked and spontaneous excitatory potentials in guinea-pig hippocampus. *J. Physiol.*, 378: 403-415.

Cox, D.W.G., Headley, M.H. & Watkins, J.C. (1977) Actions of L- and D-homocysteate in rat CNS: a correlation between low-affinity uptake and the time courses of excitation by microelectrophoretically applied L-glutamate analogues. *J. Neurochem.* 29: 579-588.

Crompton, M.R., Moss, S.E. & Crompton, M.J. (1988) Diversity in the lipocortin/calpactin family. *Cell*, 55: 1-3.

Cull-Candy, S.G. (1976) Two types of extrajunctional L-glutamate receptors in locust muscle fibres. *J. Physiol.*, 255: 449-464.

Curtis, D.R. & Watkins, J.C. (1963) Acidic amino acids with strong excitatory

actions on mammalian neurons. *J. Physiol.* 166: 1-14.

Danbolt, N.C., Storm-Mathisen, J. & Kanner, B.I. (1992) An $[\text{Na}^+ + \text{K}^+]$ coupled L-glutamate transporter purified from rat brain is located in glial cell processes. *Neuroscience*, 51: 295-310.

Davies, J., Francis, A.A., Oakes, D.J., Sheardown, M.J. & Watkins, J.C. (1985) Selective potentiating effect of β -p-chlorophenylglutamate on responses induced by certain sulphur-containing excitatory amino acids and quisqualate. *Neuropharmacol.* 24: 177-180.

Davis, P.K., Carlini, W.G., Ransom, B.R., Black, J.A. & Waxman, S.G. (1987) Carbonic anhydrase activity develops postnatally in the rat optic nerve. *Dev. Brain Res.*, 31: 291-298.

Dascal, N. (1987) The use of *Xenopus* oocytes for the study of ion channels. *CRC Crit. Rev. Biochem.*, 22: 317-387.

Deguchi, Y., Yamato, I. & Anraku, Y. (1990) Nucleotide sequence of *gltS*, the Na^+ /glutamate symport carrier gene of *Escherichia coli* B. *J. Biol. Chem.*, 265: 21704-21708.

Deitmer, J.W. (1992) Evidence for glial control of extracellular pH in the leech central nervous system. *Glia*, 5: 43-47.

Deitmer, J.W. & Schlue, W.R. (1989) An inwardly directed electrogenic sodium-bicarbonate co-transport in leech glial cell. *J. Physiol., Lond.*, 411: 179-194.

Deitmer, J.W. & Szatkowski, M. (1990) Membrane potential dependence of intracellular pH regulation by identified glial cells in the leech central nervous system. *J. Physiol.*, 421: 617-631.

de Vrij, W., Bulthuis, R.A., van Iwaarden, P.R. & Konings, W.N. (1989) Mechanism of L-glutamate transport in membrane vesicles from *Bacillus stearothermophilus*. *J. Bacteriol.*, 171: 1118-1125.

Do, K.Q., Mattenberger, M., Streit, P. & Cuénod, M. (1986) In vitro release of endogenous excitatory sulfur-containing amino acids from various rat brain regions. *J. Neurochem.* 46: 779-786.

Drejer, J., Larsson, O.M. & Schousboe, A. (1982) Characterization of L-glutamate uptake into and release from astrocytes and neurons cultured from different brain regions. *Exp. Brain Res.*, 47: 259-269.

Eaton, S.A., Jane, D.E., Jones, P.L.St.J., Porter, R.H.P., Pook, P.C.-K., Sunter, D.C., Udvarhelyi, P.M., Roberts, P.J., Salt, T.E. & Watkins, J.C. (1993) Competitive antagonism at metabotropic glutamate receptors by (S)-4-carboxyphenylglycine and (RS)- α -methyl-4-carboxyphenylglycine. *Eur. J. Pharmacol.*, 244: 195-197.

Edsall, J.T. & Wyman, J. Biophysical Chemistry 585 (Academic, New York, 1958).

Edwards, H.C. & Crumpton, M.J. (1991) Ca²⁺-dependent phospholipid and arachidonic acid binding by the placental annexins VI and IV. *Eur. J. Biochem.*, 198: 121-129.

Eigen, M. & de Maeyer, L. (1958) Self-dissociation and protonic charge transport in water and ice. *Proc. R. Soc. Lond. A*, 247: 505-533.

Eisner, D.A., Kenning, N.A., O'Neill, S.C., Pocock, G., Richards, C.D. & Valdeolmillos, M. (1989) A novel method for absolute calibration of intracellular pH indicators. *Pflügers Arch.*, 413: 553-558.

Endres, W., Grafe, P., Bostock, H. & ten Bruggencate, G. (1986) Changes in extracellular pH during electrical stimulation of isolated rat vagus nerve. *Neurosci. Lett.* 64: 201-205.

Engelke, T., Jording, D., Kapp, D. & Pühler, A. (1989) Identification and sequence analysis of the *Rhizobium meliloti dctA* gene encoding the C₄-dicarboxylate carrier. *J. Bacteriol.*, 171: 5551-5560.

Erecińska, M., Wantorsky, D. & Wilson, D.F. (1983) Aspartate transport in synaptosomes from rat brain. *J. Biol. Chem.*, 258: 9069-9077.

Erecińska, M. (1987) The neurotransmitter amino acid transport systems. *Biochemical Pharmacology*, 36: 3547-3555.

Fahrig, T. (1993) Receptor subtype involved and mechanism of norepinephrine-induced stimulation of glutamate uptake into primary cultures of rat brain astrocytes. *Glia*, 7: 212-218.

Fedele, E. & Foster, A.C. (1992) [³H]glycine uptake in rat hippocampus: kinetic analysis and autoradiographic localization. *Brain Res.*, 572: 154-163.

Fenwick, E.M., Marty, A. & Neher, E. (1982) A patch-clamp study of bovine chromaffin cells and of their sensitivity to acetylcholine. *J. Physiol.*, 331: 577-597.

Ferkany, J. & Coyle, J.T. (1986) Heterogeneity of sodium-dependent excitatory amino acid uptake mechanisms in rat brain. *J. Neurosci. Res.*, 16: 491-503.

Fischer-Bovenkerk, C., Kish, P.E. & Ueda, T. (1988) ATP-dependent glutamate uptake into synaptic vesicles from cerebellar mutant mice. *J. Neurochem.*, 51: 1054-1059.

Forsythe, I.D. & Clements, J.D. (1990) Presynaptic glutamate receptors depress

excitatory monosynaptic transmission between mouse hippocampal neurones. *J. Physiol.*, 429: 1-16.

Frank, G., Grisar, T. & Moonen, G. (1983) Glial and neuronal Na⁺, K⁺ pump. In *Advances in Neurobiology* (Ed: S. Fedoroff & L. Hertz; Academic Press New York), 4: 133-159.

Fykse, E.M., Iversen, E.G. & Fonnum, F. (1992) Inhibition of L-glutamate uptake into synaptic vesicles. *Neurosci. Lett.*, 135: 125-128.

Gallo, V., Patrizio, M. & Levi, G. (1991) GABA release triggered by the activation of neuron-like non-NMDA receptors in cultured type 2 astrocytes is carrier-mediated. *Glia*, 4: 245-255.

Garthwaite, G. & Garthwaite, J. (1985) Sites of D-[³H]-aspartate accumulation in mouse cerebellar slices. *Brain Res.*, 343: 129-136.

Garthwaite, G. & Garthwaite, J. (1986) Neurotoxicity of excitatory amino acid receptor agonists in rat cerebellar slices: Dependence on calcium concentration. *Neurosci. Lett.*, 66: 193-198.

Ghasemzedah, B., Cammack, J. & Adams, R.N. (1991) Dynamic changes in extracellular fluid ascorbic acid monitored by in vivo electrochemistry. *Brain Res.*, 547: 162-166.

Giacobini, E. (1962) A cytochemical study of the localization of carbonic anhydrase in the nervous system. *J. Neurochem.*, 9: 169-177.

Gonzales, R.A. (1992) Biochemical responses mediated by N-methyl-D-aspartate receptors in rat cortical slices are differentially sensitive to magnesium. *J. Neurochem.* 58: 579-586.

Graham, S.H., Shiraishi, K., Panter, S.S., Simon, R.P. & Faden, A.I. (1990) Changes in extracellular amino acid neurotransmitters produced by focal ischaemia. *Neurosci. Lett.*, 110: 124-130.

Grassl, S.M. & Aronson, P.S. (1986) Na⁺/HCO₃⁻ co-transport in basolateral membrane vesicles isolated from rabbit renal cortex. *J. Biol. Chem.*, 261: 8778-8783.

Greenamyre, J.T., Penney, J.B., Young, A.B., D'Amato C.J., Hicks, S.P. & Shoulson, I. (1985) Alterations in L-glutamate binding in Alzheimer's and Huntington's diseases. *Science*, 227: 1496-1499.

Griffiths, R., Grieve, A., Allen, S. & Olverman, H.J. (1992) Neuronal and glial plasma membrane carrier-mediated uptake of L-homocysteate is not selectively blocked by β -p-chlorophenylglutamate. *Neurosci. Lett.*, 147: 175-178.

Grünewald, R.A. & Fillenz, M. (1984) Release of ascorbate from a synaptosomal fraction of rat brain. *Neurochem. Int.*, 6: 491-500.

Hablitz, J.J. & Langmoen, I.A. (1982) Excitation in hippocampal pyramidal cells by glutamate in the guinea-pig and rat. *J. Physiol.* 325: 317-331.

Hagberg, H., Lehmann, A., Sandberg, M., Nyström, B., Jacobson, I. & Hamberger, A. (1985) Ischemia-induced shift of inhibitory and excitatory amino acids from intra- to extracellular compartments. *J. Cereb. Blood Flow Metab.* 5: 413-419.

Hamill, O.P., Marty, A., Neher, E., Sakmann, B. and Sigworth, F.J. (1981) Improved patch-clamp techniques for high-resolution current recording from cells and cell-free membrane patches. *Pflügers Arch.*, 391: 85-100.

Hansen, A.J. (1985) Effect of anoxia on ion distribution in the brain. *Physiol.*

Rev., 65: 101-148.

Harder, R. & Bönisch, H. (1985) Effects of monovalent ions on the transport of noradrenaline across the plasma membrane of neuronal cell (PC-12 cells). *J. Neurochem.* 45: 1154-1162.

Harvey, J. & Collingridge, G.L. (1992) Thapsigargin blocks the induction of long-term potentiation in rat hippocampal slices. *Neurosci. Lett.*, 139:197-200.

Hayashi, Y., Tanabe, Y., Aramori, I., Masu, M., Shimamoto, K., Ohfuné, Y. & Nakanishi, S. (1992) Agonist analysis of 2-(carboxycyclopropyl)glycine isomers for cloned metabotropic glutamate receptor subtypes expressed in Chinese hamster ovary cells. *Br. J. Pharmacol.*, 107: 539-543.

Hediger, M.A., Coady, M.J., Ikeda, T.S. & Wright, E.M. (1987) Expression cloning and cDNA sequencing of the Na⁺/glucose co-transporter. *Nature*, 330: 379-381.

Heginbotham, L. & MacKinnon, R. (1992) The aromatic binding site for tetraethylammonium ion on potassium channels. *Neuron*, 8: 483-491.

Hell, J.W., Maycox, P.R., Stadler, H. & Jahn, R. (1988) Uptake of GABA by rat brain synaptic vesicles isolated by a new procedure. *EMBO J.*, 7: 3023-3029.

Hertz, L., Schousboe, A., Boechler, N., Mukerji, S. & Fedoroff, S. (1978) Kinetic characteristics of the glutamate uptake into normal astrocytes in cultures. *Neurochem. Res.*, 3: 1-14.

Hertz, L. (1979) Functional interactions between neurons and astrocytes. I. Turnover and metabolism of putative amino acid transmitters. *Prog. Neurobiol.* 13: 277-323.

Hille, B. (1992) Ionic channels of excitable membranes. Sinauer, pp 393-397.

Hoffman, B.J., Mezey, E. & Brownstein, M. (1991) Cloning of a serotonin transporter affected by antidepressants. *Science*, 254: 579-580.

Hollmann, M., Hartley, M. & Heinemann, S. (1991) Ca²⁺ permeability of KA-AMPA-gated glutamate receptor channels depends on subunit composition. *Science*, 252: 851-853.

Houamed, K.M., Kuijper, J.L., Gilbert, T.L., Haldeman, B.A., O'Hara, P.J., Mulvihill, E.R., Almers, W. & Hagen, F.S. (1991) Cloning, expression, and gene structure of a G protein-coupled glutamate receptor from rat brain. *Science*, 252: 1318-1321.

Iijima, T., Ciani, S. & Hagiwara, S. (1986) Effects of the external pH on Ca channels: experimental studies and theoretical considerations using a two-site, two-ion model. *Proc. Natl. Acad. Sci. USA*, 83: 654-658.

Ikeda, M., Nakazawa, T., Abe, K., Kaneko, T. & Yamatsu, K. (1989) Extracellular accumulation of glutamate in the hippocampus induced by ischemia is not calcium-dependent - in vitro and in vivo evidence. *Neurosci. Lett.*, 96: 202-206.

Isaakson, J.S., Solis, J.M. & Nicoll, R.A. (1993) Local and diffuse actions of GABA in the hippocampus. *Neuron*, 10: 165-175.

Isakov, N., McMahon, P. & Altman, A. (1990) Selective post-transcriptional down-regulation of protein kinase C isoenzymes in leukemic T cells chronically treated with phorbol esters. *J. Biol. Chem.*, 265: 2091-2097.

Ito, I., Hidaka, H. & Sugiyama, H. (1991) Effects of KN-62, a specific inhibitor of calcium/calmodulin-dependent protein kinase II, on long-term potentiation in the rat hippocampus. *Neurosci. Lett.*, 121: 119-121.

Iwasaki, Y., Ikeda, K., Shiojima, T. & Kinoshita, M. (1992) Increased plasma concentrations of aspartate, glutamate and glycine in Parkinson's disease. *Neurosci. Lett.*, 145: 175-177.

James, J.H., Ziparo, V., Jeppson, B. & Fischer, J.E. (1979) Hyperammonæmia, plasma aminoacid imbalance, and blood-brain aminoacid transport: a unified theory of portal-systemic encephalopathy. *Lancet*, 2: 772-775.

Jessel, T.M. & Kandel, E.R. (1993) Synaptic transmission: a bidirectional and self-modifiable form of cell-cell communication. *Neuron* 10 (Suppl.): 1-30.

Johnson, J.W. & Ascher, P. (1987) Glycine potentiates the NMDA response in cultured mouse brain neurons. *Nature*, 325: 529-531.

Johnston, G.A.R., Kennedy, S.M.E. & Twitchin, B. (1979) Action of the neurotoxin kainic acid on high affinity uptake of L-glutamic acid in rat brain slices. *J. Neurochem.*, 32: 121-127.

Kaila, K. & Voipio, J. (1987) Postsynaptic fall in intracellular pH induced by GABA-activated bicarbonate conductance. *Nature*, 330: 163-165.

Kaila, K., Saarikoski, J. & Voipio, J. (1990) Mechanism of action of GABA on intracellular pH and on surface pH in crayfish muscle fibres. *J. Physiol.*, 427: 241-260.

Kanai, Y. & Hediger, M.A. (1992) Primary structure and functional characterization of a high-affinity glutamate transporter. *Nature*, 360: 467-471.

Kanner, B.I. (1978) Active transport of γ -aminobutyric acid by membrane vesicles isolated from rat brain. *Biochemistry*, 17: 1207-1211.

Kanner, B.I. (1993) Glutamate transporters from brain. A novel neurotransmitter

transporter family. *Febs Lett.*, 325: 95-99.

Kanner, B.I. & Sharon, I. (1978a) Active transport of L-glutamate by membrane vesicles isolated from rat brain. *Biochemistry* 17: 3949-3953.

Kanner, B.I. & Sharon, I. (1978b) Solubilization and reconstitution of the L-glutamic acid transporter from rat brain. *FEBS Lett.*, 94: 245-248.

Kanner, B.I. & Marva, E. (1982) Efflux of L-glutamate by synaptic plasma membrane vesicles isolated from rat brain. *Biochemistry*, 21: 3143-3147.

Kanner, B.I. & Schuldiner, S. (1987) Mechanism of transport and storage of neurotransmitters. *CRC critical reviews in Biochem.*, 22: 1-38.

Keirstead, S.A. & Miller, R.F. (1992) Trans-ACPD evokes increases in intracellular free calcium concentration in isolated retinal glial (Müller) cells. *Soc. Neurosci. Abstr.*, 18: 1030.

Kerkerian, L., Dusticier, N. & Nieoullon, A. (1987) Modulatory effect of dopamine on high-affinity glutamate uptake in the rat striatum. *J. Neurochem.*, 48: 1301-1306.

Keyes, S.R. & Rudnick, G. (1982) Coupling of transmembrane proton gradients to platelet serotonin transport. *J. Biol. Chem.* 257: 1172-1176.

Keynan, S., Suh, Y.-J., Kanner, B.I. & Rudnick, G. (1992) Expression of a cloned γ -aminobutyric acid transporter in mammalian cells. *Biochemistry*, 31: 1974-1979.

Kim, J.P., Koh, J.-Y. & Choi, D.W. (1987) L-homocysteate is a potent neurotoxin on cultured cortical neurons. *Brain Research* 437: 103-110.

Kimelberg, H.K. (1981) Active accumulation and exchange transport of chloride

in astroglial cells in culture. *Biochim. Biophys. Acta*, 646: 179-184.

Kimelberg, H.K, Pang, S. & Treble, D.H. (1989) Excitatory amino acid-stimulated uptake of $^{22}\text{Na}^+$ in primary astrocyte cultures. *J. Neurosci.*, 9: 1141-1149.

Klann, E., Chen, S.-J. & Sweatt, D. (1991) Persistent protein kinase activation in the maintenance phase of long-term potentiation. *J. Biol. Chem.*, 266: 24253-24256.

Kraig, R.P., Ferreira-Fihlo, C.R. & Nicholson, C. (1983) Alkaline and acid transients in cerebellar microenvironment. *J. Neurophysiol.*, 49: 831-850.

Kuhar, M.J. & Zarbin, M.A. (1978) Synaptosomal transport: a chloride dependence for choline, GABA, glycine, and several other compounds. *J. Neurochem.*, 31: 251-256.

Kvamme, E., Schousboe, A., Hertz, L., Torgner, I.A. & Svenneby, G. (1985) Developmental change of endogenous glutamate and gamma-glutamyl transferase in cultured cerebral cortical interneurons and cerebellar granule cells, and in mouse cerebral cortex and cerebellum in vivo. *Neurochem. Res.*, 10: 993-1008.

Kyte, J. & Doolittle, R.F. (1982) A simple method for displaying the hydrophobic character of a protein. *J. Mol. Biol.*, 157: 105-132.

Langley, O.K., Ghandour, M.S., Vincendon, G. & Gombos, G. (1980) Carbonic anhydrase: an ultrastructural study in rat cerebellum. *Histochem. J.*, 12: 473-483.

Lehmann, A. & Hansson, E. (1987) Amino acid content in astroglial primary cultures from different brain regions during cultivation. *Neurochem. Res.*, 12: 797-800.

Levi, G. & Patrizio, M. (1992) Astrocyte heterogeneity: endogenous amino acid

levels and release evoked by non-N-methyl-D-aspartate receptor agonists and by potassium-induced swelling in type-1 and type-2 astrocytes. *J. Neurochem.*, 58: 1943-1952.

Levy, W.B. & Steward, O. (1979) Synapses as associative memory elements in the hippocampal formation. *Brain Res.*, 175: 233-245.

Linden, D.J., Sheu, F.-S., Murakami, K. & Routtenberg, A. (1987) Enhancement of long-term potentiation by *cis*-unsaturated fatty acid: relation to protein kinase C and phospholipase A₂. *J. Neurosci.*, 7: 3783-3792.

Logan, W.J. & Snyder, S.H. (1971) Unique high affinity uptake systems for glycine, glutamic and aspartic acids in central nervous tissue of the rat. *Nature*, 234: 297-299.

Lux, H.D. & Neher, E. (1973) The equilibration time course of $[K^+]_o$ in cat cortex. *Exp. Brain Res.*, 17: 190-205.

Lynch, G., Dunwiddie, T. & Gribkoff, V. (1977) Heterosynaptic depression: a postsynaptic correlate of long-term potentiation. *Nature*, 266: 737-739.

Lynch, G. Larson, J., Kelso, S., Barrionuevo, G. & Schottler, F. (1983) Intracellular injections of EGTA block induction of hippocampal long-term potentiation. *Nature*, 305: 719-721.

MacDermott, A.B., Mayer, M.L., Westbrook, G.L., Smith, S.J. & Barker, J.L. (1986) NMDA-receptor activation increases cytoplasmic calcium concentration in cultured spinal cord neurones. *Nature*, 321: 519-522.

MacDonald, J.F. & Nowak, L.M. (1990) Mechanisms of blockade of excitatory amino acid receptor channels. *Trends in Pharmacol. Sci.*, 11: 167-172.

Malenka, R.C., Kauer, J.A., Zucker, R.S. & Nicoll, R.A. (1988) Postsynaptic calcium is sufficient for potentiation of hippocampal synaptic transmission. *Science*, 242: 81-84.

Malinow, R., Madison, D.V. & Tsien, R.W. (1988) Persistent protein kinase activity underlying long-term potentiation. *Nature*, 335: 820-824.

Marc, R.E., Liu, W.S., Kalloniatis, M., Raiguel, S.F. & van Haesendonck, E. (1990) Patterns of glutamate immunoreactivity in the goldfish retina. *J. Neurosci.*, 10: 4006-4034.

Marin, P., Lafon-Cazal, M. & Bockaert, J. (1992) A nitric oxide synthase activity selectively stimulated by NMDA receptors depends on protein kinase C activation in mouse striatal neurons. *Eur. J. Neurosci.*, 4: 425-432.

Martell, A.E. & Smith, R.M. (1974) Critical stability constants volume 1: amino acids, London, Plenum Press.

Masu, M., Tanabe, Y., Tsuchida, K., Shigemoto, R. & Nakanishi, S. (1991) Sequence and expression of a metabotropic glutamate receptor. *Nature*, 349: 760-765.

Maycox, P.R., Deckwerth, T., Hell, J.W. & Jahn, R. (1988) Glutamate uptake by brain synaptic vesicles. *J. Biol. Chem.*, 263: 15423-15428.

Mayer, M.L. & Westbrook, G.L. (1984) Mixed-agonist action of excitatory amino acids on mouse spinal cord neurones under voltage clamp. *J. Physiol.* 354: 29-53.

Mayer, M.L., Westbrook, G.L. & Guthrie, P.B. (1984) Voltage-dependent block by Mg^{2+} of NMDA responses in spinal cord neurones. *Nature*, 309: 261-263.

Mayer, M.L., MacDermott, A.B., Westbrook, G.L., Smith, S.J. & Barker, J.L.

(1987) Agonist- and voltage-gated calcium entry in cultured mouse spinal cord neurons under voltage clamp measured using arsenazo III. *J. Neurosci.*, 7: 3230-3244.

Mayer, M.L., Vyklický, L. & Westbrook, G.L. (1989) Modulation of excitatory amino acid receptors by group IIB metal cations in cultured mouse hippocampal neurones. *Nature*, 309: 261-264.

Mayor, F. Jr., Marvizón, J.G., Aragón, M.C., Giménez, C. & Valdivieso, F. (1981) Glycine transport into plasma-membrane vesicles derived from rat brain synaptosomes. *Biochem. J.*, 198: 535-541.

McLennan, H. (1976) The autoradiographic localization of L-[³H]glutamate in rat brain tissue. *Brain Res.*, 115: 139-144.

McNaughton, B.L., Douglas, R.M. & Goddard, G.V. (1978) Synaptic enhancement in fascia dentata: cooperativity among coactive afferents. *Brain Res.*, 157: 277-293.

Meguro, H., Mori, H., Araki, K., Kushiya, E., Kutsuwada, T., Yamazaki, M., Kumanishi, T., Arakawa, M., Sakimura, K. & Mishina, M. (1992) Functional characterization of a heteromeric NMDA receptor channel expressed from cloned cDNAs. *Nature*, 357: 70-74.

Meldrum, B. & Garthwaite, J. (1990) Excitatory amino acid neurotoxicity and neurodegenerative disease. *Trends in Pharmacol. Sci.*, 11: 379-387.

Mewett, K.N., Oakes, D.J., Olverman, H.J., Smith, D.A.S. & Watkins, J.C. (1983) In: *CNS Receptors - From Molecular Pharmacology To Behaviour* (eds. P. Mandel & F.V. DeFeudis) p163-174. Pub. Raven Press, New York.

Meyer, E.M. & Cooper, J.R. (1982) High-affinity choline transport in

proteoliposomes derived from rat cortical synaptosomes. *Science*, 217: 843-845.

Miller, B., Sarantis, M., Traynelis, S.F. & Attwell, D. (1992) Potentiation of NMDA receptor currents by arachidonic acid. *Nature*, 355:722-725.

Mobbs, P., Brew, H. & Attwell, D. (1988) A quantitative analysis of glial cell coupling in the retina of the axolotl (*Ambystoma mexicanum*). *Brain Res.*, 460: 235-245.

Monaghan, D.T., Bridges, R.J. & Cotman, C.W. (1989) The excitatory amino acid receptors: Their classes, pharmacology, and distinct properties in the function of the central nervous system. *Ann. Rev. Pharmacol. Toxicol.* 29: 365-402.

Monyer, H., Sprengel, R., Schoepfer, R., Herb, A., Higuchi, M., Lomeli, H., Burnashev, N., Sakmann, B. & Seeburg, P.H. (1992) Heteromeric NMDA receptors: molecular and functional distinction of subtypes. *Science*, 256: 1217-1221.

Moody, W.J.Jr., Futamachi, K.J. & Prince, D.A. (1974) Extracellular potassium activity during epileptogenesis. *Experimental Neurology*, 42: 248-263.

Moriyoshi, K., Masu, M., Ishii, T., Shigemoto, R., Mizuno, N. & Nakanishi, S. (1991) Molecular cloning and characterization of the rat NMDA receptor. *Nature*, 354: 31-37.

Mudd, S.H., Levy, H.L. & Skovby, F. (1989) Disorders of transsulfuration. In *Metabolic Basis of Inherited Diseases*, Eds Stanbury, J.B., Wyngaarden, J.B., Frederickson, D.S., Goldstein, J.L. & Brown, M.S. pp. 693-741. McGraw-Hill, New York.

Mutch, W.A.C. & Hansen, A.J. (1984) Extracellular pH changes during spreading depression and cerebral ischemia: mechanisms of brain pH regulation. *J. Cereb.*

Blood Flow Metab., 4: 17-27.

Naito, S. & Ueda, T. (1985) Characterization of glutamate uptake into synaptic vesicles. *J. Neurochem.*, 44: 99-109.

Nakanishi, S. (1992) Molecular diversity of glutamate receptors and implications for brain function. *Science*, 258: 597-603.

Nawy, S. & Jahr, C.E. (1990) Suppression by glutamate of cGMP-activated conductance in retinal bipolar cells. *Nature*, 346: 269-271.

Nelson, P.J., Dean, G.E., Aronson, P.S. & Rudnick, G. (1983) Hydrogen ion cotransport by the renal brush border glutamate transporter. *Biochemistry*, 22: 5459-5463.

Newman, E.A. (1984) Regional specialization of retinal glial cell membrane. *Nature*, 309: 155-157.

Newman, E.A. (1985) Voltage-dependent calcium and potassium channels in retinal glial cells. *Nature*, 317: 809-811.

Newman, E.A. & Astion, M.L. (1991) Localization and stoichiometry of electrogenic sodium bicarbonate cotransport in retinal glial cells. *Glia*, 4: 424-428.

Nicholls, D.G. (1989) Release of glutamate, aspartate, and γ -aminobutyric acid from isolated nerve terminals. *J. Neurochem.*, 52: 331-341.

Nicoletti, F., Wroblewski, J.T., Fadda, E. & Costa, E. (1988) Pertussis toxin inhibits signal transduction at a specific metabotropic receptor in primary culture of cerebellar granule cells. *Neuropharmacology*, 27: 551-556.

Nieoullon, A., Kerkerian, L. & Dusticier, N. (1983) Presynaptic dopaminergic

control of high affinity glutamate uptake in the striatum. *Neurosci. Lett.*, 43: 191-196.

Norenberg, M.D. & Martinez-Hernandez, A. (1979) Fine structural localization of glutamine synthetase in astrocytes of rat brain. *Brain Res.*, 161: 303-310.

Novelli, A., Nicoletti, F., Wroblewski, J.T., Alho, H., Costa, E. & Guidotti, A. (1987) Excitatory amino acid receptors coupled with guanylate cyclase in primary cultures of cerebellar granule cells. *J. Neurosci.*, 7: 40-47.

Nowak, L., Bregestovski, P., Ascher, P., Herbert, A. & Prochiantz, A. (1984) Magnesium gates glutamate-activated channels in mouse central neurones. *Nature*, 307: 462-465.

Obenous, A., Mody, I. & Baimbridge, K.G. (1989) Dantrolene-Na (dantrium) blocks induction of long-term potentiation in hippocampal slices. *Neurosci. Lett.*, 98: 172-178.

O'Dell, T.J., Kandel, E.R. & Grant, S.G.N. (1991) Long-term potentiation in the hippocampus is blocked by tyrosine kinase inhibitors. *Nature*, 353: 558-560.

Ohmori, S., Kodama, H., Ikegami, T. & Mizuhara, S. (1972) Unusual sulfur-containing amino acids in the urine of homocystinuric patients. III. Homocysteic acid, homocysteine sulfinic acid, S-(carboxymethylthio)-homocysteine and S-(3-hydroxy-3-carboxy-n-propyl)-homocysteine. *Physiol. Chem. Phys.*, 4: 286-294.

Okada, D., Yamagishi, S. & Sugiyama, H. (1989) Differential effects of phospholipase inhibitors in long-term potentiation in the rat hippocampal mossy fiber synapses and Shaffer/commissural synapses. *Neurosci. Lett.*, 100: 141-146.

Olney, J.W., Sharpe, L.G. (1969) Brain lesions in an infant rhesus monkey

treated with monosodium glutamate. *Science*, 166: 386-388.

Olney, J.W., Ho, O.L. & Rhee, V. (1971) Cytotoxic effects of acidic and sulphur containing amino acids on the infant mouse central nervous system. *Exp. Brain Res.* 14: 61-76.

Olney, J.W., Misra, C.H. & de Gubareff, T. (1975) Cysteine-S-sulfate: brain damaging metabolite in sulfite oxidase deficiency. *Journal of Neuropathology & Experimental Neurology* 34: 167-177.

Olney, J.W., Price, M.T., Samson, L. & Labruyere, J. (1986) The role of specific ions in glutamate neurotoxicity. *Neurosci. Lett.*, 65: 65-71.

Olney, J.W., Price, M.T., Labruyere, J., Salles, K.S., Friedrich, G., Mueller, M. & Silverman, E. (1987) Anti-parkinsonian agents are phenylcyclidine agonists and N-methyl-D-aspartate antagonists. *Eur. J. Pharmacol.*, 142: 319-320.

O'Neill, R., Fillenz, M., Sundstrom, L. & Rawlins, J.N.P. (1984) Voltammetrically monitored brain ascorbate as an index of excitatory amino acid release in the unrestrained rat. *Neurosci. Lett.*, 52: 227-233.

Orkand, R.K., Nicholls, J.G. & Kuffler, S.W. (1966) Effect of nerve impulses on the membrane potential of glial cells in the central nervous system of amphibia. *J. Neurophysiol.*, 29: 788-806.

Ottersen, O.P. (1989) Quantitative electron microscopic immunocytochemistry of neuroactive amino acids. *Anatomy & Embryology*, 180: 1-15.

Palade, P.T. & Barchi, R.L. (1977) On the inhibition of muscle membrane chloride conductance by aromatic carboxylic acids. *J. Gen. Physiol.*, 69: 879-896.

Parsons, B. & Rainbow, T.C. (1984) Localization of cysteine sulfinic acid uptake

sites in rat brain by quantitative autoradiography. *Brain Research* 294: 193-197.

Pasternack, M., Bountra, C., Voipio, J. & Kaila, K. (1992) Influence of extracellular and intracellular pH on GABA-gated chloride conductance in crayfish muscle fibres. *Neuroscience*, 47: 921-929.

Patneau, D.K. & Mayer, M.L. (1990) Structure-activity relationships for amino acid transmitter candidates acting at N-methyl-D-aspartate and quisqualate receptors. *J. Neurosci.* 10: 2385-2399.

Paulsen, R.E. & Fonnum, F. (1989) Role of glial cells for the basal and Ca²⁺-dependent K⁺-evoked release of transmitter amino acids investigated by microdialysis. *J. Neurochem.*, 52: 1823-1829.

Peterson, N.A. & Raghupathy, E. (1972) Characteristics of amino acid accumulation by synaptosomal particles isolated from rat brain. *J. Neurochem.*, 19: 1423-1438.

Petrou, S., Ordway, R.W., Singer, J.J. & Walsh, J.V.Jr. (1993) A putative fatty acid-binding domain of the NMDA receptor. *Trends in Biochem. Sci.*, 18: 41-42.

Pin, J.-P. & Bockaert, J. (1989) Two distinct mechanisms, differentially affected by excitatory amino acids, trigger GABA release from fetal mouse striatal neurons in primary culture. *J. Neurosci.*, 9: 648-656.

Pines, G., Danbolt, N.C., Bjørås, M., Zhang, Y., Bendahan, A., Eide, L., Koepsell, H., Storm-Mathisen, J., Seeberg, E. & Kanner, B.I. (1992) Cloning and expression of a rat brain L-glutamate transporter. *Nature*, 360: 464-467.

Pullan, L.M., Olney, J.W., Price, M.T., Compton, R.P., Hood, W.F., Michel, J. & Monahan, J.B. (1987) Excitatory amino acid receptor potency and subclass specificity of sulphur-containing amino acids. *J. Neurochem.*, 49: 1301-1307.

Putnam, R.W., Roos, A. & Wilding, T.J. (1986) Properties of the intracellular pH-regulating systems of frog skeletal muscle. *J. Physiol.*, 381: 205-219.

Ransom, R.W. & Stec, N.L. (1988) Cooperative modulation of [³H]MK-801 binding to the N-methyl-D-aspartate receptor-ion channel complex by L-glutamate, glycine, and polyamines. *J. Neurochem.*, 51: 830-836.

Rehncroa, S., Westerberg, E., Åkesson, B. & Siesjö, B.K. (1982) Brain cortical fatty acids and phospholipids during and following complete and severe incomplete ischaemia. *J. Neurochem.*, 38: 84-93.

Relton, J.K., Strijbos, P.J.L.M., O'Shaughnessy, C.T., Carey, F., Forder, R.A., Tilders, F.J.H. & Rothwell, N.J. (1991) Lipocortin-1 is an endogenous inhibitor of ischemic damage in the rat brain. *J. Exp. Med.* 174: 305-310.

Rice, M.E. & Nicholson, C. (1988) Behavior of extracellular K⁺ and pH in skate (*Raja erinacea*) cerebellum. *Brain Res.* 461: 328-334.

Rink, T.J., Tsien, R.Y. & Pozzan, T. (1982) Cytoplasmic pH and free Mg²⁺ in lymphocytes. *J. Cell. Biol.*, 95: 189-196.

Robinson, M.B., Hunter-Ensor, M. & Sinor, J. (1991) Pharmacologically distinct sodium-dependent L-[³H]-glutamate transport processes in rat brain. *Brain Res.*, 544: 196-202.

Robinson, M.B., Sinor, J.D., Dowd, L.A. & Kerwin, J.F., Jr (1993) Subtypes of sodium-dependent high-affinity L-[³H]glutamate transport activity: pharmacologic specificity and regulation by sodium and potassium. *J. Neurochem.*, 60: 167-179.

Rosenberg, P.A, Amin, S. & Leitner, M. (1992) Glutamate uptake disguises neurotoxic potency of glutamate agonists in cerebral cortex in dissociated cell culture. *J. Neurosci.*, 12: 56-61.

Roskoski, R.Jr. (1978) Net uptake of L-glutamate and GABA by high affinity synaptosomal transport systems. *J. Neurochem.*, 31: 493-498.

Rothman, S. M. (1984) Synaptic release of excitatory amino acid neurotransmitter mediates anoxic neuronal death. *J. Neurosci.*, 4: 1884-1891.

Rothman, S. M. (1985) The neurotoxicity of excitatory amino acids is produced by passive chloride influx. *J. Neurosci.*, 5: 1483-1489.

Rothman, S. M., Thurston, J. H. & Hauhart, R.E. (1987) Delayed neurotoxicity of excitatory amino acids *in vitro*. *Neuroscience*, 22: 471-480.

Rothstein, J.D. & Tabakoff, B. (1984) Alteration of striatal glutamate release after glutamate synthetase inhibition. *J. Neurochem.*, 43: 1438-1446.

Rothstein, J.D., Tsai, G., Kuncl, R.W., Clawson, L., Cornblath, D.R., Drachman, D.B., Pestronk, A., Stauch, B.L. & Coyle, J.T. (1990) Abnormal excitatory amino acid metabolism in amyotrophic lateral sclerosis. *Annals of Neurology*, 28: 18-25.

Rothstein, J.D., Martin, L.J. & Kuncl, R.W. (1992) Decreased glutamate transport by the brain and spinal cord in amyotrophic lateral sclerosis. *New Engl. J. Med.*, 326: 1464-1468.

Rudnick, G. (1977) Active transport of 5-hydroxytryptamine by plasma membrane vesicles isolated from human blood platelets. *J. Biol. Chem.*, 252: 2170-2174.

Sánchez-Prieto, J. & Gonzalez, P. (1988) Occurrence of a large Ca²⁺-independent release of glutamate during anoxia in isolated nerve terminals (synaptosomes). *J. Neurochem.*, 50: 1322-1324.

Sarantis, M., Everett, K. & Attwell, D. (1988) A presynaptic action of glutamate

at the cone output synapse. *Nature*, 332: 451-453.

Sarantis, M. & Attwell, D. (1990) Glutamate uptake in mammalian retinal glia is voltage- and potassium-dependent. *Brain Res.*, 516: 322-325.

Sarantis, M., Ballerini, L., Miller, B., Silver, R.A., Edwards, M. & Attwell, D. (1993) Glutamate uptake from the synaptic cleft does not shape the decay of the non-NMDA component of the synaptic current. *Neuron*, in press.

Sather, W., Dieudonné, S., MacDonald, J.F. & Ascher, P. (1992) Activation and desensitization of N-methyl-D-aspartate receptors in nucleated outside-out patches from mouse neurones. *J. Physiol.*, 450: 643-672.

Saugstad, J.A., Segerson, T.P., Mulvihill, E.R. & Westbrook, G.L. (1992) Isolation of novel metabotropic glutamate receptor cDNAs from rat olfactory bulb. *Soc. Neurosci. Abst.*, 18: 1363.

Schmidt, B.H., Weiss, S., Sebben, M., Kemp, D.E., Bockaret, J. & Sladeczek, F. (1987) Dual action of excitatory amino acids on the metabolism of inositol phosphates in striatal neurones. *Mol. Pharmacol.*, 32: 364-368.

Schoepp, D.D., Bockaert, J. & Sladeczek, F. (1990) Pharmacological and functional characteristics of metabotropic excitatory amino acid receptors. *Trends Pharmacol. Sci.*, 11: 508-515.

Schon, F. & Kelly, J.S. (1974) Autoradiographic localization of [³H]GABA and [³H]glutamate over satellite glial cells. *Brain Res.*, 66: 275-288.

Schousboe, A., Fosmark, H. & Hertz, L. (1975) High content of glutamate and of ATP in astrocytes cultured from rat brain hemispheres: effect of serum withdrawal and of cyclic AMP. *J. Neurochem.*, 25: 909-911.

Schwartz, E.A. (1987) Depolarization without calcium can release γ -aminobutyric acid from a retinal neuron. *Science*, 238: 350-355.

Schwartz, E.A. & Tachibana, M. (1990) Electrophysiology of glutamate and sodium co-transport in glial cell of the salamander retina. *J. Physiol.*, 426: 43-80.

Shiells, R.A. & Falk, G. (1990) Glutamate receptors of rod bipolar cells are linked to a cyclic GMP cascade via a G-protein. *Proc. R. Soc. Lond.*, 242: 91-94.

Siesjö, B.K. (1985) Acid-base homeostasis in the brain: physiology, chemistry, and neurochemical pathology. *Prog. in Brain Res.*, 63: 121-154.

Siesjö, B.K. (1990) Calcium, excitotoxins and brain damage. *News in Physiol. Sci.*, 5: 120-125.

Sigworth, F.J. (1980) The conductance of sodium channels under conditions of reduced current at the node of Ranvier. *J. Physiol.*, 307: 131-142.

Silverstein, F.S., Buchanan, K. & Johnston, M.V. (1986) Perinatal hypoxia-ischaemia disrupts striatal high-affinity [^3H]-glutamate uptake into synaptosomes. *J. Neurochem.*, 47: 1614-1619.

Sladeczek, F., Pin, J.-P., Récasens, M., Bockaert, J. & Weiss, S. (1985) Glutamate stimulates inositol phosphate formation in striatal neurones. *Nature*, 317: 717-719.

Somjen, G.G. (1984) Acidification of intestinal fluid in hippocampal formation caused by seizures and by spreading depression. *Brain Res.*, 311: 186-188.

Sommer, B., Köhler, M., Sprengel, R. & Seeburg, P.H. (1991) RNA editing in brain controls a determinant of ion flow in glutamate-gated channels. *Cell*, 67: 11-19.

Speciale, C., Hares, K., Schwarcz, R. & Brookes, N. (1989) High affinity uptake of L-kynurenine by a Na⁺-independent transporter of neutral amino acids in astrocytes. *J. Neurosci.*, 9: 2066-2072.

Spray, D.C., Harris, A.L. & Bennett, M.V.L. (1981) Gap junctional conductance is a simple and sensitive function of intracellular pH. *Science*, 211: 712-715.

Stallcup, W.B., Bulloch, K. & Baetge, E.E. (1979) Coupled transport of glutamate and sodium in a cerebellar nerve cell line. *J. Neurochem.*, 32: 57-65.

Stevens, C.F. & Wang, Y. (1993) Reversal of long-term potentiation by inhibitors of haem oxygenase. *Nature*, 364: 147-149.

Storck, T., Schulte, S., Hofmann, K. & Stoffel, W. (1992) Structure, expression, and functional analysis of a Na⁺-dependent glutamate/aspartate transporter from rat brain. *Proc. Natl. Acad. Sci. USA*, 89: 10955-10959.

Sugiyama, H., Ito, I & Hirono, C. (1987) A new type of glutamate receptor linked to inositol phospholipid metabolism. *Nature*, 325: 531-533.

Swanson, R.A. (1992) Astrocyte glutamate uptake during chemical hypoxia in vitro. *Neurosci. Lett.*, 147: 143-146.

Syed, S. E.-H. & Engel, P.C. (1990) A pH-dependent activation-inactivation equilibrium in glutamate dehydrogenase of *Clostridium symbosium*. *Biochem. J.*, 271: 351-355.

Sykova, E. (1989) Activity-related extracellular pH changes in spinal cord. *Acta Physiol. Scand.* 136 (suppl. 582): 62.

Syková, E. & Svoboda, J. (1990) Extracellular alkaline-acid-alkaline transients in the rat spinal cord evoked by peripheral stimulation. *Brain Res.*, 512: 181-189.

Szatkowski, M.S. & Thomas, R.C. (1986) New method for calculating pH_i from accurately measured changes in pH_i induced by a weak acid and base. *Pflügers Arch.*, 407: 59-63.

Szatkowski, M., Barbour, B. & Attwell, D. (1990) Non-vesicular release of glutamate from glial cells by reversed electrogenic glutamate uptake. *Nature* 348: 443-446.

Szatkowski, M., Barbour, B. & Attwell, D. (1991) The potassium-dependence of excitatory amino acid transport: resolution of a paradox. *Brain Res.*, 555: 343-345.

Szczepaniak, A.C. & Cottrell, G.A. (1973) Biphasic action of glutamic acid and synaptic inhibition in an identified serotonin-containing neurone. *Nature, new Biol.*, 241: 62-64.

Tanabe, Y., Masu, M., Ishii, T., Shigemoto, R. & Nakanishi, S. (1992) A family of metabotropic glutamate receptors. *Neuron*, 8: 169-179.

Tanaka, K. (1993) Expression cloning of a rat glutamate transporter. *Neurosci. Res.*, 16: 149-153.

Tang, C.-M., Dichter, M. & Morad, M. (1990) Modulation of the N-methyl-D-aspartate channel by extracellular H^+ . *Proc. Natl. Acad. Sci. USA*, 87: 6445-6449.

Tessier-Lavigne, M., Attwell, D., Mobbs, P. & Wilson, M. (1988) Membrane currents in retinal bipolar cells of the axolotl. *J. Gen. Physiol.* 91: 49-72.

Thomson, A.M., Walker, V.E. & Flynn, D.M. (1989) Glycine enhances NMDA-receptor mediated synaptic potentials in neocortical slices. *Nature*, 338: 422-424.

Thompson, S.M. & Gähwiler, B.H. (1992) Effects of the GABA uptake inhibitor

tiagabine on inhibitory synaptic potentials in rat hippocampal slice cultures. *J. Neurophysiol.*, 67: 1698-1701.

Tolner, B., Poolman, B., Wallace, B. & Konings, W.N. (1992) Revised nucleotide sequence of the *gluP* gene, which encodes the proton-glutamate-aspartate transport protein of *Escherichia coli* K-12. *J. Bacteriol.*, 174: 2391-2393.

Traynelis, S.F. & Cull-Candy, S.G. (1990) Proton inhibition of N-methyl-D-aspartate receptors in cerebellar neurons. *Nature*, 345: 347-350.

Traynelis, S.F. & Cull-Candy, S.G. (1991) Pharmacological properties and H⁺ sensitivity of excitatory amino acid receptor channels in rat cerebellar granule neurones. *J. Physiol.*, 433: 727-763.

Trombley, P.Q. & Westbrook, G.L. (1992) L-AP4 inhibits calcium currents and synaptic transmission via a G-protein-coupled glutamate receptor. *J. Neurosci.*, 12: 2043-2050.

Turski, W.A., Herrling, P.L. & Do, K.Q. (1987) Effects of L-cysteine-sulphinat and L-aspartate, mixed excitatory amino acid agonists, on the membrane potential of cat caudate neurons. *Brain Research* 414: 330-338.

Turski, L., Bressler, K., Rettig, K.-J., Löschmann, P.-A. & Wachtel, H. (1991) Protection of substantia nigra from MPP⁺ neurotoxicity by N-methyl-D-aspartate antagonists. *Nature*, 349: 414-418.

Urbanics, R., Leniger-Follert, E. & Lübbers, D.W. (1978) Time course of changes of extracellular H⁺ and K⁺ activities during and after direct electrical stimulation of the brain cortex. *Pflügers Arch.*, 378: 47-53.

van den Berg, C.J. & Garfinkel, D. (1971) A simulation study of brain compartments. Metabolism of glutamate and related substances in mouse brain.

Biochem. J., 123: 211-218.

van Harrevelde, A. (1959) Compounds in brain extracts causing spreading depression of cerebral cortical activity and contraction of crustacean muscle. *J. Neurochem.*, 3: 300-315.

van Slyke, D.D. (1922) On the measurement of buffer values and on the relationship of buffer value to the dissociation constant of the buffer and the concentration and the reaction of the buffer solution. *J. Biol. Chem.*, 52: 525-570.

Verdoorn, T.A., Burnashev, N., Monyer, H., Seeburg, P.H. & Sakmann, B. (1991) Structural determinants of ion flow through recombinant glutamate receptor channels. *Science* 252: 1715-1718.

Virgin, C.E.Jr., Ha, T.P.-T., Packan, D.R., Tombaugh, G.C., Yang, S.H., Horner, H.C. & Sapolsky, R.M. (1991) Glucocorticoids inhibit glucose transport and glutamate uptake in hippocampal astrocytes: implications for glucocorticoid toxicity. *J. Neurochem.*, 57: 1422-1428.

Voisin, P., Viratelle, O., Girault, J.-M., Morrison-Bogorad, M. & Labouesse, J. (1993) Plasticity of astroglial glutamate and γ -aminobutyric acid uptake in cell cultures derived from postnatal mouse cerebellum. *J. Neurochem.*, 60: 114-127.

Volterra, A., Trotti, D., Cassutti, P., Tromba, C., Salvaggio, A., Melcangi, R.C. & Racagni, G. (1992) High sensitivity of glutamate uptake to extracellular free arachidonic acid levels in rat cortical synaptosomes and astrocytes. *J. Neurochem.*, 59: 600-606.

Vyklický, L.Jr., Krusek, J. & Edwards, C. (1988) Differences in the pore sizes of the N-methyl-D-aspartate and kainate cation channels. *Neurosci. Lett.*, 89: 313-318.

Vyklický, L.Jr., Vlachová, V. & Krůšek, J. (1990) The effect of external pH changes on responses to excitatory amino acids in mouse hippocampal neurones. *J. Physiol.*, 430: 497-517.

Waniewski, R.A. & Martin, D.L. (1983) Selective inhibition of glial versus neuronal uptake of L-glutamic acid by SITS. *Brain Res.*, 268: 390-394.

Waniewski, R.A. (1992) Physiological levels of ammonia regulate glutamine synthesis from extracellular glutamate in astrocyte cultures. *J. Neurochem.*, 58: 167-174.

Watkins, J.C. (1986) Twenty five years of excitatory amino acid research, in *Excitatory amino acid*, pp: 1-39; Ed P.J. Roberts, J. Storm-Mathisen & H.F. Bradford.

Wenthold, R.J., Yokatani, N., Doi, K. & Wada, K. (1992) Immunochemical characterization of the non-NMDA glutamate receptor using subunit-specific antibodies. *J. Biol. Chem.*, 267: 501-507.

Westbrook, G.L. & Mayer, M.L. (1987) Micromolar concentrations of Zn^{2+} antagonize NMDA and GABA responses of hippocampal neurons. *Nature*, 328: 640-643.

Wheeler, D.D. (1979) A model of high affinity glutamic acid transport by rat cortical synaptosomes - a refinement of the originally proposed model. *J. Neurochem.*, 33: 883-894.

White, R.D. & Neal, M.J. (1976) The uptake of L-glutamate by the retina. *Brain Res.*, 111: 79-93.

Williams, K., Dawson, V.L., Romano, C., Dichter, M.A. & Molinoff, P.B. (1990) Characterization of polyamines having agonist, antagonist and inverse agonist

effects at the polyamine recognition site of the NMDA receptor. *Neuron*, 5: 199-208.

Wilson, D.F. & Pastuszko, A. (1986) Transport of cysteate by synaptosomes isolated from rat brain: evidence that it utilizes the same transporter as aspartate, glutamate, and cysteine sulfinatate. *J. Neurochem.*, 47: 1091-1097.

Wilson, J.X. & Dixon, S.J. (1989) Ascorbic acid transport in mouse and rat astrocytes is reversibly inhibited by furosemide, SITS, and DIDS. *Neurochem. Res.*, 12: 1169-1175.

Winter-Wolpaw, E. & Martin, D.L. (1984) Cl⁻ transport in glioma cell line: evidence for two transport mechanisms. *Brain Res.*, 297: 317-327.

Wong, E.H.F., Kemp, J.A., Priestley, T., Knight, A.R., Woodruff, G.N. & Iversen, L.L. (1986) The anticonvulsant MK-801 is a potent N-methyl-D-aspartate antagonist. *Proc. Natl. Acad. Sci. USA*, 83: 7104-7108.

Wyllie, D.J.A., Mathie, A., Symonds, C.J. & Cull-Candy, S.G. (1991) Activation of glutamate receptors and glutamate uptake in identified macroglial cells in rat cerebellar cultures. *J. Physiol.*, 432: 235-258.

Yamamoto, F., Borgula, G.A. & Steinberg, R.H. (1992) Effects of light and darkness on pH outside rod photoreceptors in the cat retina. *Exp. Eye Res.*, 54: 685-697.

Zhuo, M., Small, S.A., Kandel, E.R. & Hawkins, R.D. (1993) Nitric oxide and carbon monoxide produce activity-dependent long-term synaptic enhancement in hippocampus. *Science*, 260: 1946-1950.